Aerospace System Design

AERO 483

The University of Michigan

Project UM-Haul

UnManned Heavy pAyload Unloader and Lander

The design of a reusable lunar lander with an independent cargo unloader

NASA/USRA

April 1991

Table of Contents

Foreword

Aerospace Engineering 483, "Aerospace System Design", is one of a number of design courses available to students in Aerospace Engineering at The University of Michigan. Each year, in this course, a different topic is selected for the preliminary design study, which is carried out by the entire class as a team effort. There are no exams or quizzes in this course, but the total output of the study consists of three parts: a) a formal oral presentation at the end of the semester, b) a scale model of the design, and c) a final report. The UM-Haul system is the second of two designs completed this year and the thirty-sixth in the series, started in 1965 by the late Professor Wilbur C. Nelson.

Project UM-Haul is the preliminary design of a Reusable Lunar Transportation Vehicle that travels between a lunar parking orbit and the lunar surface. The design is suggested by the 1990/91 AIAA/INDUSTRY competition. A detailed statement of design objectives and requirements has been published by AIAA and formed the guideline of the project. This vehicle is an indispensable link in the overall task of establishing a lunar base as defined by the NASA Space Exploration Initiative.

Our response to this need is a system which consists of two independent vehicles: lander and unloader. The system can navigate and unload itself with a minimum amount of human intervention. The design addresses structural analysis, propulsion, power, controls, communications, payload handling and orbital operations.

The Lander has the capability to descend from low lunar orbit (LLO) to the lunar surface carrying a 7000 kg payload, plus the unloader, plus propellant for ascent to LLO. Taking advantage of specially designed legs and retractable engines, the Lander deploys the Unloader by way of a motorized ramp. The Unloader is a terrain vehicle capable of carrying cargos of 8,500 kg mass and employs a lift system to lower payloads to the ground. It can stay on the surface between missions, or return with the Lander to orbit for use at another site. The system can perform 10 missions before requiring major servicing.

As is customary, the students in the course elected a Project Manager and an Assistant Project Manager at the beginning of the semester and subsequently organized themselves into technical groups, one for each of the major subsystems of the design. The work of each group is directed by a Group Leader. The Managers direct and control the team activity and integrate the group inputs into a single, coherent design. The concept of a system approach to design was carried throughout the design process.

A Final Report Committee, with representatives from each group, was assigned the major task of integrating the team inputs into this document, to be published in June, 1991.

We gratefully acknowledge the continuation of the Grant from the NASA/USRA University Advanced Design Program. The Grant provides funding for a graduate teaching assistant, for travel, for reproduction and distribution of the final report, for construction of the scale model, and for various other operational costs. Special recognition is due Ms. Carol Hopf, Deputy Director, Division of Educational Programs, and Ms. Barbara Rumbaugh, Senior Project Administrator of the Advanced Design Program, both of USRA, Houston TX.

As integral part of the Grant, NASA Lewis Research Center gave support of key lecturers and other technical resources. NASA Lewis also hosted the mid-term design review in early March. Ms. Lisa Kohout and Ms. Barbara McKissock provided technical guidance and maintained contact with the team during the year. We are thankful to them for their support and friendship.

Professor Harm Buning April, 1991

Acronyms

AFC - Alkaline Fuel Cells
AIAA - American Institute of Aeronautics & Astronautics
ASE - Advanced Space Engine
ATDRSS - Advanced Tracking and Data Relay Satellite System
B4A - Dacron Net B4A Separator
BOL - Beginning of Life
CEC - Carbon Epoxy Composites
COI - Chase Orbit Insertion
D/FP - Docking/Fuel Ports
DCOI - Descent to the Chase Orbit Initiation
DGK - Double Goldized Kapton Reflector
DOD - Depth of Discharge
DOI - Descent Orbit Insertion
EOL - End of Life
EVA - Extra-Vehicular Activities
GH2 - Gaseous Hydrogen
GN&C - Guidance, Navigation & Control
GOX - Gaseous Oxygen
GRS - Geostationary Relay Satellite
IGS - Integrated reaction control and fuel cell Gaseous System
IOC - Initial Operating Capability
Isp - Specific Impulse
LEO - Low Earth Orbit
LH_2 - Liquid Hydrogen
LLO - Low Lunar Orbit
LOX - Liquid Oxygen
LRV - Lunar Rover Vehicle
LWLL - Lightweight Longeron Latches
MCC - Mission Control and Communications
MLI - Multi-Layer Insulation
MOLAB - Mobil Lunar Laboratory
MPD - Magnetoplasmadynamic
NTR - Nuclear Thermal Rockets
OTV - Orbital Transfer Vehicle
PDI - Powered Descent Initiation
PTM - Payload Transfer Mechanism
PV - Photovoltaic
RCS - Reaction Control System
RFC - Regenerative Fuel Cell
RTG - Radioisotope Thermoelectric Generator
SSF - Space Station Freedom
SURLL - Self-Unloading Reusable Lunar Lander
TDRSS - Tracking and Data Relay Satellite System
TPI - Terminal Phase Initiation

Team Organization

Organizational Chart

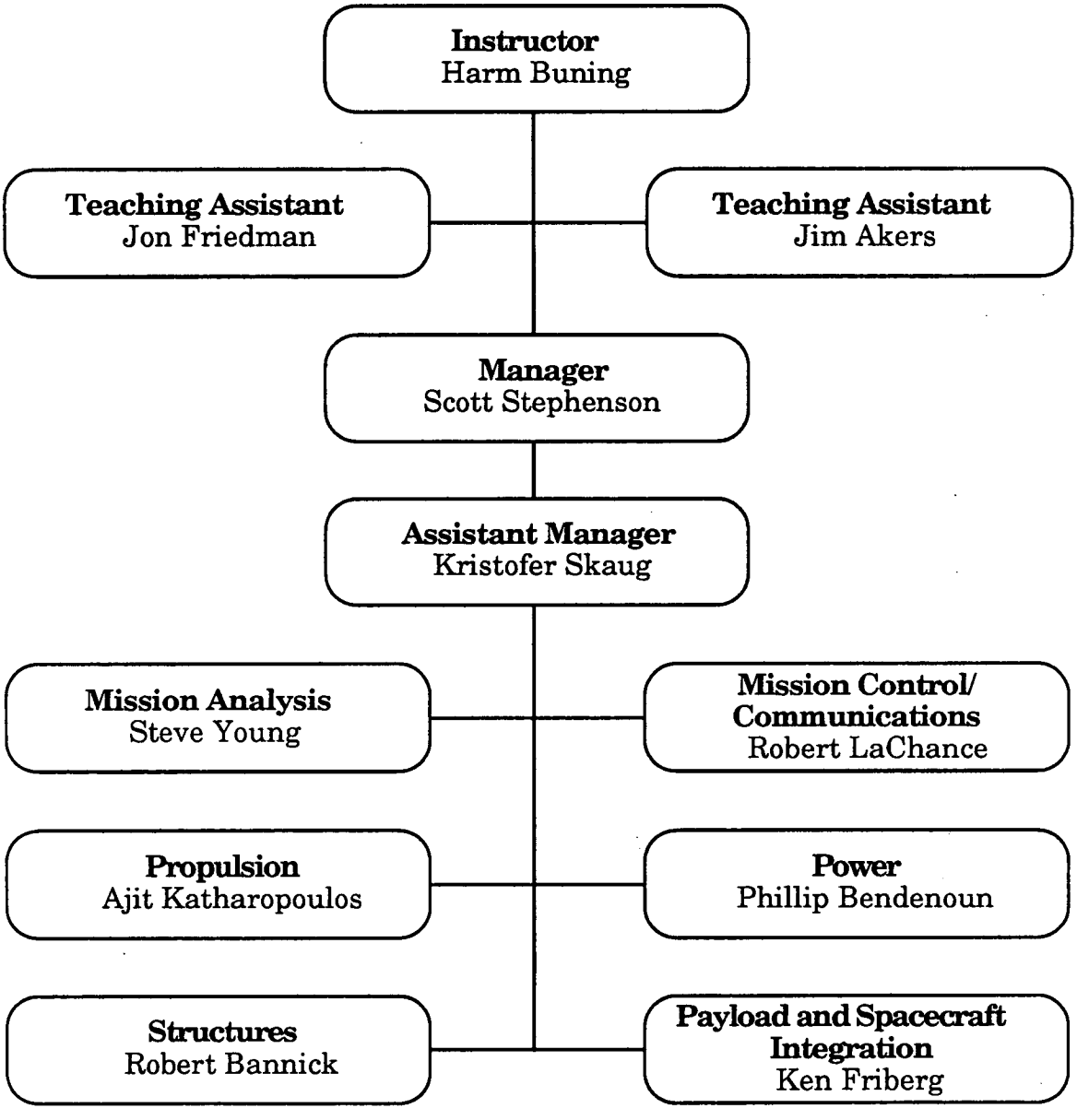

Team Roster

Aerospace Engineering 483

Project UM-Haul

Instructor: Harm Buning

Teaching Assistant: Jon Friedman

Teaching Assistant: Jim Akers

Manager: Scott Stephenson

Assistant Manager: Kristofer Skaug

Payload and Spacecraft Integration
David Dempsey
*Ken Friberg
Ken Kowalczyk

Power
*Philip Bendenoun
Dan Darga

Structures
*Robert Bannick
Alexa McCulloch
Douglas Murphy
Dan Payne

Control and Communications
*Robert LaChance
Gardiner Leverett
Karen Sinclair

Propulsion
Edmond Chang
Karen Gorny
*Ajit Katharopoulos

Mission Analysis
Jodie McGrew
Corey Schumacher
*Steve Young

(* Denotes Group Leader)

Ad-Hoc Committee for the Final Report

*Dan Darga: Power

Dave Dempsey: Payload Spacecraft Integration

*Karen Gorny: Propulsion

Alexa McCulloch: Structures

Jodi McGrew: Mission Analysis

Douglas Murphy: Structures

Karen Sinclair: Control and Communications

Cover Design: Douglas Murphy

(* Denotes Chairman of Ad-Hoc Committee)

Scale Model Team

David Dempsey

*Ken Friberg

Ken Kowalczyk

(* Denotes Team Leader)

ORIGINAL PAGE
BLACK AND WHITE PHOTOGRAPH

First Row: Steve Young, David Dempsey, Karen Sinclair, Dan Darga, Ken Kowalczyk, Kristofer Skaug
Second Row: Harm Buning, Edmond Chang, Jodi McGrew, Dan Payne, Alexa McCulloch, Ken Friberg, Karen Gorny **Third Row:** Doug Murphy, Phillip Bendenoun, Corey Schumacher, Gardiner Leveritt, Ajit Katharopoulos, Robert LaChance, Robert Bannick, Scott Stephenson

Chapter 1

Introduction

1.1 Mission Justification

1.2 Project UM-Haul

1.3 References

1.1. Mission Justification

1.1.1. Human Expansion into the Solar System

Ever since the triumphant 1969 Moon landing of Apollo 11, Mankind has had the confidence that it could travel to and explore other worlds. We will soon be evolving into a "solar species", utilizing the entire space, matter and energy of a solar system to build and sustain our civilization. In our thrust to expand to new worlds, a first step must be to learn how to handle hostile environments with the aid of technology, and furthermore to take advantage of the resources present on other worlds so as to make human colonization self-sustained and economically viable.

Due to the favorable conditions on our home planet, as a species we face a critical lack of adaptability to different environments. Humans can only live within a narrow band of climates, and need an Oxygen atmosphere of severely bounded composition and pressure ranges to sustain themselves. Adding to this problem, humans depend on specific bacterial soil cultures for production of food. Most such cultures are even more sensitive to environmental changes than humans. Therefore, human colonization of planets even slightly different from Earth requires significant isolation from the outside environment and an elaborately simulated Earth ecosystem within the artificial habitats. Testing of prototype colonies is currently underway, for example in Project "Biosphere II" in Arizona, where humans are sealed off from the outside world in a glass dome with a fully autonomous ecosystem.

The significant costs of such systems, however, necessitates the presence of strong economic incentives before large-scale colonization of other planets can be considered. Foreseeable incentives include minerals and gases, as well as the opportunities for new manufacturing techniques under different gravitational and atmospheric conditions.

However, before exploring such resources, we must ensure that our technology can meet the challenge. The large-scale environmental effect of such activities should also be determined. Finally, we must establish whether or not long-term exploitation of the given resources is profitable to the extent of outweighing the costs of colonization. In this perspective, it seems logical to look for a small-scale beginning to our endeavor, one which will teach us about our own limitations and those of our technology.

Several factors contribute to make the Moon a good first target for human colonization. The Moon offers no atmosphere, abrasive soils, extreme temperatures and low gravity. Thus it provides a hostile environment and some tough proving grounds for our technology. Being the closest extraterrestrial body we know of, the Moon also leaves us ample communication opportunities and relatively low transport costs. Once our technology has conquered the lunar environment, we will have a well justified confidence in our ability to expand further into space.

1.1.2. Establishment of a Lunar Base

In its 1986 report titled "Pioneering the Space Frontier" [1], the National Commission on Space recommends a return to the Moon with the goal of establishing permanently manned lunar bases. The resources and strategies required to reach this goal are extensive. Important links in the project include the establishment of a permanent space station in Low Earth Orbit (LEO), and so-called Transportation Nodes (TN) which will provide assembly, docking and launch facilities for interplanetary spacecraft. Furthermore, the plan calls for the development of a generic Orbital Transfer Vehicle (OTV) for bulk transport of cargo and crew modules between LEO and a Low Lunar Orbit (LLO).

As described in the study "Lunar Outpost" [2], the current NASA lunar base concept includes an inflatable habitat, a construction shack, a laboratory module, a solar dynamic or photovoltaic energy plant, an Oxygen production plant, several terrain transport and reconnaissance vehicles, and a landing/launch pad facility at a suitable distance with road connections to the base site. An illustration of a lunar outpost is shown in Figure 1.1. (Reproduced with permission from [2])

Construction of such a lunar base will require the delivery of a number of payloads to the Moon, including pressurized elements of at least the same size as a Space Station Freedom (SSF) logistics module. Other necessary payloads include elements for an energy plant (solar cell arrays, or a nuclear reactor), lunar ground vehicles, lunar Oxygen plant elements, laboratory modules, observatory elements, antennas, vehicles and necessary spare parts, food, etc.

By some ways of accounting, the cost of delivering this magnitude of masses to the Moon is on the order of $\$10^6$ per kg [3]. The transfer of integral Earth-based unloading systems (cranes, forklifts, etc.) to the Moon for the sole purpose of handling payloads would therefore be costly. Likewise, with the low degree of automation currently employed, operational costs for such systems would be high. Further removing the standard Earth-based unloader design from consideration in this scheme is the minimal compatibility with the lunar environment; the low gravity, abrasive dust and lack of atmosphere can have severe effects on the long-term operability of these systems. Hence, it would clearly be advantageous to employ a self-unloading transport system specifically designed for the lunar environment.

The general risks of human Extra-Vehicular Activities (EVA) are significant, and particularly so on a lunar construction site with reduced environmental protection and safety provisions. Considering the extensive mass of equipment and resources that need to be installed for an inhabitable base, it is therefore desirable to deliver the bulk of construction resources in advance of human arrival to the prospective base site. Through unmanned, automated transports, the actual EVA time required to assemble a lunar base can be kept to an absolute minimum.

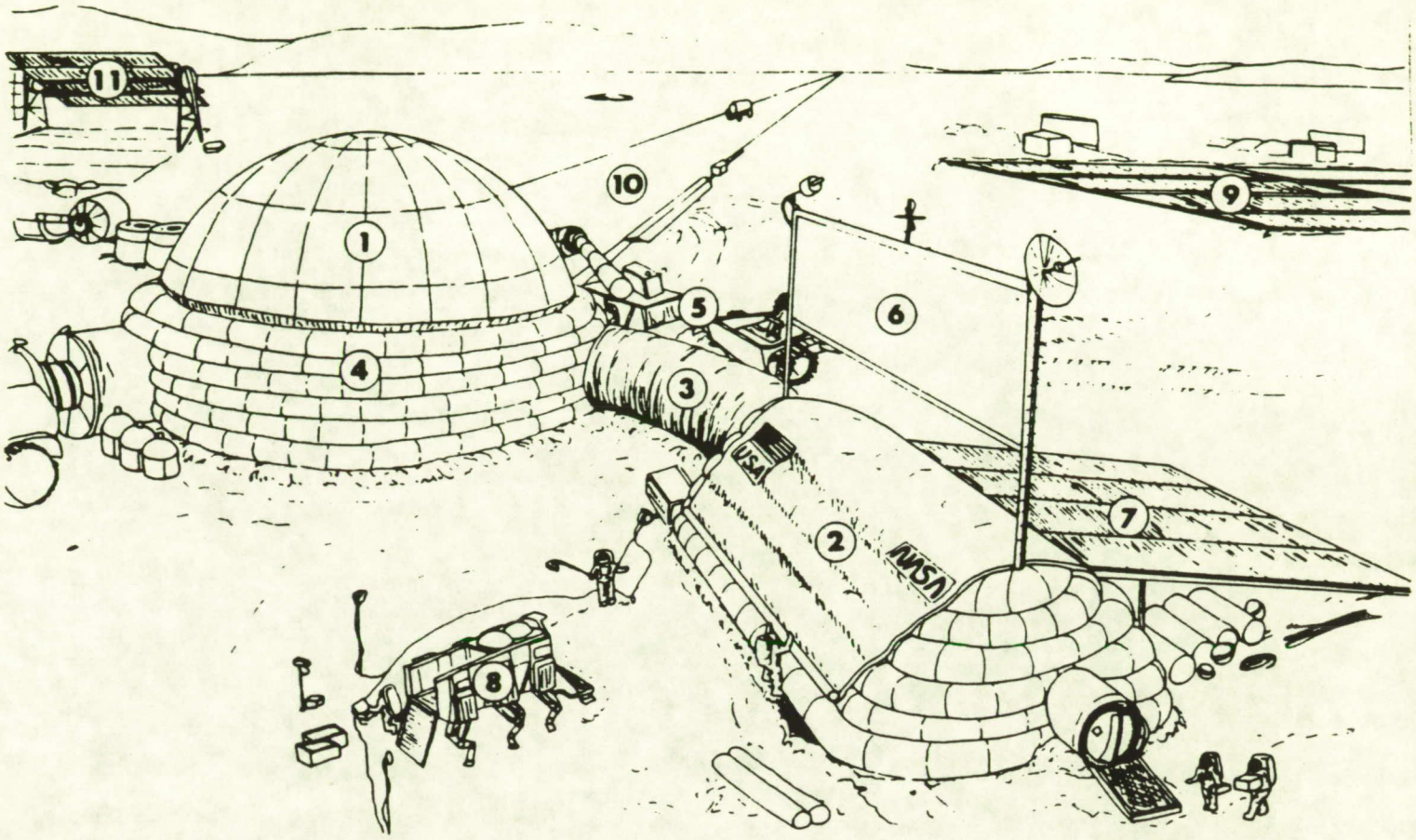

1. The inflatable habitat
2. The construction shack
3. Connecting tunnel
4. Continuous, coiled regolith bags for radiation protection
5. Regolith bagging machine, coiling bags around the habitat while bulldozer scrapes loose regolith into its path
6. Thermal radiator for shack
7. Solar panel for shack
8. Experimental six-legged walker
9. Solar power system for the outpost
10. Road to landing pad
11. Solar power system for the lunar oxygen pilot plant

Figure 1.1 - A Lunar Outpost

In this context, the idea of a "Self-Unloading Reusable Lunar Lander" (SURLL) arises naturally. A system is desired which can navigate and unload itself with little or no need for human intervention. Furthermore, a high payload capability is desired, along with a high reliability so that maintenance needs are low, even after multiple missions.

Our response to this need is UM-Haul, or the UnManned Heavy pAyload Unloader and Lander. In this report, a full system description is provided as well as preliminary risk and cost analyses.

1.2. Project UM-Haul

1.2.1. Project Objective

The stated objective of Project UM-Haul is the definition of a design and operational concept for a SURLL. This system will transport payloads crucial to the construction of a permanent manned lunar base from LLO to designated sites on the lunar surface, and unload them.

Defining the design and operation of such a system is a difficult problem. As with all design situations, there is no optimum solution: there are too many variables. Instead, one must strive to arrive at a "best" solution by achieving a satisfactory balance between conflicting factors such as cost, performance, and on-time delivery. Given an infinite budget, one could deliver a high performance system when promised, but this is generally not feasible. Trade-offs must be made, and in order to arrive at a system which achieves the "best" balance, one must have a set of criteria against which can be evaluated the pros and cons of each design option.

1.2.2. Requirements and Constraints

The UM-Haul preliminary design stage commenced with determining the critical characteristics which the "optimum" system would satisfy. The "ideal" SURLL would be reliable (long mission life with few maintenance needs), versatile (able to handle payloads of varying shape, size, weight and multiple landing sites), highly automated (able to perform its mission with little or no human intervention), and low cost. These traits were translated into a set of concrete system requirements and constraints. In the discussion that follows, the criteria [3] used for UM-Haul will be presented.

The SURLL shall meet the following design criteria:

1. Capability to descend from LLO and land on the lunar surface carrying a 7000 kg payload, the unloading mechanism, and propellant for ascent back to LLO.

2. Capability to refuel and reload in LLO for another landing.

3. Capability to carry the unloading mechanism back to LLO for later use at another landing site.

4. Capability to return to LLO without the unloading device, load a payload of mass equal to 7000 kg plus that of the unloader, and return to the landing site where the unloader waits.

5. Capability to perform 10 landing/unloading sequences before major servicing (additional sequences is desirable).

6. Feature modularized subsystems for easy maintenance.

The unloading mechanism shall meet the following design criteria:

1. Capability to unload a payload with the same diameter as a space station logistics module and with a mass of 7000 kg plus its own mass.

2. Not required to provide cooling, power, etc. to the payload.

In the preliminary design elimination phase, candidate designs were removed if they were unable to satisfy one or more of the above design criteria. The remaining candidates were judged based on versatility (both in payload and landing site), reliability (a minimum of vulnerable mechanisms), low power consumption, an efficient and safe unloading process, and easy interface with existing or proposed systems (a more detailed discussion of the evaluation process is contained in Chapter 2). In the end only one candidate remained. Figure 1.2 contains a diagram of the fully integrated UM-Haul system.

1.2.3. Description of the UM-Haul System

1.2.3.1. Lunar Lander

The primary purpose of the Lander is to rendezvous with the Orbital Transfer Vehicle (OTV), load a payload, and deliver it to the lunar surface for deployment by the Unloader. In addition, the Lander can transport the Unloader between different landing sites where payloads are to be deployed. Special features include two-fold redundant deployable ramps; retractable Helium gas shock legs; retractable engines that can be gimbaled; laser radar obstacle avoidance system; fuel cell primary power system and Sodium-Sulfur (NaS) battery secondary power system.

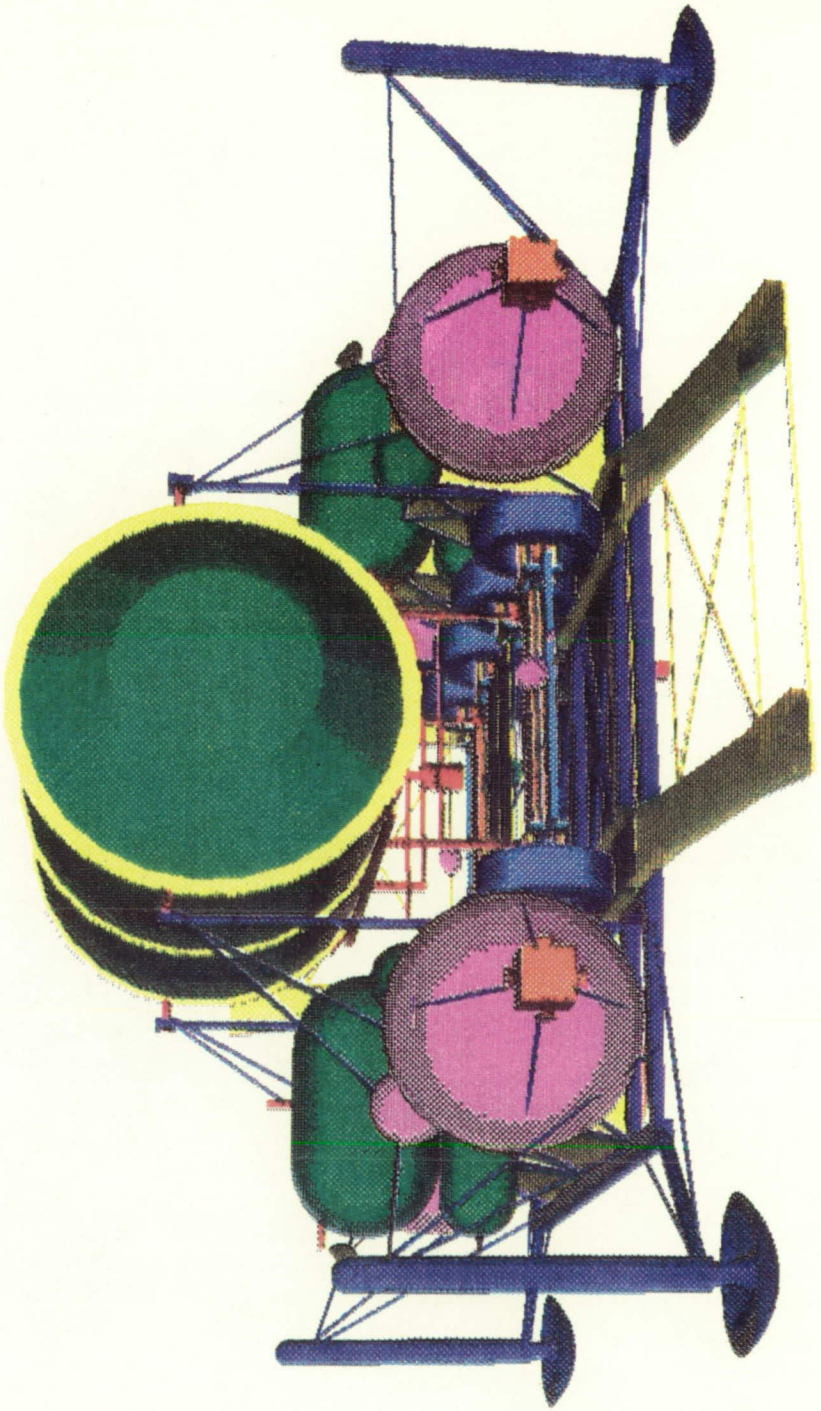

Figure 1.2 - Fully Integrated UM-Haul System

Special emphasis was placed on system and subsystem modularity in the design. Due to its size, it was necessary that the Lander could be disassembled into a minimum number of sections, each of which would fit within the confines of the Space Shuttle bay. For a LEO assembly, the number of required Shuttle launches will be three (including the Unloader). The symmetric modularity of the vehicle [see Figure 1.2] also allows assembly in LEO with a minimum number of extra-vehicular man-hours. In order to provide this modularity, it was necessary that each of the Lander pods (which house engines, propellant tanks, etc.) contain redundant and autonomous subsystems. Apart from structural members, the pod-to-pod connection needs are thus reduced to electrical cabling only.

1.2.3.2. Unloader

Designed to fit within the Lander cargo bay, the Unloader [see Figure 1.2] can carry a payload with a total mass of 8,500 kg, and the maximum dimensions of an SSF Logistics Module (4.57 m diameter, 7.32 m length). The Unloader is equipped with eight wire-mesh wheels, each independently driven, steered, and suspended. The telerobotic obstacle avoidance system for the Unloader employs a Ka-band direct video link. The Unloader will thus be guided by an Earth-based support team.

The Unloader power system consists of a 3.25 m^2 Gallium-Arsenide (GaAs) photovoltaic array, and Sodium Sulphur (NaS) storage cells. The array is mounted statically on the chassis, and is protected from debris kicked up by the Lander engines with a deployable blanket.

In order to obtain and deploy payloads, the Unloader utilizes a low-geared lifting mechanism consisting of four threaded posts. Supported by these posts is a system of rails and rocker joint cradling surfaces upon which the load-bearing bulkheads of the payload rest.

For successful unloading, a payload must be equipped with automatically deployable legs. Once these legs have been extended, the Unloader lowers the payload to a stable ground position, and drives out from underneath.

1.2.3.3. UM-Haul Fact Sheet

Figure 1.3 and Figure 1.4 contain a factual breakdown for both the Lander and Unloader subsystems.

Lander

Main Engine	Pratt and Whitney RL10-IIIB (4)
Reaction Control Thrusters	GH_2/GOX 8911 Bell Textron Thrusters (20)
Primary Power System	GH_2/GOX Fuel Cells (3)
Structure	
Material	Aluminum Lithium 2090-T87
Landing Attenuation	Helium Gas Shocks
Mass (Truss only)	1445 kg
Communication Frequency	
Primary	Ka-Band
Backup	S-Band
Obstacle Avoidance System	Laser Radar (1)
Guidance System	
Relative Frame	Star Tracker (3)
Body frame	Ring Laser Gyroscope (6)
Position, velocity, acc.	Accelerometers (6)
Communications with Unloader	Beacon (1)

Figure 1.3 - Lander Subsystem Specifics

Unloader

Primary Power System	GaAs/Ge Photovoltaic Array (4.5 m^2)
Secondary Power System	NaS Batteries (6)
Structure	
Material	Aluminum Lithium 2090-T87
Mass (Truss only)	448 kg
Communication Frequency	
Primary	Ka-Band
Backup	S-Band
Obstacle Avoidance System	Television Cameras (4)
Guidance System	
Relative Frame	Wheel Odometers (2)
Body frame	Gyrocompasses (2)
Position, velocity, acc.	Accelerometers (2)
Communication with Lander	Receiver (1)
Wheels	Wire mesh (8)
Drive Train	Independently driven wheels
Steering	Independently steered wheels
Drive Motors	746 Watts (8)
Lift motors	746 Watts (4)
Steering Motors	373 Watts (8)
Suspension	Rotational Springs

Figure 1.4 - Unloader Subsystem Specifics

1.2.4. Mission Scenario and Timeline

The basic mission plan can be divided into five well-defined segments:

1. Initial in-orbit operations
2. Transit to lunar surface
3. Lunar surface operations
4. Launch to orbit
5. Concluding in-orbit operations

The assembly of these elements into a concise UM-Haul Mission Scenario is diagrammed in Figure 1.5. Approximate figures for the time consumption in each phase is indicated in italics. The flowchart emphasizes the cyclic nature of the mission, with an open end to payload transfers from Earth. The zero time point of a cycle is assumed to be the instant when the Lander and OTV are docked in LLO.

Initial in-orbit operations for a nominal mission include payload transfer, systems check, descent planning, separation and descent countdown. *Transit to surface* consists of the descent orbit burn and a landing burn, possibly with hovering. The *lunar surface operations* involve another complete systems check, ramp deployment, Unloader activation, cargo securing and transit, unloading and finally a clearance or re-boarding maneuver by the Unloader.

Preceding *the launch to orbit* phase, yet another systems check is performed. A rapid ascent burn takes the Lander up with a minimal heat exposure on the landing gear (legs). An orbit insertion burn is required upon obtaining the desired altitude. Finally, during the *concluding orbit operations* the Lander waits in orbit for the arrival of another payload aboard an OTV; rendezvous, proximity operations and docking follows. Once safely docked, the Lander is refueled and checked by the OTV. If the ten mission cycles have been completed, UM-Haul is returned to SSF for maintenance and refurbishment; otherwise, it is ready to load another payload and begin the next cycle.

1.2.4.1. Low Lunar Orbit Operations

Figure 1.6 details the UM-Haul LLO Operations. LLO standby will range from 2 to 4 months, depending on factors such as OTV availability, OTV transit time, payload delivery needs, launch window timing, etc.

Upon arrival of the OTV in LLO, rendezvous operations will commence and be completed in 10 hours (worst case scenario). After refueling, payload transfer, and confirmation of next landing site, the mission begins.

1.2.4.2. Unloader Lunar Surface Standby

As set forth in the requirements, the Unloader is capable of waiting on the Lunar surface for the return of the Lander with an additional payload.

However, cargo delivery and unloading operations will not occur during the two week lunar night due to the absence of battery recharging capability. During this period, the Unloader will monitor vital signs (such as subsystem temperatures, battery charge levels, etc) and periodically transmit these status checks back to the Earth ground station. The flowchart in Figure 1.7 details the Unloader lunar surface standby mode.

In the event that a payload delivery is requested immediately following the end of lunar night (before sufficient battery recharging for unloading has occurred), the Unloader can charge directly from the Lander power system. This will reduce the required time for recharge from 24 to 6 hours.

Due to the dire effects of the harsh lunar surface environment on the Unloader power system, the maximum surface wait time which the Unloader can endure is 4 months. If the mission hold time will exceed this period, the Unloader must be returned to LLO with the Lander.

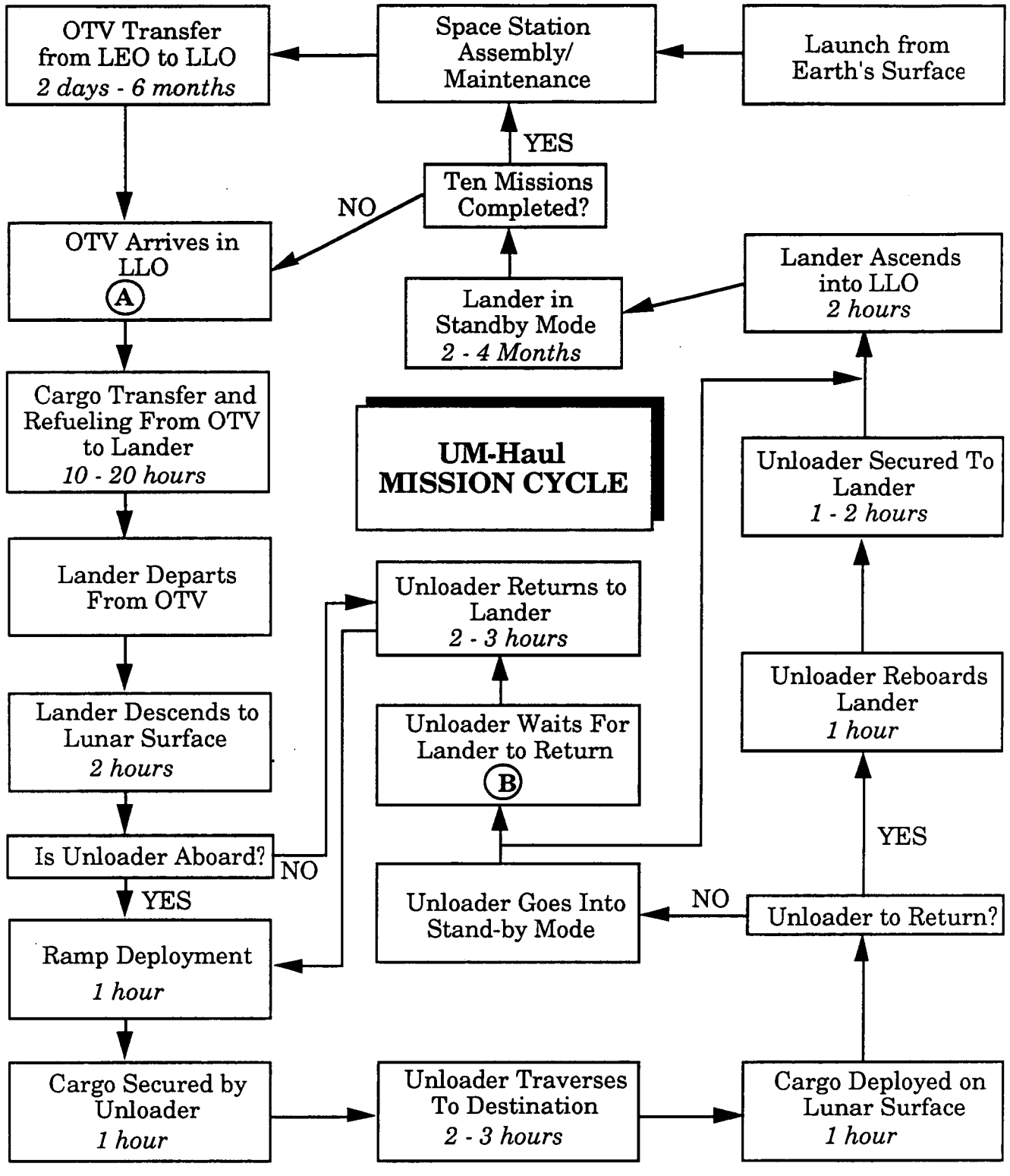

Figure 1.5 - UM-Haul Mission Scenario

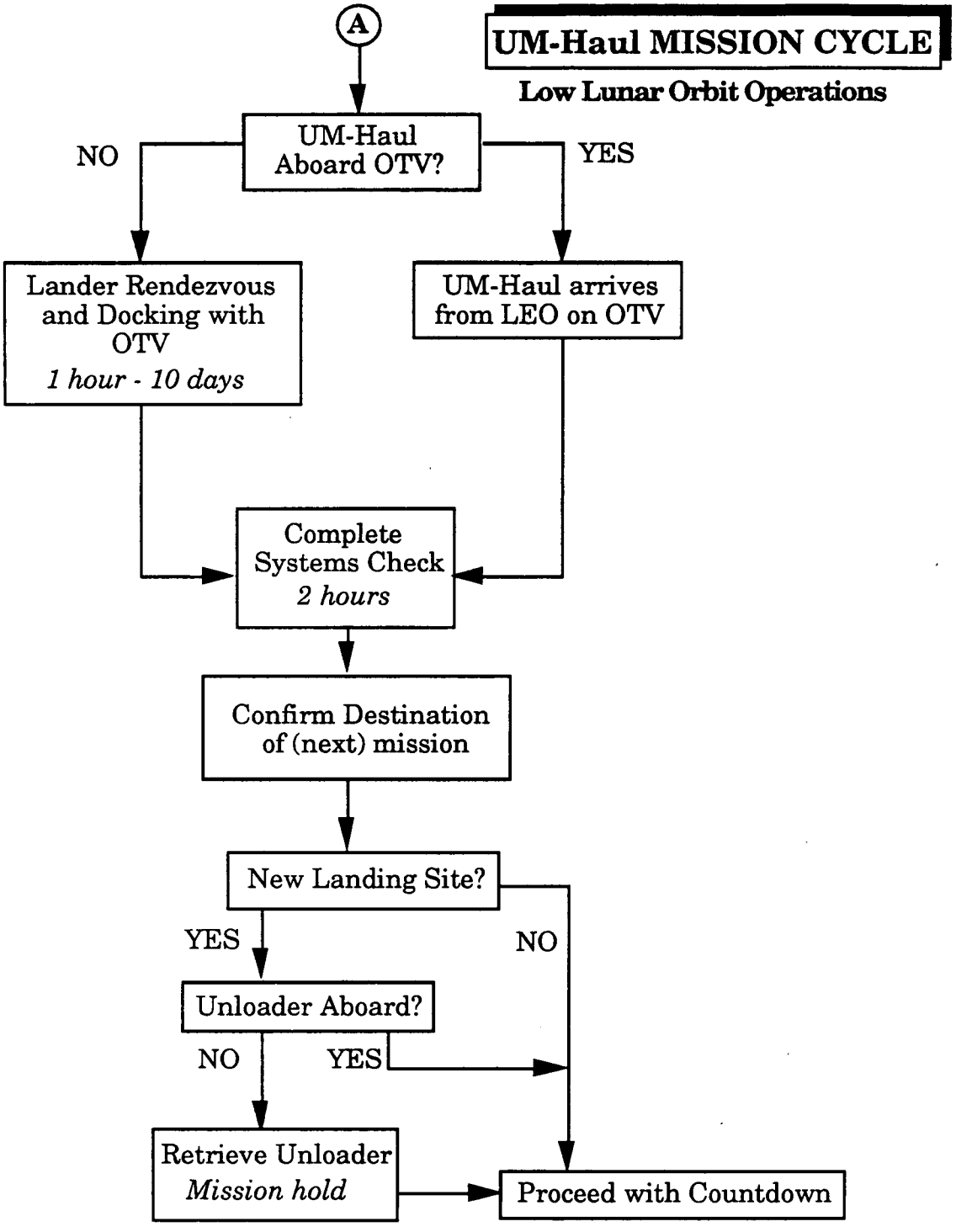

Figure 1.6 - Low Lunar Orbit Operations

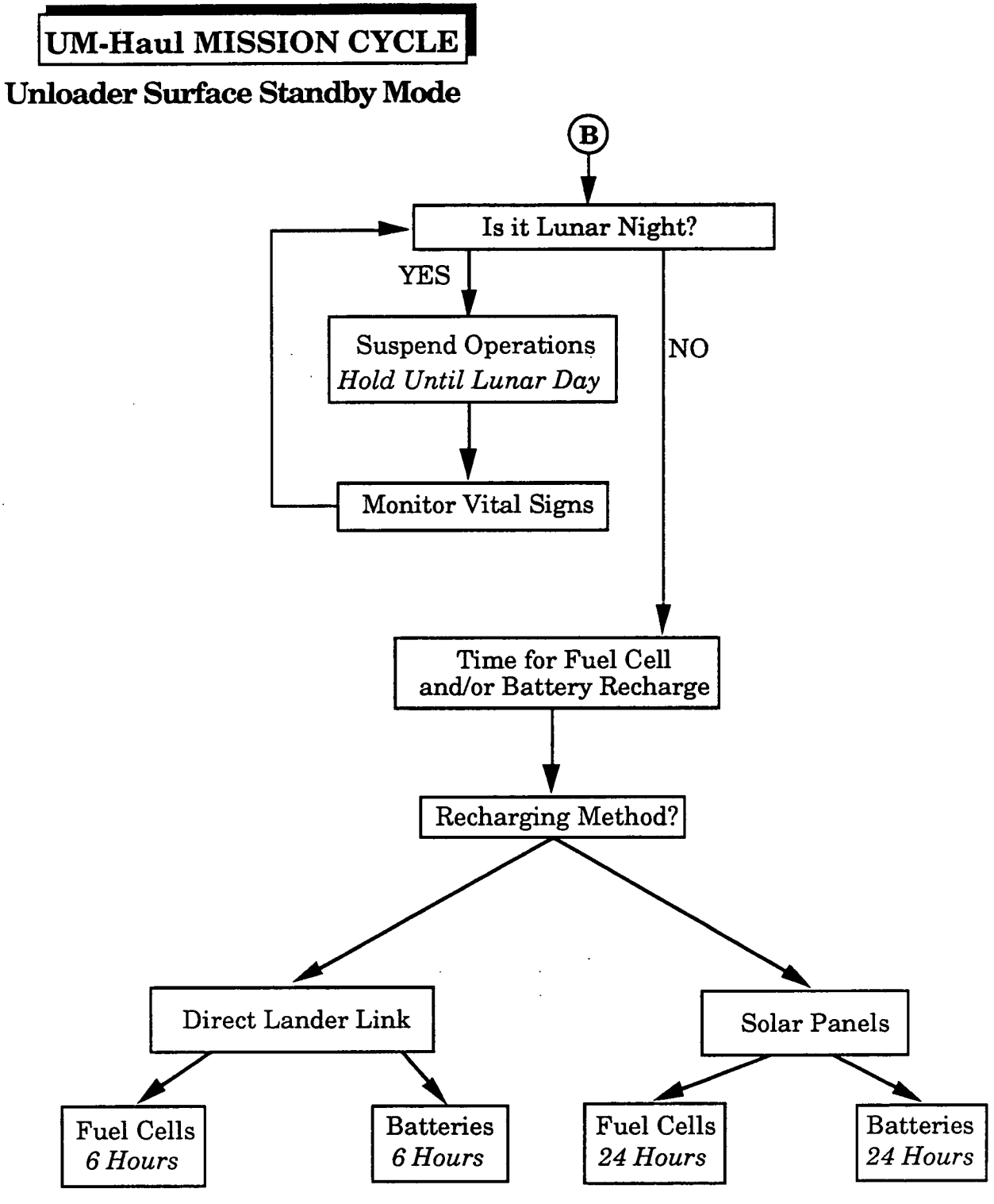

Figure 1.7 - Unloader Surface Standby Mode

1.3. References

[1] "Pioneering the Space Frontier". Report of the National Commission on Space. Bantam Books, New York 1986, p.18.

[2] Alred, John, et al.: Lunar Outpost, NASA Concept Study. Advanced Programs Office, Johnson Space Center, Houston, TX, 1989.

[3] AIAA/Industry Team Design Competition, "Request for Proposal: A Self-Unloading Reusable Lunar Lander". 1990-1991.

Chapter 2

Payload and Spacecraft Integration

2.0. Summary

Payload and Spacecraft Integration is responsible for the handling of the mission's payload and the consolidation of all subsystems into a unified spacecraft design. Payload Spacecraft Integration is where the entire design effort comes together. Several systems are addressed here giving rise to topics which are diverse in nature, but all are equally important in describing the final design.

UM-Haul consists of a Lander and an independent Unloader vehicle. The Lander consists of six basic components. These components are a payload bay with ramp, main engines, landing legs, cylindrical liquid Oxygen tanks with hemispherical caps, spherical liquid Hydrogen tanks and modularized equipment bays. These six components were integrated in such a way as to produce a vehicle with the lowest center of gravity possible. A low center of gravity increases stability during landing.

The Unloader is rectangular in shape and is propelled by eight independently driven wheels. This Unloader is capable of carrying a payload of 8500 kg. It has the capability to be left on the lunar surface while the Lander is getting another payload, or to return to orbit with the Lander.

2.1. Candidate Design Generation and Elimination

During the first two months of the design process, many original designs were generated. Each of these possible candidate designs for the Lander and the Unloader were researched and analyzed, exploring their pros and cons, until a final design was developed. The Unloader's final design originated from seven different concepts while the Lander design originated from two basic designs.

2.1.1. Unloader Designs

2.1.1.1. Crane

This design was modeled after Earth type cranes. Cranes have the ability to lift large masses and to move them to different locations. The fact that this design conformed to the design requirements that were set forth at the onset of this design process made it a desirable candidate. However, the crane did pose a problem. This problem is the need for a heavy counterbalance in order to counteract the weight of the payload. With the extreme transportation costs involved in sending payload to the moon, a heavy counterbalance is not very economical. It was therefore decided to eliminate this design from those being considered. Figure 2.1 shows a schematic of the crane design.

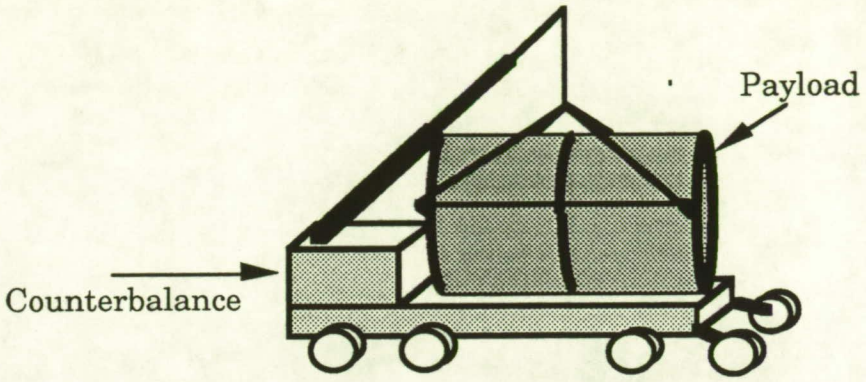

Figure 2.1 - Unloader Proposal: The Crane

2.1.1.2. Conveyor

This design features a conveyor belt which is attached to a movable payload bed. The rear of the bed lowers to the lunar surface by means of hydraulic lifters. When the surface is reached, the conveyor belt moves the payload slowly down the bed until it reaches the lunar surface. At this point, the unloader moves away and gently lowers the payload onto the surface. This design met all of the design requirements, but did have some problems. One problem is that the conveyor belt consists of many moving parts. Because of the abrasive nature of the lunar dust, this multitude of moving parts is more prone to degradation and eventual failure. The stability of a cylindrical payload on the payload bed was also questionable. Therefore, due to the instability of the conveyor design, it was eliminated. Figure 2.2 shows a schematic of the conveyor.

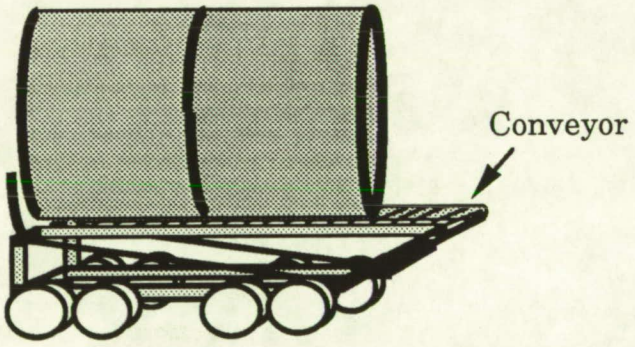

Figure 2.2 - Unloader Proposal: The Conveyor

2.1.1.3. Forklift

This design resembles Earth type forklifts. Forklifts are known for their ability to lift heavy loads and to transport them to desired locations. This feature made the forklift a reasonable design candidate. This design also fulfilled the design requirements. However, like the crane design, a heavy counterbalance would be

necessary to prevent the forklift from tipping while carrying the payload. This design also requires a large motors and heavy, stable structural arms on which the payload rests. The need for a counterbalance and a heavy structure increases the mass of the system, and therefore increases transportation costs. Due to this increase in cost and weight, it was decided to terminate the consideration of this design. Figure 2.3 shows a schematic of the forklift design.

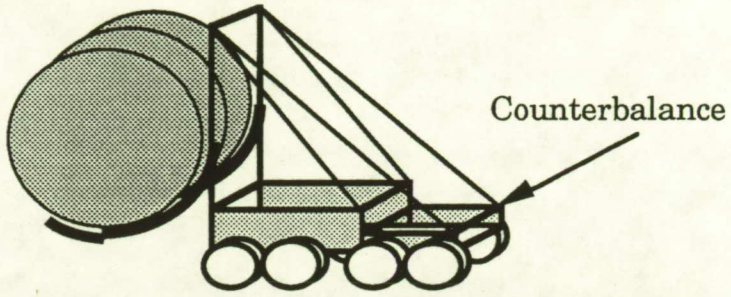

Figure 2.3 - Unloader Proposal: The Forklift

2.1.1.4. Grasping Carrier

This unloader design is bottomless and cylindrical in shape. The unloader drives over the payload and arm-like graspers, which are driven by independent motors, raise the payload off the bed of the lander. This vehicle then drives away to the desired destination. Upon reaching this location, the graspers lower the payload to the lunar surface. This design restricts variations in payload size to cylindrical shapes. One type of cylindrical payload that the grasping carrier carries is a Logistics Module. The Logistics Module is 4.6 m in diameter, and would therefore require the grasping carrier to be from 6 to 7.6 m in height. This raises the center of mass of the entire lander/unloader configuration, which incurs stability problems upon landing. The grasping carrier must also be loaded from underneath, which makes payload transfer in Low Lunar Orbit (LLO) difficult. Another disadvantage of this design is the large stresses incurred on the grasping arms. Due to the nature of these problems, this design candidate was eliminated. Figure 2.4 show a schematic of the grasping carrier unloader design.

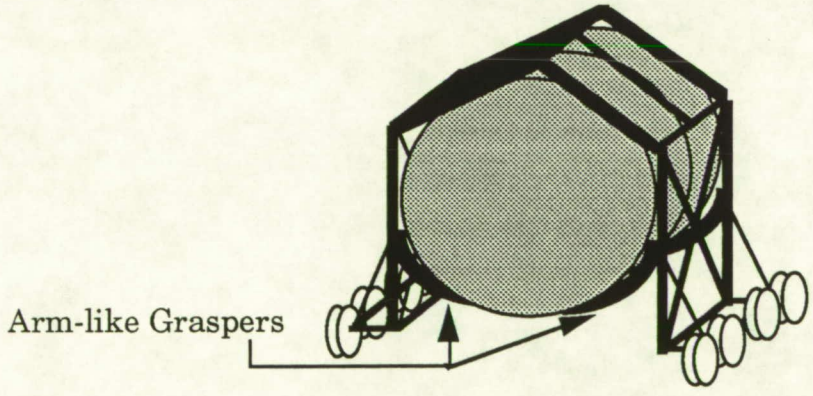

Figure 2.4 - Unloader Proposal: The Grasping Carrier

2.1.1.5. "U-ey"

This design has a "U" shaped structure that is open on the top, the bottom, and at the front of the vehicle. U-ey drives up to the payload and then by using elevator type latches, secures and lifts the payload off the bed of the lander.
When the desired destination is reached, the payload is lowered to the lunar surface and the U-ey backs away. While this design did fulfill the design requirements, there were some inherent problems. The size and weight of this vehicle was greater than that of the other designs. There was also concern about its structural stability when it moved over uneven terrain. Torsional stresses can develop which would twist the frame of U-ey. This problem could be alleviated with a modification of the structure. However, this modification would add more weight to the already heavy structure. For these reasons, further consideration of this design was abandoned. Figure 2.6 shows a schematic of the U-ey unloader design.

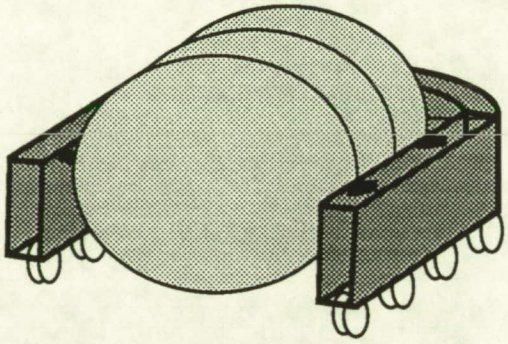

Figure 2.6 - Unloader Proposal: The "U-ey"

2.1.1.6. "O-ey"

O-ey is a cross between the structure of the grasping carrier and the payload handling capabilities of U-ey. The structure surrounds the payload on the top and sides. The two structural arcs can lower so that a payload can be lowered into the payload bay. With the same latch mechanisms as U-ey, the payload is secured and the two arcs then raise to a vertical position where they lock in place. O-ey unloads the payload just as U-ey does. However, O-ey had a few inherent problems in the design. When the arcs are lowered and raised, the entire structure is subjected to large stresses which would require massive joints in key areas. This structure is also very large and heavy, which incurs large transportation costs. Due to the risk that the structure would not be able to handle the stresses incurred upon it and due to the immense size of this unloader design,the O-ey was removed from the list of possible unloaders. Figure 2.7 shows a schematic of the O-ey unloader design.

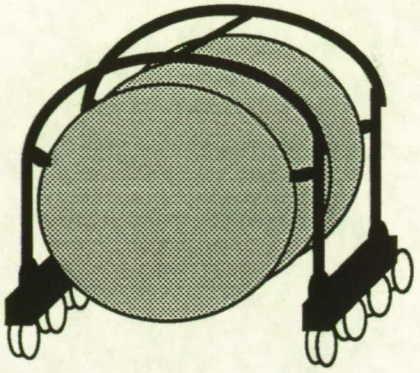

Figure 2.7 - Unloader Proposal: The "O-ey"

2.1.1.7. "Pallet" Carrier

This design is a car-like vehicle that is equipped with an adjustable bed. The bed can be raised and lowered using mechanical lifters. The payload is situated on a pallet which can stand on its own legs. The carrier drives under the pallet, raises it to attain proper ground clearance, and then drives to the desired destination. When this location is reached, the pallet is lowered until it's legs are in contact with the ground. The carrier then drives away from under the payload. This design met all of the design requirements, but the need for a pallet for every payload was an undesirable feature. The transportation and manufacturing costs that are involved in using these pallets was considered unnecessary. Hence, it was felt that further consideration of this design was not warranted. Figure 2.5 shows a schematic of the pallet carrier unloader design.

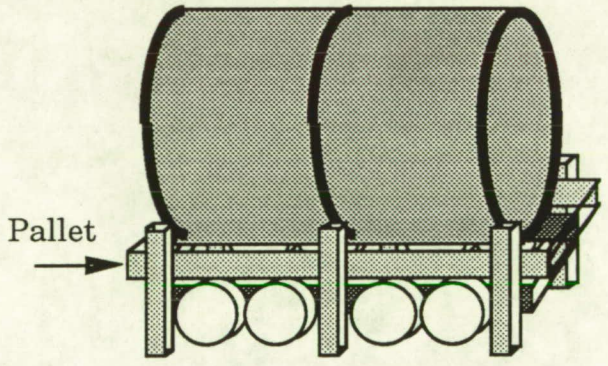

Figure 2.5 - Unloader Proposal: The "Pallet" Carrier

2.2.1.8. Module Carrier

The module carrier is the unloader design chosen for UM-Haul. It is similar to the pallet carrier concept, but it does not use a heavy pallet. Instead, the Logistics Module has four deployable legs bolted to it, which serve the same function as the pallet, but fit in the space at the ends of a logistics module as to not increase the effective payload size. The module carrier has the benefits of being a light steerable unloader with complete

redundancy and minimum complexity. Figure 2.8 shows the UM-Haul in its two configurations - raised (with payload) and lowered (without payload) .

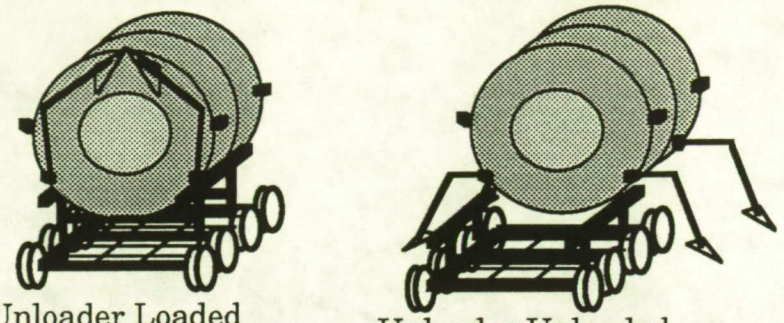

Figure 2.8 - Final UM-Haul Unloader Design

2.1.2. Lander Designs

2.1.2.1. Integrated Lander/Unloader

One of the design proposals for the lander was to integrate the lander and the unloader into one vehicle. This integrated vehicle comprises features of U-ey and that of a low center of gravity lander. The payload is situated in the payload bay which is comparable to that of U-ey. This vehicle lands on the lunar surface with the payload, lowers it to the surface and then moves away. The vehicle then returns to LLO for another payload. The advantage of the integrated lander/unloader system is that it removes the added mass of a separate unloader. However, there are several concerns regarding this design, the most prominent one is that this design does not fulfill one of the design requirements set forth for this project. Since this vehicle incorporates the lander and the unloader into a unified spacecraft, the requirement that the unloader must be able to remain on the lunar surface while the Lander secures another payload in LLO could not be met. For this reason, this design was rejected as a possible design candidate. Figure 2.9 shows a schematic of the integrated lander/unloader.

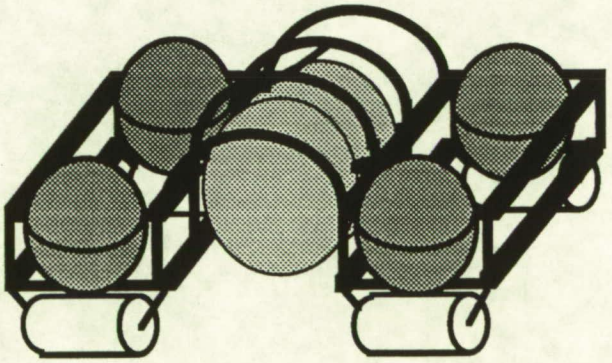

Figure 2.9 - Integrated Lander/Unloader Proposal

2.1.2.2. Centralized Engines

The engines of this design are located as close to the central vertical axis of the lander as possible. The main reason for this is to allow the lander to have maximum resilience in an engine failure scenario (i.e. the engines will gimbal a minimum amount to maintain the thrust vector through the center of mass). Some other benefits of this design include the need for less propellant piping and maximum clearance for the payload from the engines and the lunar surface. The disadvantage to this design is that the payload must be located above the engines, which causes the center of gravity to be high. A high center of gravity requires an extensive leg network in order for the lander to remain stable through the landing process. This design also requires a very long ramp or a very steep ramp. A very long ramp is massive, costly, and hard to store when not deployed. A very steep ramp makes it difficult for the Unloader to get on and off of the lander. These two disadvantages led to further research and conceptual designs. A schematic of a lander design with centralized engines is given in Figure 2.10.

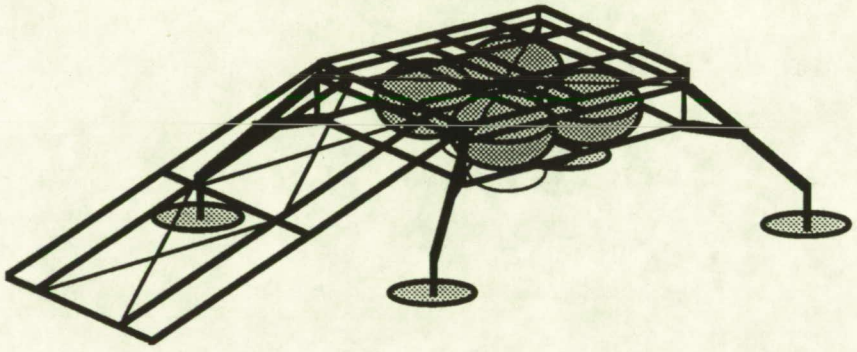

Figure 2.10 - Lander Proposal: Centralized Engines Lander

2.1.2.3. Separated Engines - Payload on Bottom

To alleviate the centralized engine problems, the main engines are separated into two clusters with the payload in between them underneath the lander structure. This dramatically lowers the center of gravity, which correspondingly stabilizes the lander during the landing cycle. Two engines are placed on each side of the payload to allow the mission to be completed for any single engine failure and all but one double engine failure. The disadvantages to this configuration are the difficulty in rendezvous with the OTV, as well as the risk to the payload during lunar touchdown. Figure 2.11 shows a schematic of the lander design with separated engines.

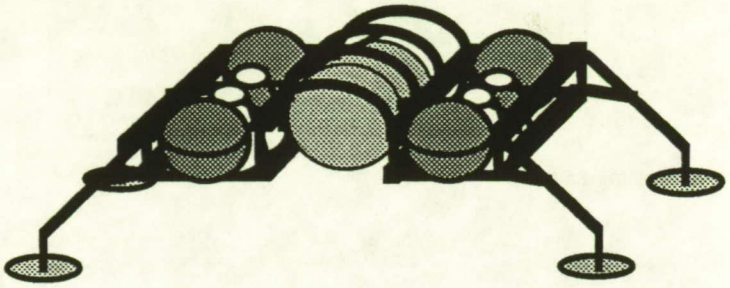

Figure 2.11 - Lander Proposal: Separated Engines Lander

2.1.2.4. Separated Engines - Payload on Top

This is the design chosen for project UM-Haul. It is identical to the separated design mentioned above except the payload is located on top of a protected lander bed. This protects the payload is from dust kickup and unexpected obstructions. It has a very low center of gravity, short unloading ramp length requirement and a compacted integrated system of high flexibility and redundancy. This design requires an Unloader (consistent with the requirements). The Unloader is shown driving off the payload bed of the UM-Haul lander in Figure 2.12.

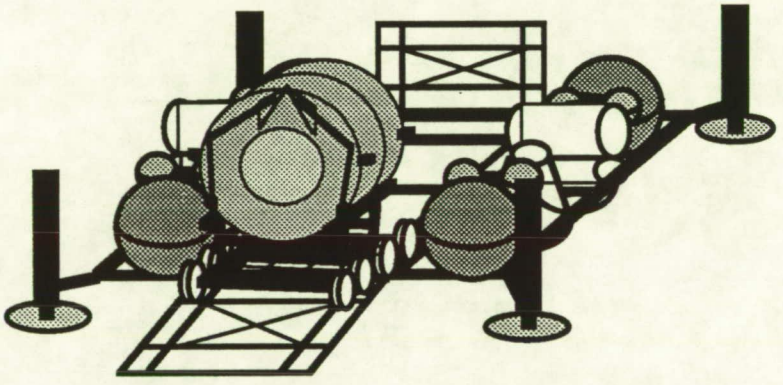

Figure 2.12 - Final UM-Haul Lander Design

2.2. Integration of Finalized Lander/Unloader Design

2.2.1. Integration of the Unloader

The Unloader consists of several components which are integrated to obtain maximum performance. Maintaining the center of mass at the center of the Unloader along with individual subsystem constraints dictated the location of the various components. The rational for each component's location on the Unloader is as follows.

2.2.1.1. Wheels

Eight wheels are located at the extremes of the chassis to provide clearance when traversing the ramp and when moving over uneven terrain. There is space between each of the wheels so that any debris picked up will not become lodged between the wheels. The wheels are also located in the shadow of the payload to give a chassis of minimum width.

2.2.1.2. Solar Array Panels

The two redundant solar array panels are located over the midsection of the Unloader, which protects the central electronics. In addition, they are far away from the NaS batteries and are fully exposed to sunlight when the payload has been unloaded.

2.2.1.3. NaS Batteries

The NaS batteries are located in two rectangular banks, one at either end of the Unloader. They are located to give maximum distance from the other components i.e. the electronics at the center of the Unloader and the cameras and antennas at the far ends. This separation distance is needed to thermally isolate the high temperature NaS batteries from the electronic components.

2.2.1.4. Power radiators

Two power radiators are suspended beneath the battery boxes on the Unloader with a total surface area of 1.25 m^2. They are placed below the Unloader to minimize sunlight exposure and to be clear of other components.

2.2.1.5. Power Regulators

The power regulators and controllers are located in a box underneath the solar panels near the central axis of the Unloader.

2.2.1.6. Computers and Transmitters

These components are all located under the solar array panel so as to be close to the solar power source, protected by the panel, and close to the center of mass of the Unloader.

2.2.1.7. High Gain Antenna

Two high gain antennas are located between the cameras at the front and rear of the chassis. This allows them to point in any direction on a bi-axis gimbal mount. They protrude from the vehicle so that the payload does not shadow them and also

so that there is no interference with any of the other components. They are also angled upwards to maintain ground clearance when the Unloader is on an inclined surface.

2.2.1.8. Low Gain Antenna

Two low gain antennas are located on the Unloader, one on each end. This allows a full sphere of coverage in order to be in constant communication with the Earth and the Lander. They are positioned at the edges to avoid interference with the high gain antenna.

2.2.1.9. Cameras

Four identical cameras are located at the front and rear of the chassis to minimize Unloader obstruction in the cameras' field of view. In addition the two cameras on each side are separated by 0.5 m for stereoscopic vision for the obstacle avoidance system.

2.2.1.10. Payload

The standard Logistics Module payload is located symmetrically on the Unloader far enough above the ground so that it will not come into contact with any surface features, the wheels or any other Unloader components.

2.2.1.11. Deployable Payload Support Legs

The four Logistics Module deployable payload legs are located on both ends of the Logistics Module. The deployment of the legs is a two step process. First, a radio controlled pyro device unlatches the legs from the stowed position. Then a spring unfolds each leg and locks it into it's final deployed position.

2.2.1.12. Unloader/Payload Interface

The payload (a Logistics Module) is situated on two support rails that are attached to the Unloader. On this rail are three rocker arms that support the payload at its support rings. A trunnion, located at the base of the Logistics Module, fits snugly into a cylindrical hardlock that is elevated above the center of the Unloader. This adds stability to the payload when the Unloader traverses a sloped surface.

Table 2.1 gives a mass breakdown of all of the aforementioned Unloader subsystems. Figure 2.13 shows a schematic of the integrated Unloader.

Table 2.2 - Unloader Mass Breakdown

SUBSYSTEM	WEIGHT (kg)	DESIGN/DEVEL ($M)	PRODUCTION ($M)
STRUCTURES	**908**	**15**	**7**
truss	448		
wheels	320		
suspension	140		
GN&C	**76.2**	**30**	**15**
antenna	11		
computers	6.4		
gyro compass	2		
accelerometers	2.6		
cameras	8		
wheel odometers	2		
receiver/trans.	44.2		
POWER	**425**	**20**	**7.4**
solar array	12		
solar shield	15		
batteries	315		
power dist.	40		
radiators/piping	43		
MOTORS	**70**	**5**	**0.6**
drive	32		
lifting	16		
turning	22		
TOTAL	**1479.2**	**70**	**30**

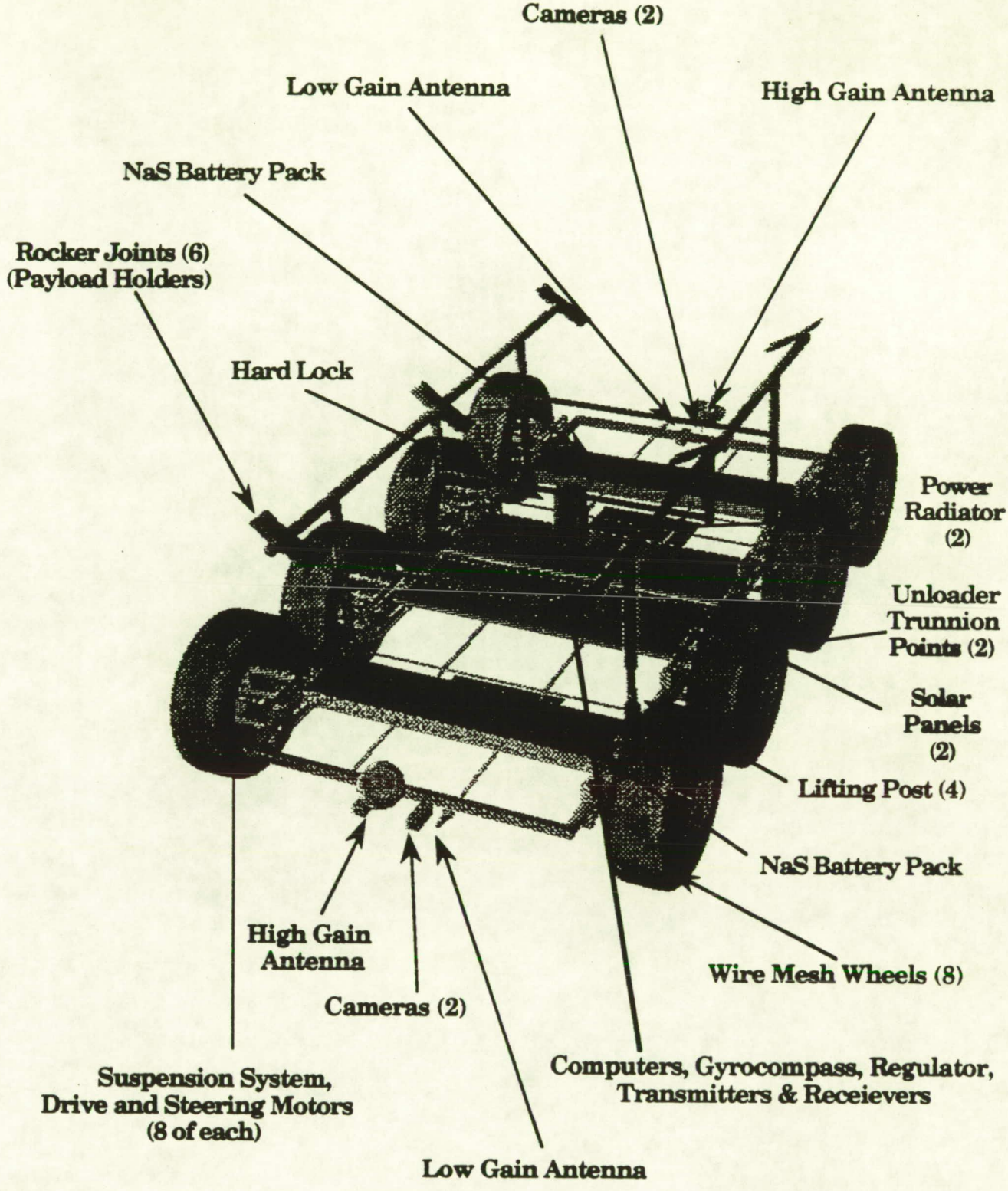

Figure 2.13 - Integrated Unloader Picture(CAD)

2.2.2. Integration of the Lander

The integration of the Lander was driven by propulsion constraints coupled with the desire to keep the center of gravity as low as possible. The desire to have the Lander as resilient as possible in an engine failure scenario also influenced much of the design. Finally, the smaller subsystems were integrated into the remaining places on the Lander with the basic desire to minimize the center of gravity and the necessary cable and propellent line lengths.

2.2.2.1. Engines

Two engines are positioned on each side of the Lander. Each set of engines are close enough to each other to allow for minimum gimbal angle in a worst case engine failure scenario, but the distance between each set of engines is also enough to allow for the maximum gimbal angle to be attained. The engines protrude 0.25 m below the Lander bed to prevent structural heating but are able to be retracted when the Lander lowers during the unloading sequence.

2.2.2.2. Liquid Oxygen (LOX) Tanks

The four cylindrical liquid Oxygen tanks with spherical ends are located between the engine shrouds, lowered down as far as reasonably possible. The separation of the LOX tanks into two tanks per side allows the center of mass to be lowered a meter on the Lander. In addition the LOX tank positions allow for an almost direct feed to the main engines. Since they are the heaviest part of the Lander, it is desirable to have the strong engine shrouds support this weight especially during main engine burns.

2.2.2.3. Liquid Hydrogen (LH_2) Tanks

The liquid Hydrogen tanks are much larger than the Oxygen tanks but are comparable in weight due to their spherical shape. They are positioned on the outer edges of the Lander because the moments that they induce are minimal, thus requiring less structural weight.

2.2.2.4. Reaction Control System (RCS) Thrusters

The reaction control system's four clusters of five 220 N thrusters are located as far away, horizontally, from the engines to allow for the greatest moment, in case an engine fails. They are located off of the lateral edge of each Hydrogen tank and are extended from the tank by a truss network. In addition, this location will minimize the plume impingement on the Lander legs and footpads.

2.2.2.5. RCS and Fuel Cell Holding Tanks

An Oxygen and Hydrogen holding tank is located between each large liquid Hydrogen tank and its corresponding engine shroud, yielding a total of eight tanks (4 Hydrogen tanks and 4 Oxygen tanks).

2.2.2.6. RCS and Fuel Cell Turbopumps

There are eight small turbopumps, one for each of the gaseous Hydrogen and Oxygen holding tanks. They are located adjacent to the gaseous Hydrogen and Oxygen holding tanks.

2.2.2.7. Fuel Cells

The three fuel cells are each located in the fuel cell bays formed between the two gaseous reaction control system holding tanks. Two fuel cells are located on one side of the Lander and one on the other.

2.2.2.8. Power Regulators

These two regulators are located in the same place as a fourth fuel cell would be located. This location is called the fuel cell bay.

2.2.2.9. Power Radiators

Two 0.5 m^2 power radiators are located on the top side of the Lander bed.

2.2.2.10. Lander/Unloader Interface

When the Unloader is properly positioned on the Lander, two trunnion latch mechanisms are deployed. These latches attach to each side of the Unloader at the trunnion locations. The trunnion latch mechanisms are centrally located and are attached to the outer edge of the chassis. The latch mechanism secures the Unloader during orbital maneuvers and throughout the landing sequence. When the Unloader is ready to leave the Lander, these latch mechanisms retract and free the Unloader.

2.2.2.11. Payload Trunnion Latches

There are four Logistics Module trunnion latches. These are located on a truss structure near the cargo bed and above and between the main engine shrouds and the LH_2 tanks. They are motorized and secure the payload during transport.

2.2.2.12. Unloader Trunnion Latches

Two trunnion points are centrally located on the Unloader, one on each side. A motorized trunnion catcher on each side of the Lander moves out and locks down the Unloader for times of transport. These trunnion points also serve as a power coupling between the Unloader and Lander.

2.2.2.13. Ramps

There is a ramp on both the front and rear sides of the payload bay. Two ramps are employed in case one of them fails.

2.2.2.14. Landing Gear

The landing gear are strategically located on the four Lander chassis corners to create a maximum footprint for stability during landing.

2.2.2.15. Landing Gear Helium Tanks

These tanks were placed on top of the landing gear to minimize helium line lengths.

2.2.2.16. Computers

There are three main computers. All three are located in the fuel cell bay with the power regulators mentioned above.

2.2.2.17. Transmitters and Receivers

There is one redundant Ka-Band transmitter and receiver and one redundant S-Band transmitter and receiver. They are both located in the fuel cell bay.

2.2.2.18. High Gain Antennas

There are two high gain antennas, one at each end of the Lander. They protrude from the ends of the large LOX tanks on the side of the Lander. This allows an unobstructed field of view for the two bi-axis gimbaled antennas.

2.2.2.19. Low Gain Antennas

The two low gain antennas are located in the same orientation as the high gain antennas. These were placed on the ends of the small LOX tanks on the side of the Lander.

2.2.2.20. Star Trackers

There are 3 star trackers on the Lander. Each is oriented along a different axis and located to be as far from Lander structure and engine plume impingements as possible. One is placed on the middle top of one of the large LOX tanks and has an upward field of view. One is placed on the end of the same tank and has a field of view from the side of the Lander. The third star tracker is located on the cargo bed and has a field of view out from the front edge of the Lander.

2.2.2.21. Laser Gyroscopes

Six laser gyros are on the Lander located underneath the small LOX tanks in clusters of three. One gyro is oriented along each axis.

2.2.2.22. Accelerometers

Each box of three accelerometers are symmetrically placed under the small LOX tanks near the gyroscopes. They are placed symmetrically along the middle axis of the Lander for maximum visibility.

Table 2.2 gives a mass breakdown of the Lander subsystems mentioned above. Figure 2.14 shows a schematic of the integrated Lander.

2.3. OTV Interface

The OTV is assumed to be the two stage, General Dynamics design [1]. The OTV is designed to deliver 36,000 kg to LLO and return with 6,800 kg. It uses the Advanced Space Engine with a mixture ratio of 6:1 and an Isp of 485 seconds. Its aerobrake is a six sided geotruss sized to fit the mission requirements. A truss structure connects eight spherical propellant tanks to it, containing over 48,000 kg of usable propellant. A docking ring is attached to the end of the truss. This ring interfaces with a payload pallet/docking port when delivering Logistic Modules to the moon. When the OTV is transporting both the Lander and its payload, the Lander is connected to the OTV with a support truss. See Figure 2.15 for a schematic of the OTV and payload docking.

Table 2.2 - Lander Mass Breakdown

SUBSYSTEM	WEIGHT (kg)	DESIGN/DEV. ($M)	PRODUCTION ($M)
STRUCTURES	**3800**	**239**	**19**
truss/chassis	1445		
landing gear(4)	1373		
ramps(2)	285		
payload latches(4)	80		
docking latches(2)	120		
runners(2)	497		
PROPULSION	**1077**	**527**	**17**
main engines(4)	780		
RCS system(4)	120		
tanks	177		
GN&C	**136.7**	**188**	**59**
antenna(4)	11		
computers(3)	6.9		
star trackers(3)	15		
laser gyroscopes(6)	27.6		
accelerometers(6)	7.8		
laser radar(1)	24.2		
receiver/trans.(2)	44.2		
POWER	**426**	**66**	**16**
fuel cells(3)	204		
power dist.	72		
radiator/piping	150		
MISC.	**100**		
pumps	60		
motors	40		
PROPELLANT	**17274**	**19**	**3**
liquid Oxygen	14827		
liquid Hydrogen	2447		
TOTAL	**22813.7**	**1039**	**114**
TOTAL DRY	**5539.7**		

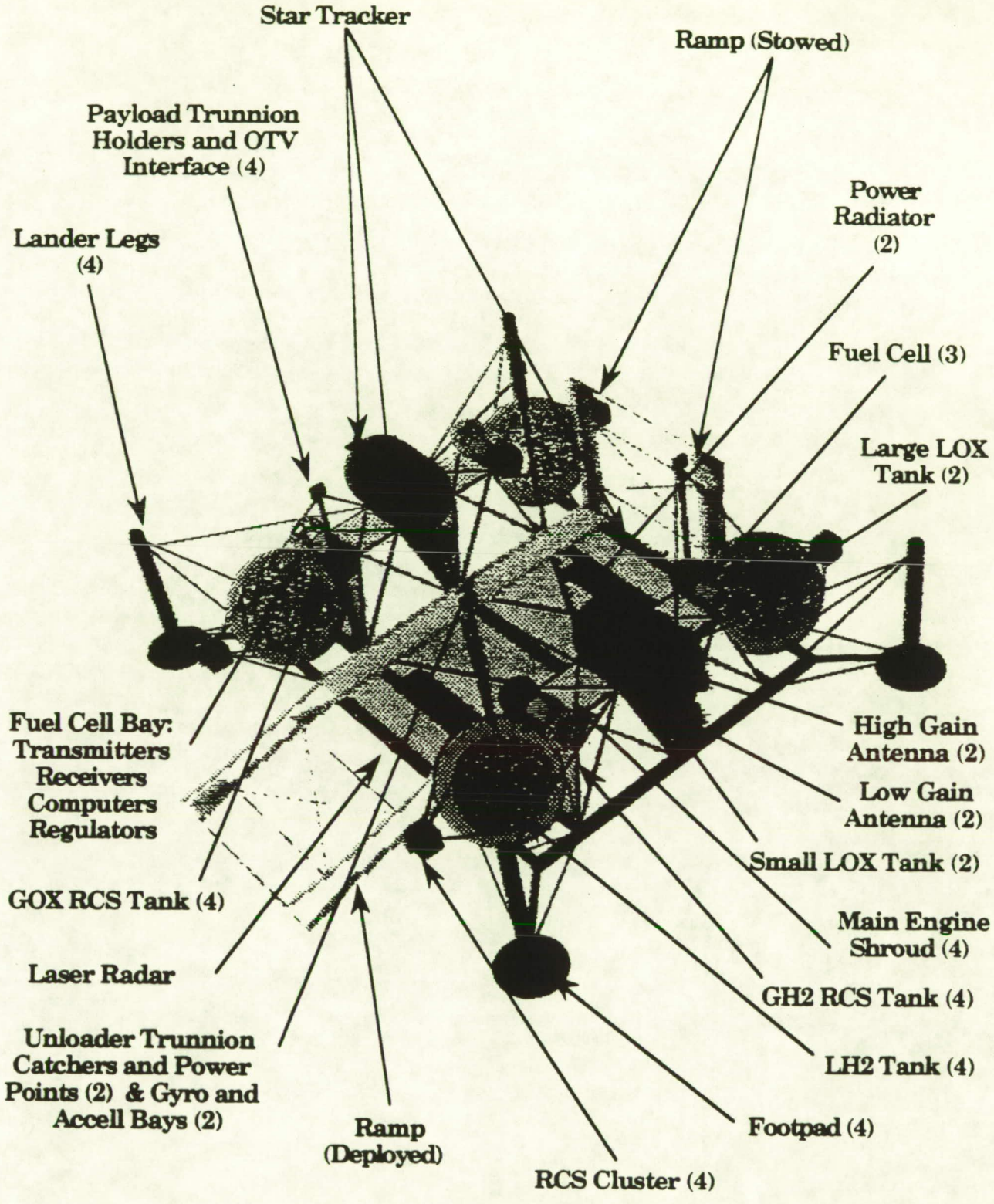

Figure 2.14 - Integrated Lander (CAD)

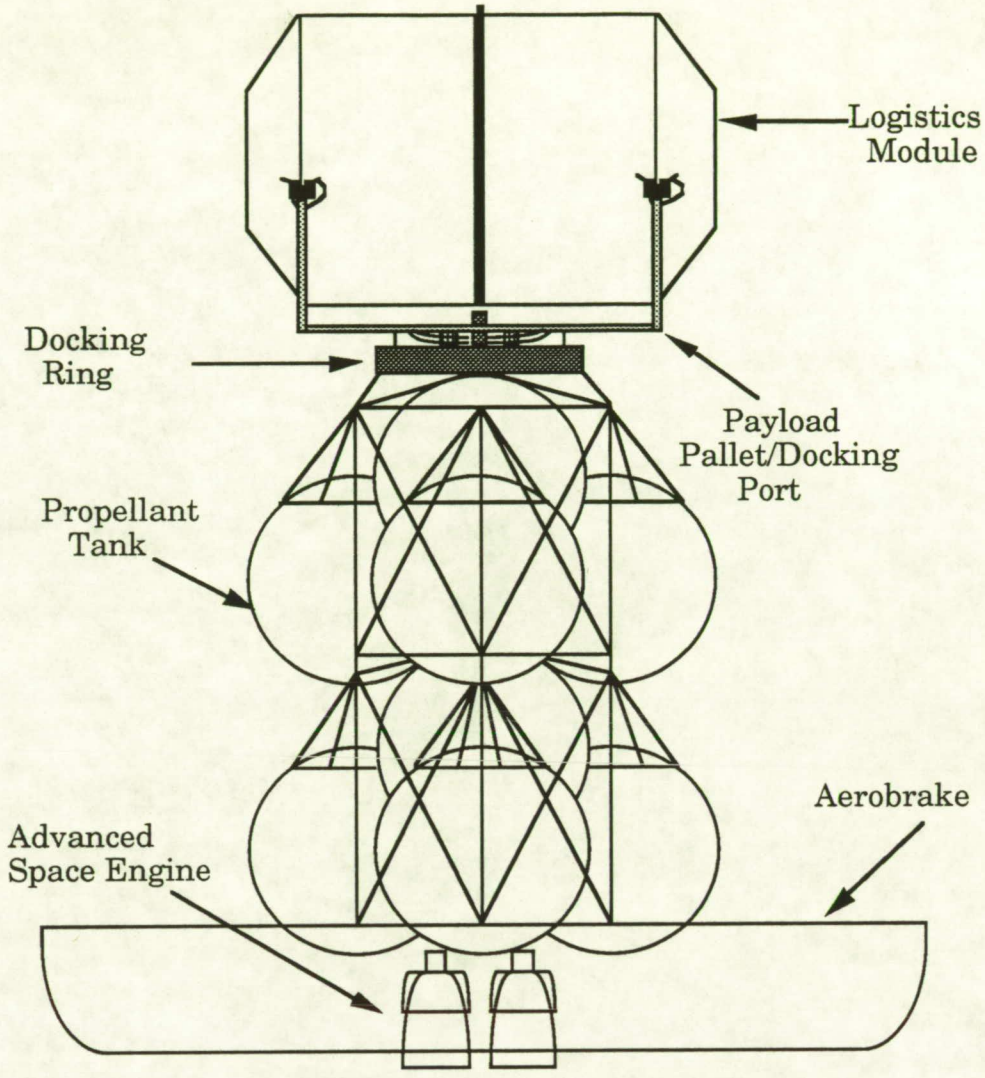

Figure 2.15 - OTV and Payload Docking

2.4. OTV Payload Pallet/Docking Port

The pallet is 6.0 meters long, 6.3 meters wide, and 2.9 meters high. The pallet holds the payload with four Lightweight Longeron Latches (LWLLs), the same as the ones used on the shuttle. The LWLL's are spaced 5.5 m apart along the length of the pallet, and 4.8 m apart along the width of the pallet. The LWLLs are placed on trusswork 2.2 m above the pallet giving a 10 cm clearance between the retracted payload transfer mechanism (PTM) and the payload. The PTM is located in the middle of the pallet and is designed to guide the payload to the Lander after the LWLLs release the payload. The total distance traveled by the PTM to transfer the payload is 40 cm. The pallet also has four docking/fueling ports (D/FP) located on the outside of the pallet at the same height as the LWLLs. From the D/FP run Hydrogen and Oxygen lines. These lines lead to ports that connect to the OTV. Figure 2.16 shows a schematic of the pallet/docking port.

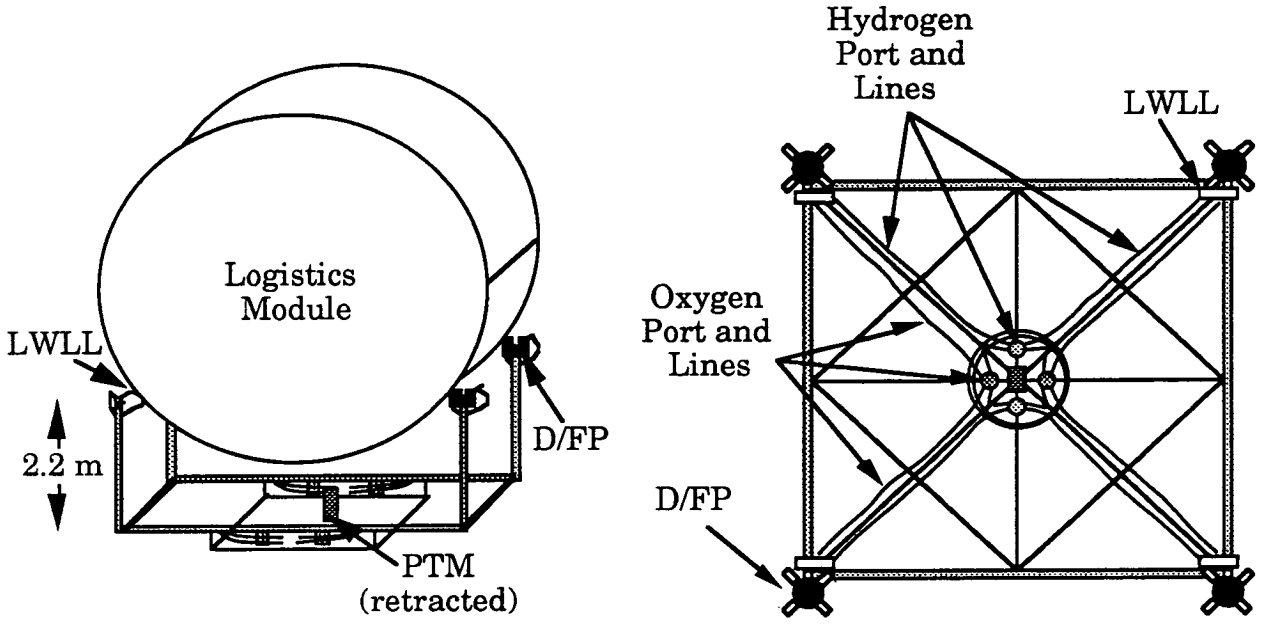

Figure 2.16 - OTV Payload Pallet Docking Port

2.5.1. Lightweight Longeron Latches (LWLL)

The Lightweight Longeron Latches consist of an Aluminum frame and gear box with steel gears. They have a total mass of 20 kg. The latches also have dual AC motors and brakes with a redundant drive differential that can open or close the latch in 30 sec. If only one motor is functional, the latch opens or closes in 60 sec. The LWLLs require a 28 volt DC power source and can operate in a temperature range of -73.3 to 176 degrees Celsius. These latches have a ready-to-latch/ejection arm that can deliver a force of 53 N to help release the payload from the latches. Guides located on the latches, 25 cm in length, ensure that the payload is transferred correctly to the Lander's latches. The Lander's latches do not have the ejection arm feature. This is because the Unloader lifts the payload from the latches. See Figure 2.17 for a schematic of a LWLL.

2.5.2 Docking/Fuel Ports (D/FP)

Each docking/fuel port has four conical alignment guides extending outward at a 45 degree angle, spaced 90 degrees apart. The OTV and the Lander's ports have a mass of 40 kg and 30 kg, respectively. Each port houses a 10 cm diameter Hydrogen cryogenic line and a 5 cm diameter Oxygen line. Figure 2.18 shows a picture of the docking/fuel port. The latching mechanism requires a minimum force of 400 N to mate with the Lander's passive ports. The capture hook then pulls the Lander's docking port until it is in the locked position. Figure 2.19 details the capture hook.

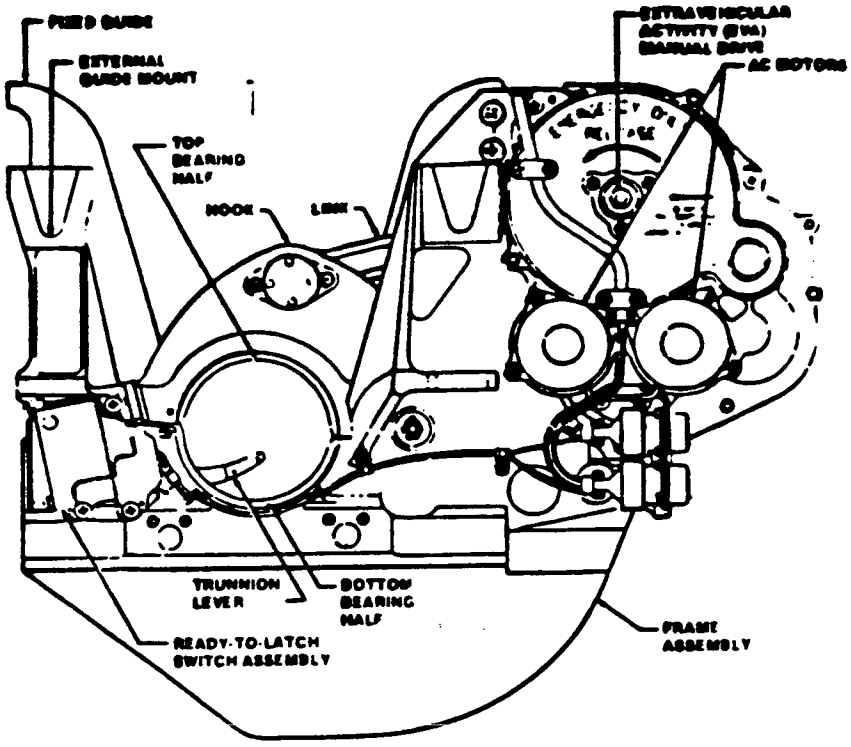

Figure 2.17 - Lightweight Longeron Latch

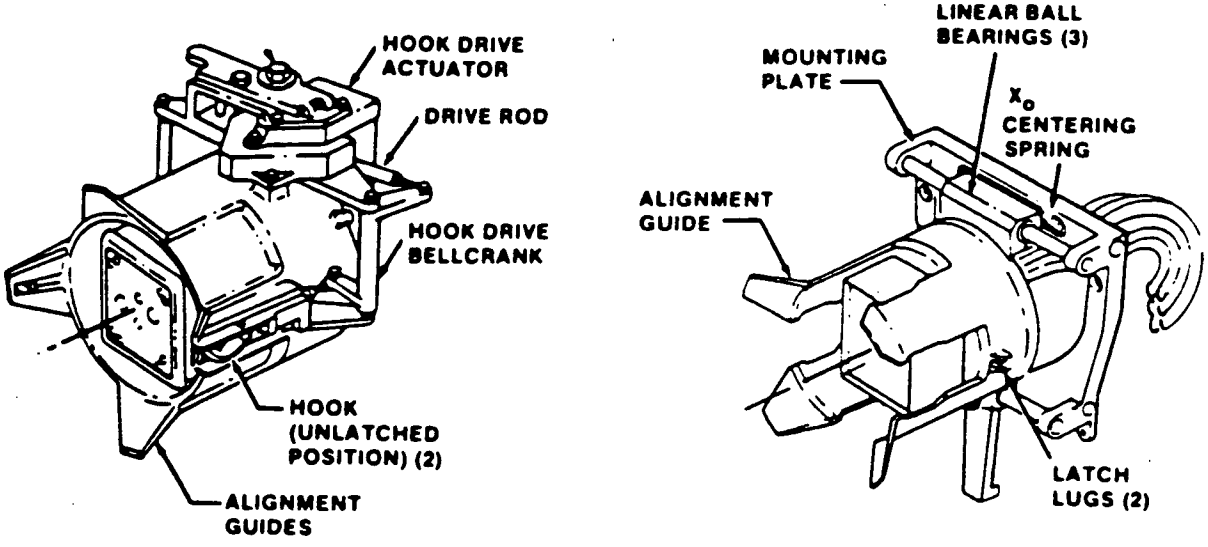

OTV DP/F **Lander DP/F**

Figure 2.18 - Docking/Fuel Ports

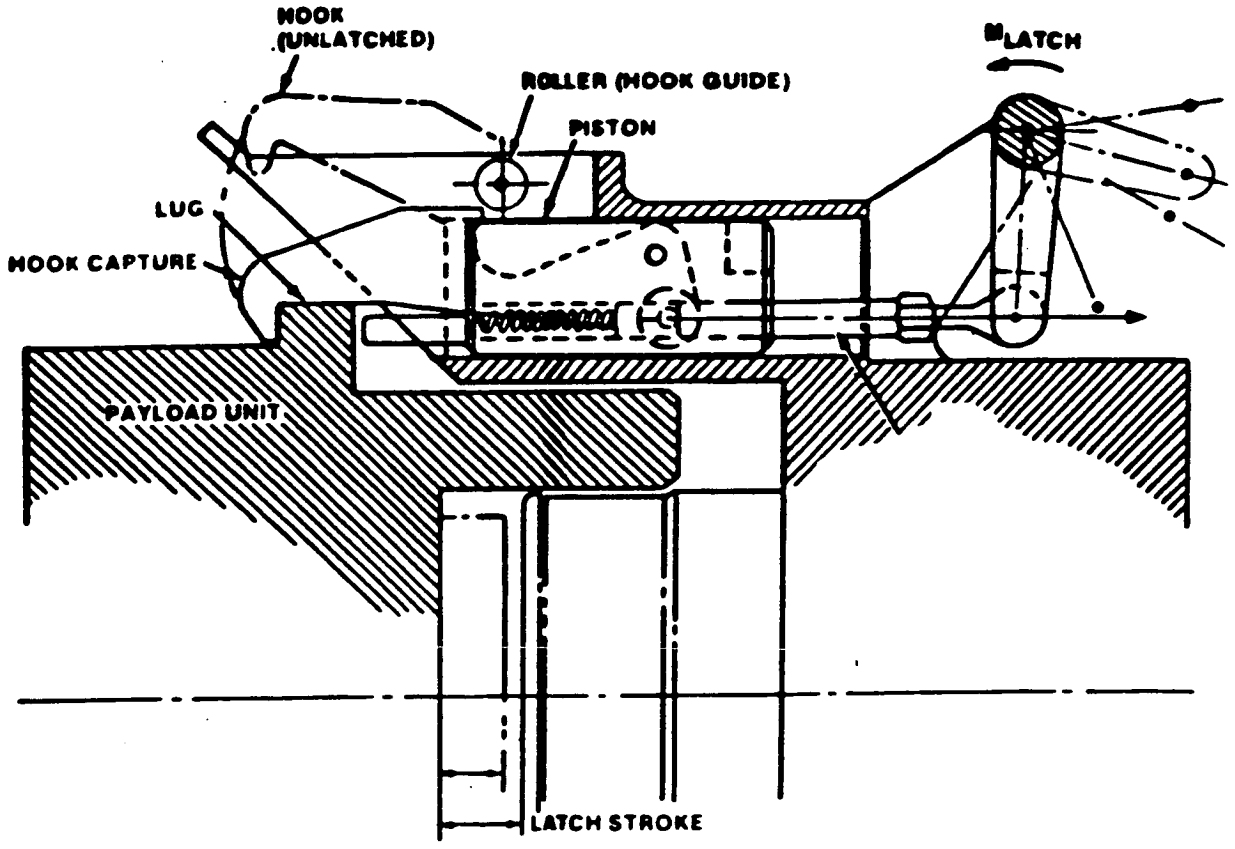

Figure 2.19 - Capture Hook

2.5.3. Payload Restrictions

The Lander and Unloader are capable of carrying other types of payloads to the moon. The three major restrictions on the payload are its size, weight and trunnion locations. If the Unloader is aboard the Lander when the cargo is being transferred to the Lander (in lunar orbit), the maximum size of the payload is 7.4 m in length and 4.6 m in diameter, and has a mass of 7000 kg. If the Unloader is not aboard the Lander, the maximum mass is 8500 kg with the same dimensions. If the payload does not have the required trunnion points or if more than one payload will be loaded at once, then a pallet must be used [see Figure 2.20].

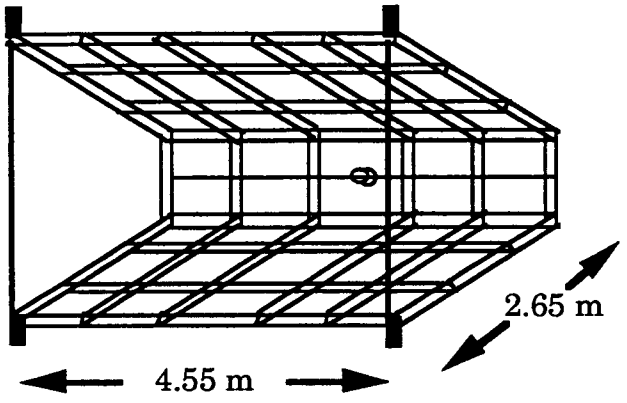

Figure 2.20 - Alternate Payload Pallet

2.5. Alternate Payloads

Payloads other than the Logistics Module can also be transported by the Lander. One alternate payload considered is an inflatable habitat package without its secondary structure. The dimensions of the habitat package is 4.5 m in diameter and 4.87 m in length. This payload could be carried by the Unloader using a pallet. Another payload which employs a pallet is a fluid shipping module [see Figure 2.21]. The module can carry 2,500 kg of liquid fuels. Two such modules could be carried if the Unloader is not on the Lander during descent. The total mass of the two modules is 8,050 kg. The two modules would be transported as shown in Figure 2.22. The last payload considered that employs the use of a pallet is the SP-100 space nuclear reactor. It has a mass of 3,000 kg and has dimensions of 4.5 m in diameter and 6.1 m in length.

Other payloads that the Lander can transport, which do not require a pallet, are various lunar vehicles. One such vehicle is the Mobile Lunar Laboratory (MOLAB) which has dimensions of 7.39 m in length, 3.78 m in width and a mass of 3,658 kg. The only necessary modification to the Lander is to adjust the ramps and payload bay supports to match the width of MOLAB.

2.6. Earth Launch Vehicle

A major consideration in this design was the decision on what earth launching mechanism would be used to transport UM-Haul to Earth orbit. Initially, the research process centered around a heavy launch vehicle which would have the dimensional cargo capacity to bring UM-Haul to earth orbit fully assembled.

Upon further consideration of the mission scenario, it was decided that to expedite the integration of this design into present NASA trends, the Space Shuttle Orbiter Cargo Bay would be utilized. The cargo bay is a cylinder 18.288 m (60 ft) long and 4.572 m (15 ft) in diameter. Three Space Shuttle launches would be required to move the entire system (Lander and Unloader) to Earth orbit in pieces. Once in

LEO, UM-Haul would be reassembled for orbital transfer to LLO. The propellants would be transported to the space station in a smaller launch vehicle after the dry components, for deposit in the main propellant and reaction control holding tanks.

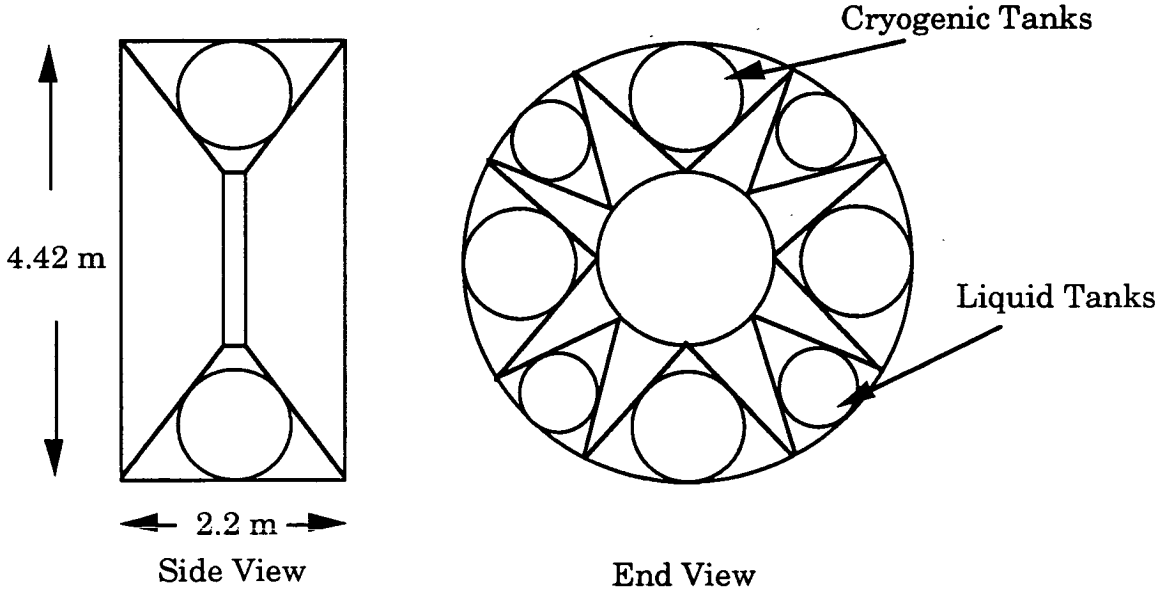

Figure 2.21 - Fluid Shipping Module

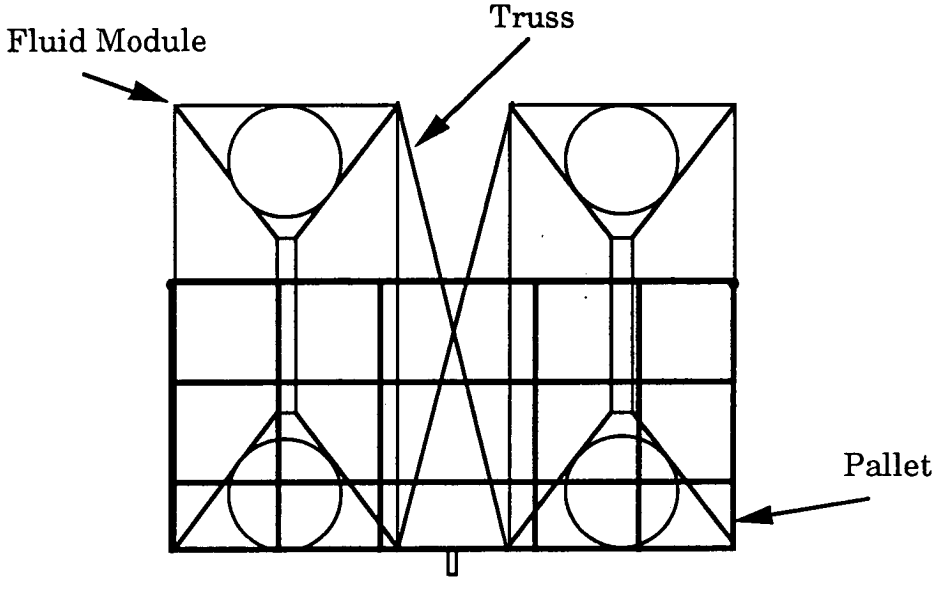

Figure 2.22 - Transport of Two Fluid Shipping Modules

2.7. References

[1]. OTV Concept Definition and Systems Analysis Study Final Report; Volume 2 Book 2; General Dynamics Space Systems Division - December 1986

[2]. "Lunar Base Scenario Cost Estimates"; Lunar Base Study Task 6.1, (Eagle Engineering) October 31, 1988; NASA-CR-172103

[3]. Maintenance and Supply Options; NASA-CR-17062 - (Eagle Engineering) May 1988

[4]. "Lunar Surface Locomotion Concepts"in F.I. Ordwax Ed; Advances in Space Sciences and Technology 34 - Volume 9, New York, John Wiley Publishing1967, pgs. 297-326

[5]. "Lunar Surface Transportation Systems"; Conceptual Design Lunar Base Systems Study Task, (Eagle Engineering) July 7, 1988, NASA-CR-172027

[6]. Space Shuttle System Payload Accommodations; NST 507700 Volume 14, Revision J, Appendix 10

[7] Intersociety energy conversion; Volume 1, 1985 , Pgs. 1.21-1.24 Sp-100

Chapter 3

Structures

3.0. Summary

The structures subsystem includes the structural design of both the Unloader and the Lander. The goal was to create strong, durable, and efficient systems with minimum mass. Static analysis using beam theory was used to predict the performance of the structures under their maximum loads. Reliability and redundancy were strong considerations because both vehicles are required to complete ten mission cycles without major servicing. Both the Unloader and Lander have been further divided into their major sections, which are described in detail below.

The main components of the Unloader structure include supports to secure the cargo, a main chassis, a truss grid, solar array protection and support, wheels, and a suspension and steering system.

The main Lander structures consist of a main platform, shrouds to house the main engines, landing legs, and a retractable ramp to allow deployment of the Unloader. Because the Lander will not be fully assembled on Earth, considerations for assembly in space have been addressed.

An overview of material selected for the main structural beams, fatigue and corrosion factors, and major redundancy features for both vehicles has also been included.

3.1. Unloader Structure

The Unloader was designed using beam theory, therefore it was assumed that all members of the structure undergo small deflections only. These members were also considered to be isentropic, homogeneous materials with constant cross-sectional area. In order to maximize the strength while minimizing the size and mass, the structural members will be hollow and thin walled. The inner to outer radius ratio is .75 m unless otherwise noted.

The loads on the structure were initially approximated at 7,000 kg, the mass of the payload. Since one of the requirements of the Unloader is to have the ability to carry its own mass plus the payload mass, the structural mass had to be iterated and added to the payload mass to give a final maximum loading of 1,438 kg. The Unloader structure is designed to withstand this load. These calculations are shown on an Excel spreadsheet in Appendix A. A picture of the Unloader structure is shown in Figure 3.1. An in depth discussion of the Unloader follows, beginning with a description of the cargo interface and lifting mechanisms.

3.1.1. Cargo Interface and Lifting Mechanisms

The cargo interface and lifting mechanisms of the Unloader include the rocker joints, the support rails, the threaded posts, the support rail posts, the hard lock

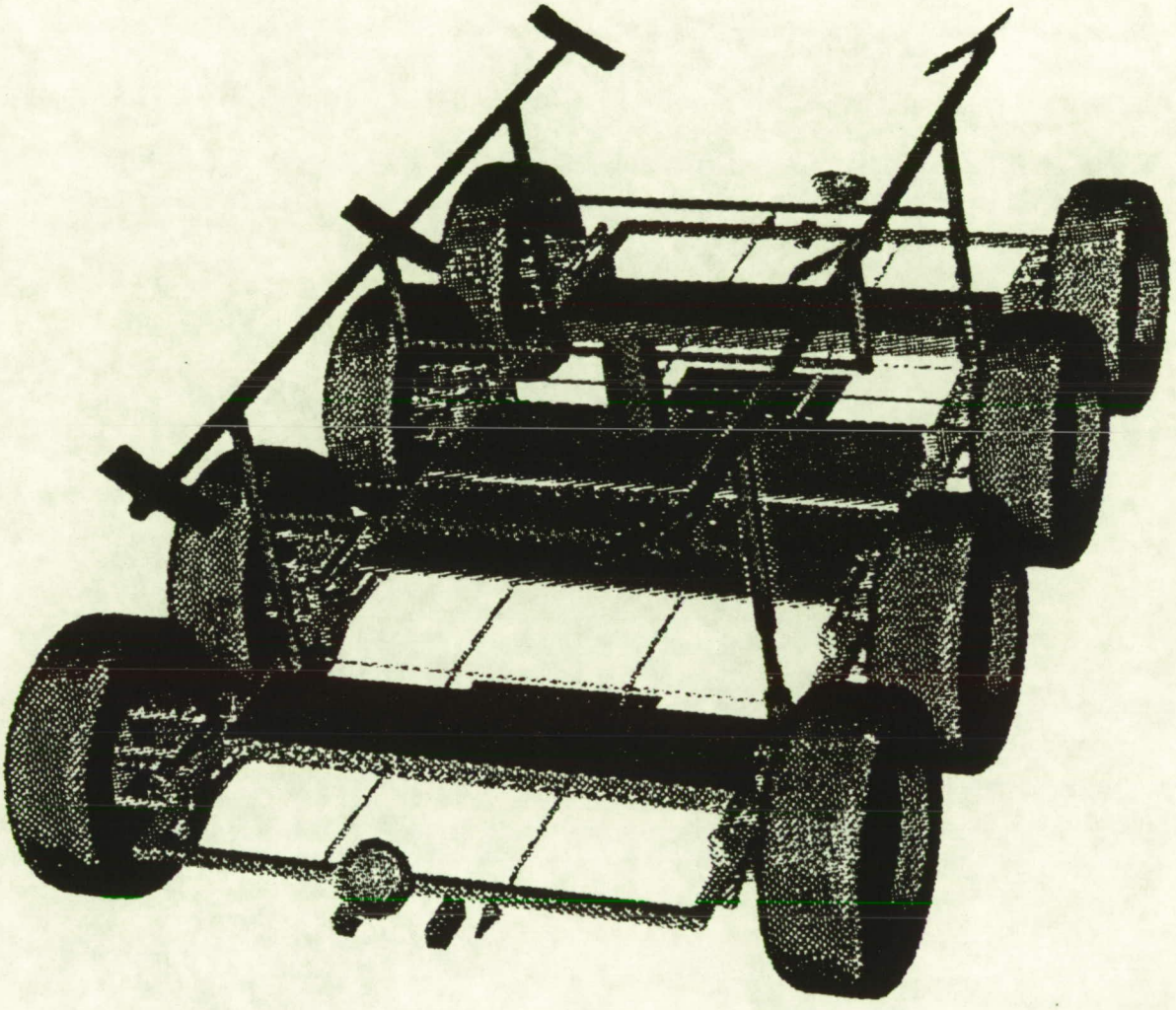

Figure 3.1 - The Unloader

supports, and the cross beams. A detailed description of each is given in the following paragraphs.

3.1.2.1. Rocker Joints

The Logistics Module has three bulkheads located on it, one at each end, and one in the center. These bulkheads are designed to support their own weight, and therefore, they are used to support the payload on the Unloader system. This is achieved by using a series of curved plates of arc length of 0.5 meters, called rocker joints. This value of 0.5 m was decided upon because of the large circumference of the Logistics Module (28.7 m), and the desire to match its curvature. The curved plates function to cradle the Module, preventing lateral movement. Use of beam theory shows that the thickness of the rocker joint, with a safety factor of 3.0, must be 0.031 m. The curved plate is mounted on a slightly rotatable joint, hence its name, "rocker joint". This small rotational play allows for slight changes in the curved surface of the Module. This is primarily for the case when another curved surface other than the Logistics Module is carried, or one that is of not the exact curvature. The width of the rocker joint, 0.25 m, allows for ease of "finding" the bulkhead, since the rocker joint is twice as wide as the bulkhead. Figure 3.2 shows a schematic of the rocker joint.

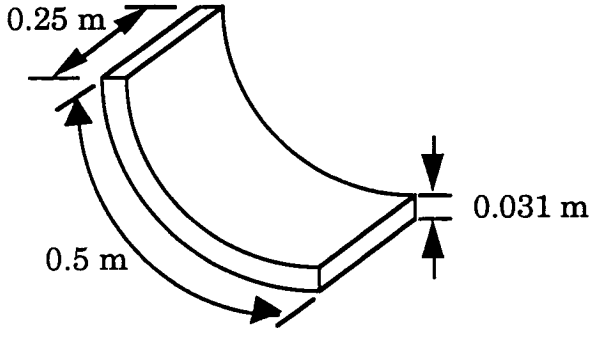

Figure 3.2 - Rocker Joint

3.1.2.2. Support Rails

The next piece of the cargo interface is the support rails. The support rails are two beams which run along the length of the Logistics Module. They are designed to carry the loads from the rocker joints and transmit them to the lifting mechanism. The support rails are designed to resist transverse loads and shears. The rails are 5.8 m in length (the length between the outer bulkheads on the Logistics Module), have on outer radius of 0.043 m, and an inner radius of 0.032 m. Figure 3.3 shows a schematic of one of the support rails.

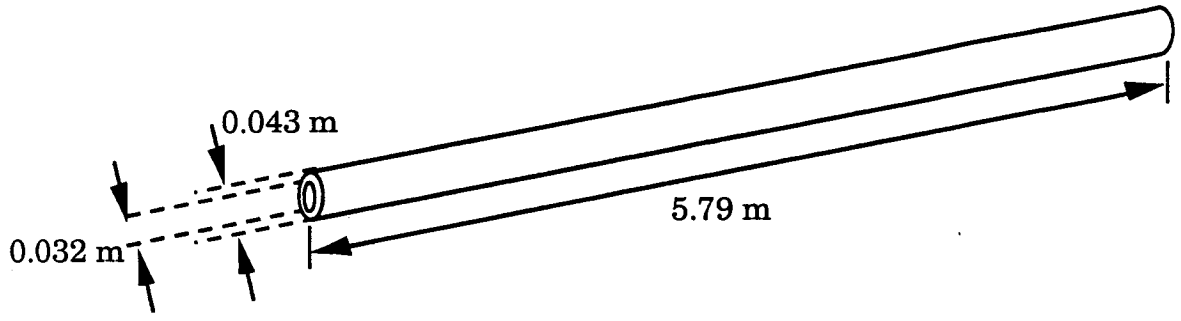

Figure 3.3 - Support Rail

3.1.2.3. Threaded Posts

The threaded posts are rotated by a motor, and act to lift the support rail poles (thereby lifting the support rails, the rocker joints, and the cargo). These posts experience a nominal axial load. In cases where the Unloader is tipped or on an incline, the posts must be able to withstand transverse loads as well. The maximum load was calculated both axially and transversely, and compared to find the limiting case, which was found to be the transverse or cantilevered case. With this specification defined, and the further specification of a 0.6 m travel distance, the threaded post is determined to have an outer radius of 0.0399 m, an inner radius of 0.02 m, and a length of 0.6 m.

3.1.2.4. Support Rail Posts

The support rail post is threaded on the inside, and houses the threaded post. When the threaded post rotates, the support rail post either raises or lowers, as applicable. It is designed for both axial and transverse loads, but as above, the transverse load is the limiting case. The length of the support rail post is 0.95 m. Since in many industrial cases (dies, lifts, etc...) threads are used to lift enormous loads, the reliability of the threads against the loads is not in question. Beam theory shows that the inner diameter of the support rails must be at least 0.025 m, but since the support rail post must house the outer diameter of the threaded post (0.0399 m), this sets the inner diameter. Using the 0.75 inner to outer diameter ratio, [see the remarks in the summary above], the outer diameter is found to be 0.053 m. The threaded post integrated with the support rail post is shown in figure 3.4.

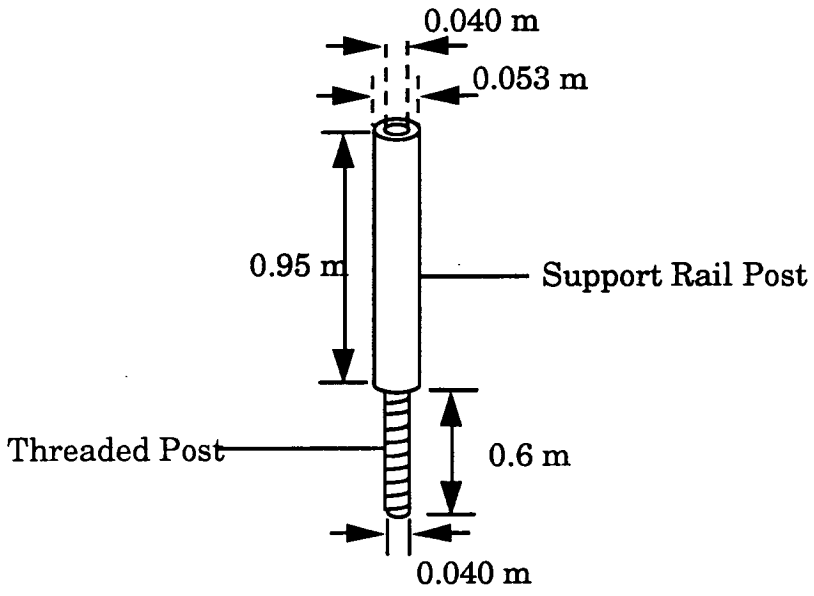

Figure 3.4 - Threaded Post and Support Rail Post

3.1.2.5. Hard Lock and Supports

The hard lock is used to physically restrain the Logistics Module. It is supported by several beams arranged on the support rail. These beams are rods with outer radii of 0.034 m and inner radii of 0.026 m. They support both lateral and longitudinal stresses. The two hard lock supports shown in Figure 3.5 are 0.65 m high, joined together by a 3.0 m rod of the same radii.

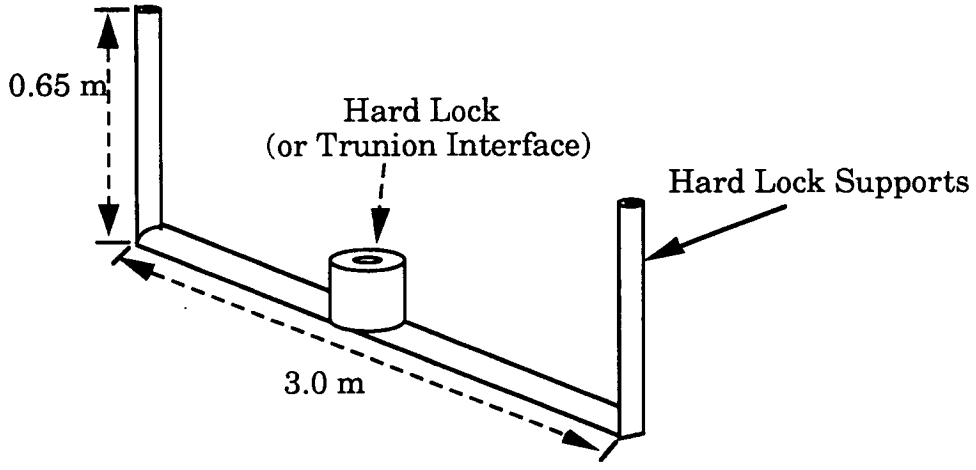

Figure 3.5 - Hard Lock Bars with Hard Lock Shown

3.1.2.6. Cross Beams

The cross beams were initially designed to prevent bending in the threaded posts. The calculations revealed that the cross beam would only have to be 4 mm in diameter! Since this is nearly a wire, we decided to look further into the deflections of the threaded rods and support rail posts. While the deflections in the y-z plane are restrained by the wire-thin beam, any cantilever-type deflections (transverse loads) on the cross beam would mean failure of the beam. Although transverse stresses are not expected, a beam strong enough to resist transverse stresses would allow one side of the support rail post to hold the entire weight of the cargo. Therefore, calculations were performed to size the cross beam in the event that a maximum load is applied to the cross beam. This gives a rod 3 m wide, with an outer radius of 0.057 m and an inner radius of 0.043 m.

3.1.3. Chassis Design and Static Analysis

The analysis of the Unloader continues with the chassis. The chassis is the main support frame upon which all other sub-systems are attached. The chassis is responsible for withstanding all stresses due to these sub-systems, in addition to nominal loads due to operations.

3.1.3.1. Chassis Beams:

The chassis beams run longitudinally (±x direction), and are made of square tubing. Refer to Appendix [A] for the shear and moment diagrams used to size the beams. Beam theory, then, gives an outer wall length (H_{outer} max) of 0.041 m and an inner wall length (H_{inner} max) 0.0306 m. However, to be consistent with the size of the chassis spar [see below] an H_{inner} of 0.0635 m and an H_{outer} of 0.0762 m is used. The chassis beams are 7.0 m in length.

3.1.3.2. Chassis Spar:

The chassis spars function to tie together the chassis beams. The incorporated chassis spars are also designed to resist twisting moments in the Unloader. Rotational beam theory gives, for an arbitrary cross section, H_{outer} of 0.0762 m and H_{inner} of 0.0635 m. Initial calculations showed that in order for one beam to resist all torque, it must be almost 0.1 m in radius! Since this was much too large for the structure, multiple beams were used. Two beams are used in the center of the chassis beams and one at each end to tie the chassis together in a "block eight" shape. The length of the chassis spars is 2.88 m. Figure 3.6 shows a schematic of the chassis beams with the supporting chassis spars.

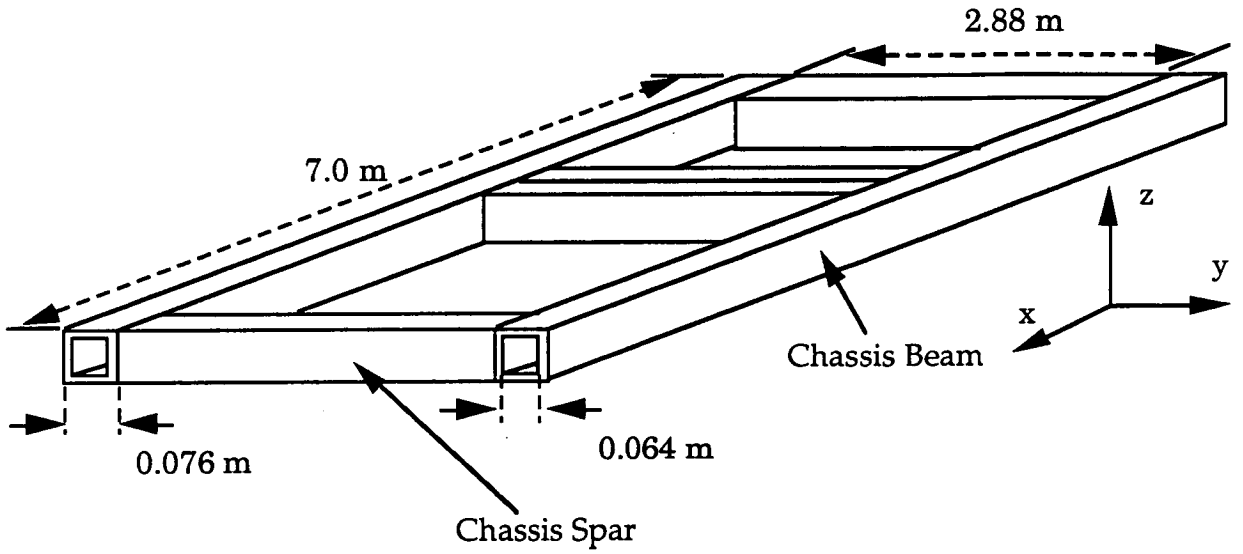

Figure 3.6 - Chassis Beams and Spars

3.1.4. Component Security of other Unloader Subsystems

Components of the other Unloader subsystems (such as power units and controls) will be secured to the structure using a truss grid. This truss grid will be composed of lightweight rods, 0.011 m outer radius and 0.008 m inner radius. The rods are spaced apart at center-lines of approximately 1.0 m, and therefore, grid the open areas in the "block eight" of the chassis. They are rated for approximately 50 Kg per opening in the grid. In areas where either particularly heavy loads or very delicate components are supported, additional truss rods may be added.

3.1.5. Unloader Solar Array Shielding and Support

The solar arrays are supported by the truss grid and must be protected from damage due to the vibration of the Unloader and due to lunar dust. The truss grid, together with the suspension, chassis, and wheels, damps out any vibrations that could damage the solar panels. In order to protect the solar arrays from the lunar dust, they are shielded with a dust cover similar to a window shade. The dust cover is made of a lightweight material that is initially rolled up and connected to a rotary spring. The spring is in its uncompressed position when the dust cover is rolled up. The cover is attached to the Unloader chassis at one end of the solar arrays. A set of thin cords located at either end of the cover traverses over the array to a motor at the other end. When the solar array needs

to be covered, the motor turns, pulling the cords, and thereby the dust cover, over the solar array. The dust cover also has a lip over its leading edge to prevent dust from sliding off of the cover and onto the solar panels. When the panels are to be exposed again, the motor reverses direction and unfurls the cover. To prevent the cover from sliding against the panels and damaging them, it will travel on a track a centimeter above the array, and be taut to prevent sagging in the middle.

3.1.6. Unloader Wheels

The varying loads experienced by the chassis and gridwork while driving over the lunar surface will be transmitted via the wheels and the suspension system. These systems, described below, were selected for their ability to minimize these loads in order to allow the Unloader to efficiently drive over the lunar terrain without disrupting the cargo or the other Unloader subsystems.

3.1.6.1. Tracks vs. Wheels

Initially, the option of using tracks instead of wheels as a means of locomotion for the Unloader was considered. However, it was determined that it was more advantageous to use wheels for the following reasons:

1. The motion resistance/weight ratio of tracks is higher than that of wheels in the lunar soil.

2. The driving forces required for the skid steering of the tracks may exceed by many times those required for normal driving thus leading to excessive weight in the track design.

3. Tracks have poor wear characteristics and a high frequency of breakdown.

3.1.6.2. Wheel Selection

Having eliminated the use of tracks, the remaining options were to use rigid or flexible wheels. Rigid wheels do not deform appreciably under a given load, (for example, a train wheel), while a flexible wheel would show deformation, (like an automobile tire). The flexible wheel was chosen because it has a higher drawbar-pull to weight ratio, which is a measure of the vehicles ability to perform useful work [1]. The flexible wheel candidates considered were the metal-elastic wheel, the cone wheel, and the wire mesh wheel, which was used on the Apollo Lunar Rover. The three wheel candidates are shown in Figure 3.7.

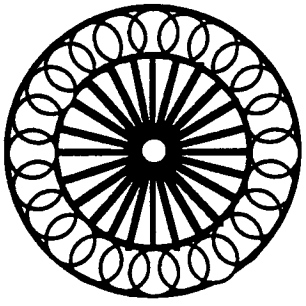

Metal-Elastic Wheel

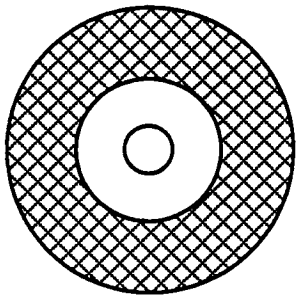

Wire Mesh Wheel

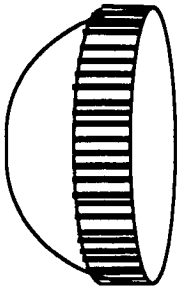

Cone Wheel

Figure 3.7 - Flexible Wheel Candidates

The following design criteria were established in order to make a selection from among the three types of wheels:

1. Size: The wheel had to be narrow enough so that the combined width of the wheels, suspension, and chassis would not exceed the 4.6 m diameter of the Logistics Module. With the chassis being 3.1 m wide, and the suspension system extending 0.5 m out from the chassis, it was determined that the diameter of the wheel could be no larger than 1.5 m to allow for suspension deflection, and the width of the wheel could not be greater than 0.5 m.

2. Mass: Among the wheels that met the size requirement, the least massive would then be selected.

3. Ground contact pressure: The lunar soil can support ground contact pressures between 7 and 10 kPa [2]. Therefore, to allow for a margin of safety, it was desired that each wheel not exceed a ground contact pressure of 7 kPa.

Each wheel was evaluated using the above criteria. The cone wheel was rejected because, for a given contact pressure, it would be larger than the metal-elastic or wire mesh wheels. The remaining two wheels were of comparable size; therefore, it was necessary to evaluate their relative masses.

Since no data was available on the mass of a metal-elastic wheel, it was necessary to estimate it. Using the known dimensions of a smaller metal-elastic wheel [1] and assuming it was made of Aluminum 6061 (in reality, most of it would be composed of spring steel so our mass would be a lower limit), we computed the mass of the wheel and then scaled it to the dimensions of the Apollo Lunar Rover wire mesh wheel (diameter=0.82 m, width=0.23 m) [3]. The estimated metal-elastic wheel mass was 22 kg as compared to the Lunar Rover wire mesh wheel mass of 5.4 kg. Thus, the wire mesh wheel was selected due to its lower mass.

3.1.6.3. Number of Wheels

The next step in the design of the Unloader was to determine the number of wheels the vehicle should have. Six wheels gave a ground contact pressure that was slightly over 7 kPa. Eight wheels, however, gave a contact pressure of about 6 kPa. A six-wheeled vehicle would be lighter and easier to steer, but would also have lower wheel redundancy and experience greater stresses on each wheel. An eight-wheeled vehicle, on the other hand, would have greater wheel redundancy, better performance, and lower wheel stresses, but would be heavier and more difficult to steer. Feeling that the advantages outweighed the disadvantages, it was decided to use an eight-wheel design on the Unloader. Table 3.1 gives the final wire mesh wheel characteristics.

Table 3.1 - Final Wire Mesh Wheel Characteristics

Type	Wire Mesh
Number	8
Diameter	1.5 m
Width	0.5 m
Static Deflection	0.15 m
Contact Area	0.33 m^2
Contact Pressure	6.1 kPa
Sinkage	0.0074 m
Mass per Wheel	40 kg
Total Mass (Eight Wheels)	320 kg

3.1.7. Suspension and Steering

The independent suspension system and steering mechanism that will be used for the Unloader are shown in Figure 3.8. This system is designed to allow the Unloader to traverse any terrain expected to be found in the vicinity of the landing sites without any of the wheels losing contact with the surface. The total distance the wheel can move vertically is 0.78 m. The electric motor is shown as single crosshatching on the drawings. Steering is accomplished with the push/pull rod shown in solid black on the top view and perspective drawings. The rod is driven by a small motor mounted to the chassis. Figure 3.9 shows a side view and an enlargement of the suspension and steering system.

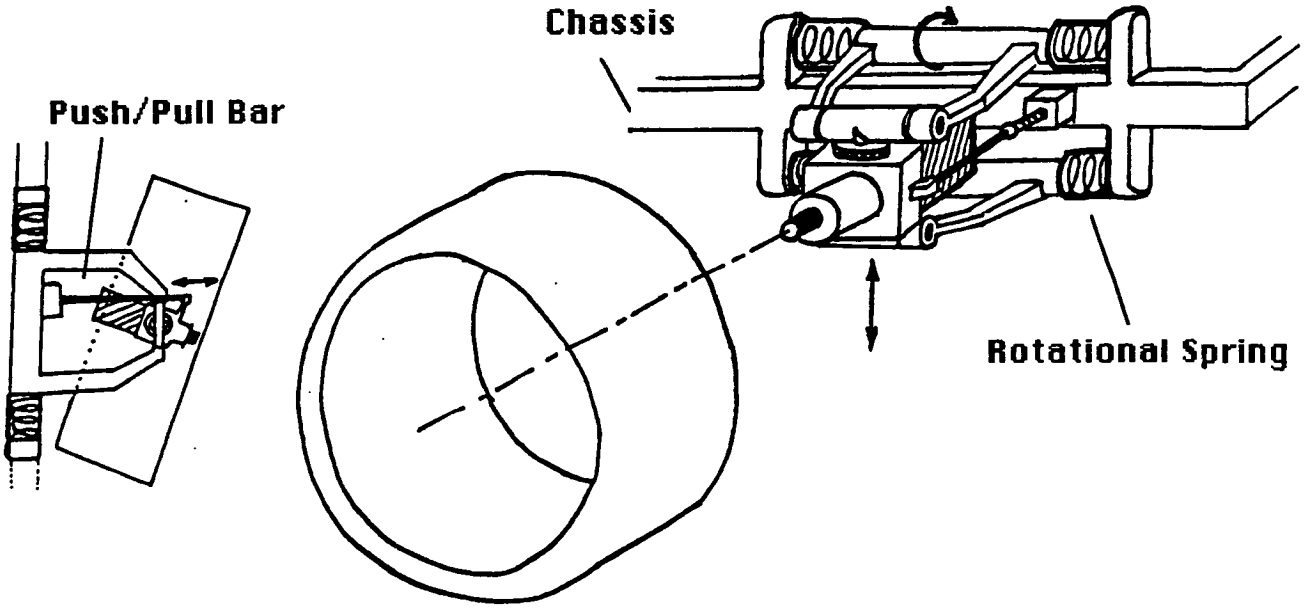

Figure 3.8 - Suspension System and Steering Mechanism (Top View & Perspective)

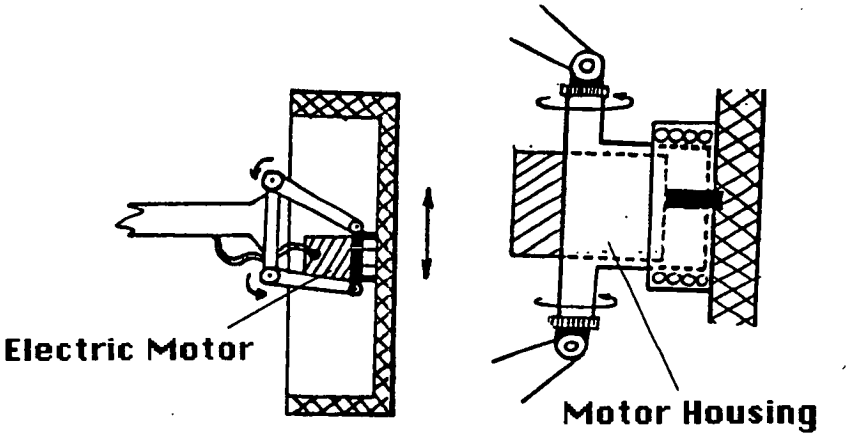

Figure 3.9 - Suspension System (Side View & Enlargement)

The enlargement of the side view shows how the weight of the vehicle is being supported by a large bearing and transmitted to the motor housing instead of directly to the motor axle.

This style of suspension is similar to that used on many Earth off-road vehicles. The advantages of the system are:

1. Independent suspension for each wheel

2. Independent steering for each wheel
3. Modular design
4. Durability

The disadvantages of the system are that it is heavier than some simple suspensions and has more parts. However, because the Unloader must complete ten missions without servicing, the durability of the design is an overriding factor.

Among the systems considered initially was the torsion bar suspension used on the lunar rover of the Apollo missions. This consists simply of a single metal bar connected to the wheel and the chassis. As the wheel moves up and down the bar is twisted, and resists an amount determined by the stiffness of the bar. Because the ability of this system to operate in the long term without fracture was uncertain, it was not chosen for the final design.

3.1.8. Braking

In general, the large mass of the system and the low velocities of the Unloader tend to make braking unnecessary. However, if the Unloader is stopped on an incline or needs immediate braking, a wear pad and friction contact has been provided. This is similar to an automobile's disc brakes. A material with a high frictional constant (achieved by geometry) is placed around the hub of the wheel, and an electronically controlled gripping-arm makes contact with the frictional pad to allow for braking.

3.2. Lander Design

The second task in the design of the structures subsystem was the analysis and design of the Lander. This included a static analysis of the structure and a study of the forces encountered during landing. As in the design of the Unloader, beam theory was used, which assumed small deflections of all the members. All beam members were also considered to be made of isotropic, homogeneous materials with constant cross sectional areas. A safety factor of 1.5 was used throughout the Lander design instead of a safety factor of 3 as was used on the Unloader. This was because the dynamic loading conditions of the Unloader (i.e. traveling over uneven terrain, raising and lowering cargo, etc.) were more complex than the dynamic loading of the Lander (i.e. landing impact). Therefore, it was felt that since the loads on the Lander were known more precisely, a smaller safety factor could be used, and a substantial weight savings could be realized. All structures were designed to be made of the Aluminum-Lithium alloy 2090-T87 unless otherwise stated. The design of the Lander can be broken down into the following components: platform and Unloader bay, engine shrouds, ramp, and landing legs. There will also be a brief overview of how the vehicle might be assembled in orbit. Figure 3.10 gives an isometric view of the Lander.

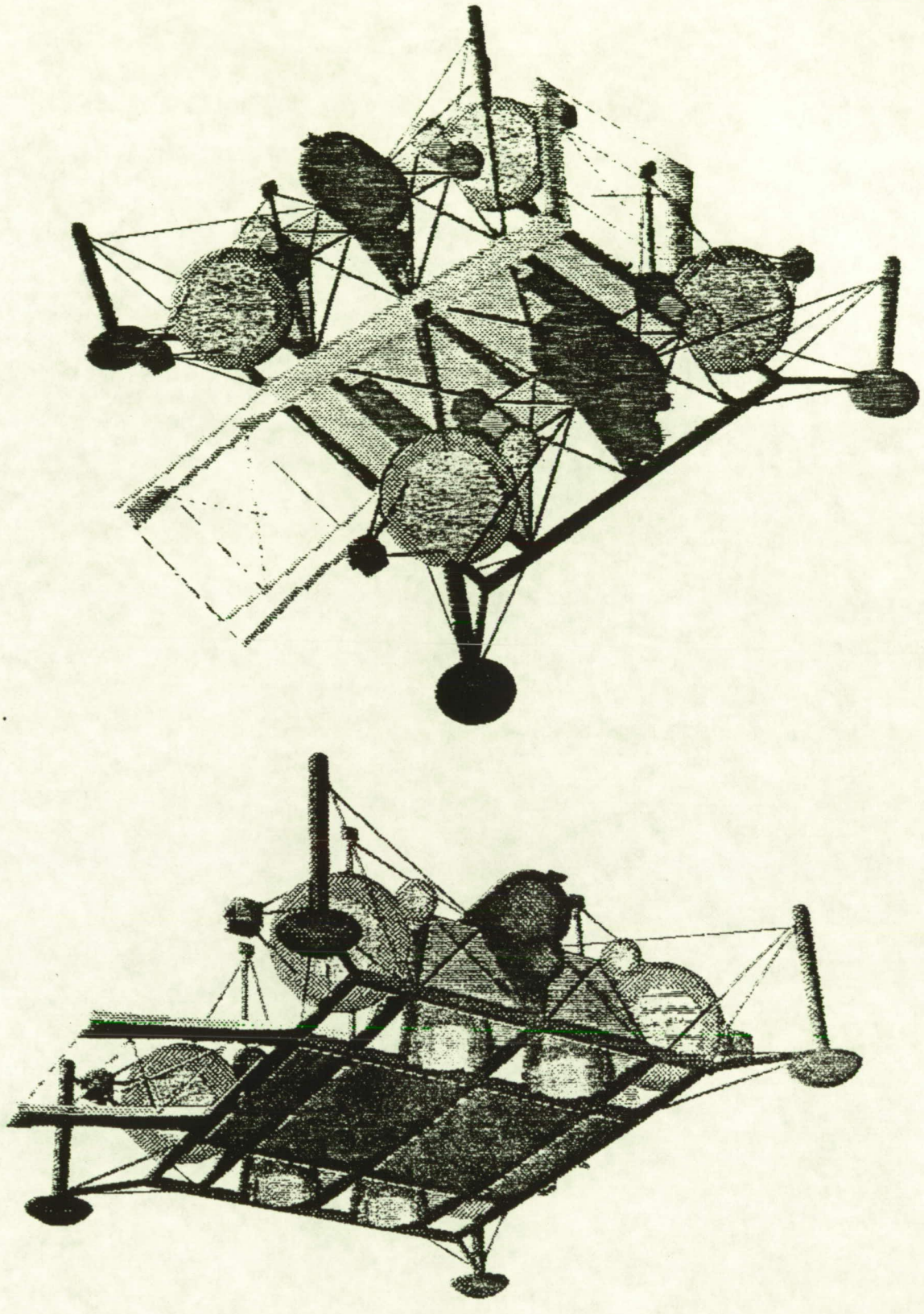

Fig 3.10 - UM-Haul Lander Structure

3.2.2. Platform and Unloader Bay

The first major component of the Lander is the platform and the Unloader bay. The platform of the Lander, as shown in Figure 3.11, is the "backbone" of the structure to which all the other components are attached. The primary design considerations for the platform were that it had to be able to statically support its own weight, the weight of the Unloader and the payload, and also be able to withstand a 1g deceleration during landing. This would be equivalent to designing the Lander to statically support its own weight under Earth's gravity. Applying the beam theory and iterating, the optimum beam size for the platform was obtained. Figure 3.11 shows the final cross-section of the platform beams and spars.

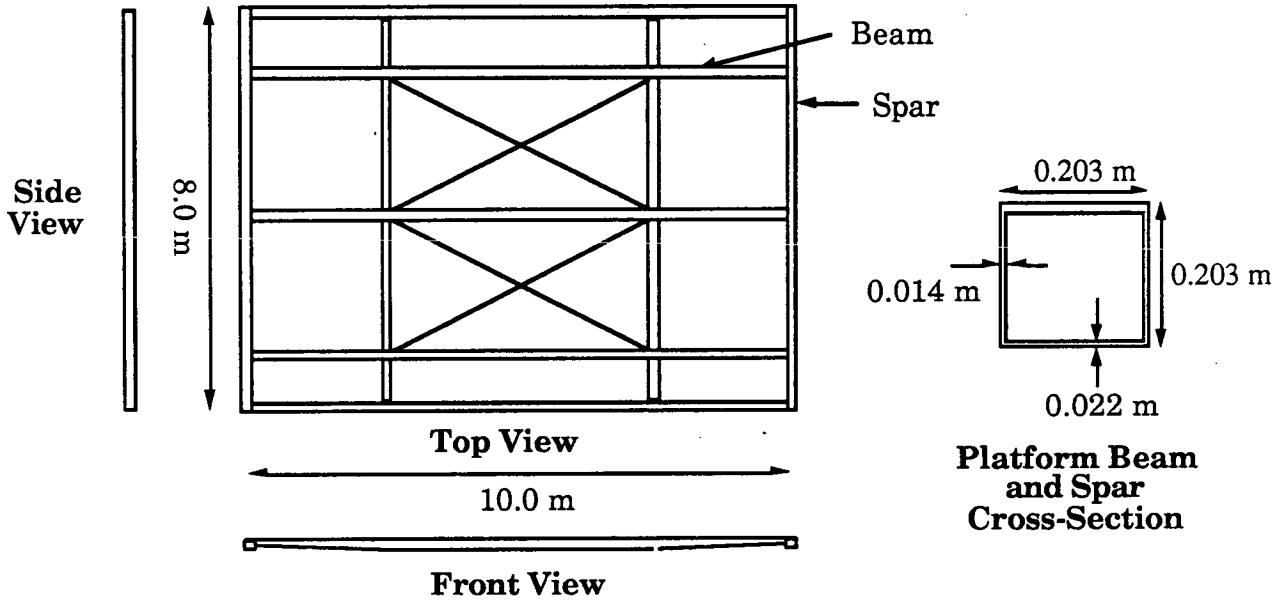

Figure 3.11 - Platform and Beam and Spar Cross-Sections

The Unloader bay is the area where the Unloader and/or the payload will be secured while the Lander is in transit. It consists of an area 5 m wide by 8 m long in the middle of the platform [see Figure 3.12]. On each side of this bay are runners 0.75 m wide that run the length of the bay. These runners are designed to support the Unloader while it is driving on or off the Lander. Each runner consists of two main supports, a truss network, side guides for the Unloader wheels, and a series of metal plates.

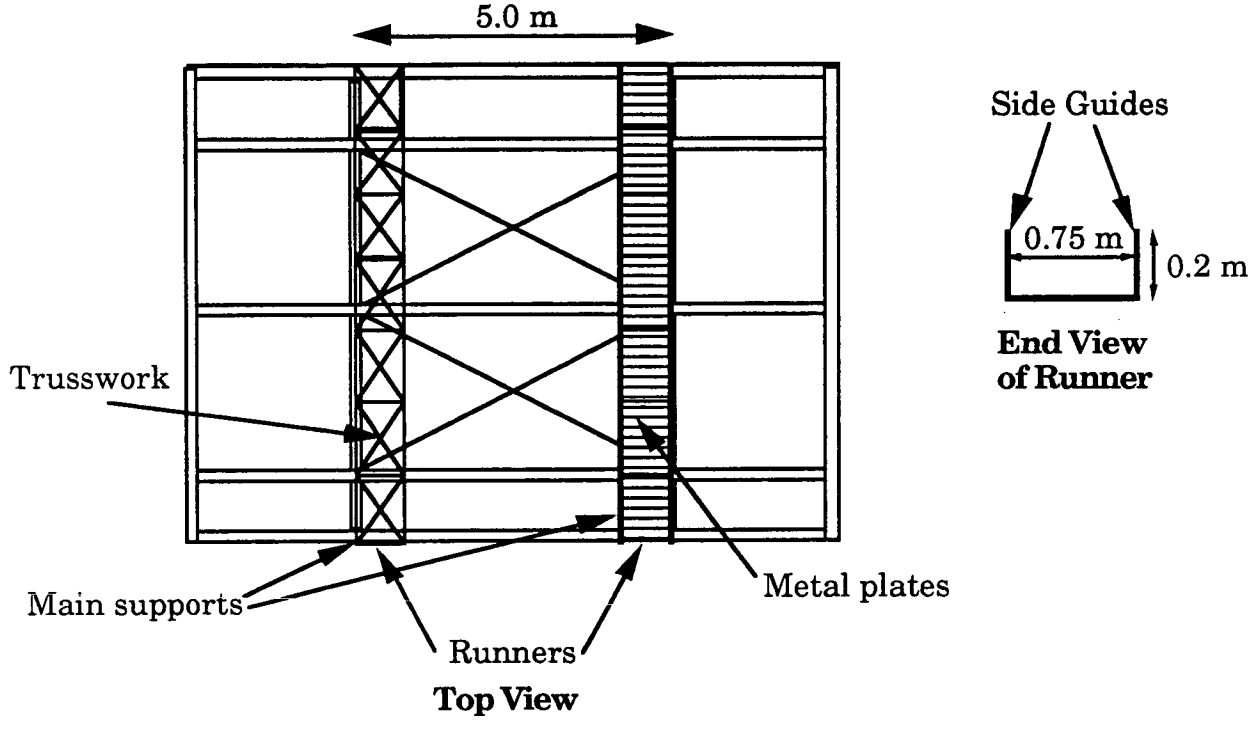

Figure 3.12 - Unloader Bay

3.2.2.1. Engine Shrouds

The four main engines of the Lander are attached to the platform by an engine shroud. Each shroud is a truss designed to statically carry the weight of the engine and to withstand the force the engine exerts while firing. The maximum thrust of each engine (33,000 N) was used as a worst-case situation. Using an analysis method similar to the one used for the platform, the shroud design shown in Figure 3.15 was arrived at. Each member of the truss is a rod with an inner radius of 0.012 m and an outer radius of 0.016 m.

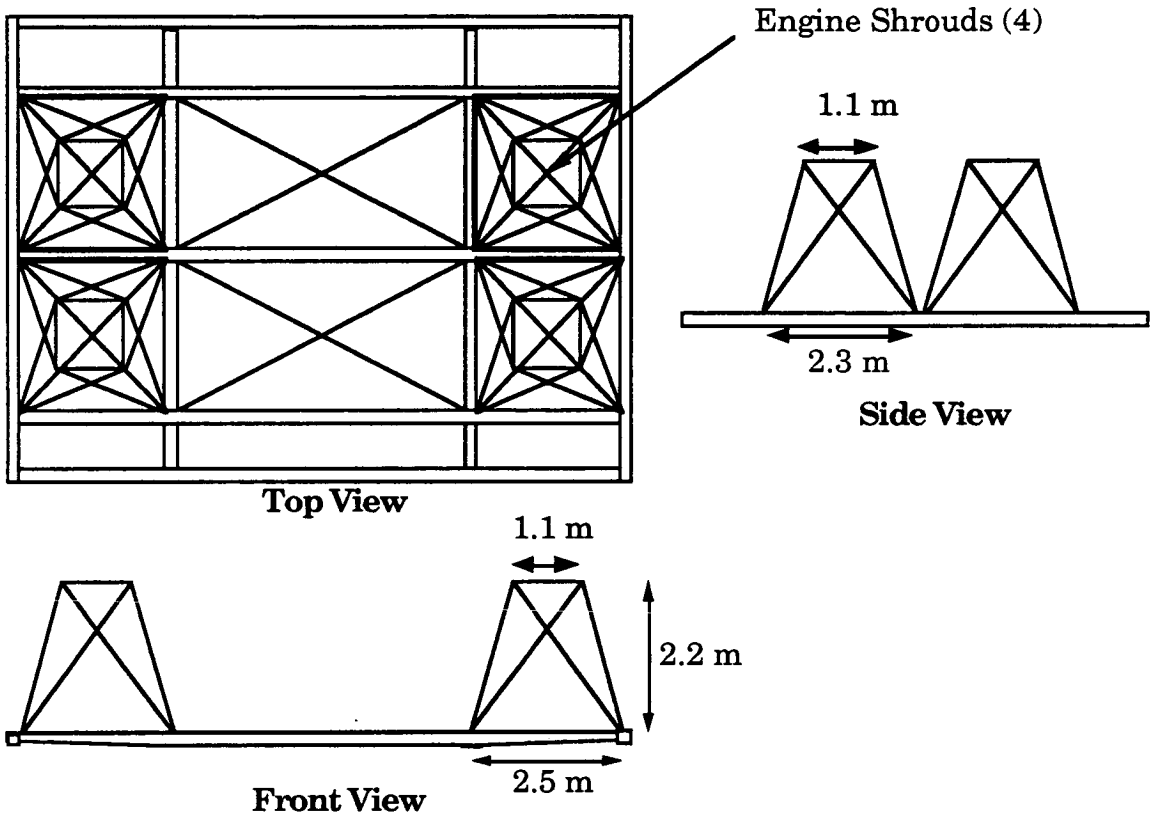

Figure 3.13 - Engine Shrouds Connected to the Platform

3.2.2.2. Ramp

In order to get the Unloader on and off the Lander, two ramps are located at each end of the Unloader bay. Each ramp consists of two tracks, connected to each other by trusswork, which are similar in construction to the runners in the Unloader bay. At the end of each track, the side guides and track are flared out in order to ensure that the Unloader wheels travel straight along the track. Metal ridges on the surface of each track are used to improve the traction between the Unloader wheels and the ramp. Figure 3.14 shows a schematic of the Lander's ramp.

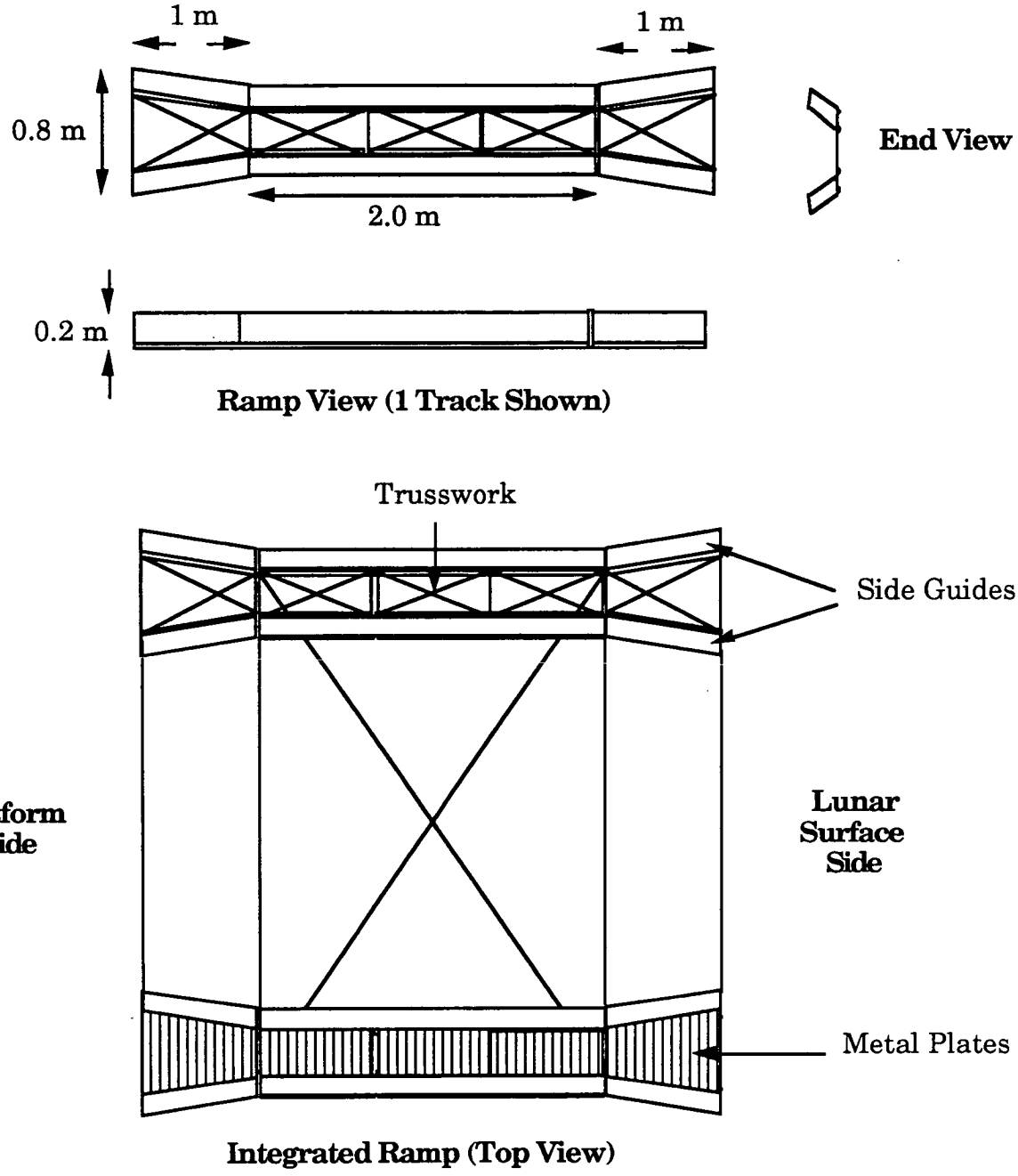

Figure 3.14 - Single Track and Integrated Ramp

3.2.3. Landing Impact Absorption System (Legs)

The Lander has four landing legs which use the compression of Helium gas to absorb the force of the landing impact [see Figure 3.15]. Helium gas was chosen because it will not react with the Aluminum-Lithium alloy shells of the leg. Each leg is made up of three components: the leg shell, the leg post, and the landing

pad. The leg is attached to the chassis with a main support and four rods. The leg shell is an open-ended cylinder with an inner radius of 0.151 m and an outer radius of 0.161 m. Into this shell fits the leg post, a tube with an inner radius of 0.128 m and an outer radius of 0.151 m. Both the inside of the leg shell and the outside of the leg post are coated with a dry-film lubricant. The landing pad is attached to the leg post. Helium gas fills the space between the top of the leg post and the top of the inside of the leg shell. Seals on the top circumference of the leg post prevent the Helium from leaking out. Upon landing impact, the gas is compressed and absorbs the energy of the landing impact. A friction clamp, located near the bottom of the leg shell, begins to close around the leg post when the landing deceleration is detected and dissipates the energy stored in the gas, eventually bringing the Lander to rest with a 1 meter clearance between the bottom of the chassis and the lunar surface.

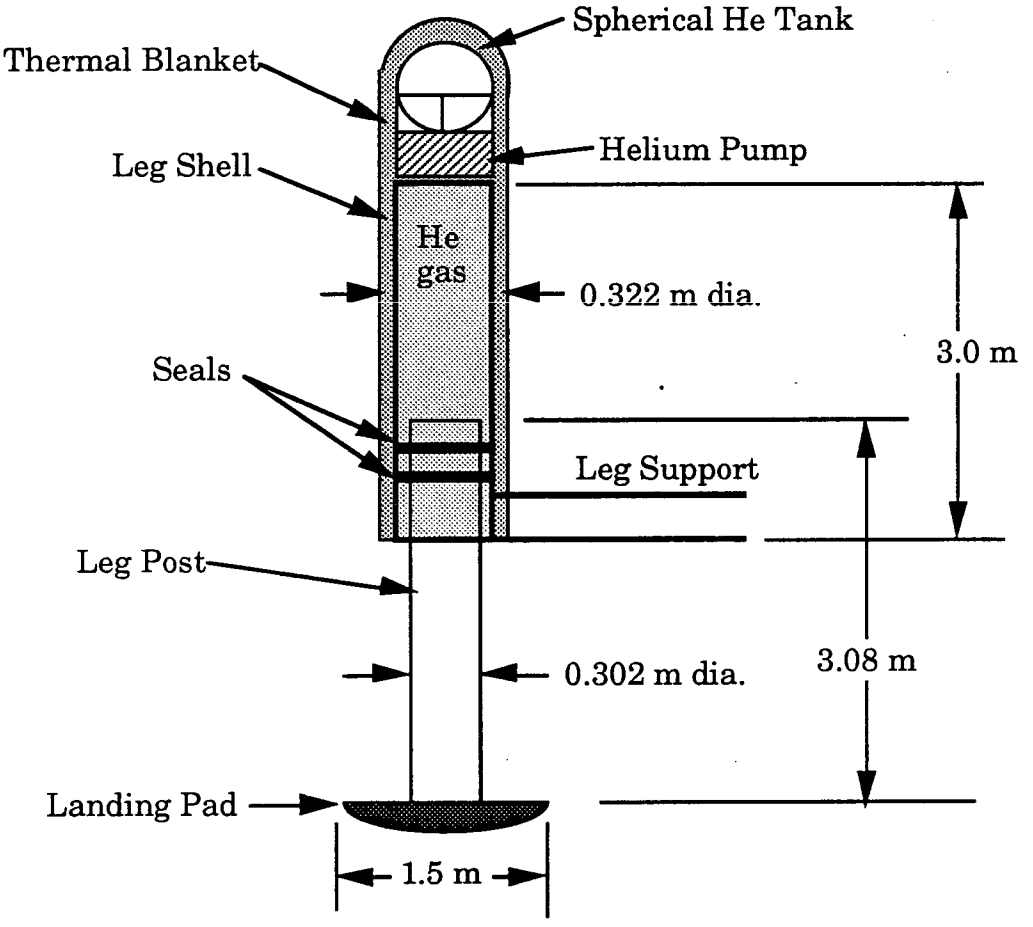

Figure 3.15 - Landing Legs

Some of the Helium gas is pumped out of the leg into a holding tank in order to lower the Lander down to 0.5 meters above the lunar surface before the ramp is deployed. Just before the Lander takes off, the gas is pumped back into the legs to raise the legs so the engines have a sufficient ground clearance to fire. Both the Helium tank and the leg shell of each leg will be covered by a thermal blanket and a small heating system to keep the gas at a relatively constant temperature. The

Helium gas will be maintained at roughly the same temperature as the outside legs in order to minimize heat transfer.

3.2.4. Lander Assembly

Due to the large size of the Lander, it will not be possible to launch the vehicle into low Earth orbit in one piece. Therefore, the Lander will have to be packaged into a launch vehicle and then reassembled at the Space Station. Assuming the Space Shuttle is used as the launch vehicle, the unassembled Lander and the Unloader with only the wheels removed could be delivered to orbit in three flights. If the Unloader chassis were also disassembled, the entire system could most likely be delivered in only two flights, but would require more assembly operations in orbit. In either case, the beams and spars of the Lander platform will be launched unassembled, and then joined in orbit using fasteners. The platform was designed to be constructed using a minimum number of beams and spars in order to reduce the number of fastening operations. Once this base structure is completed, the remaining components of the Lander will then be attached.

3.3. Materials Selection for Structural Components

The structures group has decided to use Aluminum Lithium Alloy for the structural components of the Unloader and Lander. This material was chosen primarily because of it's relatively high yield strength and low density. A list of desirable characteristics used in the selection of materials for the structural components is given below:

1. Low density
2. High strength
3. Non-brittle
4. Resistant to corrosion and wear that may be caused by the sand-like lunar soil
5. Resistant to radiation and atomic Oxygen that may be encountered in space
6. Good fatigue properties with respect to repeated loadings and variations of lunar surface temperature
7. Weldability
8. Resistance to high temperatures (For components in proximity to Lander thrusters)
9. Materials proven in space are a plus

10. Developing materials must be expected to be obtainable and usable for construction of the craft by the year 2000.

3.3.1. Candidate Materials

Initial investigation showed that the following materials might be suitable for the Lander and Unloader structures (ordered from most promising to least) Each material meets a majority of the desirable characteristics described above.

1. Aluminum Lithium (such as 2090-T841, or 7075-T651): Low density, much higher yield strength compared to other alloys, untested in space, not yet widely available [4].

2. Aluminum 6061-T6 : Proven in space, widely available, inexpensive, relatively light, less prone to cracking than similar widely used aluminums [4].

3. Aluminum Magnesium : Very light, low yield strength [5].

While not yet widely used, Al-Li alloys are rapidly developing and are being considered by NASA in other proposals for future space missions. In general, Al-Li alloys have nearly three times the yield strength of Al 6061 and can be up to 15% lighter [6]. These advantages were felt to outweigh the disadvantage due to the "newness" of the material, and therefore Al-Li was chosen as the material for all of the structures.

Materials that have been looked at but not been strongly considered for main structural components are: composites, including graphite-epoxy and Aluminum-boron, titanium, and ceramics. Composites require a plastic to hold the fiber matrix, which will tend to disintegrate in the space environment. Titanium is difficult to weld, while ceramics have good heat resistance but are generally too brittle.

3.4. Fatigue, Corrosion, and Redundancy Factors

Because the Lander and Unloader will be operating over an extended period, consideration must be given to the possible degradation of the system over time. Therefore, the structures and components must be designed to resist failure due to effects of operating in a harsh environment. The following analysis shows how the system is prepared to withstand the effects of fatigue and corrosion, and outlines some of the major redundancy features in UM-Haul.

3.4.1. Structural Resistance to Fatigue

The structural elements used in the UM-Haul Lander and Unloader will experience a reduction in yield strength due to fatigue. This is caused by cyclic loading of the structure due to the following factors: 1. Driving over uneven

terrain, 2. Heating and cooling of the structural elements, 3. Loading and unloading of cargo, 4. Launch and landing. Corrosion of the metal can exacerbate the problems of fatigue depending on the extent of the damage. The first two sources of fatigue listed are the overriding factors, and an approximate prediction for the extent of fatigue was conducted based on this assumption.

Driving over uneven terrain causes the deformation of the structure and results in constantly varying stresses in the structure beams. A round trip of 2 km (farther than the Lander is expected to travel) over rough terrain was chosen as a worst case example. In order to get an approximate value for the number of loading cycles encountered during the trip, the terrain was modeled as sinusoidal. The "wavelength" of the surface was set at 0.6 meters, roughly meaning that the Unloader would be driving over 0.3 meter wide craters spaced 0.3 meters apart throughout the whole trip. If the Unloader drives at 0.1 km/hr, the frequency of loading would be 0.05 cycles/sec. The total number of cycles for a mission over this surface was estimated to be around 4,000, giving a ten mission total of 40,000. Since the fatigue of Al-Li is almost negligible before a hundred thousand cycles at this low of a frequency [7], the structure will be well equipped to handle fatigue due to driving. Taking into account some corrosion of the material due to lunar dust and engine exhaust contaminates, the estimated reduction in yield strength due to fatigue is less than 10%.

Fatigue due to heating and cooling also causes repeated loadings on the structure. Because the cycle of heating and cooling will be slow, fatigue due to the cyclic thermal stresses will be minimal. The main problem caused by the variation in the temperature is creep, or the propagation of cracks in the structure due to stresses in the beams under elevated temperatures. The problem gets worse over time and with higher temperatures. The creep rate of Al-Li in the lunar environment was not calculated due to lack of data. However, the lunar temperatures will not be high enough for creep to be an immediate problem. Testing of Al-Li in a lunar environment is recommended before the mission.

The fatigue limit of Al-Li is 83 MPa for notched (pitted) Al-Li, and 220 MPa for smooth Al-Li [7]. The yield strength will never get below these values regardless of the number of loading cycles. Our structure was designed assuming a yield strength of 206 MPa (after including safety factors). This means that if the Aluminum can be relatively well protected by paint or coating, the design would be able to accommodate unlimited loading cycles. Creep and corrosion will eventually lower the fatigue limit, but the structures should still be in tact after 10 missions.

3.4.2. Corrosion of Structures and Mechanisms

Corrosion will decrease the operating lifetime of both the structures and the components aboard UM-Haul. The main sources of corrosion for both the Lander and Unloader are: 1. Sand-like lunar dust, 2. Contaminates from propulsion systems, 3. Solar radiation. Lunar dust is abrasive and will wear down areas in mechanisms or surfaces in which it becomes trapped. Contaminates from the propulsion system, including atomic Oxygen and water, will tend to corrode the

metals of the structure. Solar radiation may increase the creep rate of the materials.

Corrosion protection for the structures is included mainly with the choice of material used. Aluminum is a good reflector of solar radiation, and can be made more so by the application of white Aluminum paint. Aluminum alloy is also resistant to engine contaminants, as it forms an oxide coating while on Earth, which is resistant to corroding species. Deterioration of the structure due to damage by lunar dust will not seriously affect fatigue characteristics, as the frequency of loading variations is small.

Protection for mechanisms and electronic components aboard the Lander and the Unloader will be provided by coverings. Flexible bellows will be used around moving components such as the Unloader suspension and steering linkages. Thin walled Aluminum boxes will house electronic parts aboard the Lander and Unloader.

A three mm thick Aluminum plate covers the underside of the Lander to deflect dust particles. Due to the configuration of the four engines, the dust plumes created on takeoff will tend to "fountain" upwards and impact the bottom of the Lander. While the acceleration of the Lander on takeoff should quickly move the craft away from the dust plume, the plate was added to protect components against pitting and becoming coated with dust.

3.4.3. Redundancy and Contingency Features

The vital elements of the Lander and Unloader have been designed with a factor of safety that will allow for continued operation after unforeseen contingencies. The Unloader structure has been designed with a safety factor of three, and the Lander structure with safety factor of 1.5.

3.4.4. Unloader Redundancy

The Unloader has eight independently driven, steered and suspended wheels. Four of the eight 1/4 horsepower motors can be lost while still maintaining full maneuverability. More than that will result in a reduced ability to climb hills.

Inability to drop off the cargo will result in the failure of the Unloader to return to the Lander, thus the cargo lifting mechanisms are redundant. The support arms will be constructed so that a failed lifting mechanism can be ejected, and the load can be handled by the remaining lifting arms. The Unloader can lose two of the four lifting arms, assuming that the two failed arms are not both on the same end of the Unloader.

The frame is designed to resist torsion using only two bars running through the center of the "block eight" chassis. Further torsion resistance is provided by the beams on the ends of the block eight configuration.

Should the trunnion point of the cargo fail to lock with the Unloader, the cargo can still be moved and carried with a roll angle of up to twenty degrees.Fifty percent of the solar cell arrays aboard the Unloader can be damaged while still allowing power required for full operation.

3.4.5. Lander Redundancy

The Lander structure is fully capable of handling required loads before the addition of small trusswork. The trusswork will be needed to hold component bays and mechanisms, and will add to the structural integrity of the craft.

The Lander is still operational after the loss of any one main engine, two diagonally opposed engines, or one engine on each side of the cargo bed. Re-aligning the thrust through the center of mass after the failure of two engines on the same side of the cargo bed may exceed the gimballing capability of the engines.

An area of concern for the Lander is the legs. There are no redundant legs, and the craft must be built to withstand ten landings without failure.

3.5. Future Developments in Structural Technology

The ability to alloy Lithium with Aluminum is a fairly recent development. Lithium, which is a highly reactive substance, is unstable during certain alloying processes. Only small amounts of Lithium are needed to improve the mechanical properties of Aluminum. For each weight percent of Lithium that is added to the Aluminum alloys, the density is reduced by approximately 3% and the elastic modulus is increased by approximately 6%. These values are good for Lithium additions up to 4 weight percent. Aluminum Lithium (Al-Li) has high ductility, good damage tolerance, good corrosion resistance, excellent mechanical properties and ease of formation and production using conventional equipment and methods.

Elements such as Sodium, Potassium, Sulfur and Hydrogen can adversely affect the performance of Al-Li alloys at low levels of contamination. These elements generally appear as impurities in the Lithium. Since these elements have no solubility in Aluminum, they may lead to unwanted segregation at the grain boundaries of the alloy. One way to over come this problem is to add other elements to the alloy that would form harmless compounds with the unwanted elements. Improvements in the aging of this alloy and new thermal mechanical treatments designed to develop either a very fine recrystallized grain structure or a completely uncrystallized grain structure could also alleviate the problems caused be these impurities in the Lithium.

Since Al-Li is a fairly new alloy, its stability in a space type environment is currently unknown. After more research and experimentation, future spacecraft can be constructed from this alloy.[9]

A structural material that is still under development is Carbon Epoxy Composites (CEC). CEC consists of Carbon fibers encased in a resin matrix. There are several types of resins suitable for this matrix. The modulus of the Carbon fibers is approximately 20 times that of the matrix. When a load is applied, the matrix will distribute the load so that each fiber supports part of the load. The Carbon fibers are generally elastic right up to their breaking strain. CEC would make a better structural material as compared to Al-Li, Aluminum or steel [see Table 3.2]. They have properties that give them 1/2 of the density of Al-Li and three times its yield strength. This corresponds to a six times increase in yield strength over conventional space Aluminum. Low density and a high strength makes CEC a prime candidate for aerospace structural materials. CEC has favorable mechanical properties including high strength, easy fabrication, good thermal conductivity, low thermal expansion and high electrical conductivity. CEC has been used in a few satellites already orbiting the Earth.[8]

Table 3.2 - Materials Comparison

Material	Density (kg/m^3)	Tensile Strength (GPa)
Carbon Fiber	1800	3.1-4.6
Aluminum Lithium	2685	0.556
Aluminum	2800	------
Steel	7870	1.5

3.6. References

[1] Bekker, M. G.; Joseph P. Finelli and Ferenc Pavlics. "Lunar Surface Locomotion Concepts." Advances in Space Science and Technology. Ed. Frederick I. Ordway III. New York, NY: Academic Press, Inc. ; 1967: 297-326.

[2] Alred, J. and A. Bufkin, "Lunar Surface Transportation Systems Conceptual Design," Eagle Engineering Report No. 88-188, NASA Contract NAS9-17878 (CR-172077), July 7, 1988.

[3] Costes, N.; J. Farmer and E. George, "The Lunar Roving Vehicle: Terrestrial Studies: Apollo 15 Results", NASA TR-R401, December 1972.

[4] Frazier, William E., et. al., "Advanced Lightweight Alloys for Aerospace Applications," Journal of Metals, May 5, 1989, p. 23

[5] Wadsworth, J., "Developments in Metallic Materials for Aerospace Applications," Journal of Metals, May 5, 1989, p. 15

[6] Ronald, Terence M.F.,"Advanced Materials to Fly High in NASP," Advanced Materials and Processes, May 1989, p.29

[7] Taketani, H., McDonald, M.J., and Chionis, W.G.,"Properties of Al-Li Alloy 2090-T3 Sheet," Advanced Materials and Processes, April 1990, p.113

[8] Drestelhaus, M.S. et. al., Graphite Fibers and Filaments, Volume 5, 1988

[9] Starke, E.A.,T.H. Sanders, and I.G. Palmer, New Applications to Alloy Development in the Al-Li System, Georgia Inst. of Technology/Lockheed, Palo Alto Research Laboratory.

Chapter 4

Propulsion

4.0. Summary

The propulsion system must have the ability to carry the Lander with its payload from the lunar orbit to the moon and back to lunar orbit. The system is also responsible for attitude control operations. This chapter is divided into four main sections.

The first section evaluates different propulsion system candidates. Cryogenic liquid chemical propulsion, using hydrogen (LH_2) and oxygen (LOX) as the propellants, was chosen as UM-Haul's primary propulsion system with Pratt & Whitney's RL10-IIIB as the main engine.

The propellant system is discussed in the second section. This includes the required propellant mass, and a study of the propellant storage and feed system.

The third section details the Reaction Control System (RCS) and explains the integration of the primary propulsion system with the RCS and the fuel cell power system.

The last section discusses the lunar dust radius caused by the engines upon the landing and the take-off of the Lander.

4.1. Propulsion Systems

Several propulsion systems were considered to be used on the Lander. These included electric, nuclear, laser, solar, and chemical propulsion systems. The requirements that must be fulfilled by the propulsion system are many. First, the system must have a high thrust capability, (on the order of 35,000 N per engine). It must also have a high specific impulse (Isp). Specific impulse is an efficiency rating of how much thrust an engine produces per unit mass of propellant. It also must have the capability to be throttled, (i.e., to control reactant flow rate to the engine), and, finally, it must be available by the mid-to-late 1990's.

Based on extensive research, it was determined that a liquid chemical bipropellant propulsion system would best suit the mission of UM-Haul. Currently available liquid propulsion systems are capable of producing high thrust and high Isp, and are capable of being throttled. A summary of each propulsion system is given below.

4.1.1. Electric Propulsion

Several forms of electric propulsion were considered. These included magnetoplasmadynamic (MPD) and ion thrusters. MPD systems use an electric current to create a magnetic field which forces a propellant (a plasma) through a nozzle at high speeds. Ion thrusters use electric power to ionize and expel the ions at high velocities.

Although both of these types of electric propulsion have high Isp, neither can provide the thrust required for Lander missions. Light-weight power systems which can fulfill power requirements for high thrust electric propulsion applications have yet to be developed.

4.1.2. Nuclear Propulsion

Nuclear Thermal Rockets (NTR) were considered for nuclear propulsion. NTR systems contain a nuclear reactor which heats the propellant and expels it at very high velocities. NTR systems, which have yet to be developed, theoretically provide high values of Isp. However, the technology to develop and build such a propulsion system is prohibitive for UM-Haul in terms of time, cost, and environmental concerns due to radiation from the nuclear reactor.

4.1.3. Laser Propulsion

Laser propulsion systems function on the premise that a laser pulse excites a field of gaseous propellant, which then is expanded through the aft quarter of the engine at very high velocity to provide thrust. This system works with extremely high Isp and with a variety of propellants. However, a laser propulsion system needs a large amount of power to operate. For example, a laser-driven system needs 20 MW of power to place a 170 kg object in low earth orbit (LEO) from the surface. Laser propulsion systems are still very theoretical. The technology to develop and build this type of system, along with the immense power consumption of the system, prevented the feasibility of this system for UM-Haul.

4.1.4. Solar Propulsion

Solar propulsion systems, in general, work by using large, concentrating mirrors to gather and focus solar energy into a light-absorbing heat exchanger. This energy heats a propellant which is exhausted to produce thrust. These systems are typically very large and extremely costly. The future goal of solar thermal propulsion systems is to have two mirrors, each 30 m in diameter, deliver 1.5 MW of power to two thrusters operating at 222.5 N thrust at 900 sec Isp. Today's solar technology has only produced a 4.45 N thruster at a 650 sec Isp from a 25 kW power source. Solar propulsion systems with thrust levels suitable for UM-Haul will not be available by the mid-to-late 1990's.

4.1.5. Chemical Propulsion

The two types of chemical propulsion systems considered were a solid propellant propulsion system and a liquid propellant propulsion system. Both systems are currently available and have shown consistent performance for use in spaceflight applications.

A solid propellant system employs a propellant initially in a solid state. Upon ignition, the propellant combusts and the gaseous products exit at high velocity from the nozzle. Solid propellant systems are capable of providing high thrust

and high Isp, but are not throttleable. This means that once the propellant has been ignited, it does not stop burning until all of the propellant has been used.

The principle of a liquid propellant system is similar to that of a solid propellant system, except that the propellant is in liquid state. Liquid propellant systems are capable of high thrust, high Isp, and are throttleable. They can use monopropellant or bipropellant inputs. A monopropellant system requires only one substance for combustion, whereas bipropellant systems employ two reactants, called a fuel and an oxidizer. Monopropellants typically yield much lower thrust levels and Isp than bipropellants. Because of these reasons, it was decided to concentrate on bipropellant chemical propulsion systems.

4.2. Propellant Types

There are two main categories of liquid propellant. These are classified as hypergolic and cryogenic. The propellant type chosen for UM-Haul is a cryogenic bipropellant system using liquid hydrogen as the fuel and liquid oxygen as the oxidizer. A comparison of the two propellant types is given below.

4.2.1. Hypergolic Propellant

Propellant is considered hypergolic if the two reactants ignites on contact. Most types can be stored on earth. The hypergolic bipropellant combination considered was monomethylhydrazine (MMH) as the fuel and nitrogen tetroxide (N_2O_4) as the oxidizer. Since hypergolic propellant systems ignite on contact, they are more reliable. Another advantage is that these propellants do not require thermal management.

4.2.2. Cryogenic Propellant

A cryogenic propellant must be stored at very low temperatures because of the extremely low boiling points of the fuel and oxidizer. The cryogenic propellant considered was liquid hydrogen (LH_2) as the fuel and liquid oxygen (LOX) as the oxidizer. The advantage of the cryogenic propellant system is that it has high Isp. This increases the performance of the engine by requiring less propellant mass per mission (as compared to a hypergolic propellant system), and therefore decreases the mission cost. A cryogenic propellant system is also advantageous because the present Orbital Transfer Vehicle (OTV) design operates on LH_2 and LOX. Since the mission scenario for UM-Haul is to refuel at the OTV, it would be more convenient, and also more economic, if both systems ran on the same propellant.

Although there are storage problems associated with cryogenic fluids, the advantages of the increased performance due to a higher Isp, the economic benefits, and the compatibility of integration with the Orbital Transfer Vehicle (OTV) design outweighs the drawbacks. Therefore, UM-Haul's design incorporates a LH_2 and LOX cryogenic system. Figure 4.1 describes the decision process pictorially.

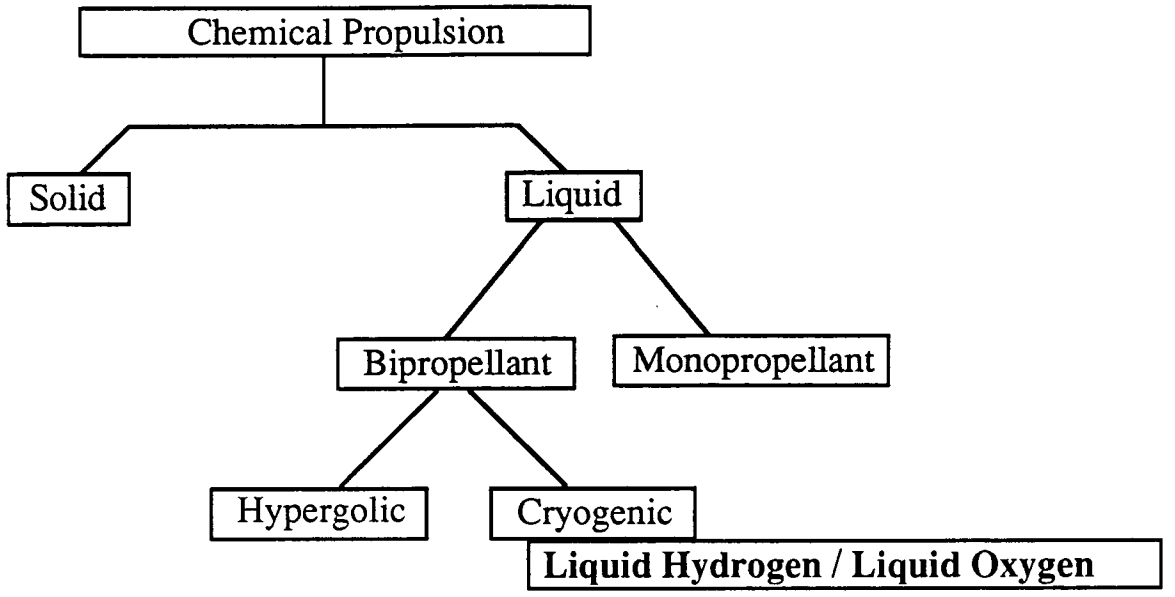

Figure 4.1 - Chemical Propulsion System Elimination Process

4.3. Cryogenic Engines

Several cryogenic engines were considered for use on the Lander. These included the Pratt & Whitney RL10 derivatives, and different advanced cryogenic designs. It was determined that the RL10-IIIB would be used on UM-Haul. A discussion of the most feasible engine candidates follows.

Four cryogenic engines were considered for the Lander. These included Pratt & Whitney's RL10-IIB and RL10-IIIB (derivatives of the Centaur's RL10A-3-3A), the Advanced Space (ASE) engine, which is under development and the Initial Operating Capability (IOC) engine, which is also under development. Table 4.1 below gives some statistics for each type of engine considered.

Table 4.1 - Cryogenic Engine Comparisons

Engine	Thrust (N)	Specific Impulse (sec)	Mass (kg)	Dev. Cost (millions of $)
RL10-IIIB	33360	470	180	104
RL10-IIB	67000	460	195	98
ASE	33360	483	90	350
IOC	33360	475	125	175

As Table 4.1 shows, all four engines have similar performance capabilities. The RL10-IIB has a thrust of 67,000 N (compared to the RL10-IIIB's 33,360 N) but is slightly larger and more massive than the RL10-IIIB. Since the extra thrust of the RL10-IIB is not needed for the mission and since the RL10-IIIB weighs less,

the RL10-IIB was eliminated. The IOC engine is in the developmental stages, and has yet to be designed. Its technology stands as a middle ground between the near-term technology of the RL10 derivatives and the development required for the ASE design. Therefore, the two remaining candidates for UM-Haul were the RL10-IIIB and the ASE.

The main advantage of the RL10-IIIB is that it is a derivative of an existing system, the Centaur's RL10A-3-3A. Therefore, the RL10-IIIB has some certainty as to its developmental and technological needs. A prototype is presently being developed for the RL10-IIIB.

Upon comparison of the two engines, the RL10-IIIB and the ASE, it was found that their performance was comparable. The ASE offers an advanced expander cycle which will offer a predicted 13 second advantage in Isp over the RL10-IIIB, and therefore a slight advantage in propellant mass requirements. The ASE has a predicted mass half of the RL10-IIIB engine and a predicted mission lifetime twice that of the RL10-IIIB.

The ASE's strengths are balanced by three drawbacks. The first two are the high predicted cost and time of development and testing. The Advanced Space Engine incurs a developmental cost of approximately 350 million dollars compared to the corresponding 104 million dollar cost of the RL10-IIIB engine. According to [1], the ASE will return its high developmental cost in time, but this time is unspecified. The third drawback is the unknown technological needs of a system that operates at an Isp of 483 seconds. This is the highest Isp level designed for an engine.

Based on reasons outlined in the above discussion, Pratt & Whitney's RL10-IIIB derivative engine was chosen for the Lander. Four engines will be used in order to provide redundancy. Table 4.2 below gives some performance specifications for the RL10-IIIB [1 & 2].

4.4. Propellant Requirements

4.4.1. Ascent / Descent Propellant Mass

The largest portion of required propellant mass is used to achieve the necessary ΔV's for ascent and descent. ΔV requirements were computed by Mission Analysis [see Chapter 7]. In addition to ΔV requirements, extra propellant mass is needed for various reasons [3]. These reasons are outlined in the Total Propellant Mass Budget shown in Table 4.3.

Table 4.2 - Performance Specifications for the Pratt & Whitney RL10-IIIB Engine

Performance Specifications	
Thrust (N)	33360
Mixture Ratio (O/F)	6/1
Chamber Pressure (MPa)	2.76
Specific Impulse (s)	470
Length, installed (m)	1.4
Mass (kg)	195
Nozzle Area Ratio	400
Life (Ms/hrs)	10/5 (190 starts)
Throttleability	20:1
Cost ($/engine)	20 million
($/DDT&E)	104 million

Figure 4.2 shows a schematic of the Pratt & Whitney RL10-IIIB engine [2].

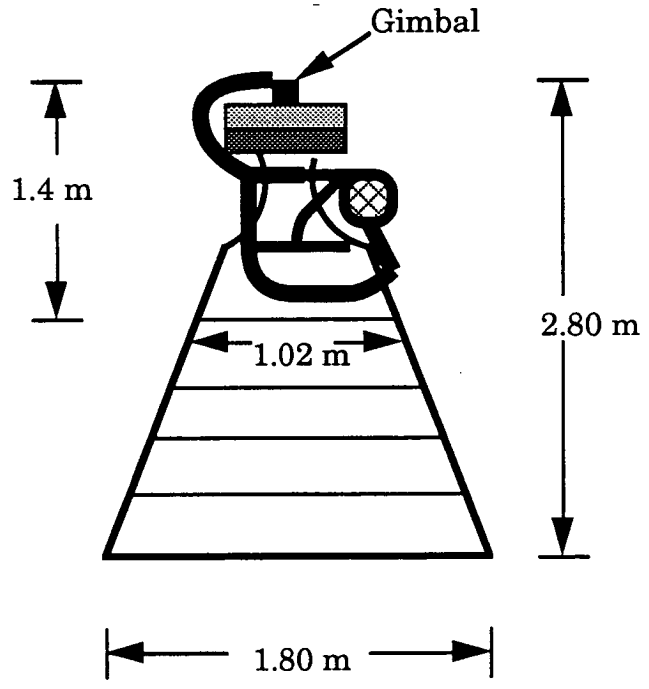

Figure 4.2 - A Schematic of Pratt & Whitney's RL10-IIIB Engine

Item (2) of the budget takes into account the boil-off of the cryogenic fuel and oxidizer while the Lander waits on the lunar surface. Boil-off rates of 4% per month for liquid hydrogen and 1.5% per month for liquid oxygen were used [4].

Item (9) budgets in the propellant which will be trapped in tanks, left over in fuel lines, or any other residual propellant. Item (10) factors in the uncertainty associated with loading propellant from the OTV to the Lander.

Table 4.3 - Total Propellant Mass Budget

Total Propellant Mass Budget	Mass (kg)
1. Mass to achieve ascent ΔV	3937
2. Compensate for Boil-off on lunar surface	8.53
3. Mass to achieve descent ΔV	10168
4. Nominal Propellant total = (1) + (2) + (3)	14114
5. Allowance for Off-Nominal performance = .75% of (4)	106
6. Mission Margin (reserves) = 7.5% of (4)	1058
7. Contingency = 7.5% of (4)	1058
8. Required Propellant total = (4) + (5) + (6) + (7)	16336
9. Residual = 1.5% of (8)	245
10. Loading Uncertainty = .5% of (8)	82
11. Mass for RCS thrusters (including factor of safety)	63.4
12. Mass for Power reactants	548
13. **Total Propellant** = (8) + (9) + (10) +(11) + (12)	17274

A spreadsheet was used to quickly compute the total propellant mass for different Lander masses [see Appendix B]. In addition, the spreadsheet could easily be changed to compute the total for varying Unloader masses.

The total mass of the propellant required to transport the Lander, of mass 6,162 kg, with a 7000 kg payload and a 1,502 kg Unloader to and from the moon is 17,274 kg. With an oxidizer to fuel ratio of 6:1 for the main engines, and a mixture ratio of 8:1 for the power reactants and RCS thrusters, the amount of LOX required is 14,827 kg, and 2,447 kg of LH_2 is required.

4.4.2. Propellant Delivery System

The propellant delivery system delivers the propellant from the tanks to the engines. There are two items that must be considered. The first item considered is propellant acquisition from the tanks in zero gravity. The second item considered is the propellant feed system to the engines.

4.4.2.1. Propellant Acquisition from Tanks in Zero Gravity

Inside every tank is a bubble called a ullage bubble. This bubble of propellant vapor or inert gas is used to pressurize the tanks and to force the propellant out of the tanks. In zero gravity, the propellant and the ullage bubble tend to float randomly about the tank. Some configurations of propellant at zero gravity are given below in Figure 4.3.

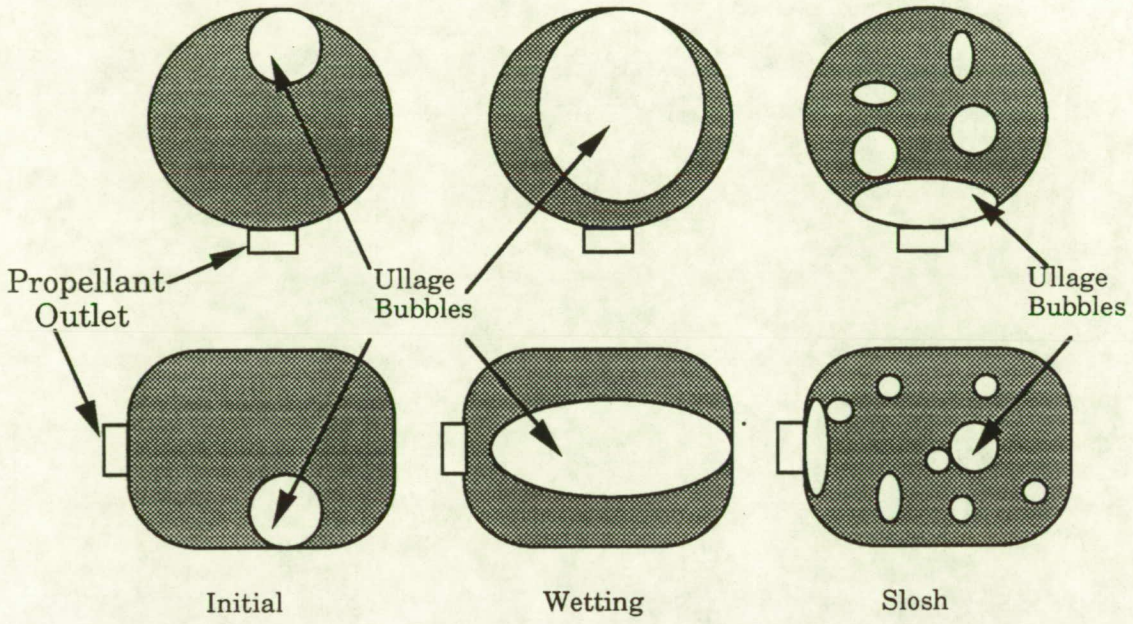

Figure 4.3 - Propellant Configurations in Zero Gravity

A problem occurs if the ullage bubble is located at the propellant outlet. In this case, when the engine starts it will receive vapor instead of fuel, which prevents the immediate ignition of the engine. Since each mission is on a specified time sequence, this delay cannot occur.

In order to ensure that the engine will receive propellant each time it is started, an anti-vortex baffle will be placed over the propellant outlet, and slosh baffles will be placed along the tank walls. The anti-vortex baffle is a metal screen dome that is placed over the propellant outlet. It acts to keep enough propellant held within it in order to start the engines. The anti-vortex baffle holds propellant by virtue of its surface tension and by the fact that the propellant tends to "stick" to the metal walls of the anti-vortex baffles in zero gravity. The slosh baffles are metal dividers placed along the tank walls in order to control the motion of the propellant.

Figure 4.4 shows the propellant storage tanks with anti-vortex and slosh baffles [5].

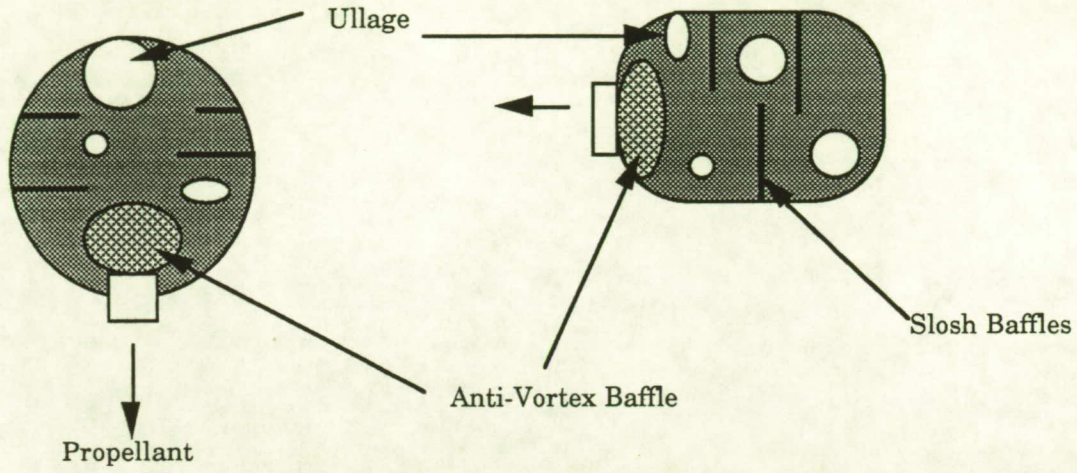

Figure 4.4 - Propellant Storage Tanks in Zero Gravity

4.4.2.2. Propellant Feed System

The purpose of the propellant feed system is to provide propellant delivery to the engines so that they can produce enough thrust to fulfill the mission scenario. There are two types of systems that can be used to deliver propellant to the engines. These are a pressure-fed system and a pump-fed system. A pressure-fed system delivers an inert gas at high pressure, like helium, to the propellant tank. The pressure of the helium forces the propellant out of the tank to the engine. For spacecraft applications such as UM-Haul, the extra weight from the high pressure helium tanks is not practical. Therefore, a pump-fed system will be used. The pump-fed system employs a turbopump and a turbine to pump the propellant to the engine. Figure 4.5 shows a configuration of the turbopump fed system with regeneration that is used on the RL10-IIIB engine. Regenerative cooling employs the propellant to cool the engine nozzle [6].

As shown in Figure 4.5, the liquid hydrogen is first discharged from its tanks to the boost pumps. The boost pumps act to collapse any ingested vapor bubbles at the pump. The boost pumps also discharge the low pressure (34.474 kPa) LH_2 and LOX at 137.9 kPa to the engine turbopumps [7]. The LH_2 is pumped from the turbopumps to the cooling jacket in the engine nozzle in order to cool the nozzle. Once in the cooling jacket, the LH_2 becomes a vapor. Most of this vapor goes directly to the turbine which runs the turbopumps. From the turbine, the vaporized LH_2 goes to the combustion chamber where it reacts with the vaporized LOX to produce thrust. Some of the vapor from the nozzle also is directed back to the tanks in order to keep the tanks pressurized at 34.474 kPa [6].

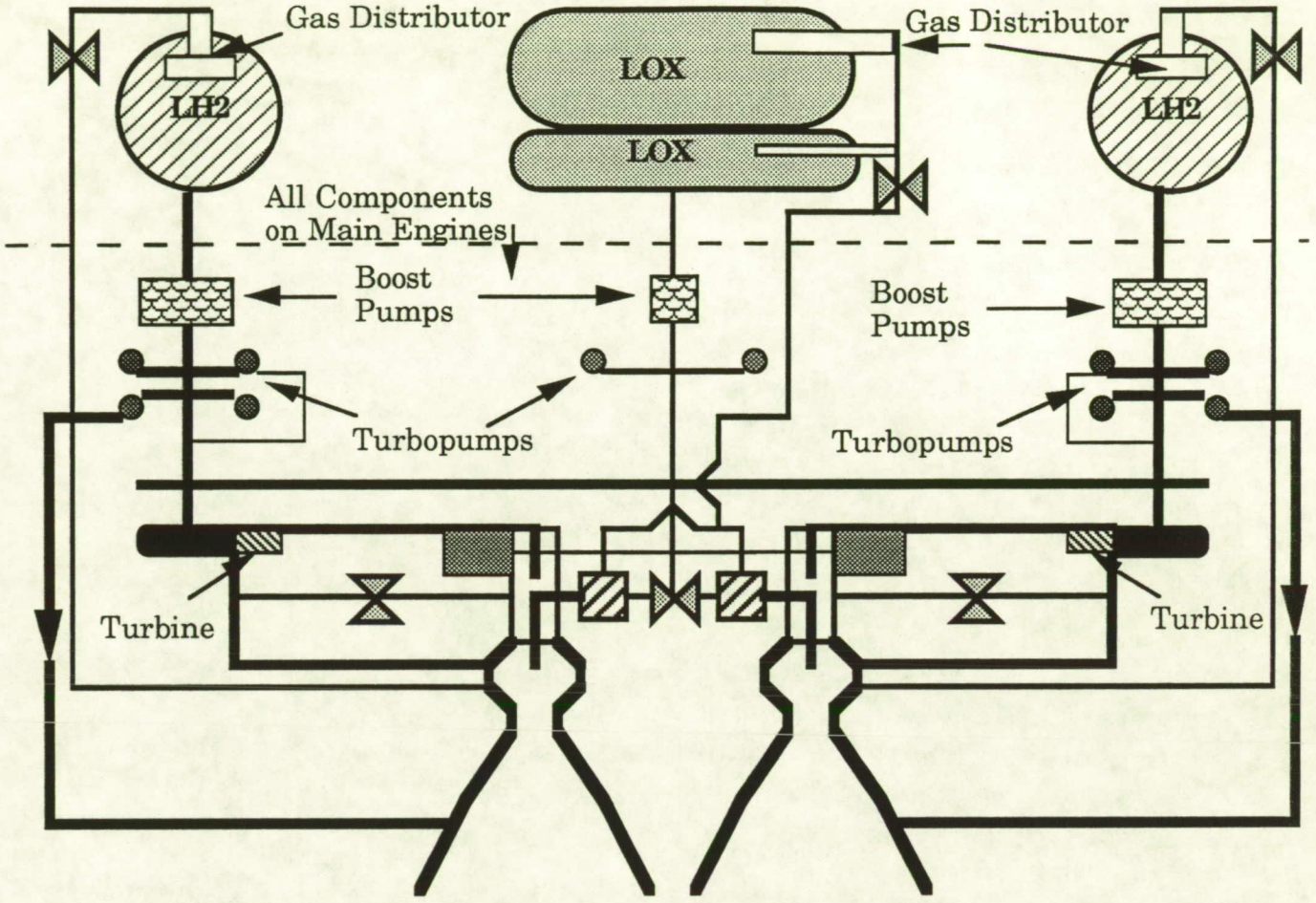

Figure 4.5 - Turbopump Fed System With Regeneration

This regenerative system is able to start by the cryogenic properties of hydrogen. Before ignition, there will be LH_2 in the engine chamber walls. The chamber walls have enough heat capacity in them to vaporize the hydrogen. The vaporized hydrogen, then, supplies the initial power to run the turbine and bring the pumps up to speed so that the propellants can be injected into the combustion chamber.

Initial prepressurization of the LH_2 and the LOX tanks will be done by adding helium from the OTV. Each LOX tank will need 0.300 kg of helium for prepressurization, and each LH_2 tank will need 0.402 kg of helium for prepressurization. This gives us 2.208 kg of helium needed for one mission, and 22.08 kg of helium needed for ten missions [7].

4.4.3. Propellant Storage System

4.4.3.1. Low Pressure Cryogenic Propellant Tanks

The Lander is solely a spaced-based vehicle, i.e., it will only operate in the vacuum environment of space. Because of this fact, the Lander can be designed to be capable of operating solely in a vacuum environment. This also includes the propellant tanks.

In the past, the propellant tanks on every space vehicle have been designed to be maintained at vapor pressures at or above atmospheric pressure (101.3 kPa). This is because, in the past, most space vehicles have been designed to re-enter the earth's atmosphere. Because the Lander will never re-enter the earth's atmosphere, the propellant storage tanks can be maintained at vapor pressures lower than atmospheric pressure. The lowest vapor pressure that is currently feasible to maintain the propellant storage tanks at is 34.474 kPa.

Lowering the vapor pressure inside the propellant storage tanks means that the propellant, LH_2 and LOX, must be "conditioned" down to a pressure of 34.474 kPa. This is because LH_2 and LOX are normally produced and bought in the saturated condition with a vapor pressure of one atmosphere on the ground. LH_2 and LOX can be conditioned down to a lower vapor pressure in one of two ways: by refrigeration, which does not cause any losses due to boil-off, or they can be boiled down, with a 10%-14% boil-off loss.

There are many advantages of reducing the operating pressure of the propellant storage tanks. At lower operating pressures, the tank containment structure can be thinner, therefore requiring less material, and therefore, the containment structure is lighter. The decrease in weight of the storage tanks at lower operating pressures reduces the amount of propellant consumed per mission. This, therefore, reduces the propellant weight and the propellant cost [1].

Because of the economic advantages of low pressure cryogenic tanks for a long mission cycle such as ours, it was decided that UM-Haul would these tanks. It was decided to use refrigeration to conditioning down the propellants to the required low pressure. This method was chosen because the boil down method results in a 10-14% boil-off of the propellant.

4.4.3.2. Tank Material

The first phase in the propellant storage system is deciding the material to make the tanks from. The requirements for tank materials is given below.

1. High Strength
2. High stiffness of elastic moduli, E
3. Excellent fabricability and corrosion resistance

4. Readily available
5. Low cost
6. Easily welded
7. Superior cryogenic fracture toughness
8. Lightweight

Many Aluminum alloys, specifically Al 2219, fulfill all of the above requirements, and have been used in many storage applications. A new material that has been undergoing testing recently is the Aluminum-Lithium alloy, Al-Li 2090-T87. The Al-Li alloy 2090-T87 has been found to have a 10% higher strength, a 20% higher elastic moduli, a lower density (and therefore a lower weight), and higher fracture toughness properties than the Al 2219 alloy [8]. Properties of both the Al 2219 alloy and the Al-Li 2090-T87 alloy are shown in Table 4.4.

Table 4.4 - Properties of Al 2219 and Al-Li 2090-T87

Property	Elastic Modulus (GPa)	Density (kg/m^3)	Ultimate Strength (MPa)	Yield Strength (MPa)			Fracture Toughness (kJ/m^2)
Temp. (K)	**294**	**294**	**294**	**294**	**78**	**20**	**20**
Al-Li 2090-T87	75.8	2546.55	565	535	600	615	10.33
Al 2219-T87	72.4	2823.35	434	386	461	512	7.71

Since the Al-Li 2090-T87 alloy is a "new" tank storage material, other factors still need to be looked into. These factors include the manufacturing requirements and the capability of producing sound welds with adequate cryogenic toughness. The data acquired as of yet on these factors has been promising. Since this material should be fully tested before the mid-to-late 1990's, the Lander should be able to employ Al-Li 2090-T87. Therefore, because of the higher strength and stiffness, the lower density, and higher fracture toughness, the Al-Li 2090-T87 alloy was chosen as the tank storage material.

The thickness of the Al-Li 2090-T87 tank walls is determined from the lower of either the yield strength with a factor of safety of 1.1 or the ultimate strength with a factor of safety of 1.4. In the space environment and at low temperatures, the yield strength with a factor of safety of 1.1 is the lower of the two properties for determining tank wall thickness [1].

4.4.3.3. Tank Shape, Size, & Weight

The second phase in the propellant storage system is to decide the tank shapes, sizes and weights based on the propellant mass requirements. The liquid hydrogen tanks will be considered first, and then the liquid oxygen tanks.

Liquid Hydrogen Tanks

The total amount of liquid hydrogen required is 2,452 kg. Four spherical tanks are used, each containing 613 kg of LH_2. The advantage of spherical tanks is that they enclose the largest volume of fuel for its given surface area, and therefore provide the lightest weight tanks. Table 4.5, given below, provides the tank volume, tank thickness, and tank weight specifications for the LH_2 tanks [9].

Table 4.5 - Specifications of Each Spherical Liquid Hydrogen Tank

Total Volume	8.9 m^3
Radius of Tank (no insulation)	1.286 m
Outer Radius (with insulation)	1.324 m
Tank Wall Thickness	0.173 mm
Tank Mass	9.16 kg
Insulation Mass	20.64 kg
Total Mass	29.8 kg

Liquid Oxygen Tanks

The total amount of liquid oxygen required is 14,858 kg. Although spherical tanks enclose the largest volume for a given surface area, and therefore the lightest weight tanks, it was decided to use four cylindrical tanks with spherical ends for the LOX storage. There will be two large cylindrical LOX tanks and two small cylindrical LOX tanks, both of the same length. The main reason for this choice of shape for the LOX tanks was because they provided the best integration with the Lander, yet still maintained low weights. Tables 4.6, 4.7, and 4.8, given below, provide the tank volume, tank thickness, and tank weight specifications for each of the LOX tanks [9].

Table 4.6 - Specifications of the Spherical Ends on the LOX Tanks

Spherical Ends	Small Tank	Large Tank
Total Volume (one end)	0.146 m^3	1.11 m^3
Inner Radius	0.4119 m	0.81 m
Outer Radius	0.4500 m	0.8481 m
Wall Thickness at Knuckle	0.076 mm	0.150 mm
Wall Thickness at Crown	0.0568 mm	0.112 mm
Mass (one end)	0.154 kg	1.176 kg
Mass (both ends)	0.308 kg	2.352 kg
Insulation Mass (both ends)	2.111 kg	8.162 kg
Total Mass (both ends)	**2.42 kg**	**10.51 kg**

Table 4.7 - Specifications of the Cylindrical Sections of the LOX Tanks

Cylindrical Section	Small Tank	Large Tank
Volume	1.16 m^3	2.84 m^3
Length	2.18 m	1.38 m
Wall Thickness	0.114 mm	0.224 mm
Wall Thickness at Juncture	0.120 mm	0.235 mm
Mass	1.64 kg	4.0 kg
Insulation Mass	5.58 kg	6.95 kg
Total Mass	**7.22 kg**	**10.95 kg**

Table 4.8 - Specifications of the LOX Tanks

LOX Tanks	Small Tank	Large Tank
Total Volume	1.454 m^3	5.06 m^3
Total Weight	9.64 kg	21.46 kg

The wall thickness at the knuckle and at the juncture are thicker than other parts of the tank wall in order to provide extra stability for attachments and welds.

4.4.3.4. Tank Insulation and Tank Meteoroid/Debris Protection

The third phase in the propellant storage system is to choose an adequate insulation and meteoroid/debris protection system to protect our tanks from heat sources and particles in space and on the moon. The tank insulation and the meteoroid/debris protection have dual purposes. The first is to keep the LH_2 and LOX at temperatures below their boiling point and above their freezing point. The purpose of keeping the propellants below their boiling points is to prevent the propellant from boiling off. The boiling point of LH_2 is 20.21 K and the freezing point is 13.82 K. The boiling point of LOX is 90.37 K, and the freezing point is 54.26 K. The second purpose of the tank insulation and the tank meteoroid/debris protection is to protect the Aluminum-Lithium tank wall from being penetrated by small particles in space.

The desirable features of tank insulation and tank meteoroid/debris protection are low weight, low cost, ease of application, ease of repair, reasonable ruggedness, reliability, and low heat conductivity.

Based on the above features, a multi-layer insulation (MLI) made up of two 1.9 cm thick blankets of 10 layers of perforated double goldized Kapton (DGK) reflectors with Dacron net B4A separators (B4A) were chosen as both the insulation and the meteoroid/debris protection [10]. Figure 4.6 below shows a cutaway view of the insulation (not to scale).

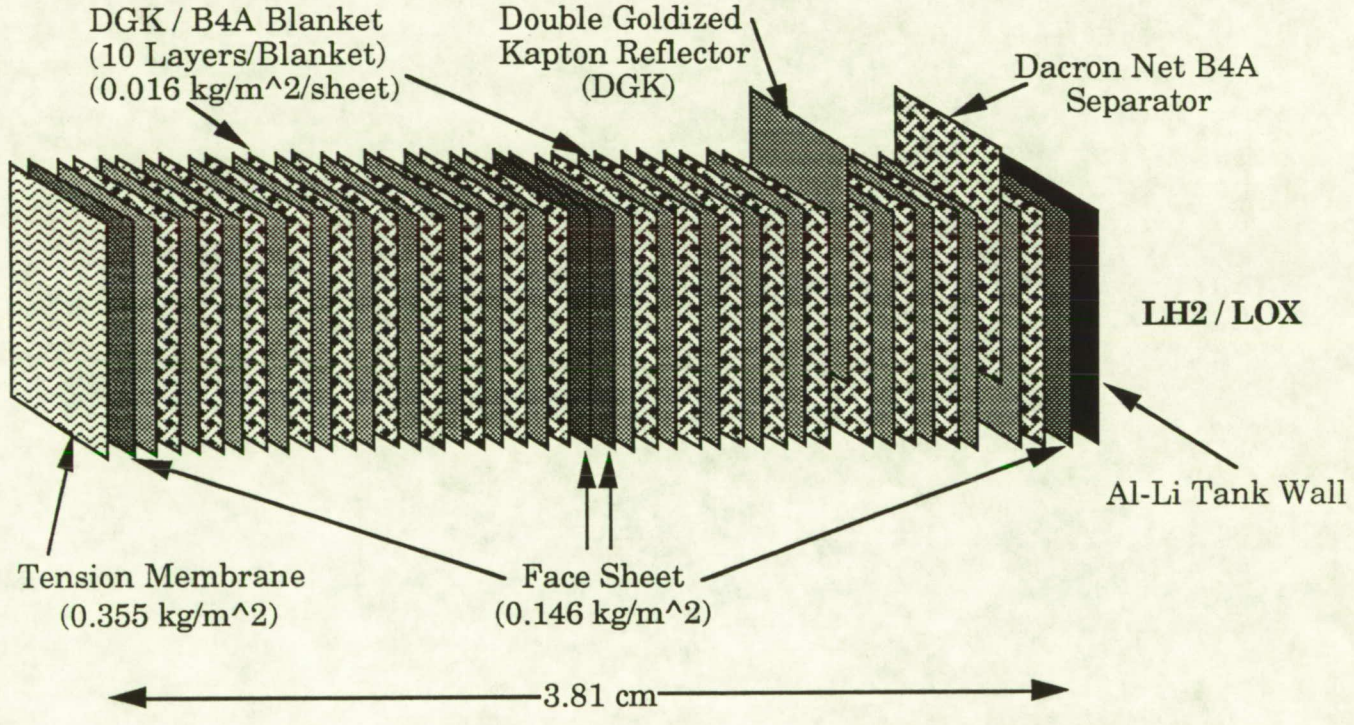

Figure 4.6 - Multi-Layer Insulation and Meteoroid / Debris Protection

The inner and outer face sheets along with the insulation provide adequate meteoroid/debris protection for the propellant tanks within the NASA requirements of providing a probability greater than 0.995 of no meteoroid penetration [11]. The inner face sheets are made of Nomex fabric HT-287 and silicone resin. The outer face sheets are made of Nomex fabric HT-287 and a polyimide resin. The tension membrane over the insulation is made of Nomex fabric HT-287, and it prevents ballooning of the insulation. The total insulation weight with 20 layers of DGK/B4A is 0.99 kg/m^2.

4.5. Reaction Control System (RCS)

Reaction control systems (RCS) are low-thrust propulsion units that perform any tasks that the main engines cannot in terms of stability, attitude control, and rendezvous maneuvering [see Chapter 6]. The Lander's reaction control system is the gaseous 8911 Thruster from Bell Aerospace Textron (developed for NASA Lewis Research Center) [12]. The 8911 Thruster uses gaseous hydrogen (GH2) and gaseous oxygen (GOX) as its reactants for combustion. Its figures of merit are tabulated below in Table 4.9. These thrusters perform all directional maneuvers for the Lander. Although the main engines can be gimballed to perform directional maneuvers, this capability is not be used. Gimballing of the engines will only occur in the event of engine failure. In this case, the remaining engines would be gimballed to produce a resultant thrust vector in the same direction as the original.

Table 4.9 - The Bell Aerospace 8911 GOX/GH2 Thruster

Performance Specifications	
Thrust (N)	223 / 320
Mixture Ratio (O/F)	4:1 / 8:1
Chamber Pressure (kPa)	517.1 / 662.
Specific Impulse (sec)	430
Length (m)	0.4
Mass (kg)	2.69
Nozzle Area Ratio	40:1
Performance	60 starts/sec
Throttleability	none
Life (max sec/start)	1000

The unique trait of this thruster is that it utilizes a reverse flow combustion chamber. The reverse flow process is based on the use of gas vortex mixing to create a simplified combustor. The hydrogen is injected as a sheet at a station in the nozzle convergent section. It then flows toward the front of the spherical combustor, where the flow is reversed and mixes with a vortexing stream of oxidizer. The combination of these two flows form large chamber mixing vortices, which aid in the combustion process [12]. Figure 4.7 shows a schematic of the 8911 GOX/GH2 Thruster.

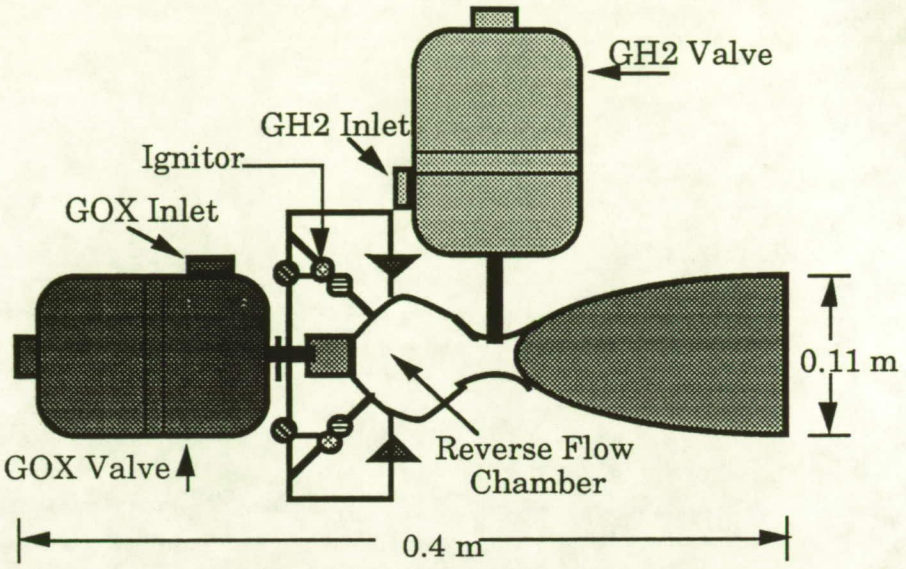

Figure 4.7 - Schematic of the GOX/GH2 Thruster

4.6. Integration with RCS and with Fuel Cells

Because of the convenience and cost-savings of using the same propellant for all of the main systems of the Lander, it was decided to integrate the main engine system with the RCS and the fuel cells. Therefore, each system will run on a hydrogen/oxygen combination, similar to the main engines. Figure 4.8 gives a schematic of the integrated system [13].

As shown in Figure 4.8, the LH2 and LOX tanks that feed the entire system are located in the upper left of the schematic, with redundant pressure transducers that monitor the tank vapor pressure. The solid black boxes depict boost pumps that pressurize the low pressure (34 kPa) propellant in the tanks to 101.3 kPa. The boost pumps are run mechanically, by direct link with the turbomachinery of each system.

The main engines are depicted directly below the tanks. The right side of Figure 4.8 features two valves leading to two more boost pumps, which begin the pressurization of the Integrated reaction control and fuel cell Gaseous System (IGS).

From the IGS boost pumps, lines run to two small heat exchanger cycles. Referring to the labels in Figure 4.8, mini-turbopumps, labeled (1), force the LH2 and LOX through vaporization processes (2). This pressurizes small accumulator tanks (3) to 1.4 MPa, which is a pressure high enough to feed the RCS and the fuel cells. From each accumulator a line also runs to small combustors (4) which operate both the mini-turbopumps and the vaporization process in a regenerative-type cycle.

Therefore, the IGS system provides pressurization and reactants to the RCS and the fuel cells in a regenerative-type process.

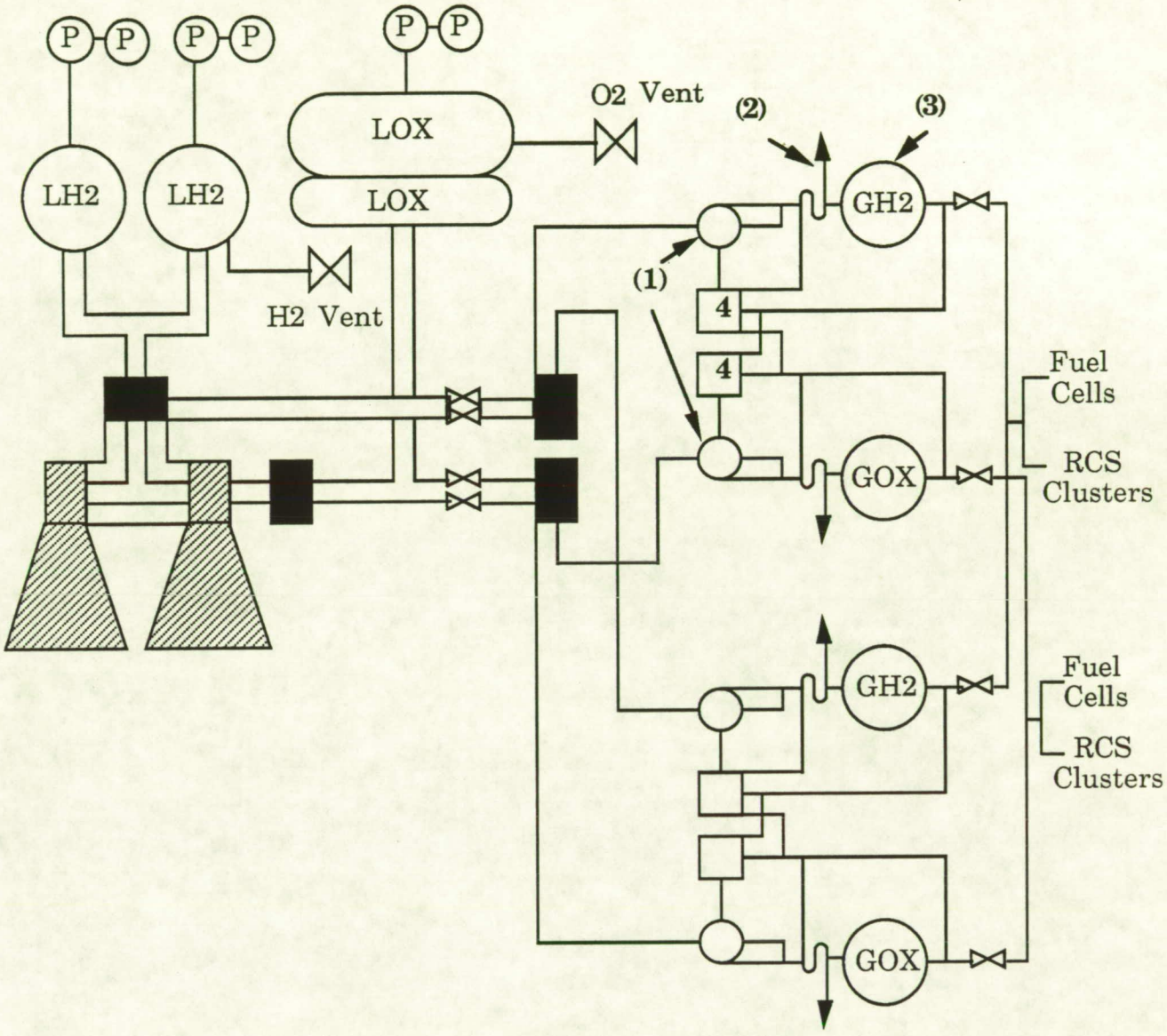

Figure 4.8 - Integration of the Main Engine System, the RCS, and the Fuel Cells

4.7. Blast Radius Considerations

The effects of lunar dust kick-up due to the exhaust plume of the main engines were examined in order to calculate the minimum safe distance that the Unloader with the payload must travel to be safe from the kick-up.

The analysis of the lunar dust kick-up included modeling the forces which a dust particle would experience. These forces are shown below in Figure 4.9.

C2

The large upward force, F, is created by the stagnation pressure of the exhaust plume underneath the dust particle, multiplied by the underside surface area of the grain. The particle also feels two downward forces: W, its own weight, and D, the drag created by direct impingement of the plume. The resultant pushes the particle in the direction shown in Figure 4.9.

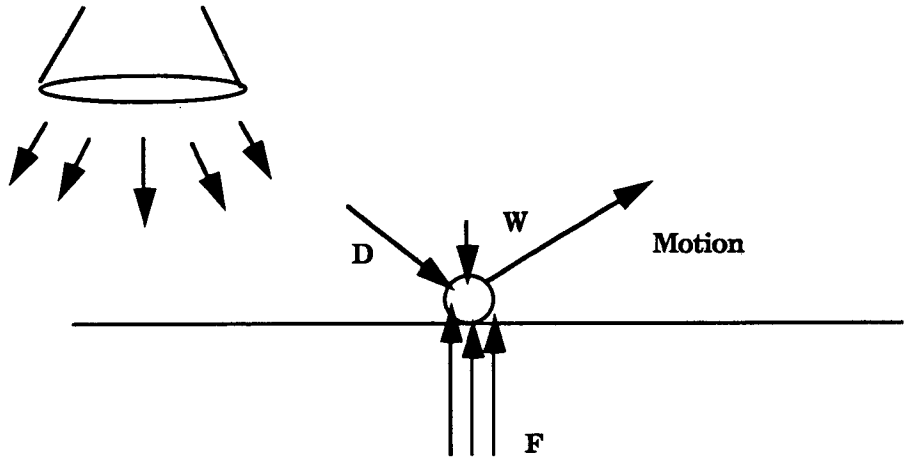

Figure 4.9 - Forces Experienced by a Lunar Dust Particle Due to Engine Exhaust

Eagle Engineering's calculations for blast radii assumed a 50,000 N thrust, 50 μ diameter particles, 50% of flux particles impacting the object surface, and a 5 sec descent.[14] In order for the analysis data to be useful for UM-Haul purposes, the data was scaled to 33,360 N thrust. The worst case scenario was also used. This is the case where the Lander returns to the same site all 10 times, subjecting the payload to the greatest number of sprayings. See Appendix B for the method used to calculate the flux of particles, the number of impacts, the crater diameter, and finally, the percentage of an object's surface which would be pitted [14].

For metal objects, it was determined that the minimum safe distance from the landing site is 300 m. After 10 landings, 1.5% of the surface would be pitted. This is less than the 5% surface pitting standard deemed acceptable in order that surface properties of the metal are not affected.

Uncovered glass objects would require the Unloader to travel a minimum distance of 1 km from the landing site before being deemed safe. Yet, even at 1 km, after 10 landings 8.2% of the surface would be pitted. Because of power and time restraints on the travel distance of the Unloader, any glass surfaces should be covered and pointed away from the landing so that the 300 m safe distance can be used.

4.8. Future Developments in Propulsion Technology

In terms of high thrust engines, turbopump failure is a major concern. High thrust correlates to high propellant flow rates. Consequently, if either fuel or oxidizer pump fails the mission as a whole is jeopardized. If redundant engines are incorporated into the design (hence redundant turbopumps), the possibility of a mission ending pump failure is less of a concern. The two components of a turbopump that are most likely to failure during operation are the shaft's bearings and seals.

This shaft rotates on bearings at high angular rates. Typically these bearings are of the rolling element type. While this type of bearing is well understood in terms of performance, there are still problems inherent to it's design. They are limited in how fast they can roll and in their performance life before failure. Due to these problems, industry is researching better performing bearings which have a longer life. Two of the most recent developments in bearing research are the hydrostatic and the hydrodynamic bearings. Hydrostatic bearings have no speed limitations and an unlimited life as far as rubbing is concerned. Also, they are well damped, high load capacity and high stiffness. Their limitations include the need for an external feed and a high flow rate.

Although there has not been much experience concerning the hydrodynamic bearings, it is known that they do not need any external feeds and they have good anti-whirl characteristics. Unfortunately, these bearings have a limited load capacity.

Currently being researched for future applications are magnetic bearings. Research on this type of bearing is still in its infancy but certain aspects of its performance are known. Its load capacity is independent of its speed and they can be controlled at times of critical speed.

Seals are another area for concern in high speed turbomachinery. If a seal ruptures, the working fluid is no longer confined and can move to all areas in the immediate vicinity of the rupture. In designing seals, there is always a tradeoff between the life of a seal and its performance. The life of the seal is more important than its performance in larger devices. Two types of seals are hydrodynamic and hydrostatic.

The hydrodynamic seal creates a separating force between itself and the sealing surface by generating a pressure differential across the seal as the sealing surface rotates.

Hydrostatic seals need an external high pressure source applied to it to generate this separating force.[13]

4.9. References

[1] General Dynamics, Space Systems Division, OTV Concept Definition and System Analysis Study, Phase 2, Detail Summary, Vol. IX, 1986

[2] Foust, Robert, R., RL10 Derivative Engines for the OTV, Pratt & Whitney Engineering Division, West Palm Beach, Fla., 1985, [AIAA-85-1338 (or A85-39732)]

[3] Sackheim, Robert L., Robert S. Wolf, and Sidney Zafran, Space Mission Analysis and Design, Edited by Wertz, James R. and Larson, Wiley J., Kluwer Academic Publishers, The Netherlands, 1991, pg. 599

[4] Scheer, Dean, and Margaret Proctor, NASA-Lewis Research Center, Private letter, dated February 15, 1991

[5] Press Information, Space Shuttle Transportation System, Rockwell International, January 1984

[6] Purser, Paul, E., Maxime A. Faget, Norman F.Smith, Manned Spacecraft: Engineering Design and Operation, Fairchild Publications, Inc., N.Y., 1964

[7] "NASA Space Vehicle Design Criteria (Chemical Propulsion)", Pressurization Systems for Liquid Rockets, October 1975 [NASA SP-8112]

[8] Torre, C.N., J. A. Witham, E. A. Dennison, R. C. McCool, and M. W. Rinker, Analysis of a Low Vapor Pressure Cryogenic Propellant Tankage System, 1987, General Dynamics, Space Systems Division, San Diego, CA [AIAA-87-2068]

[9] Huzel and Huang, Design of Liquid Propellant Rocket Engines, Rocketdyne Division, North American Rockwell, Inc., 2nd edition, 1971, [NASA SP-125]

[10] NASA-Marshall Space Flight Center, Baseline Tug Definition Document, Rev. A, June 26, 1972 [Received from Dean Scheer of NASA-Lewis Research Center]

[11] General Dynamics Convair Aerospace Division, Reusable Centaur Study, Vol. II, Final Report, pg. 2-40, 1973 [Received from Dean Scheer of NASA-Lewis Research Center]

[12] Senneff, J. M., Bell Aerospace Textron, Buffalo, N.Y., Richter, G.P., NASA-Lewis Research Center, Cleveland, OH, A Long-Life 50 lbf H2/O2 Thruster for Space Station Auxiliary Propulsion, 1986, [AIAA-86-1404]

[13] Scheer, Dean and Proctor,Margaret , Spacecraft Propulsion Presentation, The University of Michigan, February 11,1991

[14] Eagle Engineering, Inc., Lunar Base Launch and Laundry Facility Conceptual Design, report to NASA-Johnson Advanced Programs Office, March 25, 1988

Other References Used

General Dynamics Convair Aerospace Division, Centaur/Shuttle Integration Study, Vol II, Technical, Final Report, pgs. 3-25 to 3-30, 1973, [Received from Dean Scheer of NASA-Lewis Research Center]

Martin Marietta, OTV Concept Definition and Evaluation - OTV Concept Definition, OTV Concept Definition and System Analysis Study, Vol. II, Book 2, 1985

Martin Marietta, System and Program Trades, OTV Concept Definition and System Analysis Study, Vol. III, 1985

Project Argo, Aerospace Engineering Department, Aerospace System Design (Aero 483), The University of Michigan, April 1989

Project Lustar, Aerospace Engineering Department, Aerospace System Design (Aero 483), The University of Michigan, April 1985

Orbital Transfer Vehicle Concept Definition & System Analysis Study, Configuration and Subsystem Trade Studies, Final Report, Vol. II, Book 3, December 1986, Boeing Aerospace Company, Seattle, WA

Advanced Space Propulsion, *Aerospace America*, pgs 60-64, July 1990

Aerospace Forecast and Inventory, *Aviation Week and Space Technology*, pg. 131, March 1991

Nuclear Rockets Gain Support for Propelling Mars Missions, *Aviation Week and Space Technology*, pgs 24-25, March 1991

General Dynamics, Space Systems Division, OTV Concept Definition and System Analysis Study, System & Program Trades, Vol. III, 1986

Chapter 5:

Power

5.0. Summary

A wide variety of power sources were investigated based on present and near future technology. Included in the initial research were Solar Dynamic Power, Nuclear Reactors (in particular the SP-100 under current development), Dynamic Isotope Power Systems, and Microwave Beam Power. The power systems for project UM-Haul were then determined by which systems best satisfy the project's power requirements.

Based on present and near term technology available by the year 2000, primary power sources were investigated and selected for the Unloader and the Lander. The power systems that best satisfy the requirements of UM-Haul are Alkaline Fuel Cells (AFCs), Photovoltaic (PV) arrays and battery system, and Radioisotope Thermoelectric Generators (RTGs). It is from among these three power sources that the final power systems were chosen.

The Unloader power system uses a GaAs/Ge fixed horizontal planar array with NaS as the battery source. The array is body mounted and situated to minimize shadowing, array deflection, and temperature effects. The Lander provides the initial heating of the NaS batteries on the Unloader, and the batteries are supplied with a phase change energy storage system to maintain their operating temperature.

The Lander will use three primary fuel cells to provide power during all mission phases. The Lander's power system is very flexible and can provide a large amounts of power. The three fuel cells allow for triple redundancy. The reason for scaling the Lander's power system so broadly is that the mass of the system was not greatly affected by allowing for larger power output levels and system redundancy. As a result, the Lander can be used in a variety of other missions as a general reusable Lander. The fuel cells utilize the same cryogenically stored Hydrogen and Oxygen reactants that are used in the propulsion system.

Finally, a thermal management system is also briefly discussed. A general system is common between both the Lander and the Unloader. This system consists of Aluminum heat pipes filled with Mercury, creating a thermal link between all the heat generating components of the two vehicles and the radiators located on them. Because the chosen batteries operate at a very high temperature, they require special treatment. The thermal management for the battery system includes a highly insulated box which contains the batteries, and a phase change material called Carbazole which will store excess energy during high operation times, and return the energy during dormant times in order to maintain constant temperatures.

5.1. Unloader Power System Design

5.1.1. Power Requirements

The Unloader has many components that require electrical power, including the locomotion motors, communication equipment, computers, navigation equipment, and payload deployment motors. The necessary power to operate these components must be provided. A breakdown of power needs for the Unloader is shown in Table 5.1. The values in Table 5.1 reflect values during a payload deployment cycle.

Table 5.1 Power Requirements for the Unloader (in Watts)

	Driving	Unloading	Shading	Standby
Computer	10	10	10	0
Communications	24	24	24	10
Navigation	30	0	0	0
Power System	10	10	10	5
Lifting Motors	0	746	0	0
Driving Motors	746	0	0	0
Steering Motors	373	0	0	0
Shading Motors	0	0	93	0
Total Power	1193	790	137	15

The values in Table 5.1 are based on the power needs of equipment selected for the Unloader. The drive motors were selected based on the power necessary to provide locomotion on the lunar surface for the Unloader. The requirements to drive the Unloader were determined based on two estimates. For all estimates, the Unloader's characteristics of a minimum loaded velocity of 0.1 km/hr (0.028 m/sec) and a maximum loaded mass of 10,000 kg were used.

The first estimate uses the Apollo Lunar Rover Vehicle's (LRV) energy rating of 0.1412 Wh/kg/km.[1] The linear scaling based on the LRV yields 141.2 W for locomotion. Due to the differences in purpose of the Unloader and LRV an alternative method was used to estimate the locomotive requirements. The second estimate determines the forces necessary to overcome the worst instance of rolling resistance and an incline of 30 degrees for the fully loaded Unloader traveling at 0.028 m/sec.[2] From this method a maximum power of 624 W would be necessary for locomotion.

Taking the greater value of 624 W from the two estimates for locomotion requirements, the drive motors were selected. The Unloader's eight 1/8 hp drive motors provide 746 W, which is 20% more than the maximum power needed for locomotion. The actual power encountered for locomotion will most likely be much less. Normal locomotion power to maintain the velocity 0.1 km/hr for small inclines and average rolling resistance is 350 W. This gives a range of roughly 0.8

to 1.2 kW that the Unloader can be expected to provide power during driving operations. This range of power is used to allow for operating the drive motors at different power levels to adjust for varying rolling resistances, inclinations, vehicle loaded weights, and desired vehicle speeds.

The energy requirements for the Unloader is based on the total power values of Table 5.1. The energy values are shown in Table 5.2 for one deployment cycle at full drive power. A deployment cycle involves driving the Unloader 300 km away from the Lander, unloading, and then returning to the Lander. Standby power is not included in the deployment cycle because standby power is the power necessary to maintain the Unloader's communication system while in between deployment cycles.

Table 5.2 Energy Requirements for the Unloader

	Driving	Unloading	Shading
Total Power	1193 W	790 W	137 W
Time Required	6 hrs	0.25 hrs	0.083 hrs
Total Energy	7158 Wh	197.5 Wh	11.4 Wh

The total energy of all phases of the deployment cycle is 7.37 kWh. The power system for the Unloader will be expected to supply a minimum of 7.37 kWh of energy for the deployment cycle. A power time line for the Unloader is provided in Figure 5.1.

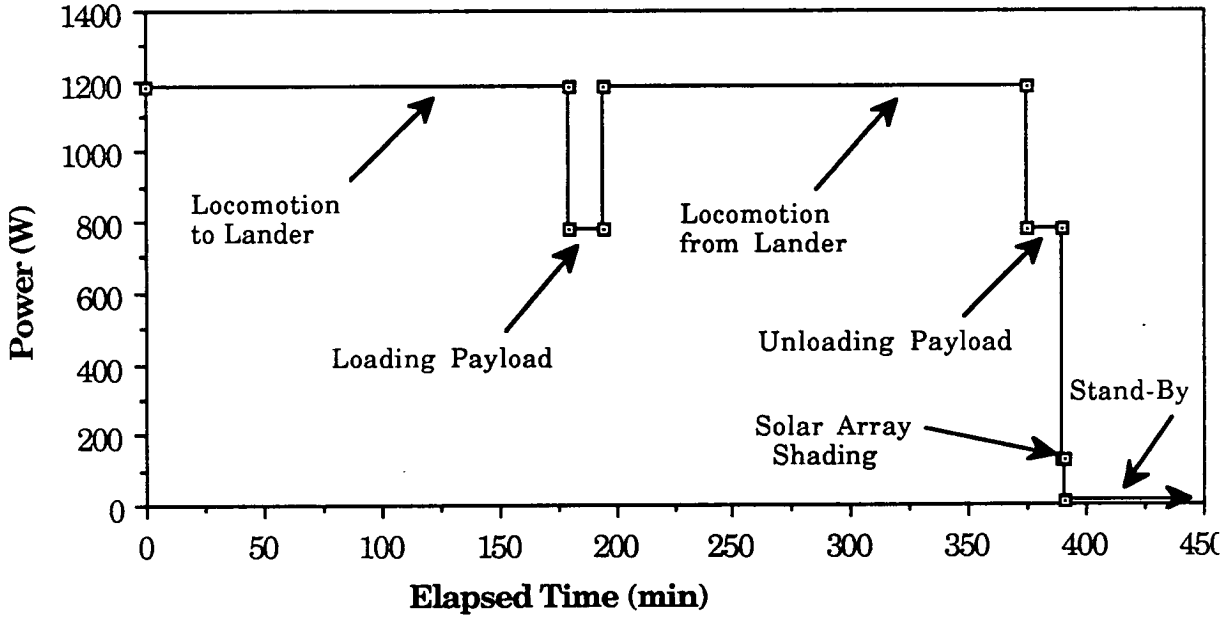

Figure 5.1 - Unloader Power Time Line

5.1.2. System Considerations

In determining the primary power sources for UM-Haul, the focus was on existing technology with a proven history of space usage. Based on proven technologies, estimates were made of future upgrades by the year 2000. The primary power sources that are available for the power needs of the Unloader include Radioisotope Thermoelectric Generators (RTGs), primary fuel cells, and photovoltaic (PV) arrays / battery system.

RTGs were considered because of several important benefits. The benefits of RTGs include long life, proven reliability, ready technology, fully autonomous, and relatively low weight in comparison with lunar night energy storage elements. Despite these benefits, RTGs were eliminated. The primary reason for elimination was the safety factors involved with using RTGs. RTGs pose safety problems due to possible radiation leakage, when human activity is in the vicinity of operations. Although UM-Haul is an unmanned system, lunar operations will involve humans as the lunar base development progresses. In addition to these factors, the high cost of Plutonium (Pu) 238 fuel and the need for extensive thermal cooling also contributed to its elimination. To avoid potential safety problems and the political difficulties in launching and using RTGs in space, RTGs were eliminated from any further consideration for lunar operations. RTGs would be more aptly used for deep space missions such as Mars rovers or spacecraft where accessibility is limited and long life necessary.

The next consideration for power sources was primary fuel cells. While this power source deserves consideration for future lunar applications, it was also eliminated. The elimination was based on the technology and the mission's needs. Using dedicated storage tanks of gaseous Hydrogen and Oxygen, the fuel cells could be used on the Unloader. The fuel cells would have to have a minimum life cycle of 3 years to complete ten payload deployments without reservicing. The current life cycle of fuel cells is about 2,000 hrs.[3] The attainment of long life fuel cells awaits further technological development. While it is likely that 3 year fuel cells will be ready for the mission, it is desired for the mission to have fuel cell lifetimes of 7 to 10 years to allow the Unloader to have a long lifetime on the lunar surface independent of the Lander and maintenance. In addition, volumetrically the fuel cell storage system would be harder to integrate into the Unloader than other storage elements such as batteries.

If fuel cells were to be used on the Unloader, they would have to be refuelled. This would shorten the lifetime of the Unloader and strengthen its dependency on the Lander. This dependency reduces the flexibility of the system. A failure to mate with the Lander at some maximum time interval will lead to a failure in the Unloader's power system. By storing more reactants on the Unloader, the advantage of low mass and volume is compromised. Consequently, the added reactants increase the difficulty of integration with the Unloader. Based on these design considerations, primary fuel cells were eliminated. However, for future missions when refueling can be satisfied by other vehicles or power sources, fuel cells are a favorable alternative due to their high specific energy, resulting in a low weight for the power system.

The third power source available was photovoltaic (PV) arrays. The use of PV arrays has several benefits, including those of space readiness and proven

technology. PV arrays have been used on a variety of space missions in the past and will be used on future projects such as the Space Station Freedom. To execute the mission tasks of the Unloader, the PV array is used in conjunction with a rechargeable secondary power source. The secondary source provides power for the Unloader's communications system during lunar night (i.e. Standby power) and for unloading operations. The PV array serves only to recharge the secondary source and to provide lunar day communications. The PV/Secondary source system is completely autonomous. There is no need for mating with the Lander at any set interval and the life cycle of the system is expected to reach up to 7 to 10 years. Based on these parameters, the PV array is the primary power source used on the Unloader.

5.1.3. Selected System: PV Array

The primary power source for the Unloader is a planar, fixed GaAs/Ge PV array, body-mounted to the Unloader. The selection of GaAs cells is based on their high efficiencies, radiation resistance, and temperature insensitivity. The use of germanium substrates will improve the array's handling characteristics and reduce the array's weight. The projected efficiency of 4 cm by 4 cm, 100 microns thick GaAs/Ge cells is 22%.[4] & [5] Based on these GaAs/Ge cells, the necessary array size is determined. The array size must reflect the power required for standby during the lunar day and for recharging the energy storage system.

The reason for choosing GaAs/Ge cells is because of their low sensitivity to solar radiation and high temperatures of near 90°c experienced on the lunar surface. Etching the solar cells on germanium substrate improves the specific power of the cells and their handling characteristics.[6] Thin film cell technology could be a future alternative, but reliability, long-term operation at high temperatures and vacuum thermal cycling stability must be confirmed. Primarily, only amorphous silicon cells have been produced on thin, lightweight polymer substrates which were used mainly for terrestrial applications.[6] As a result, GaAs/Ge is the best choice for performance, specific power, and ready technology.

5.1.3.1. Sizing of Array

The solar energy flux on the lunar surface is approximately 1350 watts/m^2. Using GaAs/Ge cells at 22% efficiency, the converted energy produced by the array is ideally 297 watts/m^2. For sizing the array, a more conservative efficiency rating of 20% is used to account for the possibility of falling short of the projected efficiencies. At 20% efficiency, the converted energy is Po = 270 watts/m^2. To determine the necessary size of the array, the energy that must be generated by the array during the lunar day is:

$$E_{sa} = \left[\frac{E_e}{X_e} + \frac{E_d}{X_d}\right]$$

Where E_{sa} = The necessary energy to be generated by the array.

E_e = The energy to be recharged during the eclipse cycle (i.e. lunar night).

X_e = The efficiency of the paths from the solar array, through the batteries to the individual loads.

E_d = The energy to be provided during the lunar day.

X_d = The efficiency of the path directly from the solar array to the loads.[7]

The values for the Unloader are as follows:

E_e = 34.8 kWh E_d = 3.36 kWh

X_e = 0.65 X_d= 0.85

E_{sa} = 57.74 kWh

The values for X_e, and X_d are based on a power regulation control system that uses direct energy transfer (DET). A DET subsystem uses shunt regulators in parallel to the array and shunts the array current away from the subsystem. Current is shunted when the loads or battery charging does not need as much power as the array is generating. The value for E_e was determined based on the total energy storage of secondary power source, which is rated at 34.8 kWh (see Energy Storage Requirements). The E_d value is based on 15 W for standby power to maintain necessary communications and power systems for the Unloader during the lunar day. The lunar day/night cycle is 14 days of light and 14 days of darkness. An extra two days are added the the night cycle and two days are subtracted from the day cycle to account times only when the sun has reached a level of 12.5 degrees above the horizon. For the sun angles which are less than 12.5 degrees from the horizon, the PV array will produce little power, and for these calculations it is assumed that the array contributes no useful power.

In continuing to determine the array size, the power losses due to inherent degradation are calculated.[7]

Table 5.3 Solar Array Inherent Degradation

Cause	Degradation factor
Packaging	0.85
Shadowing	1.00
Operating Temperature	0.84
Diode and Harness	0.95

The shadowing number of 1.00 in Table 5.2 reflects no losses caused by shadowing. No shadowing losses are assumed as a result of the careful integration of the array on the Unloader and the added fact that we assume no power generation for sun angles less than 12.5 degrees from the horizon. The temperature losses are based on a degradation rate of 0.25%/°C for temperatures above 25°C. The operating temperature for the array on the lunar surface is estimated to be at a maximum of 90°C, which results in a degradation factor of 0.84. The diode and harness losses are due to inefficiencies, mismatches, and similar factors. The resulting inherent degradation (I_d) is 0.67. The resulting power for no cosine losses generated by the array at the beginning of its life (P_{BOL}) is:

$$P_{BOL} = (P_o \times I_d) = (270\ W/m^2 \times 0.67) = 181\ W/m^2.$$

To determine the necessary size of the array, the array is sized according the the end of life power (P_{EOL}) of the array. P_{EOL} is determined by estimating the degradation of the array over time. The life degradation of the array is estimated at 2.5 % per year, based on 1% per year for radiation damage.[8] Solar flare damage to the array will be substantially less than orbiting arrays. This is because the Unloader's array will be exposed to solar flares only during the lunar day. In addition when the Unloader's array is not exposed to any radiation effects when it is aboard the Lander. It is noted that the life degradation factor may be reduced if such techniques as annealing radiation damaged cells are employed. Based on a life cycle of 10 years, the total life degradation (L_d) factor is 0.776. P_{EOL} for no cosine losses is determined by:

$$P_{EOL} = (P_{BOL} \times L_d) = (181\ W/m^2 \times 0.776) = 140\ W/m^2.$$

Next, the amount of energy generated by the PV array during lunar day for P_{EOL} is determined. To account for the cosine effects experienced during the lunar day, we perform the integral shown below:

$$2P_{EOL} = \int_{24}^{168} \sin(0.00936t)\, dt$$

This equation represents the total energy (in Wh/m^2) generated by the array during the lunar night phase. To account for the fact that the power generated by the array when the sun is below 12.5 degrees from the horizon, the equation eliminates in the first and last 24 hrs of lunar daylight. The number 0.00935 is the change in angle measured in radians per hour, during the lunar day. From this

equation and with P_{EOL} = 140 W/m^2, E_{array} = 29.2 kWh/m^2. The necessary array size can now be determined as follows:

$$A_{array} = \left[\frac{E_{sa}}{E_{array}}\right] = \left[\frac{57.74\ kWh}{29.2\ kWh/m^2}\right] = 1.98\ m^2$$

This area, however, does not reflect the effects of lunar dust over the life cycle of the array, nor does it account for factors such as stresses and breakage associated with transportation of the Unloader on the Lander. Lunar dust is electrostatically charged and abrasive. When some activity disturbs the lunar dust, it would adhere to the Unloader. The effects of lunar dust is to coat and degrade the performance of the solar array, as well as increase the operating temperature of the array. Because the Unloader travels at a very slow speed of 0.1 km/h and with employing a cover shield for the array, the array experiences small accumulations of lunar dust over a possible life time of 7 to 10 years.

To account for these factors, redundancy, and a contingency factor, the array area will be oversized. Due to the availability of a large surface area on the Unloader, the array can be substantially oversized to allow for redundancy and other degradation factors. The oversized array allows for over 55% array loss without sacrificing critical power needs. The newly sized array which is used on the Unloader is 4.5 m^2.

5.1.3.2. Array Characteristics

Now that the power needed to be generated by the array, and the array size have been determined, the performance of the array is now shown. The characteristics of the GaAs/Ge array are shown in Table 5.4. The dual junction GaAs/Ge cells are based on the cell types used on the HS-601 oriented flat plate array developed by Hughes Aircraft Company.

Table 5.4 Solar Array Characteristics

Array Characteristic	
Cell type	GaAs/Ge
Cell mounting	Shingled
Number of Panels	2
Number of Cells	2800
P_{BOL}	815 W
P_{EOL}	630 W
Operating temperature	81°C
Array voltage	29 V
Array mass	12 kg
Array area	4.5 m^2
Cost	$2 million

The array's P_{BOL} is 814.5 W (based on 181 W/m^2) and the array's P_{EOL} is 630 W (based on 140 W/m^2). The array's mass can be determined using projected specific powers. The array structure mass for a GaAs/Ge array is estimated at 12 kg (based on 66 W/kg specific power applied to P_{BOL})[4] & [12]. The assumption of 66 W/kg specific power is valid since lightweight arrays such as Hughes FRUSA and Lockheed SAFE designs have demonstrated such ratings. In addition, deployment mechanism and structural support elements are eliminated or reduced in body-mounting designs. The Unloader will provide the structural support for the array's substrate.

The number of cells used in the array is 2800 cells. This gives an array area of approximately 4.5 m^2. The array's operating temperature is likely to be 81°C on the lunar surface. The cost of the array is estimated assuming that advances in cell manufacturing will reduce the GaAs/Ge cell costs to be of the same order as current Silicon.[5] & [9] The cost estimate is 2 million dollars (based on $2500/W).[7]

The GaAs/Ge cell characteristics are listed in Table 5.6.[4] & [5]

Table 5.5 Solar Cell Characteristics

Cell Characteristics	
Cell type	GaAs on Ge
Cell size	4 cm x 4 cm
Cell thickness	100 microns
Cell efficiency	22%
Cell V_{oc} (28°C,BOL)	1.32 V
Cell I_{sc} (28°C,BOL)	0.491 A
Temperature Variation V_{oc}	- 0.37%/°C
Temperature Variation I_{sc}	+ 0.045%/°C

There will be two solar panels located on the opposite sides of the center line of the Unloader. There are 28 cells connected in series to form a series string. In each panel there are 50 series strings. Five of the series strings are connected in parallel to form a redundant circuit group. Ten circuit groups are connected in parallel to the panel bus.

A schematic of the elements a solar cell are illustrated in Figure 5.2.

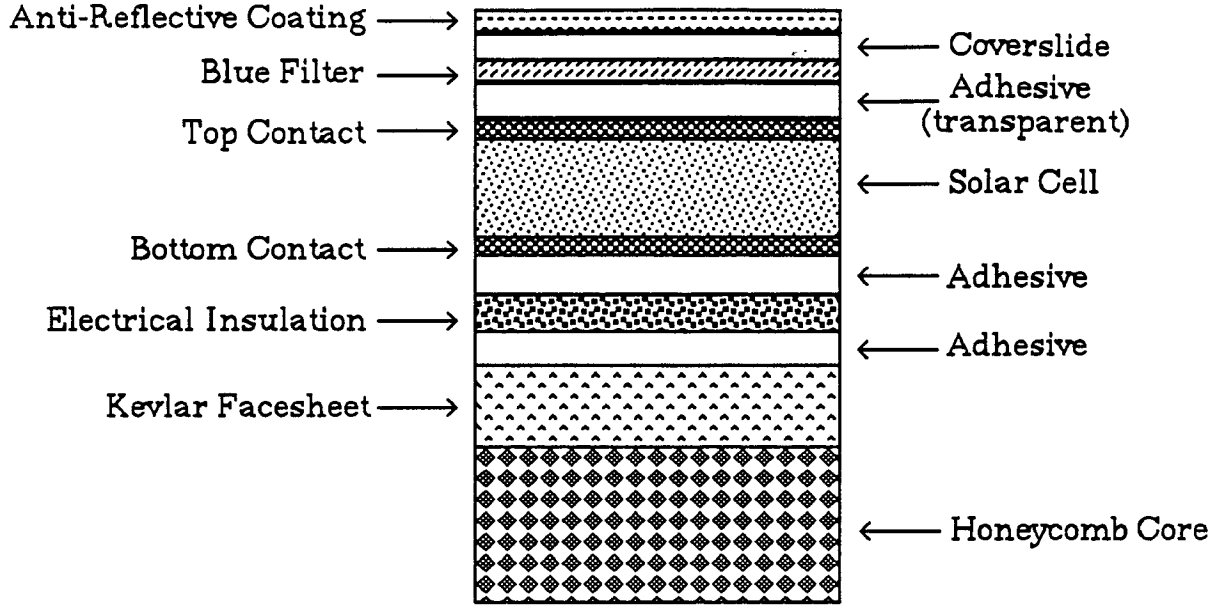

Figure 5.2 - Solar Cell Elements

The coverslide protects the cell from solar radiation, the thicker the coverslide, the greater the protection. The coverslide is textured for body-mounted cells that do not track the sun. The textured coverslide reflects incident solar energy back into the cell. A blue filter blocks ultraviolet rays which cause heating and adhesive degradation. The facesheet substrate holds the solar cell modules and their interconnections. The honeycomb core is made of Aluminum and is used for support.

5.1.3.3. Array Mounting

The array was integrated with the Unloader by body-mounting it on top of the Unloader's large surface area. Body-mounting the cells was chosen because of the large available surface area on the Unloader and for the ease of integration. The array is fixed horizontally onto the Unloader. Since, the array does not track the location of the sun, the fixed array has less complicated circuitry than tracking arrays. In addition, since the array is body-mounted, it does not have to risk failure in deployment and retraction that retractable arrays would face. The deployment and retraction of solar arrays on the lunar surface is further complicated by the effects of lunar dust adhering to the deployment mechanism.

The placement of the array reflected efforts to minimize temperature effects on or by the array with other loads. Also, the array will be placed to minimize shadowing and cell structural deflection. The cell configuration is shingled, which means the cells are series connected in stair shaped fashion as shown in Figure 5.3

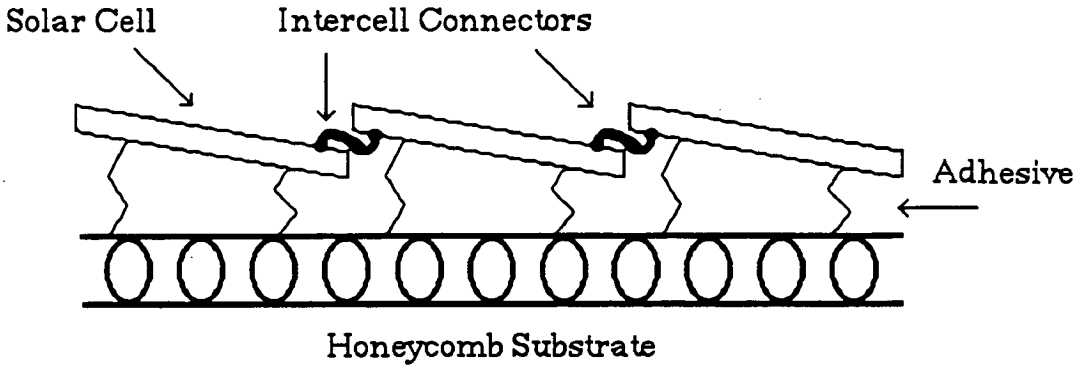

Figure 5.3 - Shingled Solar Cells

The body-mounted cells are mounted to light metallic sheets that are then attached to the Unloader. The shingled configuration will allow for more flexibility in the array to aid in adjusting to structural deflections. The cell interconnections should be of the same coefficient of thermal expansion is the same as the cell crystal. For GaAs cells, silver plated KOVAR plate can be used as the interconnector.[10]

5.1.4. Energy Storage Requirements

The secondary power source of the Unloader is expected to maintain power during lunar eclipse for standby communications and for deployment operations. The minimum energy storage for lunar night has been calculated to be 5.76 kWh. This figure reflects 15 W of standby power for 16 days. The total required energy storage has been calculated to be 16.33 kWh, which reflects both night time maintenance and daytime deployment operations (see Unloader Power Requirements), plus a 25% contingency factor. The final sizing of the energy storage system must also reflect the depth-of-discharge (DOD) of the secondary source and redundancy factors.

5.1.5. The Unloader Energy Storage System

The energy storage system for the Unloader fully satisfies the needs of the mission cycle. The charge discharge period for the Unloader is 12 days of charging and 16 days of discharging. The energy storage system was chosen to reflect a low system mass, a low self-discharge rate, and near term readiness with low development costs and risks.

Based on these criteria, the main storage contenders are regenerative fuel cells (RFCs) and Batteries. Nickel-Hydrogen batteries, although in plans to be used on a wide variety of future systems, did not meet our needs because they have a very high self-discharge rate. Over 72 hours, Ni-H2 batteries would have self-discharged to 70% their capacity.[17] Sodium-Sulfur (NaS) batteries using beta alumina electrolyte. While both technologies require further development, it is projected that NaS batteries are more likely to satisfy the Unloader's energy storage needs first. Based on this factor and the problems of obtaining long life reliable RFCs, NaS batteries were chosen. Since the NaS batteries would

experience a low number of recharging cycles (130 cycles in 10 yrs) on the lunar surface, development of the batteries is greatly facilitated for UM-Haul. However, improvements from the current status of NaS batteries must be assumed. A problem area for the NaS batteries has been the failure of its ceramic electrolyte known as beta alumina. Improvements on seals for NaS batteries must also be realized before their usage.

NaS batteries have a operating temperature of 350°C, but can still operate, although very inefficiently, at 180°C.[20] The initial heating of the NaS batteries heaters will be provided externally by the Lander. However, since the lunar night temperatures can reach 104 K and the batteries will be discharging at a slow rate, it is probable that battery freezing may occur. This requires that they have special thermal management systems to protect them. This is discussed in further detail in section 5.3.2.1.

5.1.5.1. Battery Sizing

The NaS specific power is estimated at 150 Wh/kg by the year 2000.[13] Projections for NaS batteries may increase this number to 220 Wh/kg within the near future. NaS batteries have an allowable 80% depth-of-discharge (DOD) rate during operations. To prolong the life of the NaS batteries to 7 to 10 years, the normal operation DOD is 50% for the Unloader system. The operating temperature of the NaS batteries is 350°C. NaS batteries are rated at a 90% efficiency.

To size the battery system, the following formula is used below:

$$N = \frac{P_e T_e}{(C_d C_r V n)}$$

where: C_r = Capacity rating of each battery in Ah (amp-hours).

$P_e T_e$ = Necessary energy storage in Wh.

C_d = Limit on DOD of the battery system.

N = Total number of batteries.

V = Operating voltage.

n = Transmission efficiency between battery and load.[7]

Based on V= 29 volts, PeTe being 16.33 kWh, C_d being 50%, n = 0.9, and C_r = 200 Ah the number of batteries needed are 6. The 50% DOD is only achieved if the batteries must drive both daytime deployment and nighttime power without in-between recharging. For most scenarios, the batteries recharge between the deployment operations and the night time discharge. As a result, the battery system experiences a less severe DOD than the 50% DOD used in the initial sizing.

5.1.5.2. Battery Characteristics

The six NaS batteries used as the energy storage system for the Unloader are characterized in Table 5.5.[11]

Table 5.6 NaS Battery Characteristics

NaS Batteries	6
Modules per Battery	2
Cell Series Strings in Parallel	2
Cell in Series String	14
Cell voltage	2.08
Battery voltage (V)	29
Battery Operating Temperature	623 K (350°C)
Cell Capacity (Ah)	50
Battery Capacity (kWh)	5.8
Battery System Capacity (kWh)	34.8
Battery System Mass (kg)	232
Battery System Cost ($)	3.5 million

The cost of the battery system is based on ($100 K/ kWh) and is approximately $3.5 million.[13] As indicated in Table 5.6, there are two modules per battery. Each module contains two parallel strings of 14 series connected cells. The two modules are then connected in parallel to form the battery. The cell configuration for a module is shown in Figure 5.4.

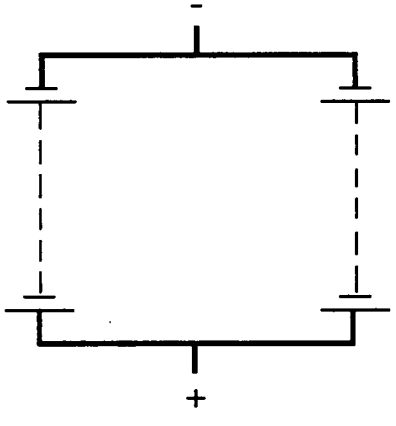

Figure 5.4 - NaS Module Cell Configuration

The specific energy rating for NaS batteries is 150 Wh/kg. This specific power value includes cells, thermal containment and control, mounting structures, and hardware. Based on the total battery capacity of 34.8 kWh for the selected 6 NaS batteries, the total mass of the battery system is 232 kg. Further attributes of the battery system is shown in Table 5.7.[11]

Table 5.7 - Module Characteristics

Number of NaS cells	28
Number Na/Na cells	2
Number of heaters	1
Length	0.76 m
Width	0.16 m
Height	0.60 m
Volume	0.073 m^3
Mass	19.3 kg

Based on the module dimensions in Table 5.7 and that there are 2 modules per battery, the total volume of the battery system is 0.875 m^3. Redundancy is factored into the system by the fact that if a cell fails in one of the series chain, the total capacity of the chain is not loss. Only after several cell failures in a series chain, will that chain no longer be able to contribute to the power system. By having the battery composed of two modules in parallel, failure of individual cells in the battery are also reduced. In this cell configuration if a cell failure occurs, the failed cell should exhibit a low resistance. If a high resistance failure occurs the battery could be incapacitated after the failure of a few cells. As a result, the cells used on the Unloader's battery system are assumed to have a low resistance failure mode.

5.1.6. Power Architecture and Control

The solar array is divided into two panels which are then connected to a two-bus configuration which provides redundant power for all critical redundant loads on the Unloader. Redundant blocking diodes are used to connect the panel power lines to the main bus lines, which prevents battery leakage into the panels. A schematic of the bus configuration is shown in Figure 5.5.

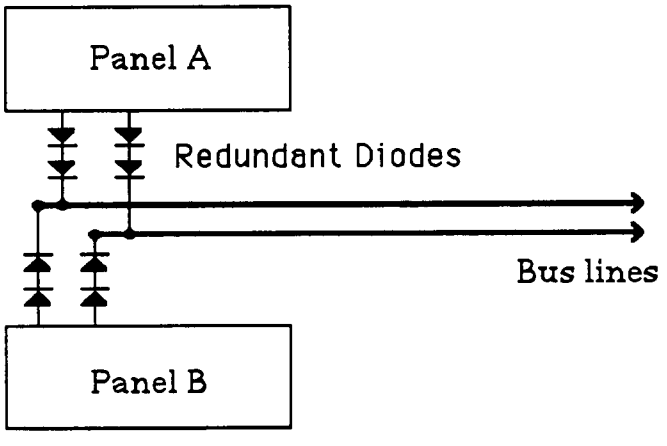

Figure 5.5 - Panel Bus Configuration

In the redundant circuit groups used in each panel, bypass diodes are provided for every four cells in series. These diodes prevent damage to the solar cells due to shadowing or current generation mismatch. Shadowing effects are important because a solar cell goes into open circuit, becoming high resistance, when it is not illuminated. For the series connected cells, the shadowing of one cell can cause the loss of the entire string. As a result, bypass diodes, which bypass groups of cells in series, help prevent damage to shadowed solar cells.

The method chosen for controlling the power generated by the solar array, is to use a direct energy transfer (DET) subsystem. The DET system will dissipate power through the use of an external bank of shunt resistors. Shunt regulation is used to maintain the bus voltage level. The shunt regulator functions in parallel to the array. Its purpose is to shunt the array current away from the subsystem when the power is not needed. As a result,the output voltage level varies. An error sensing circuit controls the shunt impedance, thereby varying the amount of bypass current so that the bus voltage remains relatively constant. This form of regulation was chosen over other forms because of its lower mass and higher efficiency at EOL.

The selected bus voltage for the Unloader is the standard 28 Volts DC . The power range for the Unloader during operations is 0.79 to 1.19 kW, which results in a current range of 28.2 to 42.5 amps. The bus for the Unloader will be fully regulated. An example of how the bus can be regulated is shown is Figure 5.6.[7]

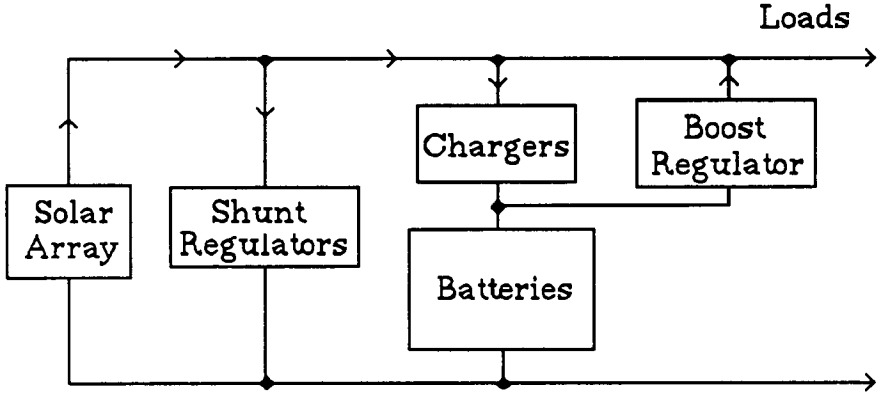

Figure 5.6 - Power Bus Voltage Control

The fully regulated bus will maintain the desired bus voltage during both battery charge and discharge. Regulating the bus voltage is necessary to maintain a near constant voltage. The battery voltage can vary from charge to discharge. A regulated bus compensates for battery voltage fluctuations.

Charging the batteries can be done either in parallel or independently. For the Unloader's power system, the batteries are charged individually with the charger in series with the battery. By charging the batteries independently, the batteries will degrade as little as possible. The batteries are all charged to their individual limits, prolonging battery life. Since the Unloader's battery system has several batteries, as battery life progresses, individual charging will adjust for battery

performance changes. There are six charger/battery units on the Unloader. The batteries will be charged using constant current limiters.

Due to complexity reasons and the high operating temperature of NaS cells, monitoring cell voltages individually is not practical. Instead, the series chain of cells will be monitored as a group of cells. To control DOD levels, Na/Na coulometers are connected in series with the series cell chain. The passage of current through a Na/beta alumina/Na cell alters the Sodium level which is detected by the Na coulometer.[11]

Charging rates for the Unloader from the solar array is C/40, which results in a battery being charged at 5 amps for 40 hours. Higher charging rates are also used. For an occasional charging from the lander, C/4 is used. This rate charges a battery in 4 hours at 50 amps.

Using Na coulometers in each series chain helps control overdischarge due to cell failure. As was mentioned previously, when a cell failure occurs, it is assumed to fail at a low resistance state. However, the failed cell will alter the voltage of that series chain. Due to the potential difference, the higher potential chain will discharge into the low potential chain. A coulometer prevents this overdischarge.

The Layout of the power system can be shown in general block diagram form in Figure 5.7.

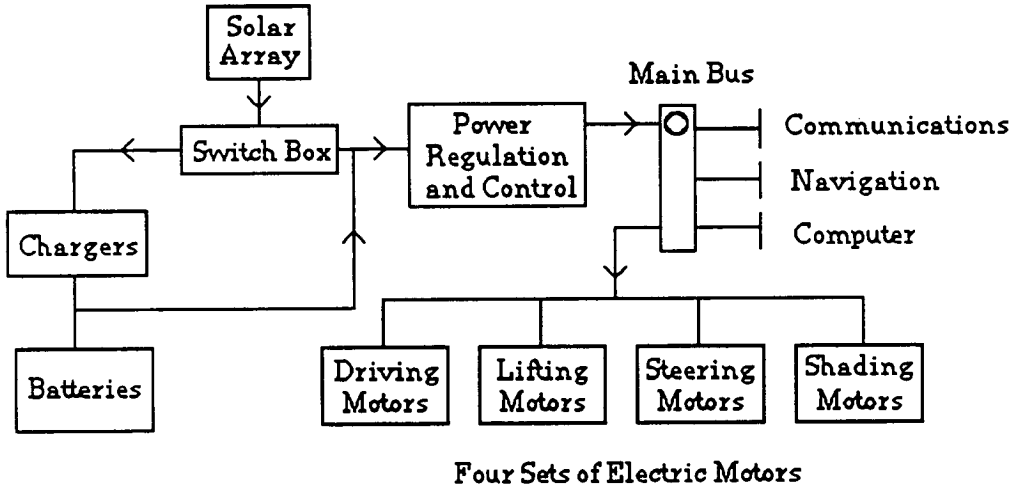

Figure 5.7 - Unloader Power System

In the Unloader's power system converters are connected in series to the individual loads. Converters alter the main bus characteristics to meet the requirements of the specific loads, such as operating voltage. Fuses connected in series with the power bus are used to protect the system against load failure. A load failure typically implies a short circuit which will draw excess power which stresses cables and drains storage. Isolating the fault is accomplished using

fuses. Fault-detection circuits can be added to essential areas of the power system to relay where the fault occurred.

The electrical power is distributed to the many subsystems around each of the vehicles via Aluminum cabling. Copper has a higher electrical conductivity rating, however, for our purposes, Aluminum cable introduces virtually negligible power losses at a significant mass reduction over Copper because of Aluminum's lower density. The cables are also be insulated by 20 layers of Multi-Layer Insulation (MLI). MLI is discussed in greater detail in Section 4.7.3.4.

The cable network to the Lander's entire Guidance, Navigation and computer systems has a diameter of 1.2 cm, resulting in a 0.34 W power loss. However, this is only 0.1 % of the total power passing through that section of cable. For other systems on either vehicle requiring more than 50 W the cable network has a diameter of 1 cm, resulting in 0.03% power loss. For the 20-50 W range, cables of 0.5 cm diameter are used, resulting in 0.5% power loss. Any cables powering systems that require smaller than 20 W loads have a diameter of 0.25 cm, resulting in a 0.05% power loss.

The total mass of the cabling and the insulation for the Lander is 19 kg, and the total mass of the cabling and insulation for the Unloader is 27.56 kg.

Based on the above power regulation and control elements, an estimate of the total mass for the power system is shown in Table 5.8

Table 5.8 Power System Mass

Solar array	12 kg
NaS batteries	232 kg
Regulator/Converters	30 kg
Control Unit	24 kg
Cables	20 kg
Miscellaneous	32 kg
Total Mass	350 kg

The masses for power regulators, converters, and the control unit are based on a scaling factor for the amount of power regulated or controlled. A final mass analysis would include thermal management factors such as radiators.

To allow for recharging of the NaS batteries by the Lander, another power line can be tied into the Unloader. This power line will go to the six charger/battery units only to provide recharging.

5.2. Lander Power System Design

5.2.1. Power Requirements

The Lander's power system has been estimated based on the Apollo Lunar Module's power needs. It had a peak power of 2.2 kW. The Lander's power requirement's were based on allocations of power estimates to specific subsystems. This design method has allowed for all the systems currently on the Lander as well as unforeseen systems and future upgrades. Table 5.9 shows the power allocation breakdown for the Lander.

Table 5.9 Lander Power Requirements

Computer	100 W
Communications	80 W
Navigation	300 W
Engines	300 W
Reaction Control Syst.	50 W
Ramp Motors	200 W
Heaters	250 W
Power System	10 W
Electric Pumps	100 W
Latching Mechanisms	20 W

Based on these allocations plus a contingency factor for unforeseen equipment, the Lander's power system should be able to provide power up to 1.5 kW. A factor not included in Table 5.9 is the capacity to recharge the Unloader's batteries, in the event that they are not sufficiently charged for a payload transfer. Also, the Lander must provide power to the NaS battery heater for the initial heating of the NaS batteries.

It may furthermore be desirable to provide power to the payload. Although the Unloader does not need to provide power to the payload, the Lander may be used in different capacities in future missions.

A power time line for the Lander is shown in Figure 5.1.

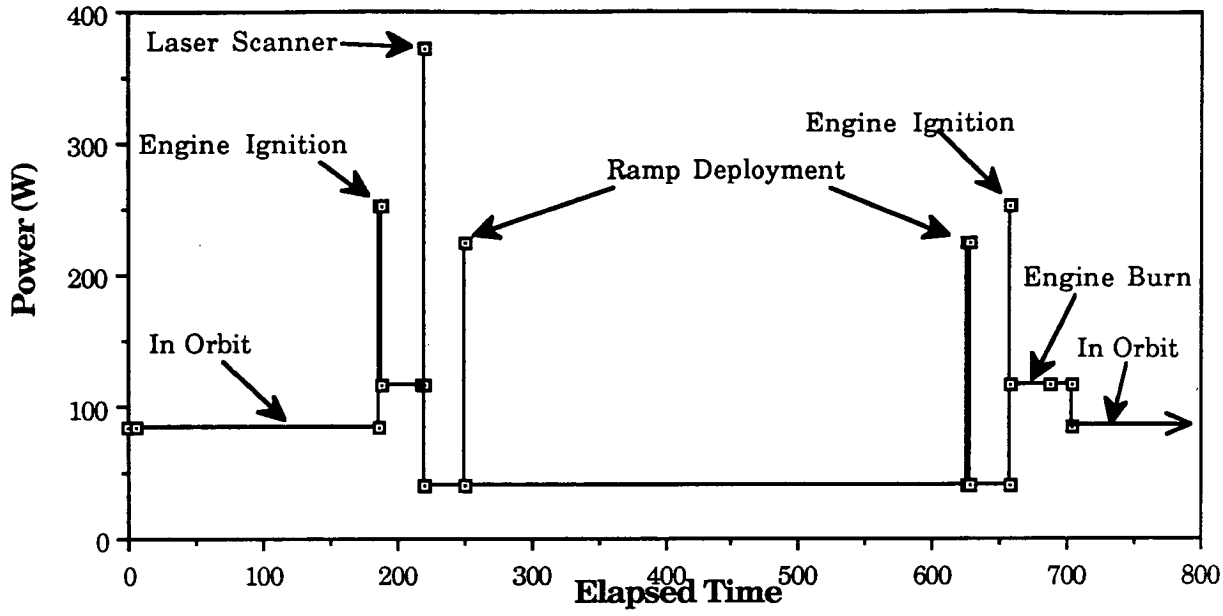

Figure 5.8 - Lander Power Time Line

5.2.2. Available Power Sources

Applying the results from the research on primary power sources for the Unloader, the two main power system candidates for the Lander were a retractable PV array/battery system and primary fuel cells.

In order to collect sufficient sunlight, a Lander-based array would have to be deployable away from the body structure. This has some disadvantages.

While a retractable PV array is currently under development, the reliability of such an array is uncertain. If the array fails to deploy or retract, the mission must be aborted and the Lander must be retrieved within a certain time frame. If the array is deployed when the failure occurs, this will complicate the docking procedure with the OTV, and the array may need to be jettisoned. In addition, the battery system on the Lander may need to withstand 10,000 recharge cycles in LLO to complete its mission. NaS batteries are not currently able to withstand such cycling, and future development of such a system would be further into the future than for low levels of cycling.

Next, Nickel-Hydrogen (Ni-H_2) batteries were considered. However, Ni-H_2 batteries have a lower specific power which results in a larger power system mass. To minimize storage mass, the Lander should recharge the Unloader batteries by means of its deployable PV array. This process, however, exposes the array to lunar dust which may effect the deployment/retracting mechanism and reduce the array output. The only alternative to supplying an extra power source or massive batteries, is to take the Unloader up to LLO and then recharge the Unloader. This is clearly very costly. As a result of the difficulties with an active Lander using a PV array/battery system, this power system was eliminated.

5.2.3. Selected Lander Power System

The power system chosen for the Lander consists of fuel cells. The only power failures that can arise in this system are due to failures at the power plant source or its internal distribution system. It is logistically easier to provide redundancy in an internal system to minimize failure possibilities. In addition, the fuel cells need not have dedicated storage tanks for the reactants. The fuel cell reactants (Hydrogen and Oxygen) are stored cryogenically with the engine propellant. The mass and volume of the fuel cell system is low.

Fuel cells have been used in the Apollo mission and on the Space Shuttle, but long life fuel cells which require little maintenance have yet to be ready for space missions. The required fuel cell life time is 3 years for this mission, after which refurbishment of the fuel cells is necessary.

Based on the figures of merit of the Space Shuttle's power system, the Lander fuel cell system is custom sized. The Space Shuttle has three fuel cells which provide power of up to 7 kW each. The Lander's power needs are modest, so the fuel cells can be remodulated to allow for a smaller size, mass and power. The fuel cells for the Lander are outlined in Table 5.10.[14]

Table 5.10 - Integrated Alkaline Fuel Cell System

Number of fuel cells	3
Reactant Mass	500 kg
Total Fuel Cell Mass	204 kg
Total Volume	0.168 m^3
Voltage	28 to 32.5 V
Power Output per Fuel Cell	4 kW
Operating Temperature	355 K (82°C)
Operating Pressure	0.4 MPa
Total Mass	704 kg
Total Cost	$6 million

The reactant storage necessary for the Lander is based on a maximum period of 4 months without refueling from the OTV. Based on a standby power of 90 W (see Fig. 5.8) over a 4 month period at a reactant consumption rate of 0.36 kg/kWh, the Lander consumes approximately 100 kg of reactants.[1] This number is bestowed with the substantial safety factor of 5, taking into account boil-off and leakage problems and a contingency for (as yet unspecified) needs for fuel cell pump power, engine control, RCS, payload tending and emergency operations. Thus emerges an estimated reactant mass of 500 kg.

Although long-term storage of reactants is shared with the propulsion systems, sets of intermediate Hydrogen and Oxygen tanks are used to house gaseous reactants. The byproduct of the fuel cell, water, is rejected to space via discharge lines. The estimated cost of the fuel cells are based on the Space Shuttle's fuel cell costs of 2 million dollars each.[12] Not included in the cost is development costs and reactant cost. A general schematic of how a fuel cell works is shown in Figure 5.9[15]

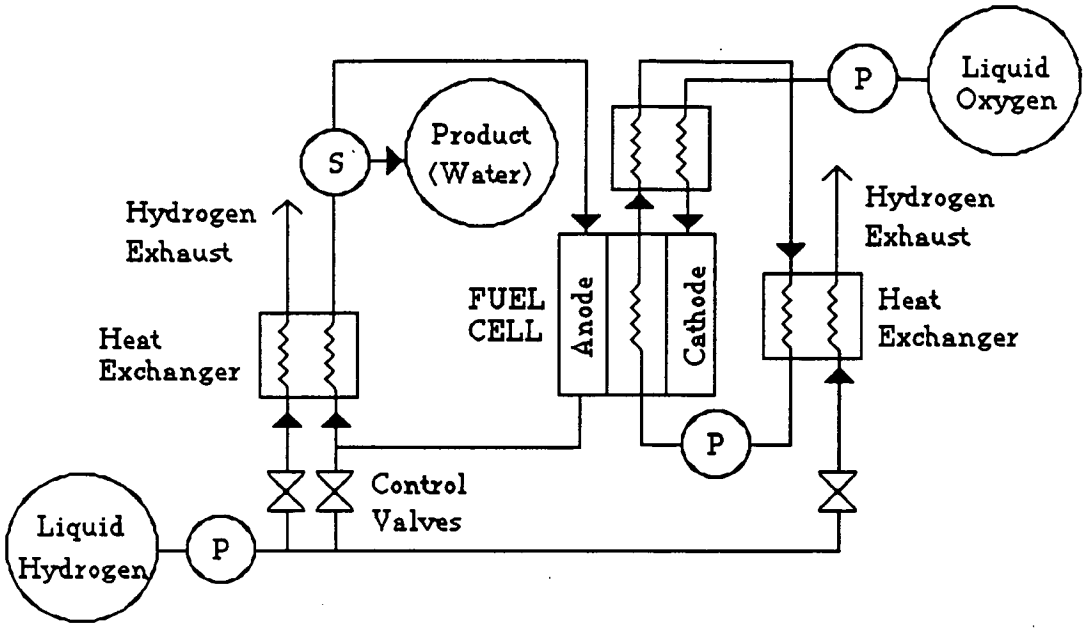

Figure 5.9 General Alkaline Fuel Cell

In Figure 5.8, a P signifies a pump, and each S represents a pump/separator. The heat exchangers are used to transform the liquid reactants to gaseous form. In the actual Lander design, there are three fuel cells, each with a set of intermediate Hydrogen and Oxygen tanks that contain gaseous reactants.

The characteristics of the fuel cells used on the Lander are shown in Table 5.11.[16]

Table 5.11 - Characteristics of Each Fuel Cell

Electrolyte	KOH
KOH Concentration	30 to 40%
Number of Cells	36
Efficiency	60 %
Length	28 cm
Width	28 cm
Height	71 cm
Volume	0.056 m^3
Mass	68 kg
Power Output	4 kW

The fuel cells have been estimated to have a life cycle of 30,000 hrs. To obtain this level of performance, further development is necessary from current technology. However, the benefits of primary fuel cells integrated with a liquid Hydrogen and liquid Oxygen system are significant, and such development will be likely for precursor vehicles such as the Orbit Transfer Vehicle (OTV). If the OTV uses fuel cells, then development costs for the UM-Haul fuel cells will be greatly reduced.

The fuel cells have purge lines to eliminate contaminants from the porous electrodes of the fuel cells. A general block diagram of the fuel cell is shown in Figure 5.10.

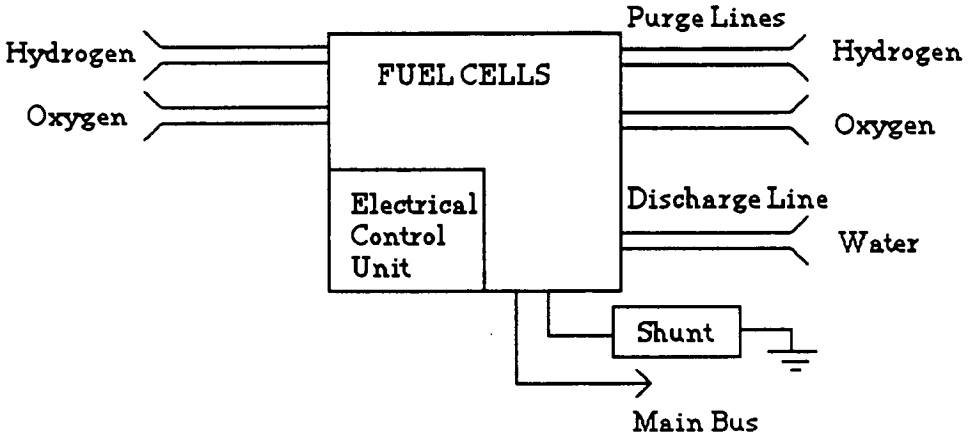

Figure 5.10 - Fuel Cell with Purge Lines

The purge lines and water discharge lines have heaters to relieve the lines of any blockage by the formation of ice. For redundancy, the are two thermostatically controlled heaters. The electrical control unit has the start-up logic as well as controls for the heaters.

5.2.4. Power Architecture and Control

To provide for system redundancy, three fuel cells are used on the Lander. Each of these will be independent resulting in three main buses. A schematic of the power system is shown in Figure 5.11.

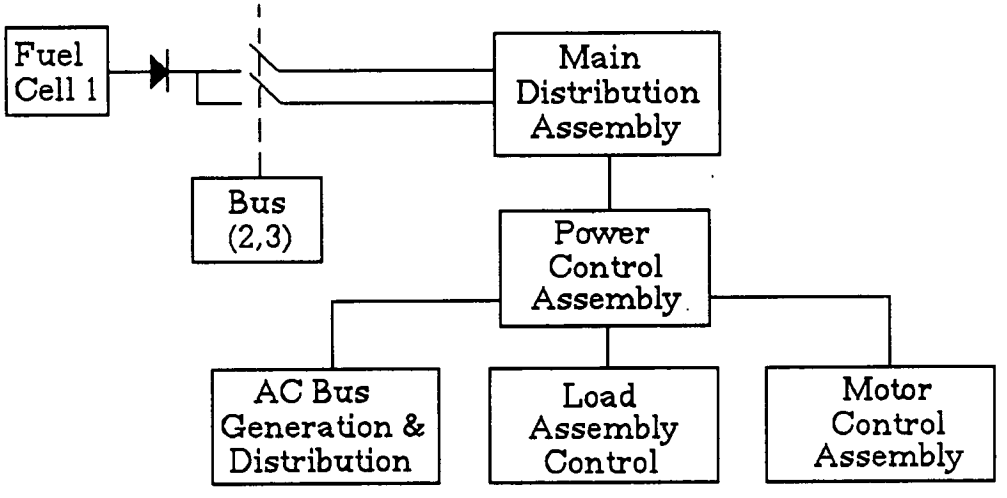

Figure 5.11 - Lander Power System

The power layout of the Lander is based on the configuration of the Space Shuttle. Less architecture is needed than in the Space Shuttle due to the decreased complexity and loads.

The three buses generated by Fuel Cells 1,2 and 3 are cross-strapped to allow for load switching in case of a failure, and the main buses operate independent of each other. The loads on the Lander are diode isolated to assure that if excess demands by a load on a particular fuel cell occurs, the load will be switched to another fuel cell. A particular heavy load on the power system would occur if the Unloader's batteries need to be recharged by the Lander. Additional load outlets will be available on the lander to provide power to the payload if such a situation becomes necessary.

The masses for the the Lander's power system are shown in Table 5.12

Table 5.12 Lander Power System Masses

Fuel Cells	204 kg
Stored Reactants	500 kg
Regulators/Converters	50 kg
Control Unit	30 kg
Cables	19 kg
Miscellaneous	47 kg
Total Mass	850 kg

5.3. Thermal Management

One of the important facts of outer space is that there is no atmosphere to contend with. In some cases this is helpful, but in the case of thermal management, it causes some major problems that need to be addressed. In space there is a great variation of temperature between sunlit areas and shaded areas because of the lack of a medium for conduction (the transfer of energy through static material by means of molecular energy) and convection (the transfer of energy via moving fluid, to equalize temperatures). Therefore, the vast majority of energy transfer is by means of radiation.

The heat transfer formulas for conduction, convection, and radiation follow:

Conduction equation: $$\frac{q}{A} = k\frac{T_1-T_2}{t}$$

Convection equation: $$\frac{q}{A} = k\,(T_1-T_2)$$

Radiation equation: $$\frac{q}{A} = \varepsilon\sigma(T_1^4-T_2^4)$$

Where

q: Heat transfer rate

A: Area of contact,

k: Thermal conductivity

T_1: Temperature of hot surface

T_2: Temperature of cold surface

h: Convection heat transfer coefficient

ε: Emissivity

σ: Stefan-Boltzmann constant

t: Thickness of material between hot and cold surfaces

While the Lander and Unloader are on the surface of the Moon, they are subject to solar radiation and heat from the surrounding landscape. Without protection, this would cause unwanted thermal gradients of large magnitudes in the structures of the systems. The gradients are also temporal, as the thermal stresses vary with the phase of the mission cycle and the occurrence of lunar night. To combat this, the vehicles are coated in white paint (solar absorptivity of 0.25)[18] to cut down on solar thermal load.

While the Lander orbits around the Moon, it will experience a greater thermal gradient because of the absence of the sunlight reflecting from the regolith. Extra protection in the form of reflective coatings, such as silvered Teflon (solar absorptivity of 0.08)[18], will be added to a side and the top of the Lander. With only one side of the Lander protected, it will then enter into a spin with the same period as the Lander's orbit around the Moon. In this fashion, the Lander will constantly expose the protected side to the Sun. The top of the Lander will be protected for the time that it is on the lunar surface. However, this provision controls only a part of the heat influx on the system; there is a considerable amount of thermal energy produced from many of the subsystems on the vehicles.

5.3.1. Thermal Energy Generated

Subsystems such as the fuel cells, the on-board computers, communication systems and the batteries all produce heat from the resistance in their electrical circuits. This thermal energy has to be controlled so that the systems do not overheat. Since there is no atmosphere, radiation is the only method for removal of this excess heat. Most of the subsystems, however, are not designed to effectively radiate thermal energy to maintain the proper working temperatures. Thus, some form of a thermal management system is needed.

In the case of most electrical systems, such as the computers and communications systems, the energy required to operate will be transformed into thermal energy produced. (For clarity, heat will be expressed in thermal Watts, W_t, and electrical power will be expressed as electrical Watts W_e) For example, if a component required 50 W_e to operate, it will produce 50 W_t in heat. However, the fuel cells on the Lander and the NaS batteries on the Unloader are special cases in terms of the amount of heat produced, because they generate energy, rather than use energy. The Lander's fuel cells operate at a 70% efficiency.[19] Therefore, in order to produce 28 V, they theoretically should be producing 40 V. The difference between the theoretical voltage and the actual voltage is the contributing factor to the thermal energy produced by the fuel cells. Therefore, with the fuel cells operating at 400 W_e (28 V and 14.3 A), the theoretical voltage would be 40 V. With these values, it can be found that the thermal energy produced by the fuel cells is

172 W_t. The Unloader's NaS batteries operate at 350 °C. For every 1W_e they produce, they will also produce 0.2 W_t.[20] Therefore, operating at a maximum of 1180 W_e, they will produce 236 W_t of heat. A breakdown of the thermal load produced by the Lander is compiled in Table 5.13 and the thermal load produced by the Unloader is compiled in Table 5.14.

Table 5.13 - Thermal Loads for the Lander

System	Thermal Load Produced (W_t)
Fuel Cells	172
Computer	15
Motors	400
Communications	24
Guidance Navigation and Control	343
Total:	**954**

Table 5.14 - Thermal Loads for Unloader

System	Thermal Load Produced (W_t)
NaS Batteries	236
Computer	10
Motors	1180
Communications	24
Guidance, Navigation and Control	30
Total:	**1480**

5.3.2. Thermal Management Systems

5.3.2.1. Sodium-Sulfur Batteries

The Sodium-Sulfur (NaS) batteries, because of their high operating temperatures, allow for special measures for their thermal control. They will be stored in a heavily insulated box. This will protect the surrounding structure and sub-systems from the unusually high temperature. To operate, the batteries must attain a temperature of at least 180 °C. During the day time, from solar radiation, they will not attain this temperature, and will require approximately 9 kW_t-hr of energy to be ready to start discharging. Once they are running at normal operating levels, they produce the heat needed for operation.

During night time operations, however, the power load on the batteries is relatively small compared to their high capacity. This creates a problem when it comes to keeping them at operating temperatures. The box, being insulated will help keep these temperatures, but no system is 100% efficient. Therefore, to maintain operating temperatures, a phase change substance is also present in the storage box. Any extra volume in this box will be filled with an organic

substance called Carbazole. Having a melting temperature of 270 °C, the substance will melt during the normal operating times, absorbing any excess energy. When the power load is relatively small, and the temperature of the batteries starts to decline, so will the temperature of the Carbazole, buffering the rate of temperature loss. Finally, when the system temperature reaches 270 °C, the Carbazole will start to solidify, releasing the energy that it had stored during the normal operating period.

This material will add 82 kg to the Unloader's mass. By taking the total mass of the Carbazole and its heat of fusion rating, the allowable amount of energy per hour lost can be calculated. With this system, if the insulation allows 11 W_t to be lost every hour, the battery system will still be maintained at operating temperatures.

5.3.2.2. Other Electrical Sub-Systems

The system for removing the heat generated by the units other than the NaS batteries will consist of heat pipes and radiators. Aluminum heat pipes filled with Mercury will course around the system requiring thermal management, absorbing the excess heat. The Mercury, after absorbing by conduction and convection the heat from the subsystem, will travel to the radiator, which will then radiate the energy to space. The heat pipe is filled with Mercury because during the day, when thermal management is a problem, Mercury is a liquid. At night time temperatures, the Mercury is a solid. When it is a solid, it severely cuts down its of thermal transport capability. This is actually beneficial because otherwise, we would run the risk of drawing too much heat from the electrical systems and freezing them. The heat pipes would then transport the thermal energy to a Copper-Carbon fiber matrix radiator. See Figure 5.12 for a schematic of the thermal management system.

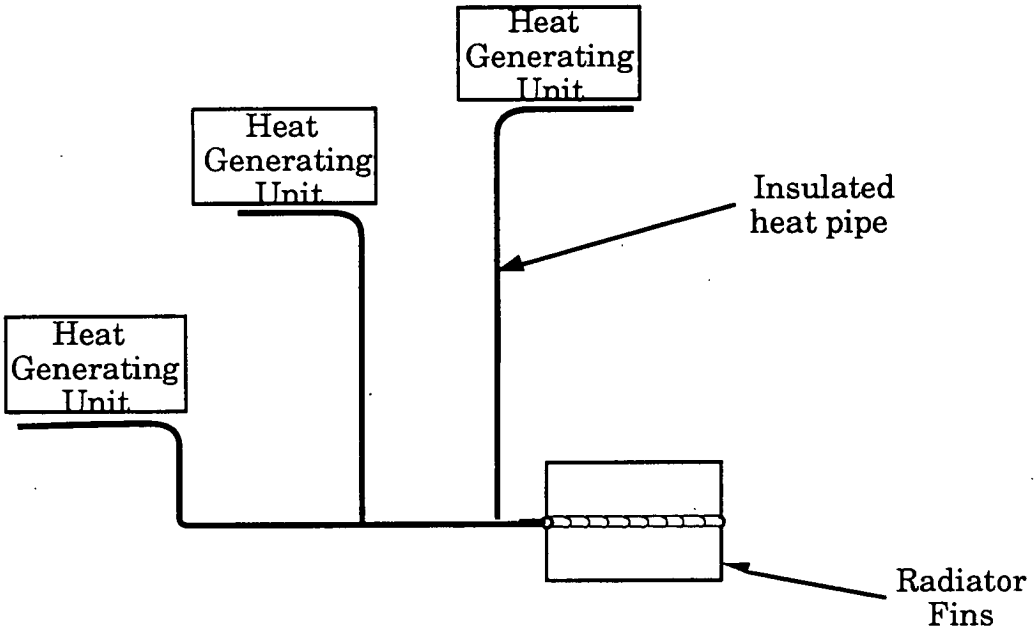

Figure 5.12: Schematic of Thermal Management Systems

Rather than working pipe across the entire span of the Lander, it will have two radiators, one for each side of the vehicle. Also, in order for the radiator to function, it must be hotter than the environment it "sees". The greater the temperature difference between the radiator and the environment it encounters, the more efficient it is, and the smaller the radiator fins need to be. This results in two adjustments. First, the heat pipes running from the heat generating source to the radiator must be heavily insulated, thus making the radiator as hot as possible. Also, to maximize the temperature gradient, the radiator will be located on a part of the vehicle which is always in the shade. The Lander's radiators will be located on the bottom of the vehicle. This will require a bit of dust shielding during landing and take-off to protect it from being coated with the very absorbant lunar dust. On the Unloader, the radiator will be located in the bottom of the vehicle, under the solar arrays. This is a centralized area, close to many of the heat generating units, and because it is on the bottom of the vehicle, it is always in the shade. The radiator will be positioned horizontally so that ground clearance is not a problem. Dust kick-up is not a problem since the Unloader will operate at a very slow speed.

The sizing of the radiator is based on these factors: The equation below, an estimation of the thermal energy to be rejected, temperature of the radiator, and the temperature of the environment the radiator is in.

$$A = \frac{q}{\varepsilon\sigma(T_1^4 - T_2^4)}$$

For the Lander, q = 954

For the Unloader, q = 1480

T1 = 450 K T2 = 380 K

$\varepsilon = 0.95$ $\sigma = 5.67 \times 10^{-8} \frac{W}{m^2 T^4}$ (Stefan-Boltzmann's Constant)

Therefore, the radiator for the lander is 1 m^2 and the radiator for the unloader is 1.5 m^2

The Copper-Carbon fiber matrix radiator have a specific mass of 6 kg/m^2.[21]. Using this figure, the density of Aluminum and Mercury, estimating the lengths and sizes of the heat pipes, the mass of the radiator and heat pipe systems were calculated. The system on the Lander will be 89 kg, and the system on the Unloader is 63 kg.

5.4. Future Developments in Power Technology

A form of energy that is free in terms of cost and available to everyone is solar energy. Harnessing this form of energy and using it to preform work is a very desirable feature to any space related activity. Solar cells are a convenient way to harness this energy. Single crystal solar cells, which have been used to date, are heavy and rigid. Vibration and bending of these solar cells could shorten their

productive life. To alleviate this degradation, thin film solar cells are currently being researched. These solar cells are much lighter than their single crystal counter part and also less rigid. These features will make systems utilizing solar cells more efficient and reliable.[23]

Batteries can be used as a secondary power source. One type of battery currently being researched in the Sodium-Sulfur (NaS) battery. Past failures of these batteries has been linked to the electrolyte. This electrolyte, known as Beta-Alumnia, is responsible for the separation of the reactants and for the provision of a conductive path for Sodium ions during operation. Currently, NaS batteries have a specific energy of approximately 150 watt-hours/kg. With the implementation of light weight, corrosion resistant materials, and upgrade design of of cell components, these batteries will be able to output in excess of 200 watt-hours/kg.[22] Improvements in other areas that would increase the life of these batteries include discharge rate capability, cycle life, uniformity of grain size and wall thickness, and methods of sealing the tube to the header. Implementation of these improvements could result in Na/S batteries that are 20% of the weight of current Nickel-cadmium batteries.[23]

5.5. References

[1] NASA CR 172-077, by Eagle Engineering Corp., 1989

[2] Colozza, A. Estimated Power Requirements for SEI Rovers, Sverdrup Technology Inc., NASA Lewis Reseach Center, May 17, 1990.

[3] Strump Guerra, Bill Annual Report Section 5.4, Surface Transportation, Eagle Engineering Corp, Aug. 11,1989.

[4] Ralph, E.L. and Michael A. Chung, Retractable Planar Space Photovoltaic Array, IEEE 21st Photovoltaic Specialist Conference, Vol 2, May 1990.

[5] Bailey. Sheila and Geoffrey Landis, Photovoltaic Superiority For Space Station Freedom Power in the 21st Century, IEEE 21st Photocoltaic Specialists Conference, May 1990.

[6] Hickman, J. Mark, Henry Curtis, and Geoffrey Landis, Design Considerations For Lunar Base Photovoltaic Power Systems, IEEE Photovoltaic Specialists Conference, May 1990

[7] Space Mission Analysis and Design,1991

[8] Landis, G.A. , S.G. Bailey, D.J. Brinker, and D.J. Flood, Photovoltaic Power For A Lunar Base, by Acta Astronautica, Vol 22, 1990, Presented at the 40th IAF Congress, Malaga Spain, Oct. 1989

[9] Photovoltaic Space Power History and Perspective, Space Power, Vol 8, No. 1/2, 1989 pp 3-10.

[10] Takata, , H, Kurakata, S. Matsuda, T. Okuno, S. Yoshida, H. Matsumoto, M. Goto, M. Ohkubo, and M. Ohmura, N. Space Proven GaAs Solar Cells, Main Power Generation for CS-3, by IEEE Photovoltaic Specialists Conference, May 1990

[11] Sudworth, J.L. and A.R. Tilley, The Sodium Sulfer Battery, 1985

[12] Withrow, Colleen A., Comparison of Power System Alternatives for SEI Rovers, Sverdrup Technology Inc., Nov. 8th, 1990

[13] Sodium Sulfer Batteries For Space Applications, Wright Research & Developement Center, 1989

[14] An Integrated Power System For Extended-Duration Shuttle Missions, Rockwell International, 1983

[15] Space Power Alternatives For Laser Radar Sensor System, TRW Space and Technology Group, 1988

[16] Lunar Lander Conceptual Design, Lunar Base Systems, Study Task 2.2, NASA CR-172051, Dec. 1987

[17] Manzo, Michelle, NASA Lewis Research Center, Cleveland OH, Telephone Interview, 11 March 1991

[18] Dr Robert K. McMordie, Space Mission and Analysis Design, Martin Marietta Astronautics Group, 1991

[19] Malone, Tom, NASA Lewis Research Center, Cleveland OH, Telephone Interview, 23 April 1991

[20] Harrold Liebecki, NASA Lewis Research Center, Cleveland OH, Telephone Interview, 13 March 1991

[21] Baker, Karl et. al. Graphite Fiber/Copper Matrix Composites for Space Power Heat Pipe Fin Applications. ms. NASA Lewis Research Center, Cleveland OH 1990

[22] Vufson, Stephen P. et. al. Sodium-Sulfur Batteries for Space Applications; Wright Research & Development Center, Wright Patterson Air Force Base.

[23] Boretz, John E., Space Power Alternatives for Laser Radar Sensor System; TRW Space & Technology Group, 1989

Chapter 6

Control and Communications

6.0. Summary

This chapter discusses the control and communications aspects of the Lander and Unloader vehicles.

The Lander's Guidance, Navigation, and Control System (GN&C) involves determining the location, attitude, and velocity of the Lander. The GN&C also involves avoiding hazards during landing and changing the orbit or trajectory of the Lander. Definitions, explanations, instrumentation, and specifications for each part of the GN&C system are given.

This chapter also briefly defines the Lander's Reaction Control System (RCS) and discusses several systems considered and the reasons behind the choice of chemical propulsion. The reader is referred to the chapter on propulsion for information concerning the reaction control engines, propellants, and associated hardware.

The Lander's on-board computers are responsible for many functions such as computation, information storage, systems coordination and actuation, and systems checks. They are essentially the "brain" of the Lander system and thus play an important role in execution of the mission cycle. The responsibilities of the computers and computer system specifications are detailed.

As the Unloader moves over the lunar terrain, its GN&C functions in avoiding hazardous obstacles, choosing a safe path to follow, and executing and verifying this path. The sensors and methods used for accomplishing these tasks are discussed. The on-board computers for the Unloader are responsible mostly for GN&C tasks, but they also function in trouble-shooting, systems management, power distribution, and mechanical actuation.

During the mission, communication of information between the vehicles and Earth is essential. Items to be communicated, optimum link configurations, carrier frequencies, and telemetry are discussed.

6.1. Lander Guidance, Navigation, and Control System

The Lander's Guidance, Navigation, and Control (GN&C) System is responsible for determining the location (in a chosen absolute reference frame), attitude (pointing direction in the absolute reference frame), and velocity (speed and direction of motion) of the Lander. The GN&C also functions in avoidance of hazards during landing and in changing the orbit or trajectory of the Lander--the GN&C must point the Lander in the selected direction, verify the pointing is correct, and restore the Lander to its operational attitude after the maneuver is complete. In order to accomplish these tasks, the GN&C system consists of four principle parts:

1. External Referencing

2. Inertial Referencing

3. Obstacle Avoidance upon Landing

4. Computer Interaction and System Integration

All instruments for the GN&C system were chosen to maximize accuracy and life and minimize mass and power requirements.

6.1.1. External Referencing

Stellar navigation first requires external referencing. External referencing is simply establishing the location and attitude of the Lander with respect to a chosen absolute reference frame. With the aid of artificial intelligence to process the data, external referencing itself consists of two parts:

1. A Vertically Stabilized Platform

2. Sensors

6.1.1.1. The Vertically Stabilized Platform.

Since the stars appear, to an Earth observer, as fixed points on a map of the heavens, an absolute reference frame with respect to the stars, such as the celestial equator reference frame, is chosen. Known stars are mapped in the chosen absolute reference frame and stored in a catalog in computer memory.

Therefore, the first aspect of external referencing is a vector, or an axis system defined with respect to this absolute reference frame. This axis system is called the vertically stabilized platform. The vertical platform is usually defined, for convenience, to coincide with one of the axes of the absolute reference frame. The mathematical definition of the vertically stabilized platform is also stored in computer memory. All changes in attitude are then measured with respect to this vertically stabilized platform.[1]

6.1.1.2. The Sensor

The second aspect of external referencing involves the use of external sensors. External sensors are used to supply information about attitude with respect to known "land marks", such as celestial bodies or fields.

Sensors Considered

Several types of external sensors were investigated and compared for use on the Lander.[2] Some of these were:

- Radio Frequency Sensors--require autotracking of a transmitted radio frequency signal. Eliminated due to communications difficulty on the far side of the Moon.

- Sun Sensors--provide course and fine Sun tracking for solar arrays. Also eliminated due to line of sight obstruction when the Lander is on the dark side of the Moon.

- Earth Sensors--sense infrared light. Eliminated due to line of sight obstruction when on the far side of the Moon.

- Surface Feature Sensors--sense visible light and rely on terrain recognition. Eliminated because terrain recognition is difficult for the Moon and this type also requires large computing capability.

- Star Trackers--sense visible light and are used for position determination, reference directions, and star pointing. This is the chosen external sensor.

The Star Tracker

UM-Haul has chosen to use three star trackers (two of which will be needed at any one time), placed on the roll, pitch and yaw axes, as the external sensors for the Lander. Star trackers have many advantages including: high accuracy; high reliability; long lifetime; low voltage requirements; space tested and proven; and no source and sensor obstruction problems. Table 6.1 summarizes some of the specifications for modern star trackers.[1] & [3]

Table 6.1 - Star Tracker Specifications for the Lander

Number	3
Placement	roll, pitch, yaw axes
Mass	5 kg each
Power Requirements	3 Watts each (6 W total at one time)
Accuracy	0.001 to 0.01 degrees
Star Fix and Update Rate	every 60-74 seconds
Lifetime	7 years continuous operation
Operation Temperature	-40 C (packaged in a vacuum housing with a thermoelectric cooler)

The star fix and update rate is the elapsed time between each iteration cycle which updates the star fix.

6.1.2. Inertial Referencing

Stellar navigation also requires inertial referencing. During the mission, the Lander experiences translation and rotation due to disturbance or induced torques, and applied forces from the reaction control or propulsion systems. So, with the aid of computations done by the Lander's on-board computer, inertial referencing is concerned with:

1. Sensing Changes in Rotation
2. Sensing Changes in Velocity

6.1.2.1. Sensing Changes in Rotation

The first aspect of inertial referencing is sensing changes in rotation. This is accomplished by rotation sensors. Several types of rotation sensors were investigated. Among these were momentum wheels, reaction wheels, two-axis position gyroscopes, rate gyroscopes, rate integrating gyroscopes, and ring laser gyroscopes. All of these are sufficient for the Lander's needs, but the ring laser gyroscope is the latest in inertial sensing devices and has several advantages over the others. These advantages include no moving parts (no drift or accumulation of angular momentum), no need for calibration, high accuracy, and high sensitivity.[4]

UM-Haul has chosen to use three ring laser gyroscopes, placed on all three body axes, as the rotational sensors for the Lander. Three additional ring laser gyros will be placed next to the first three as standby replacements should a failure occur.

Although there are no moving parts, the ring laser gyro functions like a rate integrating gyro. The ring laser gyro depends on the principle that light always propagates at speed c, with respect to an inertial frame, independent of the motion of its source and receiver. The laser gyroscope produces a laser beam, which is split into two parts, and are then directed in opposite directions around a closed, 4 kilometer path of optical quartz fiber wound on a spool. If the device is rotated about an axis perpendicular to the laser path, the inertial path followed by the laser beam moving against the rotation will be shorter than the path followed by the beam moving with the rotation. (In other words, the first beam finds the quartz crystals moving toward it.) This difference in path length causes interference patterns (since laser light is monochromatic) at the receiver. Constructive and destructive interference points shift by one bandwidth every time the path length changes by one-half a wavelength. This band pattern is used to measure the difference in the two path lengths using an optical inferometer. This relativistic change in path length between the two beams is a measure of the angular rate about the axis perpendicular to the laser path.[4] Typical ring laser gyros are sensitive enough to measure a rotation angle on the order of two arc seconds (less than 0.001 degrees).[3] Table 6.2 summarizes some of the specifications for ring laser gyroscopes.[5]

Table 6.2 - Ring Laser Gyroscope Specifications for the Lander

Number	6
Placement	2 on each of roll, pitch, yaw axes
Mass	4.6 kg each (27.6 kg total)
Power Requirements (includes pulsed	8 Watts/axis (24 W total)
electronics and power supplies)	(only 3 operate at one time)
Dynamic Range	3450 deg/sec
Sensitivity	2 arc seconds (< 0.001 degrees)
Accuracy	0.03-0.3 deg/hr
Lifetime	100,000 hours (11.4 years)

6.1.2.2. Sensing Changes in Velocity

The second aspect of inertial referencing is sensing changes in velocity. This is accomplished by accelerometers. Accelerometers measure the accelerations along each of the pitch, roll, and yaw axes. The acceleration measurements are sent to the on-board computer for integration to provide velocity and position change information. This information is then combined with previously computed and stored velocity and position information so that it may be updated as needed.

Two accelerometers are placed along each of the roll, pitch, and yaw axes. One accelerometer per axis will operate at any given time, while the other acts as a standby replacement in case its partner fails. Table 6.3 summarizes some of the specifications for accelerometers.[5]

Table 6.3 - Accelerometer Specifications for the Lander

Number	6
Placement	2 on each of roll, pitch, yaw axes
Mass	1.3 kg each (7.8 kg total)
Power Requirements	5.3 Watts each (16 W total) Includes sensor preprocessors & power supplies
Lifetime	10 years

6.1.3. Obstacle Avoidance during Landing

Stellar navigation also includes obstacle avoidance during landing. In order to ensure a safe landing, the Lander must have a way to determine the presence of and avoid hazards near the landing sight. UM-Haul has chosen to use laser radar for hazard avoidance upon landing of the Lander. The advantages of this hazard avoidance concept is that it minimizes size, mass, and power while still providing effective hazard avoidance upon landing. Although there will be no regional processing of the landing footprint area (the exact area the Lander occupies on the lunar surface upon touchdown), the concept will nearly guarantee that there will be no hazards in the landing location, assuming that landing sites have been chosen to minimize hazard distribution.

The laser radar is activated with approximately 45 seconds until touchdown. The laser radar has two types of modes, the point scan mode and the star scan mode. It begins by scanning several lines over the landing site in point scan mode in order to detect areas which contain the least amount of hazardous obstacles. A landing location is selected from this data, and the laser is directed to scan the selected location in more detail using the star scan mode. Meanwhile, the Lander is guided to the landing site. If the location continues to look good, the Lander will land at that location and the laser will not look elsewhere. If the location is found to contain a hazard or hazards, the original scan data will be utilized to obtain a second location that is still reachable given the Lander's maneuverability. The star scan could also be shifted to take advantage of the data already collected. Figure 6.1 shows a schematic of this process.

The obstacle avoidance laser radar system has a total volume of 0.04 cubic meters, total mass of 23.2 kg, total power requirement of 258 Watts, and requires 128 kilobytes of computer memory.

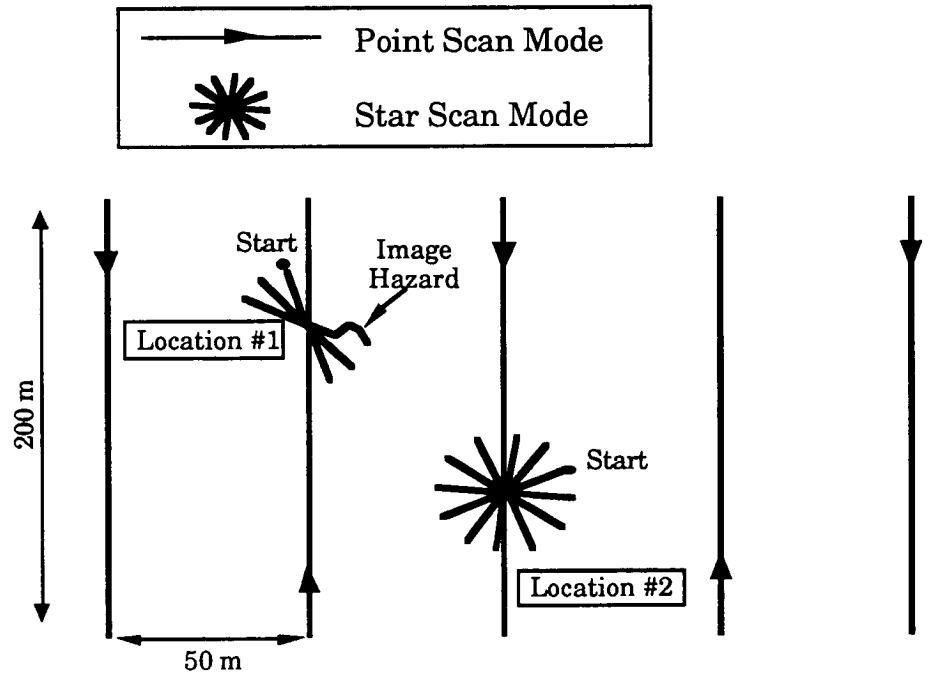

Figure 6.1 - Laser Radar--Point and Star Scan Modes

6.1.4. GN&C Computer Interaction and System Integration

The final aspect of the Lander GN&C is the computer interaction and system integration. In order to determine and control the Lander's position, attitude, and velocity, the GN&C system uses the on-board computer to store information, provide orders for desired motions, and interact with the sensors. The computer stores the star catalog, calculation algorithms, and pre-programmed flight path information for the mission. It receives, through the communications system, information from Earth regarding changes or updates in the desired motion of the Lander. The on-board computer also interacts with the star trackers, inertial motion sensors, and laser radar to integrate measurements, calculate, and continuously update location, attitude, velocity, and hazard location information.

For example, when the attitude of the Lander changes, the angular velocity is sensed by the laser gyros and then integrated by the computer to give a change in attitude measurement. The measured change in attitude is used in conjunction with the star position information from the previous star fixes to calculate the estimated new positions of the stars. If the star trackers are able to acquire new fixes, the estimated star positions and sensed magnitudes are compared with the star catalog to identify the stars. Once identified, the stars' positions are updated based on the true star positions, with respect to the vertically stabilized platform, contained in the catalog. In this way, attitude and position of the Lander are updated and accumulated errors are eliminated. If the star tracker is unable to make a new fix, it waits until the next iteration cycle to attempt to acquire a new star fix. Figure 6.2 shows a schematic of this process.

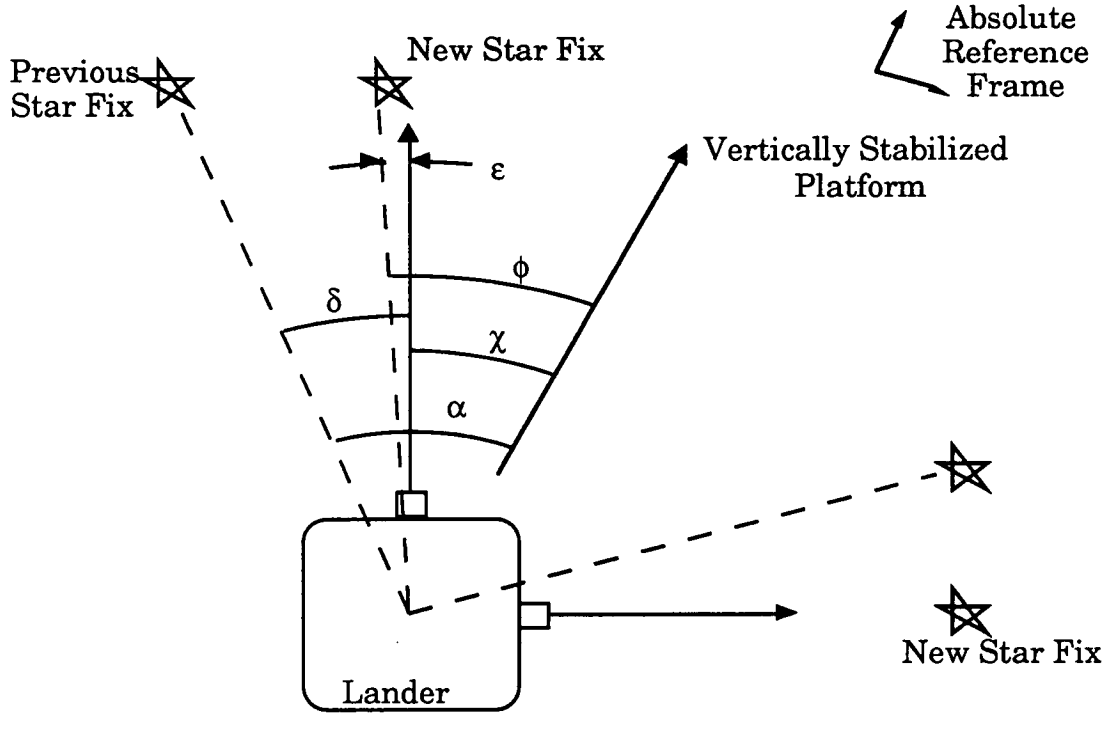

α = Previous star fix angle
δ = Displacement sensed by laser gyro
χ = Calculated, then compared with catalog
ϕ = Updated star fix angle
ε = Laser Gyro error (corrected by Star Tracker)

Figure 6.2 - The External Referencing System

When the velocity of the Lander changes, the accelerometers sense the acceleration in each direction of the body axes of the craft. The measurements are integrated by the computer to find the change in velocity, which is then added to the previous velocity. In this way, velocity and direction of motion of the Lander are updated. Figure 6.3 shows this process.

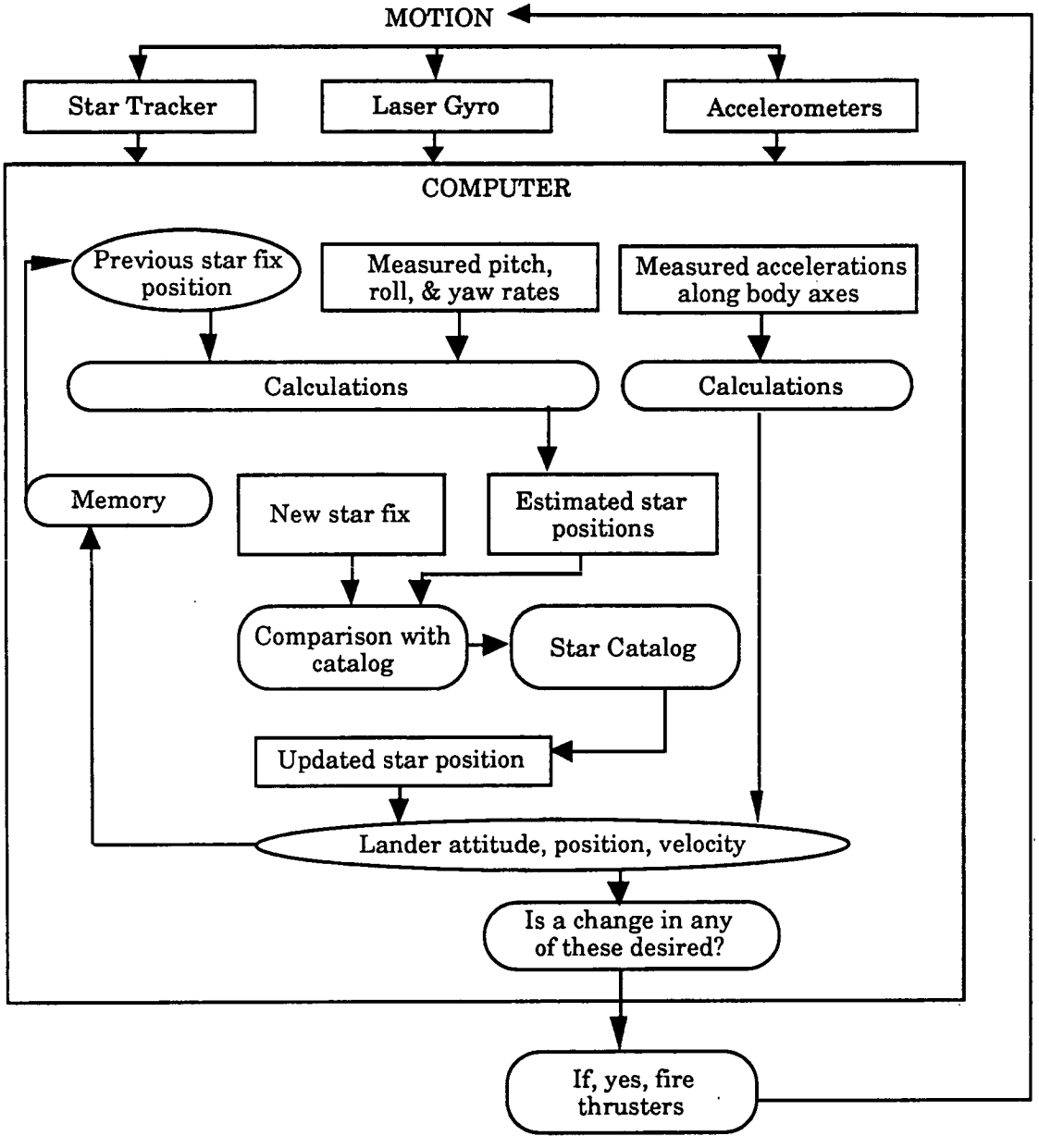

Figure 6.3 - Lander Guidance, Navigation, and Control System Integration

When the Lander is ready to land on the Moon, the computer turns on the laser radar at approximately 45 seconds to touchdown, and runs through the laser hazard detection algorithm as shown in Figure 6.4.

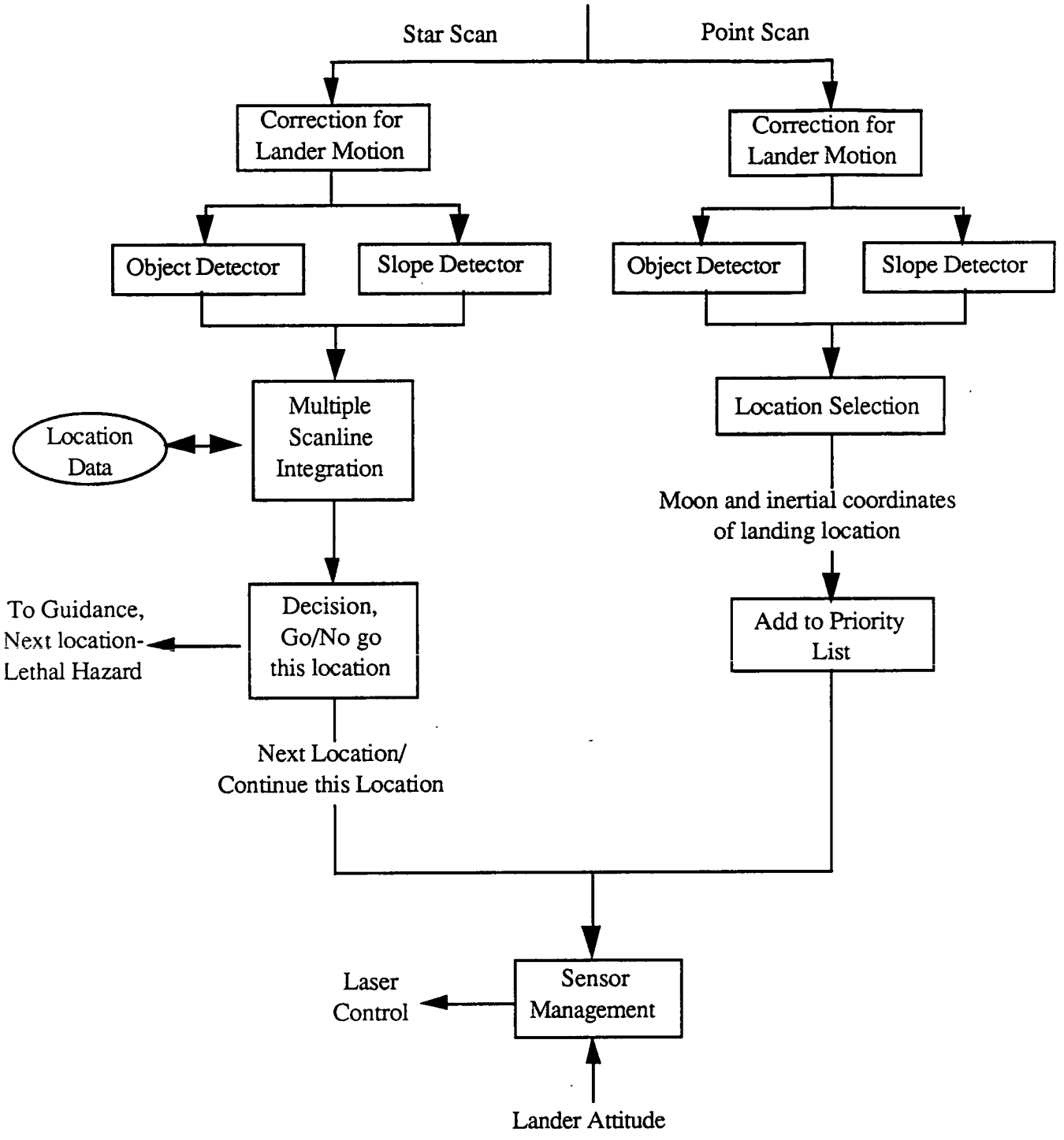

Figure 6.4 - Laser Radar Scanner Operation Block Diagram

6.1.5. The Lander GN&C System Summary

The Guidance, Navigation, and Control system is a continuous feedback loop which provides position, attitude, velocity information, and obstacle avoidance upon landing. It also makes the necessary corrections and changes that are

required for mission maneuvers. Table 6.4 gives some totals of interest (not including the on-board computer) for the Lander's GN&C system. Table 6.5 summarizes the redundancy provided for the Lander's GN&C instruments.

Table 6.4 - Lander GN&C Totals

Power Required	304 Watts
Mass	74 kg
Life	approx. 10 years (limited by accelerometers)

Table 6.5 - Number Provided for Redundancy and Error Minimization

Star Trackers	1
Laser Gyros	3
Accelerometers	3
Laser Radar	none

6.2. Lander Reaction Control System

Reaction control systems (RCS) are low-thrust propulsion units that perform any tasks that the main engines cannot in terms of stability, attitude control, and rendezvous maneuvering. The available reaction control systems are chemical and electrical propulsive systems and mechanical stabilizers, such as reaction wheels.

Reaction control wheels themselves are not complete reaction control systems; they are not able to translate the vehicle in any direction. Reaction wheels are only able to spin the vehicle on any axis. Because of this restriction, these were dismissed. Electrical propulsive systems are most commonly used on satellites and are extremely low thrust -- on the order of 4.5 - 9 Newtons, characteristically. Larger thrust electric propulsion systems are typically massive. Finally, by process of elimination, as with the main engines, chemical propulsion was selected.

Most chemical RCS are monopropellant hydrazine, which offers extremely low specific impulse. The major concern, therefore, with hydrazine is the possibility of running out of propellant, a contingency the Gemini mission explored. For the UM-Haul mission scenario, with the required 10-mission cycle, it was decided that a Hydrogen-Oxygen reaction control system be used for purposes of system integration and overall systemic uniformity.

The next decision to be made was between gaseous and liquid reactants. It became evident that a gaseous system would enable an extremely simple integration with the fuel cells (see Figure), and so the gaseous 8911 Thruster from Bell Aerospace Textron (developed for NASA Lewis Research Center) was chosen. For further specifications on gaseous 8911 Thruster, please refer to the Section 4.6.

6.3. Lander's On-Board Computer System

The Lander is equipped with three on-board computers. Each computer is fully encased to protect it from severe temperature fluctuations, radiation, lunar dust, and other environmental hazards. Including the casing, each computer unit is 0.10 x 0.25 x 0.30 m in size and has a mass of approximately 2.3 kg. Power requirements for continuous operation are on the order of mW.[6] & [7] However, 5 W per computer is allotted for worst case scenario operation. Table 6.6 provides a tabulated summary of specifications for the Lander's on-board computer system.

Table 6.6 - Lander Computer System Totals

Number	3
Size	0.10 x 0.25 x 0.30 m each
Mass	2.3 kg each (7 kg total)
Power Requirements	300 mW each (5 W each, worst case)
Number Provided for Redundancy	2

The on-board computer system has many functions throughout the integrated Lander system. It is responsible for:

1. GN&C storage, calculation, and command requirements
2. Firing sequences and timing of the RCS thrusters
3. Coordination of transmitted and received information from the communication system
4. Firing of the main engines during landing and lift-off
5. System management tasks and systems checks

The on-board computer system plays a crucial role in the operation of the GN&C system. Therefore, three computers shall operate solely in GN&C tasks during critical maneuver periods to provide failure backup and error minimization. During non-critical GN&C periods, two of the computers will either be deactivated

as standby replacements, or perform the other functions such as systems checks, communications, or system management.[8]

6.4. Unloader Guidance, Navigation, and Control System

Locomotion of the Unloader entails mobility, stability, and speed over a wide variety of terrain. The Unloader's Guidance, Navigation, and Control System (GN&C) is thus responsible for avoiding hazardous obstacles, such as boulders and craters, choosing a safe path to follow, executing this path, and verifying this path by determining distance travelled, turning, speed, and position of the Unloader. (It should be noted that full autonomy of these tasks on an excursion vehicle has not yet been attempted.) In order to accomplish these tasks, the Unloader's GN&C system consists of four parts:

1. Hazard sensing
2. Path determination
3. Motion sensing
4. On-board computer (discussed in Section 6.6).

6.4.1. Hazard Sensing

Hazard sensing is the ability of the Unloader to determine the presence of obstacles or large holes in its path. Thus, hazard sensors are used to supply information about the surrounding lunar terrain.

6.4.1.1. Sensors Considered

Several types of hazard sensors were investigated and compared for use on the Unloader. Some of these were:

- Mechanical Sweeping Device--senses physical contact with rocks and elevation dips. Eliminated because the device requires a complicated structure, flight storage mechanism, and hazard determination software package.
- Thermal Changes Sensor--senses changes in temperature, such as shadows. Eliminated due to limits on the time of day missions can be executed.
- Radar--senses obstacles and holes by radar reflection. Requires large computing capacity to be fully effective. Also eliminated because of difficulty in navigating the Lander's ramp with this type of sensor.
- Television Cameras--take three-dimensional pictures of the terrain to form an elevation mapping of the area surrounding or in the path of the Unloader. This is the chosen hazard sensor.

6.4.1.2. Television Cameras

The Unloader is equipped with television cameras as its hazard sensors. Some advantages and disadvantages of using television cameras are listed in Table 6.7.

Table 6.7 - Advantages and Disadvantages of Television Cameras as Hazard Sensors

Advantages	Disadvantages
• Three-dimensional terrain imaging • Up to 200 m of depth perception • Non-random path determination • Easier Lander ramp sensing, lining up, and ascent • Provides telerobotic capabilities and monitoring.	• Not a fully autonomous system • Requires human interaction • Time lag associated with this required data transmission and human interaction • Only effective during lunar day (can't "see" in the dark unless own source of lighting is provided) and on the near side of the Moon (for communication purposes).

There are two cameras placed on the front of the Unloader, and two on the back. This allows the Unloader to move either forwards or backwards, and also provides redundancy should one set fail. The cameras are placed with a separation of 0.5 m, which allows a depth perception out to 200 m. The television cameras are approximately 0.10 x 0.10 x 0.25 meters in size and are fully encased (transparent by the lenses) to protect them from the severe temperature fluctuations, radiation, lunar dust, and other hardships in the hostile lunar environment.

6.4.2. Path Determination

Path determination for the Unloader requires three things: a communications system for the Unloader; human interaction; and computers. As described in the Unloader GN&C System Integration section below, data from the Unloader's television is transmitted through the communication system to Earth. Operators on Earth view the three-dimensional images and designate a safe path for the Unloader to take to clear the blast radius of the Lander. Calculations for appropriate turns and path segment distances are done on an Earth-based computer and sent back to the Unloader via the communications system. These commands are stored in the memory of the Unloader's on-board computer for execution.

6.4.3. Motion Sensing

During execution of the designated path, the Unloader uses motion sensors and on-board processors to monitor its own motion and verify its path. These motion sensors include wheel odometers to measure the distance travelled, accelerometers to measure velocity, and gyrocompasses for heading. There are two of each of these instruments, one of each on the front and back of the Unloader, to provide forward and backward motion capability and for backup in case of failures.

6.4.4. Unloader GN&C System Integration

A GN&C system using television cameras is either a fully telerobotic system, or a semi-autonomous system of travel. The system used by the Unloader is semi-autonomous. There are currently two methods of semi-autonomous travel under development. These are the Semi-Autonomous Mobility (SAM) method, and the Computer-Aided Remote Driving (CARD) method.

6.4.4.1. The Semi-Autonomous Mobility Method

The SAM method provides for a more autonomous Unloader, compared to the CARD method, because the Unloader is accompanied by a satellite that orbits the surface of the Moon. This satellite uses a high-resolution camera to take pictures of the lunar terrain from two different positions in its orbit. Those pictures are then sent to Earth, where they are used to form an elevation map of a large area surrounding the Unloader. This map can be generated with a resolution of one meter. Next, a human operator draws an approximate path for the Unloader to follow, in order to avoid large obstacles, hazardous areas, and dead-ends. The Unloader is also equipped with stereo cameras, but it uses the view from these cameras to generate a depth map. From this depth map, the Unloader generates an elevation map of its local area and finds the closest correlation between it and a portion of a global elevation map sent from Earth. Using sensing elements, the Unloader determines its absolute position and compares it in relation to the path it must follow. Then the Unloader creates a revised map with very high resolution in its immediate area and calculates a feasible local path based on the approximate global path sent from Earth. Finally, the Unloader moves a given distance and repeats the process from its new position, using the map it previously received from Earth.[9] & [10] See Figure 6.5 for a schematic of the SAM method.

Unfortunately, the satellite required for this method is not in orbit around the Moon at this time. This means that one would have to be designed and deployed before this type of semi-autonomous navigation is possible. Therefore, UM-Haul is using the Computer-Aided Remote Driving (CARD) method. However, should the required orbiting lunar satellite become available at some time in the future, the SAM method would be preferred.

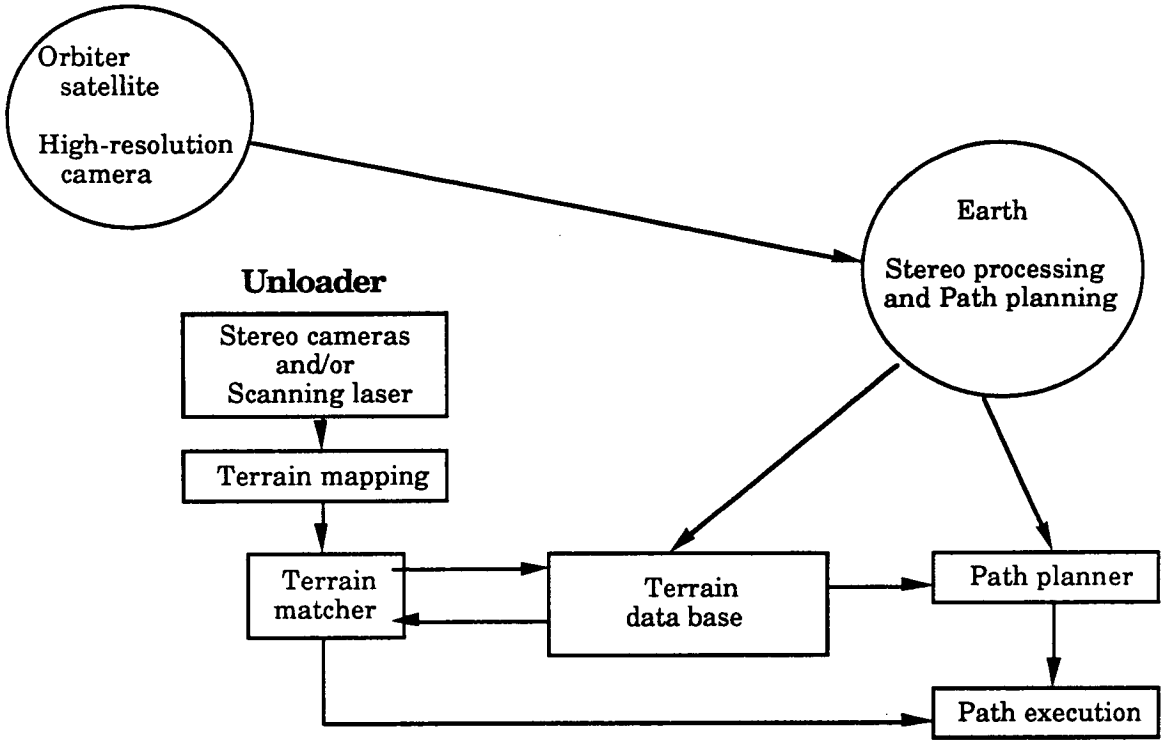

Figure 6.5 - The Semi-Autonomous Mobility (SAM) Method

6.4.4.2. The Computer-Aided Remote Driving Method

Although it is less autonomous and a somewhat slower process than the SAM method, it is the method planned for the GN&C system of the Unloader using television cameras.

In the CARD method, the Unloader is outfitted with stereo cameras that take pictures of whatever it sees. When a decision has to be made as to where it will move next, the Unloader stops and transmits three-dimensional images of the lunar terrain to Earth. A human operator views the images and designates a path for the Unloader to travel. A computer on Earth calculates appropriate turn angles and path segment distances for the Unloader to take and sends them to the Unloader's on-board computer. The Unloader executes movement commands from the on-board computer while monitoring (through the motion sensors) its own motion. When the Unloader has completed its path (or runs into an unexpected hazard) it stops and repeats the process. The Unloader can cover roughly 20 m for each iteration, depending on the terrain. See Figure 6.6 for a schematic of the CARD method.

In addition, if desired, the CARD method can be switched over to a fully telerobotic system. This type of system requires a human operator on Earth to continuously monitor the television pictures and control the motion of the Unloader through joystick commands. The human operator effectively "drives" the Unloader from the Earth. The on-board computer will shut down the system if the motion sensors encounter an extremely adverse condition. This alerts the human operator to the hazard so that he/she can move the Unloader accordingly.

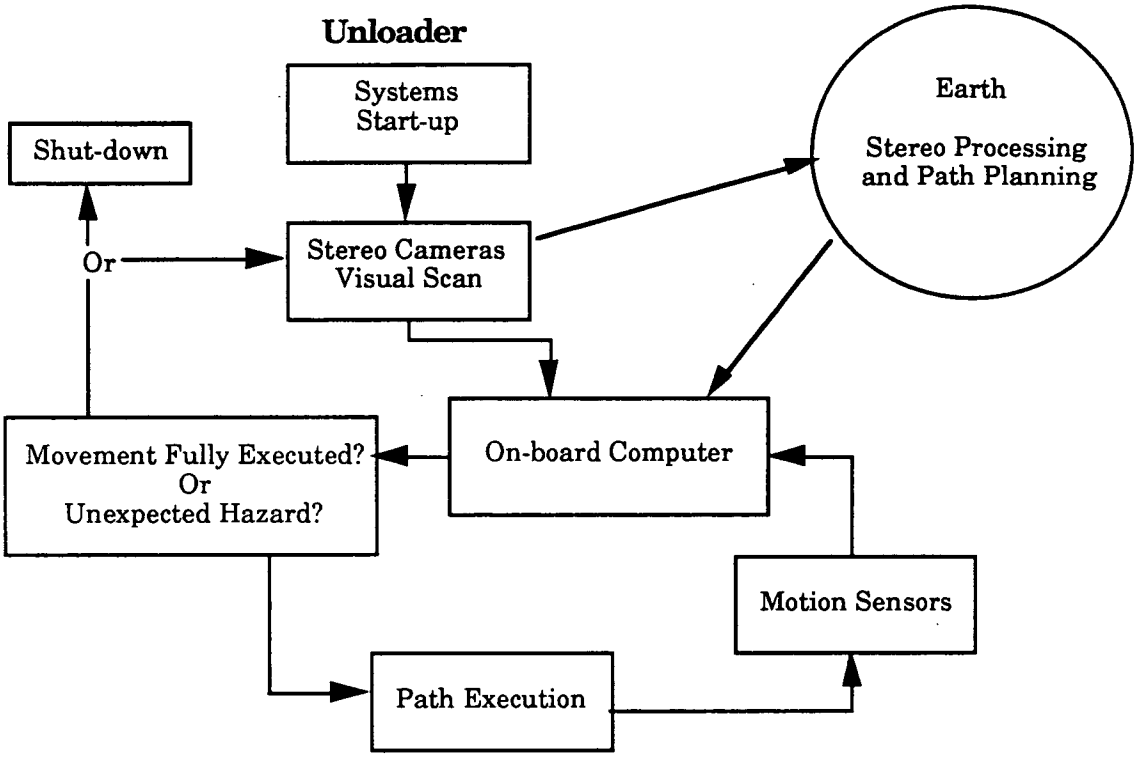

Figure 6.6 - The Computer-Aided Remote Driving (CARD) Method

6.4.5. The Unloader GN&C Summary

In summary, the Unloader Guidance, Navigation, and Control System instruments consist of 1 beacon on the Lander, 1 receiver on the Unloader, 4 television cameras (2 mounted on the front, 2 on the back, placed 0.5 m apart for depth perception), 2 wheel odometers, 2 accelerometers, 2 gyrocompasses (1 each placed on the front and back of the Unloader). The Unloader GN&C system uses the Computer-Aided Remote Driving method which requires integration with the Unloader's communication system, on-board computers, and Earth. Table 6.8 gives GN&C totals of interest for the Unloader (excluding the communication system, on-board computers, which are addressed in the following sections, and the Earth-based computers).

Table 6.8 - Unloader GN&C Totals

Power Required	30 Watts
Weight	12 kg
Life	53,000 operational hours

6.5. Unloader's On-Board Computer System

The Unloader's on-board computers are very similar to those of the Lander. There are two computers. One computer is used in GN&C to determine the presence of obstacles, initiate communications with Earth, receive and process orders from Earth, control motion actuation, and process information from the motion sensors. The second on-board computer is used for trouble-shooting, Unloader systems management, power distribution, mechanical actuation, and for back-up and error minimization for the first.

Each computer is fully encased to protect it from the hostile lunar environment, i.e., lunar dust, severe temperature fluctuations, and radiation. Including the casing, each computer is approximately 0.10 x 0.25 x 0.30 meters in size and has a mass of 2.3 kg. Power requirements for the computers during normal Unloader activity are on the order of mW each. However, up to 5 W has been allotted for each computer for a worst case scenario operation. Table 6.9 gives specifications for the Unloader's on-board computers.[6] & [7]

Table 6.9 - Unloader On-Board Computer Specifications

Number	2
Dimensions	0.10 x 0.25 x 0.30 meters each
Mass	2.3 kg each (7 kg total)
Power Requirements	300 mW each (10 W total worst case)

6.6. The Communication System

The second half of the Control and Communication aspect of Project UM-Haul, is of course, the Communication system. This system is to provide communication between the Lander, Unloader, and Earth. To do this, the communication system consists of four main parts:

1. Items to be communicated
2. An optimum link configuration
3. Carrier Frequencies
4. Necessary communications hardware
5. Telemetry & Multiplexing

6.6.1. Items to be Communicated

In order to coordinate the mission, control the motion of the UM-Haul vehicles, and initiate actuation of the proper mechanisms at the proper times, the vehicles must be able to exchange many types of information with each other and with Earth. Each subsystem has unique types of information it needs to have communicated. Some of the things each group shall be communicating are summarized in Table 6.10.

Table 6.10 - UM-Haul Items to be Communicated

Mission Analysis	Altitude Pitch, roll, yaw Pitch, roll, yaw rates Velocity Acceleration
Propulsion	propellent levels, temperatures, pressures Engine thrust level Engine characteristics: gimbal angle, nozzle temperature, pressure
Power	Power remaining, available,on reserve Temperature batteries, fuel cells
Control and Communication	Video link from Unloader & Lander Homing beacons Relative position of Unloader to Lander Relative position of Lander to OTV Down loading commands from Earth
Payload and Spacecraft Integration	Payload status Systems checks

6.6.2. Optimum Link Configuration

The optimum link configuration is the path followed by the communication signals from the Lander or the Unloader to the Earth and back. Currently, two architecture types for lunar communication links are under development by NASA. These are the geostationary relay satellite (GRS) path, and the ground terminal (GT) path.[11] For each path, there are three stages of systems deployment: initial, intermediate, and full lunar. The full lunar deployment stage is intended for use when there are one to two fully functional bases on the

Moon, so for purposes of this project, only the initial and intermediate deployment stages were compared.

6.6.2.1. The Geostationary Relay Satellite (GRS) Path

The initial deployment stage of the GRS path would use a single geostationary relay satellite in orbit around the Earth in order to communicate information to and from the Moon. No lunar relay satellites will be needed. It also would use one ground terminal antenna located within the continental U. S. The intermediate deployment stage of the GRS path would involve two geostationary relay satellites, a satellite in lunar orbit, and two ground terminal antennas at one station.

Unfortunately, a satellite has not yet been built for this type of transmission. However, NASA is currently developing an Advanced Tracking and Data Relay Satellite System (ATDRSS), similar to the currently used Tracking and Data Relay Satellite System (TDRSS system), for the purpose of implementing the GRS path.[12] Unfortunately, the ATDRSS satellite system is not operational at this time.

6.6.2.2. The Ground Terminal Path

The initial deployment of the Ground Terminal (GT) path would require three ground stations with two antennas each. The intermediate deployment stage of the GT path requires three ground stations with four antennas at each. Figure 6.7 shows a schematic of the initial and intermediate deployment stages of the GT path.

Comparisons between the two systems prove that the GRS path is better for data transmission, yet has an inherent space risk not present in the GT path. Both have similar life cycle costs, but the GRS path offers operational advantages over the GT path. However, since ATDRSS is not operational, the existing ground terminal stations currently around the Earth must be used for the linking task. Because of this, the GT path was chosen as the external communication link. When ATDRSS does become operational, the possibility to change over to the GRS path is excellent.

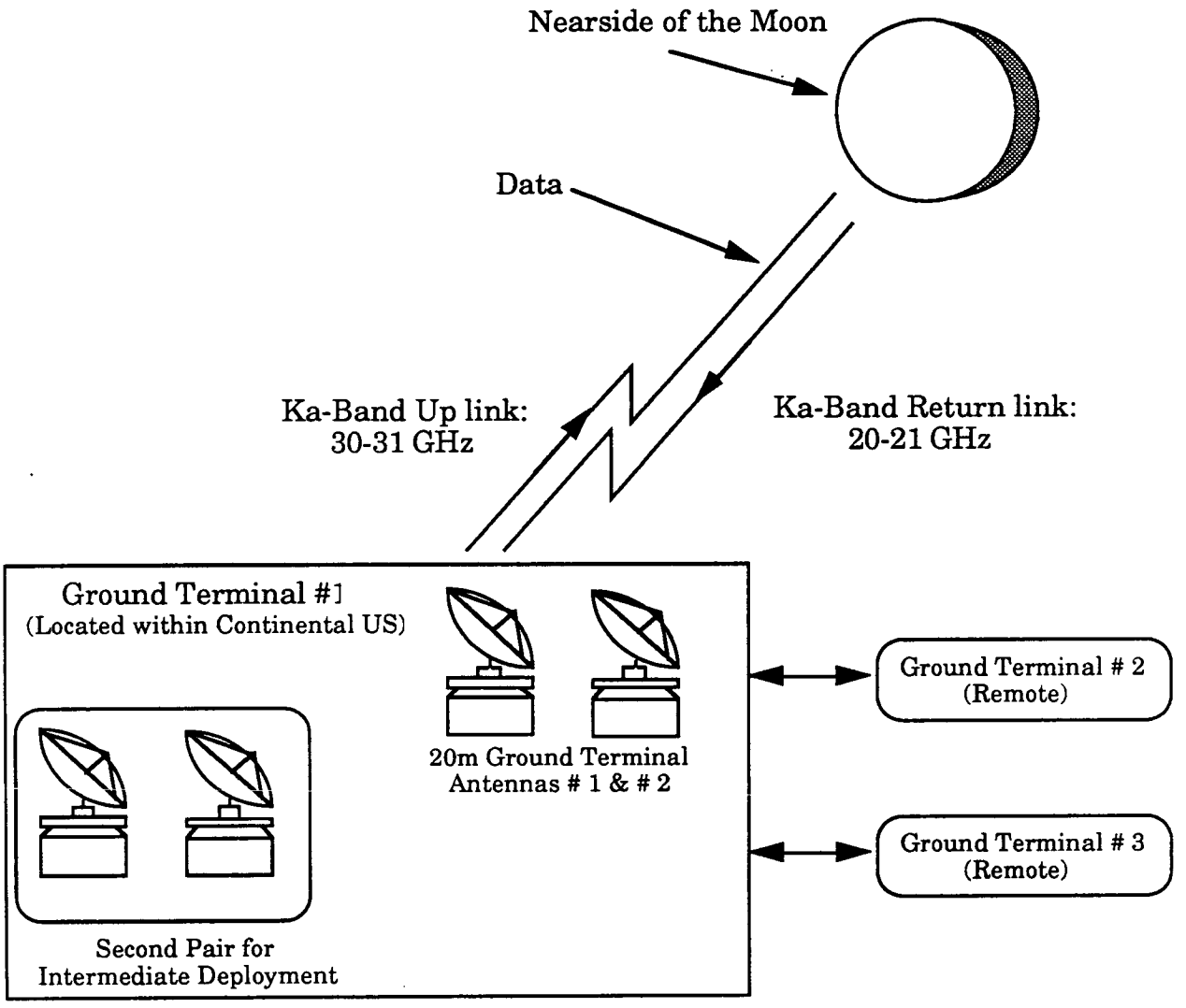

Figure 6.7 - Ground Based Architecture Earth Region Implementation

6.6.3. The Carrier Frequencies

Carrier frequencies are the frequencies over which the data is transmitted. The existing frequencies used by NASA were investigated, along with ones that might be used for the GRS or GT paths.[11] These included the Ka-band, the S-band, the Ku-band, and the X-band. The Ka-band (20GHz-40GHz) was chosen. This high frequency is useful for its capacity to transmit high rates of data, and to carry all of the signals the Lander and Unloader will be transmitting. It is also the band that NASA has plans for using in future communication systems.

As a back up to the Ka-band, both the Lander and Unloader will also be transmitting data on the S-band (2GHz-4GHz). The S-band is what is currently in use with the TDRSS system.[12] & [13] The Ka-band and the S-band together will be enough to transmit all of the necessary data.

6.6.4. Communication System Hardware

The communication system hardware are the instruments used in the UM-Haul communication system for data transmission. For example, data is transmitted on the Ka-band by parabolic antennas. The diameter of the Ka-band antenna is found by first determining the wavelength of the frequency. The diameter of the antenna must be at least half of the wavelength or greater (greater for better reception).[14] The wavelength is found by: $l = c/f$, where c is the speed of light, and f is the frequency (in Hz). Taking the lower frequency limit of the Ka-band as the minimal value, the wavelength comes out to be 0.01 meters. However, the greater the diameter of the antenna, the better the reception. Also, a larger diameter antenna also leads to greater structural stability. Therefore, the diameter of the Ka-band antennas are 0.10 meters with a height of 0.10 meters. There are two Ka-band antennas mounted on the Lander and two on the Unloader (for redundancy).

Data is transmitted on the S-band by cone-shaped antennas. The length of the cones is 0.20 meters. There are two S-band antennas on the Lander and two on the Unloader. Further communication system hardware specifications are given in Table 6.11.

Table 6.11 - Communication System Hardware Specifications

	Number on Lander	Number on Unloader	Mass (kg)	Power (Watts)	Dimension (Meters)
Ka-band antennas	2	2	3.5	0	0.10 diam. 0.10 height
Ka-band transmitter/ receiver transponder	1	1	12	25	0.17 x 0.34 x 0.09
Ka-band filter/ switches	1	1	1.2	0	0.08 x 0.19 x 0.04
S-band antennas	2	2	2	0	0.20 cone length, 0.06 shaft
S-band transmitter/ receiver transponder	1	1	29	62.5	0.14 x 0.33 x 0.14
S-band filter/ switches	1	1	2	0	0.15 x 0.30 x 0.06

6.6.5. Telemetry & Multiplexing

The communication system must be able to send and receive large amounts of data, of many different types. Telemetry is a process by which large amounts of data is compressed in order to be transmitted on one carrier frequency . Sending different types of data signals on the same carrier frequency is accomplished through multiplexing.

To better understand telemetry and multiplexing, it is helpful to look at an example. Imagine Figure 6.8 and Figure 6.9 represent data signals from two different types of sensing equipment. In order to transmit this all on the same carrier frequency, the data is multiplexed together [10]. In this fashion, it takes a number of time intervals to transmit all the data. Therefore, if Figure 6.8 is multiplexed with Figure 6.9, the result might be Figure 6.10 (with the number values being time intervals).

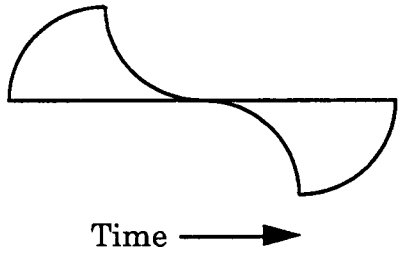

Figure 6.8 - Data Signal from Sensor A

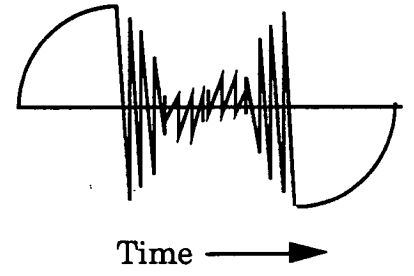

Figure 6.9 - Data Signal from Sensor B

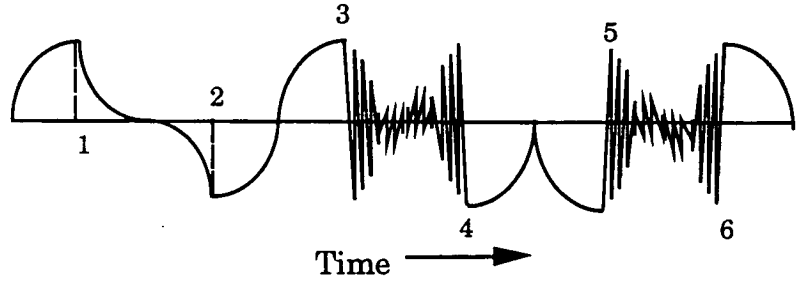

Figure 6.10 - Multiplexed Data Signals

Once the data is sent, the signal is demultiplexed back into its original form so that it can be analyzed.

This example is greatly simplified, since there may be up to thirty or forty different signals multiplexed together at one time, but this is how the data from the Lander and Unloader will be sent back to Earth. Both the Lander and Unloader are equipped with multiplexing circuitry which is included with the transponder.

6.6.6. Summary of the Communications System

Communications is an integral part of the UM-Haul mission cycle. Many types of signals, such as video signals, telemetry data, computer system control commands, reaction control sensing and maneuvering data, and radar signals, to name a few, must be transmitted to the vehicles and to Earth. The communication system is composed of a ground terminal path, with its associated ground stations and antennas. The main carrier frequency is the Ka-band and the back up carrier frequency is the S-band. The Lander and Unloader each have their own antennas, transponders, and filters/switches to transmit and receive signals. Large amounts of data can be transmitted using telemetry and multiplexing.

The communication system also plays a crucial role in the shut down and reactivation of the power systems. As part of the mission cycle, it is necessary to shut down and operate the Lander or Unloader in a "sleep mode" during inactive times. To do this, the proper signal is sent to the Unloader along the Ka-band. Then the receiver systematically turns off the power to every power piece of equipment on the Unloader, ending with the transmitter. The receiver stays on, requiring only 4.5 watts of continuous power, until another signal is sent to tell it to reactivate the other equipment.[8] The receiver will thus act like a "stand-by receiver", just waiting until the proper signal is received to resume operation.

6.7. Future Developments in Communication Technology

Lunar operations require communication between the moon and earth. Ground based communication systems have been used to date. A major problem with this type of system is the handover of data from ground station to ground station. To alleviate this and other problems, the Advanced Tracking and Data Relay Satellite System (ATDRSS) is being developed to provide a direct link between the moon and earth. This satellite would be positioned in Geostationary Orbit. ATDRSS is a derivative of the TDRSS satellite which is used for earth to earth communications. ATDRSS is scheduled for production in the late 1990's. This satellite would mostly eliminate the handover of data between ground stations. Data transmissions can increase from the current 100 megabyte per second (mbps) to over 300 mbps. ATDRSS will be easily integrated to the NASA Space Network. Because it will be quite comparable to TDRSS in user handling, the user will not need to re-learn how to operate the communication system.[15] & [16]

6.8. References

[1] McCauless, Floyd, and Quasius, Glen, Star Trackers and Systems Design, Macmillan & Co., Ltd., London distrib., Spartan Books pub., 1966.

[2] Sorensen, Albert, and Williams, I.J., "Spacecraft Attitude Control", Quest Technology at TRW Electronics and Defense, Vol. 5, Number 2, Article Reprint, Summer 1982.

[3] McGraw Hill, Encyclopedia of Science and Technology, New York, McGraw Hill Book Co., 1987.

[4] Wiesel, William, Spaceflight Dynamics, McGraw-Hill Book Co., New York, 1989, p. 165-166.

[5] "Mars Rover/Sample Return (MRSR) Program", Contract # NAS9-17868, Sept. 2, 1988, Lockheed and Honeywell, Johnson Scace Center, Houston, TX.

[6] Bollinger, Steve, and Falkenburg, Advanced Visualization Facility, U. of Michigan College of Engineering, 763-3070.

[7] McClay, Paul, Advanced Visualization Facility, U. of Michigan College of Engineering, 761-9272.

[8] Jenkins, Dennis R., "Rockwell International, Space Shuttle", 1989.

[9] "Real-time software controls Mars Rover robot", Computer Design, Vol. 27, No. 20, Nov. 1, 1988, p. 60-61.

[10] "Designing a Mars surface rover", Aerospace America, Vol. 23, No. 11, Nov., 1985, p. 54-58.

[11] Computer Science Corporation, System Science Division, Beltsville, Maryland, Evaluation and Comparison of Alternative Communications Architecture for Lunar Exploration, Volume 1, Prepared for NASA Goddard Space Flight Center, Greenbelt, Maryland. Contract number NAS5-31500, Task Assignment 01 113, November 1990.

[12] Caprna, Giovanni, The Complete Encyclopedia of Space Satellites, Portland House New York, NY 1986.

[13] Larson, Wiley S., and Wertz, James, Space Mission Analysis Design, Klunder Academics Publications Norwell, MA 02061

[14] Carlson, Kurt, Antenna engineering student, University of Michigan, interview.

[15] Evaluation & Comparison of Alternative Communication Architectures for Lunar Exploration; Volume 1, NAS5-31500-01113; Goddard Space Flight Center

[16] Weinberg, Aaron, An Overview of Reference User Services During Pre-ATDRSS Era; Stanford Telecommunications, Inc.

Other Sources of Reference

Entry Data Analysis for Viking Landers, NASA-CR-159888, Final Report Nov. 1976.

Roberts, Arthur, ed., Radar Beacons, McGraw-Hill Book Co., New York, 1947.

Ross, Bob, Avionics, Inc., Interview, La Guna Beach, CA, (1-800-ELT-LABS), Apr. 8, 1991.

Space-Qualified Kearfott Inertial Reference Unit (SKIRU-IV), Kearfott Guidance and Navigation Corporation, 150 Totowa Rd., Wayne, NJ 07474-0946, (201) 785-6000.

Strock, O.J., Telemetry Computer Systems-An Introduction, Instrument Society of America, Prentice-Hall, Inc. Englewood, NJ 1983

Various, Quest for Space, Crescent Books New York, NY 1986

Vesecky, Professor of Atmospheric and Oceanic Sciences, University of Michigan, Ann Arbor, MI, Apr., 1991.

Zuzek, John, Communications Technology, NASA Lewis Research Center Cleveland, Ohio, interview

Chapter 7

Mission Analysis

7.0. Summary

The success of a UM-Haul mission depends a great deal on mission planning. UM-Haul mission planning began with the selection of several landing sites suitable for the construction of a lunar base. Next, a lunar parking orbit was chosen which would remain stable and allow access to all of the landing sites. Then, a mission profile was developed for UM-Haul, including timing of operations, trajectory planning, determination of velocity changes (ΔV's) required for each mission, and rendezvous calculations. Finally, communications windows between the different UM-Haul vehicles and the Earth were determined.

Each UM-Haul mission follows the same general pattern. The mission begins when the orbital transfer vehicle (OTV) arrives from the Earth and is inserted into a parking orbit where the Lander has been waiting for it in a standby mode. The Lander then descends to a lower chase orbit and the rendezvous phase begins. After a successful rendezvous and cargo transfer between the OTV and the Lander, the vehicles separate, and the Lander begins its descent to the lunar surface. When surface operations are complete, the Lander ascends to the parking orbit and waits in standby mode for the next OTV to arrive from the Earth.

7.1. Landing Site Selection and Survey

The location of the landing site affects operations in several areas, including communications, power, and launch and landing operations. The four landing sites which are considered here are Lacus Veris, Taurus-Littrow, Mare Nubium, and Mare Marginis. Lacus Veris, Taurus-Littrow, and Mare Nubium are located on the near side of the Moon, and Mare Marginis is located on the far side of the Moon. The locations of the four landing sites are shown in Figure 7.1.

7.1.1. Lacus Veris

Lacus Veris is located on the western limb of the Moon at 87.5°, W 13° S, near Mare Orientale [1]. This site was chosen primarily for its proximity to features of scientific interest. Other influencing factors include access to the far side of the Moon, ruggedness of the terrain, soil chemistry, and lighting conditions.

Lacus Veris provides valuable access to the far side of the Moon. In fact, it is actually on the far side for up to 10 days each month due to the libration of the Moon [2]. Libration is due to the eccentricity of the Moon's orbit around the Earth. The rotation of the Moon on its axis is uniform, but the angular velocity of its orbit around the Earth is not since it moves faster near perigee, the point in the moon's orbit where it is closest to the earth, and slower near apogee, the point in the moon's orbit where it is furthest from the earth. This permits as much as 7.75° around each limb to be seen from the Earth in a month, although the maximum amount varies from month to month [3].

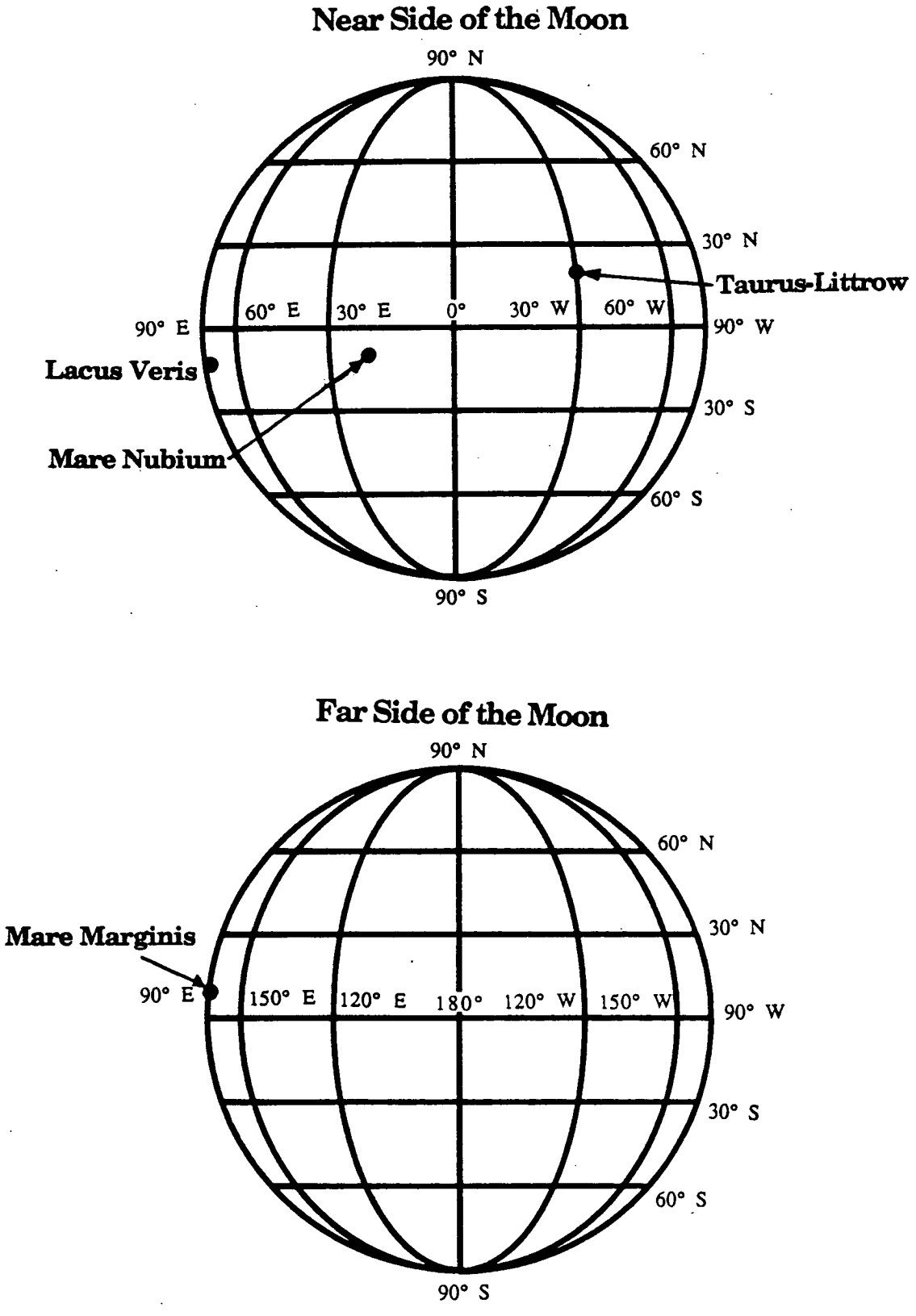

Figure 7.1 - Locations of the UM-Haul Landing Sites

Access to the far side is very important for astronomical observation. Astronomy on the Moon is difficult for two reasons. First, the full Earth shines sixty times more brightly than the full Moon, washing out the nighttime sky for optical astronomers. Second, man-made electromagnetic interference originating on the Earth affects radio astronomy. Both of these problems may be solved by locating either a permanent or a temporary observatory on the lunar far side [2].

Lacus Veris is located in a relatively smooth mare region, which reduces wear on landing pads, and aids in surface transportation and habitat site preparation [2]. Soil thicknesses in mare regions are typically fairly thin, extending only two to five meters before hitting bedrock. This is important if radiation protection for a module is to be provided by either by burying it or by covering it over. Obviously, digging into bedrock would be a time consuming activity [1]. Therefore, any equipment deployed here would be covered.

Another advantage of locating a base in a mare region is that such a site would have a relatively high concentration of the mineral ilmenite which can be extracted and used to produce Oxygen. Finally, lighting conditions are good at Lacus Veris because of its proximity to the equator [2].

There is one drawback to locating a base at Lacus Veris. Because of the libration of the Moon, the Earth as seen from Lacus Veris is below the horizon for as long as ten days out of each lunar month and thus out of direct line-of-sight communications. In order for a Lacus Veris base to maintain an uninterrupted communications link with Earth, either relay stations or communications satellites (or both) will be required. This problem is discussed in more detail later under the topic of communications windows [1].

7.1.2. Taurus-Littrow

Taurus-Littrow was the site chosen for the Apollo 17 landing. The success of Apollo 17 proves that landing approaches over mountainous terrain are feasible. The landing site was located at about 30° E, 20° N [4], in a flat mare-floored valley with average slopes of 5 - 7°. The flanking North and South Massif have average slopes of 20 - 30°. Locating a Taurus-Littrow base in a mare region would make it a good source of ilmenite for Oxygen production. However, access to the far side from Taurus-Littrow would be much more difficult than from Lacus Veris, because the far side is over 2000 km away [1].

7.1.3. Mare Nubium

The Mare Nubium site is located at about 20° W, 10° S [5], near the Apollo 12 landing site. It is in an area of fairly young mare basalts which means that the terrain should be fairly smooth and that there should be plenty of ilmenite available for Oxygen production. However, far side access from Mare Nubium would be even more difficult than from Taurus-Littrow, because the far side is over 2400 km away [1].

7.1.4. Mare Marginis

The Mare Marginis site is located at about 92.5° E, 9.5° N [6] on the far side of the Moon. It is in a mare region, so the terrain should be fairly smooth, and there should be enough ilmenite available for Oxygen production. This site is on the far side of the Moon for at least 17 days each month, so it will share all of advantages for astronomical observation which were mentioned in the description of Lacus Veris. Libration of the Moon causes Mare Marginis to rotate onto the near side for up to 10 days each month. However, the only way to maintain constant communications with the Unloader and the Lander at Mare Marginis is to place two communications satellites in orbit around the Moon or to use the Lander as a relay station. Both options are certainly a possibility, but probably would not be considered until a permanent base had been established on the near side. Since the Unloader requires constant communications with the Earth in order to maneuver on the lunar surface and it would be unreasonable to restrict operations to only 10 days per month, far side operations are not possible until a permanent communications link has been established between the far side and the Earth. Therefore, only near side landing sites will be considered for UM-Haul.

7.2. Parking Orbit

The parking orbit which was chosen for the Lander is a circular low lunar orbit (LLO) at an altitude of 111 km. The orbit is inclined at an angle equal to the latitude of the next landing site. The inclination of the orbit is the angle which the orbital plane makes with the lunar equatorial plane. So, for a landing at Lacus Veris, the inclination of the parking orbit must be 13°. The inclination must be 20° for a landing at Taurus-Littrow and 10° for a landing at Mare Nubium. These are the lowest orbital inclinations which will allow a landing at each of the landing sites. Figure 7.2 defines the inclination of the orbit and the latitude of the landing site.

Low lunar orbit is any orbit about the Moon at an altitude between 93 km and 111 km. Lower altitudes are preferable because ΔV's are lower. Experience from the Apollo program indicates that orbits below 93 km tend to be unstable due to the gravitational field of the Earth. The outer limit of 111 km was chosen to supply a satisfactory factor of safety. A spacecraft in this parking orbit will travel once around the Moon every 119 minutes at a velocity of 1.63 km/s. This orbital velocity is called the local circular velocity of the orbit (V_{lc}).

7.3. Mission Profile

The UM-Haul system is required to complete ten mission cycles before major servicing. The missions would be divided between the three landing sites. For example, a typical mission profile might include having the first three landings be made at Mare Nubium. The next four landings could be made at Lacus Veris and the final three landings could be made at Taurus-Littrow. The time between each mission will range from two to four months.

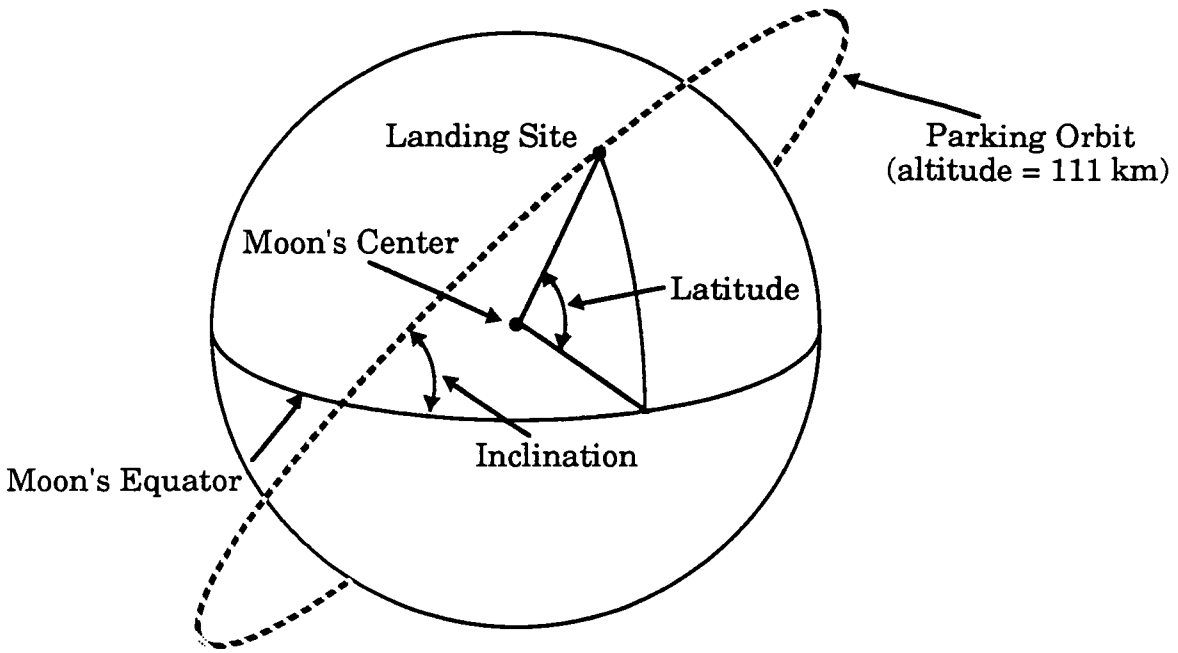

Figure 7.2 - Parking Orbit

Prior to the first mission to Mare Nubium, the OTV and the Lander will be inserted into a 10° inclination, 111 km altitude parking orbit. Since the inclination of this orbit is equal to the latitude of the Mare Nubium landing site, the site will rotate into the plane of the parking orbit once a month. A landing site is said to be in the plane of the parking orbit when the site passes directly under the ground track of the parking orbit. The exact time each month is determined by the time at which the OTV and the Lander are inserted into LLO.

After the first landing at Mare Nubium, the Lander will be launched into the same 10° inclination orbit, and a small plane change will be needed in order to correct for the rotation of the Moon while the Lander is on the lunar surface. This will insure that the Lander returns to exactly the same parking orbit it was in before the landing. This is necessary so that the landing opportunity is at the same time each month and does not eventually drift into the lunar night (see Section 7.5. Landing Opportunities). After rendezvousing with a new OTV, the Lander will repeat the mission cycle two more times. After the third landing, the Lander will be launched into a 13° inclination parking orbit so that it is able to service Lacus Veris at 13° S latitude next. After four landings at Lacus Veris, the Lander will be launched into a 20° inclination parking orbit so that it is able to service the final landing site at Taurus-Littrow at 20° N latitude for the final three mission cycles.

The sections that follow are a detailed description of the UM-Haul mission. The mission begins with a rendezvous between the Lander and an OTV which has just arrived from the Earth with a new cargo. The Lander then descends to the lunar surface to deliver the cargo to the chosen landing site. After surface

operations are completed, the Lander ascends to the parking orbit to wait for the next OTV, and then the entire mission cycle is repeated.

7.3.1. Rendezvous

The first major event in the UM-Haul mission is the rendezvous between the Lander and the OTV in LLO. Each of the phases of the rendezvous procedure will be discussed in detail in this section along with the different methods of rendezvous which were considered for UM-Haul.

7.3.1.1. Rendezvous Method

Two different rendezvous methods were considered for UM-Haul. The first method is to insert the Lander into a lower orbit, called a chase orbit, and allow it to catch up with the OTV. This is possible because an orbit at a lower altitude will have a greater angular velocity than an orbit at a higher altitude according to the equation:

$$\omega = \sqrt{\frac{\mu}{r^3}} \tag{7.1}$$

where: ω = angular velocity of the orbit

μ = gravitational constant of the Moon = 4.893×10^{12} m^3/s^2

r = Moon radius + orbit altitude = $R_{Moon} + h$

The second method is a rendezvous from the same orbit called orbit walking. If the Lander is initially trailing the OTV, then the Lander is placed into an elliptical orbit with a period shorter than the period of the OTV orbit. The Lander will then catch up to the OTV after a specified number of orbits. If the Lander is initially leading the OTV, then the Lander is placed into an elliptical orbit with a period greater than the period of the OTV orbit. The OTV will then catch up to the Lander after a specified number of orbits.

The orbit walking method presents one major difficulty. If the initial phase angle between the Lander and the OTV is greater than 39.9°, then the Lander is out of the line-of-sight of the OTV and unable to communicate with it. Figure 7.3 defines the phase angle as the angle between a line drawn from the OTV to the Moon's center and a line drawn from the Lander to the Moon's center. It is crucial for the two vehicles to be able to communicate with each other in order to determine their initial phase angle, since this angle determines the period of the elliptical orbit that the Lander will be placed in. The initial phase angle (ϕ_i) between the vehicles is determined when the OTV is inserted into LLO , so the orbit walking method would require more restrictions on the launch of the OTV from the Earth

than the chase orbit method. Therefore, the chase orbit method will be used for UM-Haul.

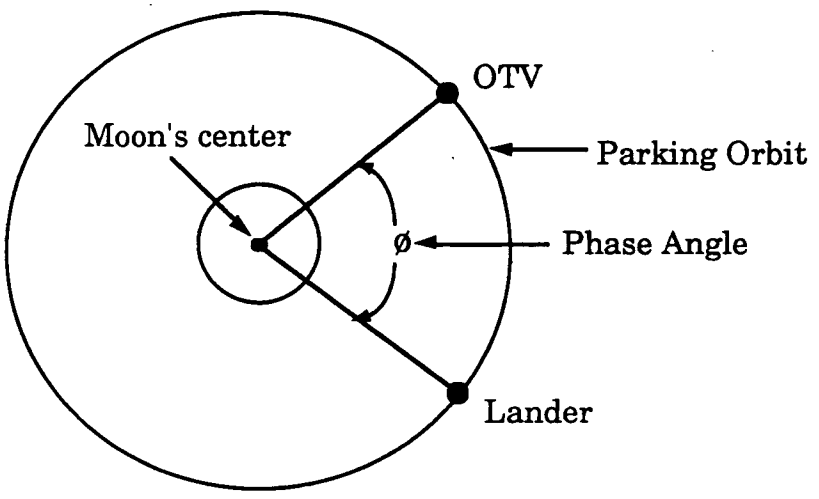

Figure 7.3 - Definition of the Phase Angle between the OTV and the Lander

7.3.1.2. Selection of the Chase Orbit Altitude

The altitude of the chase orbit that the Lander is placed in affects both the wait time and the ΔV's for the rendezvous maneuvers. The wait time (T) is the amount of time it takes for the Lander to catch up to the OTV after being placed in the chase orbit and is given by:

$$T = \frac{\phi_i - \phi_f}{\omega_L - \omega_O} \qquad (7.2)$$

where: ϕ_i = initial phase angle

ϕ_f = final phase angle or desired phase angle

ω_L = angular velocity of the Lander

ω_O = angular velocity of the OTV

The maximum wait time occurs when $\phi_i - \phi_f = 360°$. Since ω_L decreases as the altitude of the chase orbit increases, the wait time will increase as the altitude of the chase orbit increases. Note that the chase orbit always remains lower than the parking orbit. The wait time approaches infinity as ω_L approaches ω_O, or as the altitude of the chase orbit approaches the altitude of the parking orbit. The effect of the chase orbit altitude on the wait time is shown in Figure 7.4.

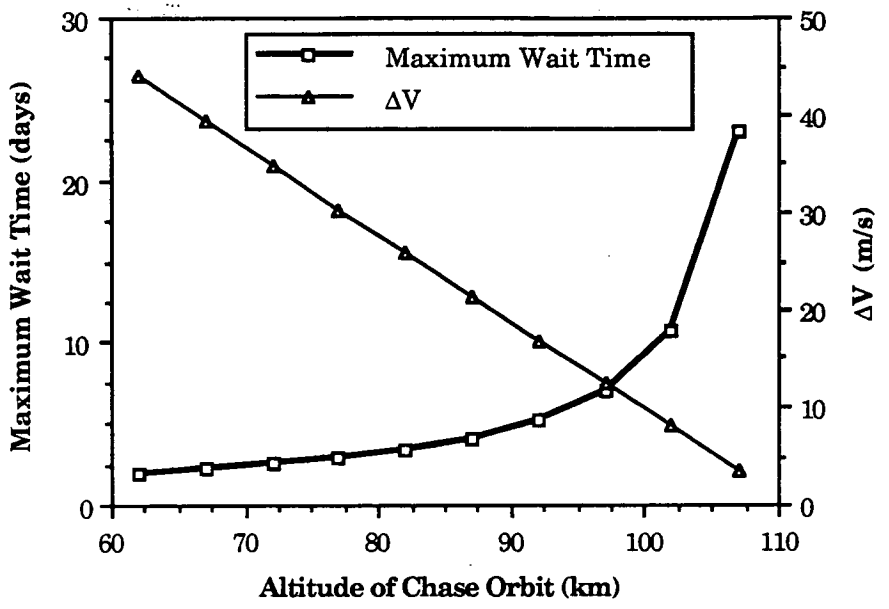

Figure 7.4 - Effect of the Altitude of the Chase Orbit on the Rendezvous Wait Time

Figure 7.4 also shows the effect of the chase orbit altitude on the rendezvous ΔV's. The rendezvous ΔV's are almost insignificant when compared to the descent and ascent ΔV's, so they were not a major concern in the selection of a chase orbit altitude. The stability of the chase orbit was a major concern. The lowest lunar orbit considered to be stable is 93 km. Thus, the chase orbit altitude must be above 93 km but must not force an extremely long wait time for rendezvous. The maximum wait time was fixed at 10 days, corresponding to a chase orbit altitude of 101 km. This orbit is sufficiently stable, and it will also allow a reasonable launch window from the Earth for the OTV.

7.3.1.3. Descent to the Chase Orbit

After the OTV has been inserted into the 111 km altitude parking orbit, the Lander will begin the Descent to the Chase Orbit Initiation (DCOI) maneuver. The Lander will descend to the 101 km altitude chase orbit using an orbital maneuver called a Hohmann transfer. A Hohmann transfer is a transfer between two circular orbits via a doubly-tangent transfer ellipse (see Appendix C). This method of transfer between orbits requires the smallest ΔV. The Hohmann transfer, shown in Figure 7.5, requires two engine burns. The first burn will impart a ΔV of 2.21 m/s to the Lander and will place it in an elliptical transfer orbit which will cross the chase orbit at its perilune, the point in the Lander's orbit around the moon where it is closest to the moon. The second burn will impart a ΔV of 2.21 m/s to the Lander and will insert it into the chase orbit. Thus, the second burn is called the Chase Orbit Insertion (COI). The descent to the chase orbit requires 59 minutes and 13 seconds to complete.

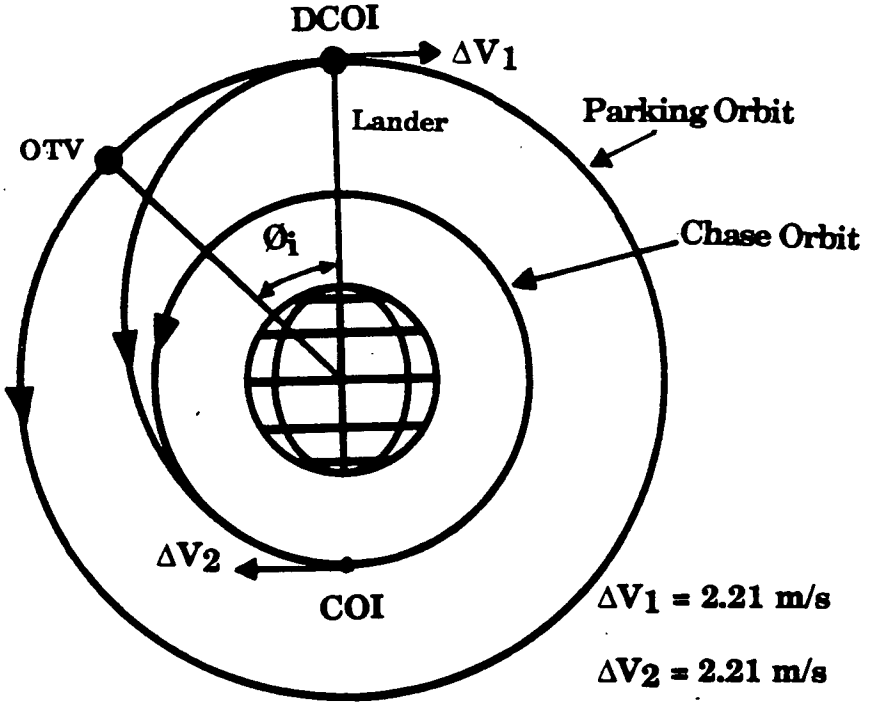

Figure 7.5 - Descent to the Chase Orbit

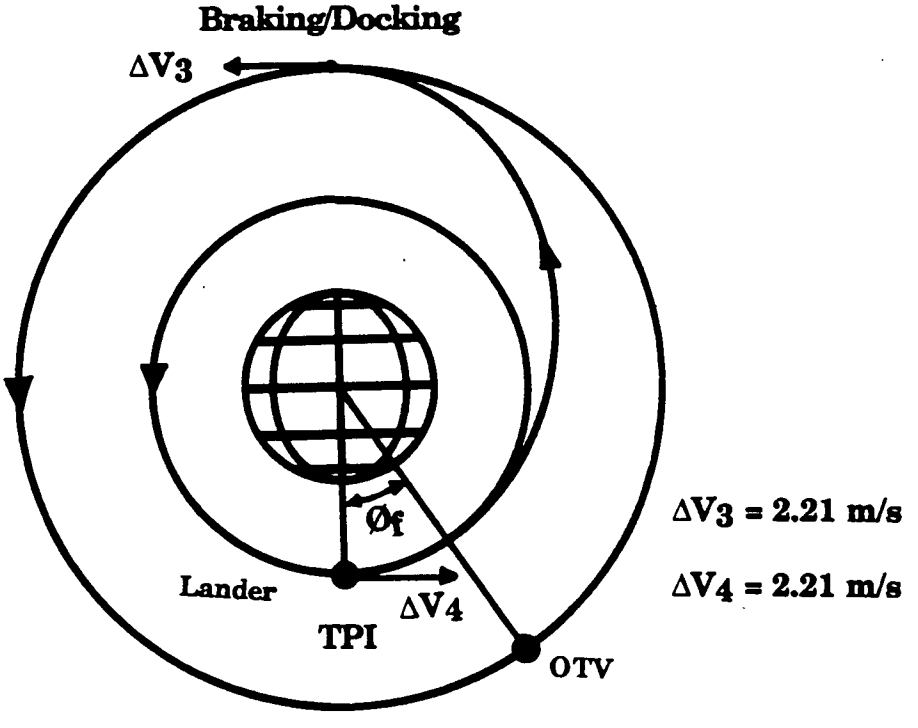

Figure 7.6 - Terminal Phase Maneuvers

7.3.1.4. Phasing

The Lander will begin to catch up to the OTV once it has been inserted into the chase orbit. This portion of the rendezvous procedure is called phasing. The wait time,T, for phasing is determined by the difference between the initial phase angle, ϕ_i, and the desired phase angle, ϕ_f, as shown in equation (7.2) earlier. The initial phase angle is determined by the exact time at which the OTV is inserted into the parking orbit and is not precisely controllable. The desired phase angle is 0.725°. The calculation of this angle will be explained in the next section. Thus, the wait time required for phasing will range from 0 seconds for the case where $\phi_i = \phi_f$ to about 10 days for the case where $\phi_i - \phi_f = 360°$. It is true that if the phase angle were to be greater than 180°, the OTV could go into a chase orbit and catch up with the Lander for a shorter waiting time, but keeping the mission scenario as simple as possible, and to design for the worst case scenario, this method of phasing was chosen. Figure 7.7 is a plot of the wait time for phasing as a function of the initial phase angle.

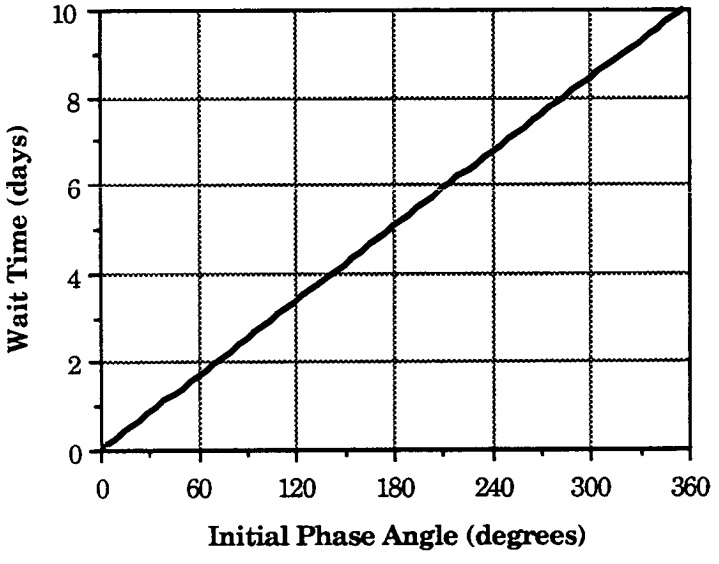

Figure 7.7 - Rendezvous Wait Time as a Function of the Initial Phase Angle

7.3.1.5. Terminal Phase Maneuvers

The rendezvous procedure is completed with the Terminal Phase Maneuvers which require two engine burns. The first burn, or the Terminal Phase Initiation (TPI) burn, places the Lander on a trajectory which will allow it to intercept the OTV in the parking orbit. The second burn is a braking burn. These maneuvers are actually just Hohmann transfers with the same total ΔV (4.42 m/s) as the descent to the chase orbit. The TPI burn imparts a ΔV of 2.21 m/s to the Lander and places it in an elliptical orbit which will cross the OTV parking orbit at its apolune. The braking burn imparts a ΔV of 2.21 m/s to the Lander which inserts it into the parking orbit by matching the velocity of the Lander to the velocity of the OTV.

In order to insure that the Lander intercepts the OTV at the apolune of the transfer ellipse, the phase angle at TPI (ϕ_f) must be 0.725°. The final phase angle was calculated with the following equation:

$$\phi_f = 180 - (T_{Hohmann} \times \omega_O) \qquad (7.3)$$

where: $T_{Hohmann}$ = time required to complete Hohmann transfer

ω_O = angular velocity of the OTV

Figure 7.6 shows the terminal phase maneuvers. The time required for the terminal phase maneuvers is 59 minutes and 13 seconds, the same as the time required for the descent to the chase orbit. The total ΔV required for the entire rendezvous is 8.84 m/s, which is very small compared to the descent and ascent ΔV's.

7.3.1.6. Rendezvous Timeline

The wait time for phasing varies depending on the initial phase angle between the Lander and the OTV. The wait time ranges between 118 minutes, 26 seconds for the case where $\phi_i = \phi_f$ and 10 days, 4 hours, 36 minutes for the case where $\phi_i - \phi_f = 360°$. Figure 7.8 is a timeline for the rendezvous assuming the worst case where the wait time for phasing is 10 days. In this case, the OTV has a window of about 16 days to arrive from the Earth. This leaves one day for the cargo transfer and refueling so that the Lander is able to make its descent when the landing site is in the plane of the parking orbit. The landing site is only in the plane of the parking orbit once every month. For the best case where there is no wait time for phasing, the OTV has an arrival window of about 26 days.

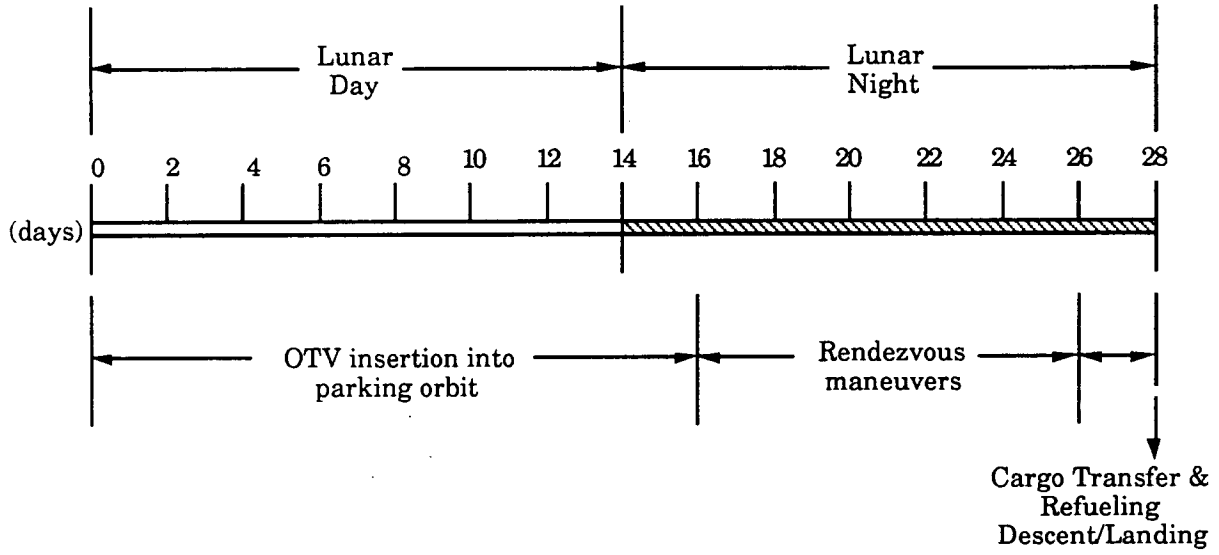

Figure 7.8 - Rendezvous Timeline for a 10 Day Wait Time for Phasing

The large window for the arrival of the OTV even in the worst case allows for reasonable flexibility in Earth launch timing. If the insertion of the OTV into LLO can be timed precisely enough to control the initial phase angle, then the wait time for phasing may be determined in advance. If this is not possible, then the OTV should be required to arrive from the Earth within the 16 days allowed in the worst case rendezvous timeline. This will insure that the Lander is able to descend to the surface during the same month when the landing site rotates into the plane of the parking orbit.

7.3.2. Descent

After the cargo has been transferred from the OTV to the Lander and the refueling of the Lander is complete, the Lander is ready to begin its descent to the lunar surface. The Lander provides clearance between itself and the OTV with a small burn imparting a ΔV of 0.8 m/s to the Lander. Approximately one-half orbit after separation from the OTV, the Lander begins its descent. The different parts of the descent procedure are explained in this section.

7.3.2.1. Descent Orbit Insertion

The first portion of the descent is the Descent Orbit Insertion (DOI). This maneuver is a Hohmann transfer which places the Lander into an elliptical orbit with an apolune of 111 km and a perilune of 15.24 km. An engine burn will impart a ΔV of 21.8 m/s to the Lander in order to place it into the transfer orbit. DOI will begin at about 59 minutes and 31 seconds (or one-half orbit) after the Lander separates from the OTV. The DOI maneuver is shown in Figure 7.9.

7.3.2.2. Powered Descent Initiation

The Lander will reach the perilune of the transfer orbit at an altitude of 15.24 km above the lunar surface 57 minutes and 11 seconds after DOI. At this point, the Lander will begin its Powered Descent Initiation (PDI) burn. The PDI burn imparts a braking ΔV of 1693.8 m/s to the Lander. This slows the Lander from its orbital velocity as it begins its powered descent to the lunar surface. The PDI burn is also shown in Figure 7.9.

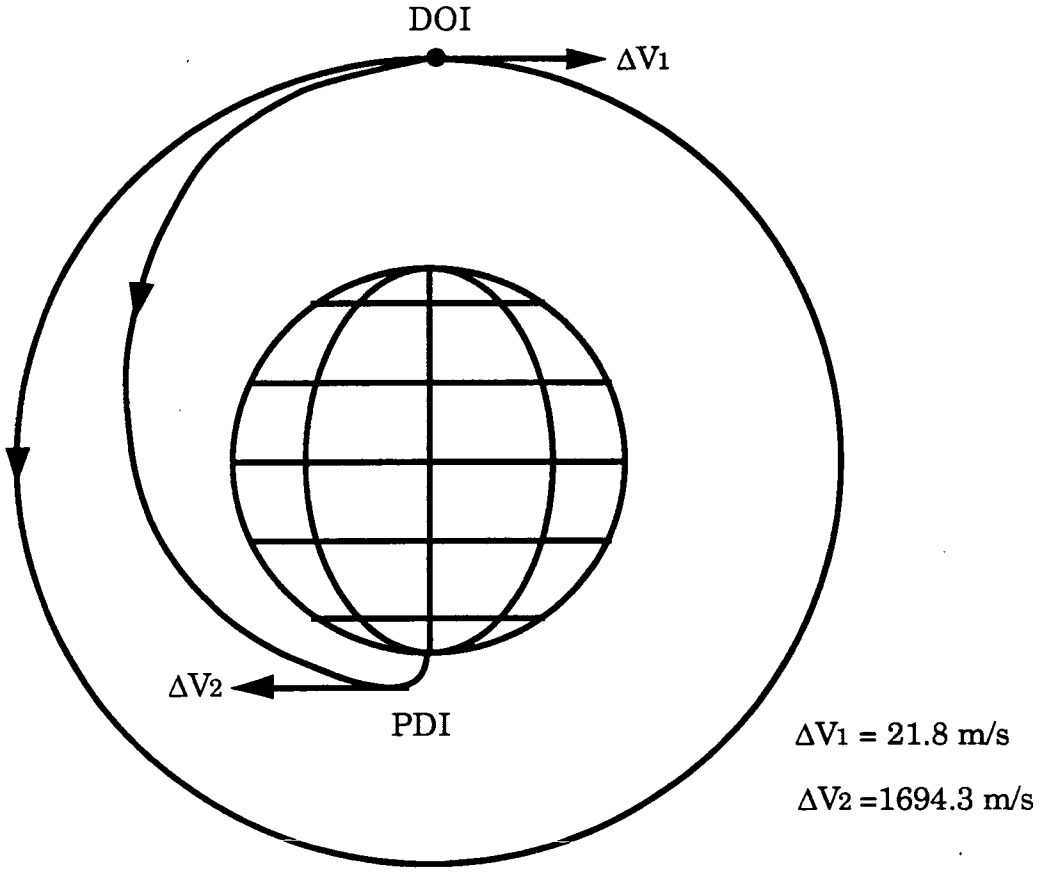

Figure 7.9 - Descent Trajectory

7.3.2.3. Powered Descent to the Lunar Surface

The powered descent to the lunar surface begins at PDI and is designed to brake the Lander from its orbital velocity to a velocity of 9.8 m/s by the time it reaches an altitude of 880 m above the lunar surface. This point in the descent trajectory is called High Gate. It is the beginning of a part of the powered descent during which the Lander will be descending at a constant velocity of 9.8 m/s. During the 90 seconds of constant velocity descent, the Lander engines are firing at a thrust level which is just high enough to counter the acceleration due to gravity of the Moon. After descending for 90 seconds, the Lander will reach a point in the descent trajectory called Low Gate at an altitude of 45.7 m above the lunar surface. The ΔV required from High Gate to Low Gate is just the gravitational acceleration of the Moon (g_m = 1.623 m/s^2) multiplied by the time of the descent (t = 90 s) as shown in equation 7.4:

$$\Delta V = g_m \times t \qquad (7.4)$$

The ΔV required from High Gate to Low Gate is 146 m/s. When the Lander reaches Low Gate, a braking ΔV of 9.8 m/s is applied to cancel its descent velocity.

During the descent from High Gate to Low Gate, the Lander will be able to scan the terrain of the proposed landing site to search for a clear landing zone. If the Lander has not found a clear zone by the time it reaches Low Gate, it may hover for up to 45 seconds and continue to scan the surface. The ΔV required for hovering may also be calculated using equation (7.4). The ΔV for a 45 second hover is 73 m/s. After a suitable landing spot has been located, the Lander will continue its descent to the surface at a rate of 1.0 m/s. If no hovering is required, a braking ΔV of 8.8 m/s will be applied at Low Gate instead, and the descent will continue at a rate of 1 m/s. The final descent to the surface will take 45.7 seconds and will require a ΔV of 74.2 m/s as calculated using equation (7.4). The Lander will land on the lunar surface at a velocity of 1.0 m/s.

7.3.3. Ascent

After activities on the lunar surface are complete, the Lander is ready to begin its ascent to the parking orbit. The ascent of the Lander will include a vertical rise off of the lunar surface before insertion into the parking orbit at the proper altitude. Finally, a Dog-Leg Maneuver will be performed to insure that the parking orbit is in the correct plane. The ascent trajectory is shown in Figure 7.10.

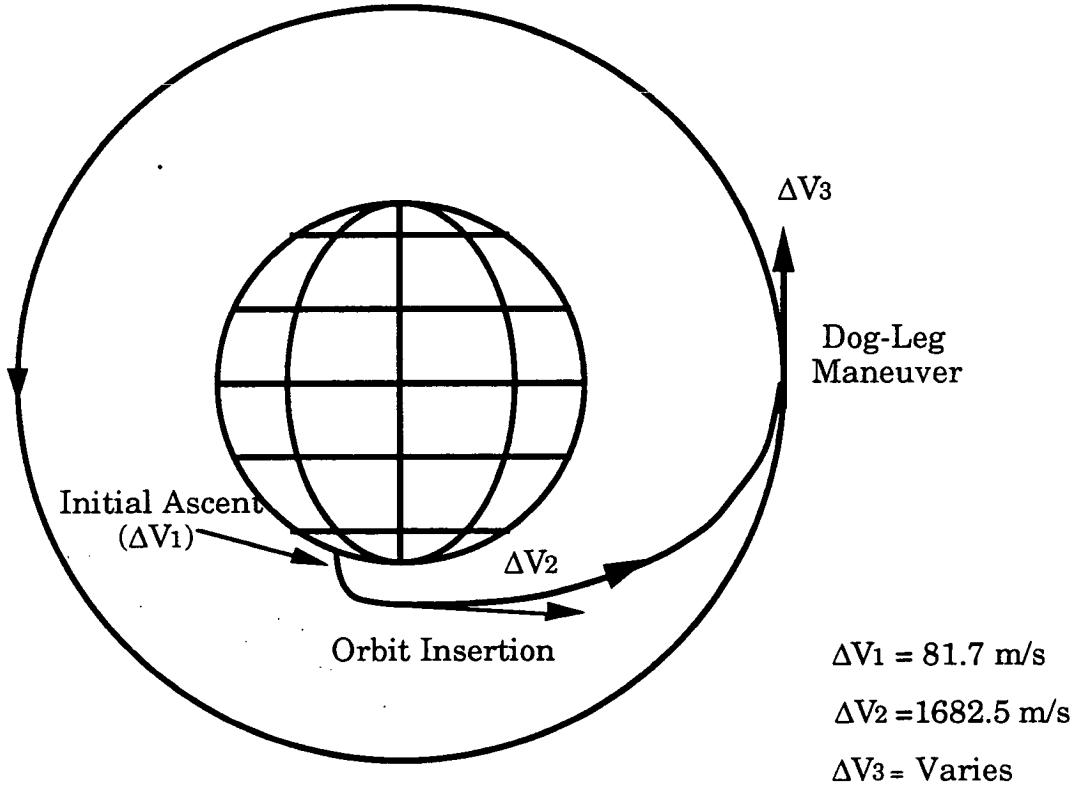

Figure 7.10 - The Ascent Trajectory

7.3.3.1. Initial Ascent

The initial ascent of the Lander consists of a vertical rise and then an ascent to an altitude high enough to insert the Lander into the parking orbit. The vertical rise

portion of the ascent trajectory has been included to insure that the Lander has risen high enough off of the lunar surface to allow it to avoid obstacles when it pitches over into horizontal flight. The Lander will first rise vertically off of the lunar surface to an altitude of 200 m. It will then begin to pitch over toward the horizontal as it continues to ascend toward the orbit insertion point at an altitude of 18.3 km. A ΔV of approximately 81.7 m/s will be required for the initial ascent of the Lander and it will take about 7 minutes.

7.3.3.2. Orbit Insertion

The initial ascent of the Lander will carry it to an altitude of 18.3 km. This altitude is sufficient to begin the insertion of the Lander into the parking orbit. The orbit insertion will require a ΔV of 1682.4 m/s and will take 29 minutes and 56 seconds. The calculation of this ΔV is explained in more detail in Appendix C.

7.3.3.3. Dog-Leg Maneuver

It will be necessary for the Lander to perform a Dog-Leg Maneuver once it has been inserted into the parking orbit. This maneuver is a combined orbit circularization and plane change and is explained in detail in Appendix C. A plane change is necessary in order to correct for the rotation of the Moon while the Lander is on the surface. The ΔV required for the Dog-Leg Maneuver will vary depending on the amount of time that the Lander spends on the surface. Figure 7.11 is a plot of the ΔV required for the Dog-Leg Maneuver as a function of the amount of time that the Lander spends on the surface (i = inclination of parking orbit, l = latitude of landing site).

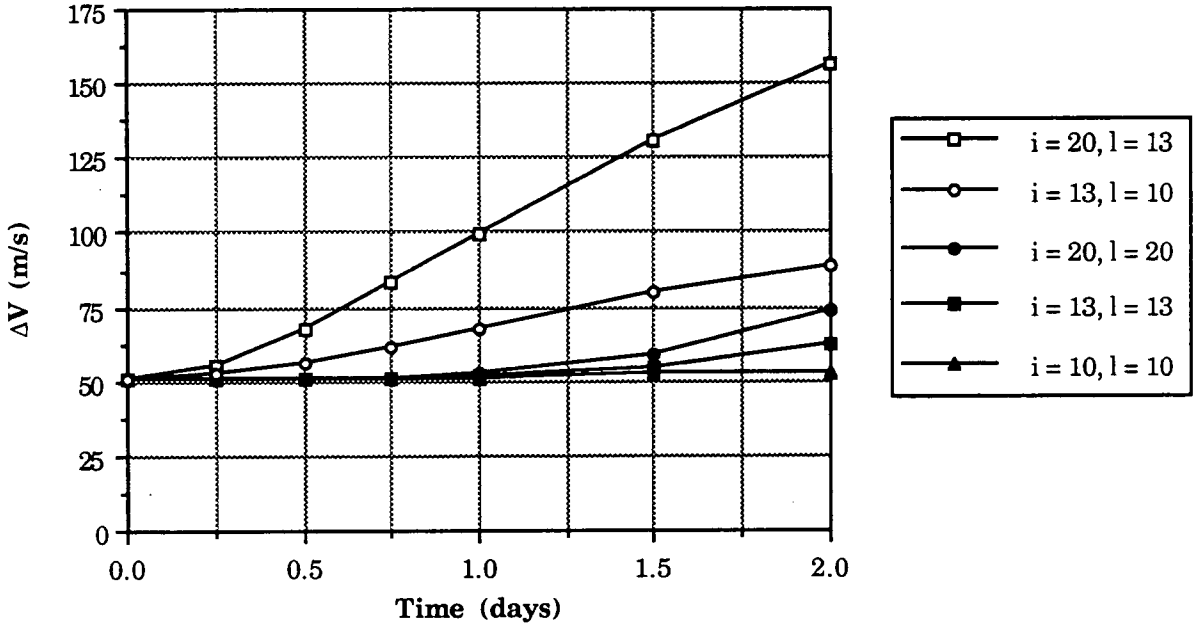

Figure 7.11 - ΔV Required vs. Time Spent on the Lunar Surface for Dog-Leg Maneuver

7.3.4. Mission Profile and Event Summary

The following chart is a summary of all of the major events in a UM-Haul mission. Included in the summary are the ΔV's required for each event, the time before the next event occurs, and the altitude of the Lander at the beginning of each event.

UM-Haul Mission Profile and Event Summary

Event	ΔV (m/s)	Time Before Next Event (min. : sec.)	Initial Altitude	Comments
Rendezvous				
DCOI	2.21	59:13	111 km	• Lander enters Hohmann transfer orbit (111 km x 101 km) to descend to the chase orbit.
COI	2.21	varies (0 - 10 days)	101 km	• Lander is inserted into the101 km chase orbit. • Lander begins phasing to catch up to the OTV.
TPI	2.21	59:13	101 km	• Lander enters Hohmann transfer orbit (111 km x 101 km) to intercept the OTV when the phase angle between the OTV and the lander is 0.725°.
Braking / Docking	2.21	-----	111 km	• Lander enters 111 km parking orbit, brakes, and docks with the OTV. • Cargo is transferred to the lander after docking.
Descent				
Separation	0.8	59:27	111 km	• Provides clearance between the lander and the OTV before the lander begins the descent to the lunar surface.
DOI	21.8	57:10	111 km	• Occurs about 1/2 orbit after separation of the lander and the OTV. • Lander enters Hohmann transfer orbit (111 km x 15.24 km) to begin the descent to the lunar surface.
PDI	1694.3	8:00	15.2 km	• Lander begins powered descent to the lunar surface. • Lander velocity begins to decrease from orbital velocity.
Powered Descent				
High Gate	146	1:30	880 m	• Lander begins approach to the lunar surface.
Low Gate	9.8	-----	45.7 m	• Lander descent rate decreases to zero. • If no hover is required, ΔV is 8.8 m/s and descent rate decreases to 1 m/s.
Hover	73	00:45	45.7 m	• If necessary, lander hovers while searching for a suitable landing site.
Final Descent	74.2	00:45.7	45.7 m	• Lander begins final descent to the lunar surface at a rate of 1 m/s.
Ascent				
Initial Ascent	81.7*	7:00*	0	•Vertical rise to 200 m. • Lander continues to ascend to 18.3 km for orbit insertion.
Orbit Insertion	1682.5	29:56	18.3 km	• Lander is inserted into the parking orbit.
Dog-Leg Maneuver	varies	-----	111 km	• Simultaneous orbit circularization and plane change. • See Figure 7.12 for ΔV.

* - approximate

7.4. The Requirement for a Daylight Landing

In order to satisfy power and communications needs, all of the UM-Haul landings must occur during the lunar day. Each of the landing sites is in daylight for approximately one-half of each month, but a landing at any site is only possible once every month when the site rotates into the plane of the parking orbit. A landing site is said to be in the plane of the parking orbit when an orbiting vehicle passes directly over that site. The most efficient landing is possible when the landing site is in the plane of the parking orbit, because otherwise a plane change would be needed to reach the site. Plane changes require significant ΔV's which are costly in terms of propellant use.

The initial parking orbit of the Lander when it arrives from the Earth with the OTV will determine what time of the month the first landing site is in the plane of the parking orbit. That landing site will then be in plane at the same time each subsequent month, assuming that the parking orbit is inertially fixed. The other landing sites will then be in the plane of the parking orbit at other times during the month. Thus, it is necessary to design the UM-Haul mission such that all of the landing opportunities will occur during the lunar day.

7.5. Landing Opportunities

Figure 7.12 shows the ground track of an orbit with an inclination, i, equal to the latitude of the landing site, l. The angle Ω is called the right ascension of the ascending node and is measured with respect to an inertially fixed direction in space. The angle δ may be found using spherical trigonometry as follows:

$$\sin(\delta) = \frac{\tan(l)}{\tan(i)} \tag{7.5}$$

A landing opportunity will occur when the right ascension of the landing site, α, is equal to $\Omega + \delta$. In general, the right ascension of the landing site is given by:

$$\alpha = \alpha_0 + \lambda + \omega(t - t_0) \tag{7.6}$$

where: α_0= Right ascension of the zero longitudinal line at time t_0

λ = East longitude of the landing site

ω = Angular velocity of the Moon = 13.187° per day

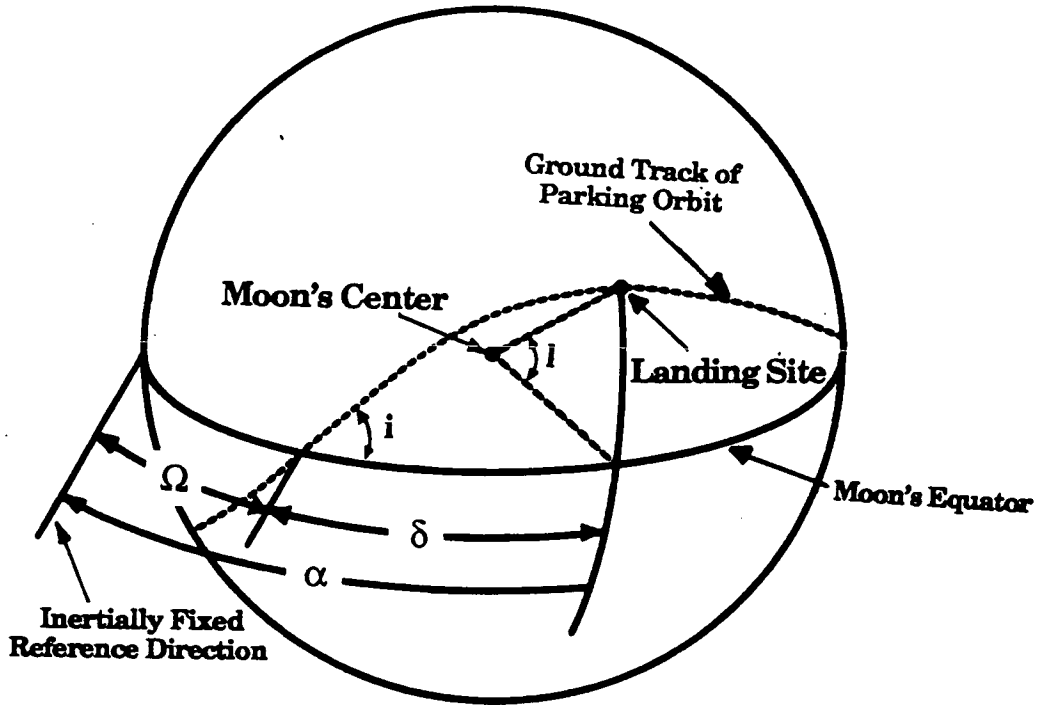

Figure 7.12 - Ground Track of Parking Orbit for Landing Opportunity at Arbitrary Landing Site

Substituting $\alpha = \Omega + \delta$ into equation (7.6) gives:

$$t = t_0 + \frac{\Omega + \delta - \alpha_0 - \lambda}{\omega}$$

(7.7)

for the landing time. The constants α_0 and t_0 are determined by the timing of the first insertion of the OTV and the Lander into the parking orbit. The timing must be controlled such that the time t is in the lunar day. Different landing sites will have different values of t so that it takes a time of $\Delta t = t_2 - t_1$ between landing opportunities for two different sites. This time difference (Δt) may be calculated using equation (7.7) as:

$$\Delta t = t_2 - t_1 = \frac{(\lambda_1 - \lambda_2) - (\delta_2 - \delta_1)}{\omega}$$

(7.8)

since Ω and α_0 are constants. When the Lander returns to the parking orbit after servicing Mare Nubium for the third time, it is launched into a 13° inclination orbit (i = 13°). The other components of equation (7.8) are as follows:

$\lambda_1 = -87.5°$ $\qquad$ $\delta_1 = -49.8°$

$\lambda_2 = -20.0°$ $\qquad$ $\delta_2 = -13.0°$

Substituting these values into equation (7.8) gives $\Delta t = 2.07$ days as the time between landing opportunities at Mare Nubium and Lacus Veris. A similar calculation gives $\Delta t = 21.6$ hours as the time between landing opportunities at Lacus Veris and Taurus-Littrow. Figure 7.14 is a timeline showing the time between the landing opportunities at the three landing sites, assuming that the landing opportunity at Mare Nubium occurs at the beginning of the lunar day.

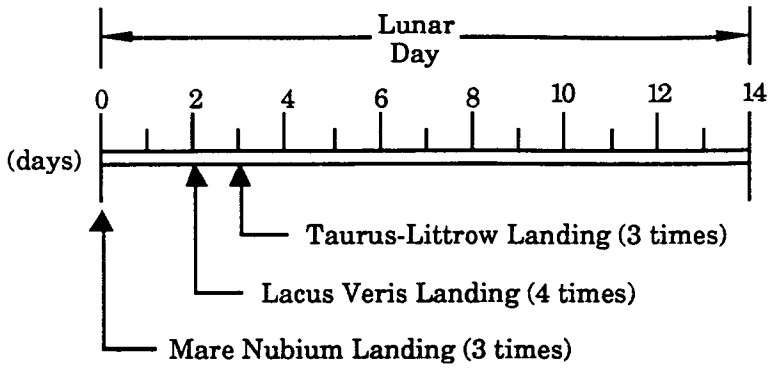

Figure 7.13 - Landing Opportunity Timeline

Thus, the landing sites at Lacus Veris and Taurus-Littrow rotate into the plane of the parking orbit approximately two and three days after the landing site at Mare Nubium, respectively. Since the landing opportunities span a period of about three days, the Mare Nubium landing must occur by the tenth day of the month in order to insure that all ten UM-Haul landings will occur during the lunar day. In order for these landing times to remain fixed, Ω must remain a constant. This is why a plane change to correct for the rotation of the Moon is needed during the ascent. If Ω were allowed to increase with the rotation of the Moon, then the landing opportunity times would eventually drift into the lunar night.

7.6. Communications Windows

Communications between the Lander, the Unloader, and the Earth play a vital role in the UM-Haul mission. The mission will be almost entirely automatically controlled, but it is necessary for personnel on Earth to be able to communicate with the Unloader in order to guide it. Personnel on Earth should also be able to monitor all operations as much as possible in order to detect any problems which may arise. Several different lines of communication between the Unloader, the Lander, and the Earth will be discussed in this section, as well as some other possible communications options.

7.6.1. Unloader Communications Windows

The Unloader will primarily communicate directly with the Earth, but it will also be able to use the orbiting Lander as a relay to the Earth. This section discusses the communications windows between the Unloader and the Earth and between the Unloader and the Lander.

7.6.1.1. Communications Between the Unloader and the Earth

An Unloader at either the Taurus-Littrow site or the Mare Nubium site will always have constant direct communications with the Earth, because both of these sites are always located on the near side of the Moon. The Lacus Veris site and the Mare Marginis site are both 2.5° away from the line of separation between

the near side and the far side of the Moon. The libration of the Moon's orbit around the Earth causes the visible portion of the Moon to vary by 7.75° each month. For approximately 10 days each month, Lacus Veris will be on the far side of the Moon and will not have direct communications with the Earth. The communications situation at Mare Marginis is exactly the opposite. Mare Marginis will only be on the near side of the Moon for approximately 10 days each month and will only have direct communications with the Earth during this period of time.

7.6.1.2. Communications Between the Unloader and the Lander

The Lander in the parking orbit has line-of-sight communications with any location on the surface that lies within a 19.95° arc of the point on the surface directly below the Lander. This means that the footprint of the Lander has a swath width of 39.9° as shown in Figure 7.14. Normally, each time the Lander orbits the Moon, the Unloader will lie inside the footprint of the Lander for some

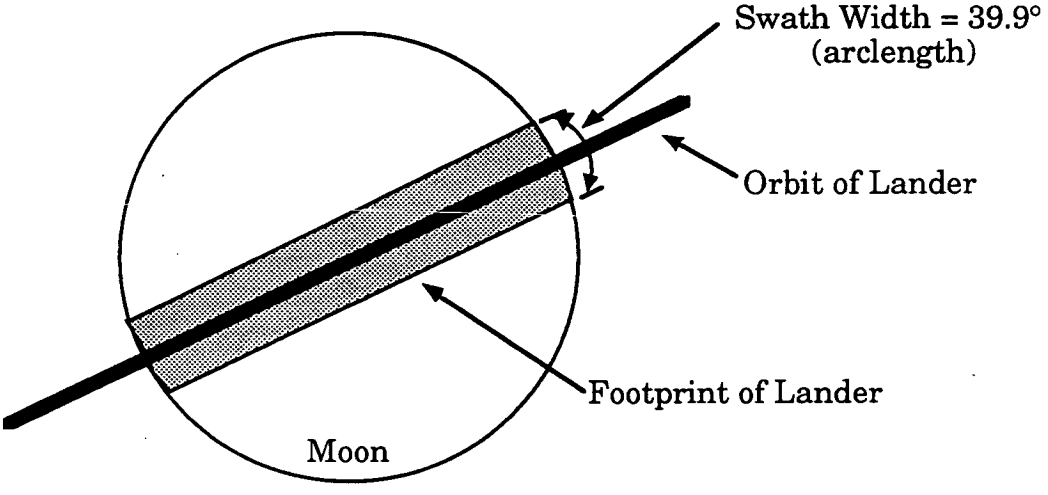

Figure 7.14 - The Footprint of the Lander in the Parking Orbit

portion of the orbit. However, the rotation of the Moon causes the amount of time during which the Lander can see the Unloader on the surface to decrease from a maximum of 13.2 minutes out of each 119 minute orbital period. The Moon eventually rotates far enough out of the plane of the parking orbit during the month so that the Lander can no longer see the Unloader. The Lander has to wait until the Unloader approaches the plane of the parking orbit again in order to communicate with it. The length of this gap in communications varies, depending on the latitude of the landing site and the inclination of the parking orbit [8]. The total communications gap for each of the four UM-Haul landing sites during each month is summarized in Table 7.1.

Table 7.1 - Total Communications Gap each Month between the Lander and the Unloader for the Four Possible UM-Haul Landing Sites

Landing Site	Location	Comm. Gap

Lacus Veris	87.5° W, 13° E	4.1 days
Taurus-Littrow	30° E, 20° N	10.6 days
Mare Nubium	20° W, 10° S	1.0 hour
Mare Marginis	92.5° E, 9.5° N	none

Locating a landing site close to the equator reduces the gap in communications. The gap is less than one orbital period for the Mare Nubium site and could be eliminated altogether by moving the landing site slightly to the North. The Mare Marginis site is less than 10° from the equator, so an Unloader at this site is visible to the Lander during every orbit. It is important to remember that on the days when the Lander and the Unloader are able to communicate, they are only able to do so for a maximum of 13.2 minutes out of every 119 minute orbit [8].

7.6.2. Lander Communications Windows

The Lander will communicate primarily with the Earth, but it must also be able to communicate with the OTV during its descent to the lunar surface. This section discusses the communications windows between the Lander and the Earth and between the Lander and the OTV.

7.6.2.1. Communications Between the Lander and the Earth

The Lander in LLO has constant direct communications with the Earth for the majority of each orbit. The exact portion of each orbit during which the Lander can communicate with the Earth depends on the inclination of the parking orbit. Table 7.2 lists the communications window from the Lander to the Earth during each orbit for each landing site and orbital inclination [9]. The communications window does not vary much with orbital inclination, so it should not influence the choice of a landing site.

Table 7.2 - Communications Window from the Lander to the Earth during each 119 Minute Orbit

Landing Site	Orbital Inclination	Comm. Window
Lacus Veris	13°	78.3 minutes
Taurus-Littrow	20°	79.3 minutes
Mare Nubium	10°	77.9 minutes
Mare Marginis	9.5°	77.8 minutes

When the Unloader is located at either Taurus-Littrow or Mare Nubium, the Lander can see the Earth at any time it is able to see the Unloader. This is not the case for Lacus Veris or Mare Marginis. Libration of the Moon causes Lacus Veris to move to the lunar far side for a portion of each month, reducing the

amount of time that the Lander can act as a relay between the Unloader and the Earth. The relay time decreases from a maximum of 13.2 minutes to 12.8 minutes when Lacus Veris reaches its farthest point on the far side. Mare Marginis is usually on the far side, but libration affects the amount of time that the Lander can act as a relay between the Unloader and the Earth. Libration will sometimes reduce the relay time from Mare Marginis from the maximum of 13.2 minutes to 12.4 minutes [9].

7.6.2.2. Communications Between the Lander and the OTV

One concern during descent is communications between the OTV and the Lander. The OTV must be able to communicate with the Lander during the entire descent. As mentioned previously, communications between the OTV and the Lander will be blocked when the phase angle between the two vehicles is greater than 39.9°. During the descent, the phase angle between the OTV and the Lander reaches a maximum at PDI. The phase angle at PDI is calculated by determining the angle that the OTV travels through in the parking orbit while the Lander moves from DOI to PDI. The phase angle at PDI is:

$$\phi_{PDI} = 180 - (T_{Hohmann} \times \omega_O)$$

(7.9)

Equation (7.9) gives a value of $\phi_{PDI} = 6.87°$ which is less than 39.9°. Since the phase angle reaches a maximum at PDI, communications between the OTV and the Lander will never be interrupted during the descent of the Lander to the lunar surface.

7.6.3. Earth Receiving Stations

Ground-based receiving stations will monitor the signals sent back to the Earth by the UM-Haul vehicles during lunar operations. Three large ground stations are presently available for use and could provide nearly continuous monitoring of signals originating from the Moon. Another option would be to use two satellites in geosynchronous orbit to monitor lunar transmissions, but this system is not yet available for use [10].

7.6.4. Other Communications Options

In order to maintain constant communications with the orbiting Lander and vehicles anywhere on the lunar surface, it is necessary to place two satellites into orbit at each of the Earth-Moon libration points. These satellites would be able to act as relays for any communications between the Earth and the Moon. It is unlikely that these satellites would be deployed until well after the establishment of a permanent lunar base, so UM-Haul would be unable to make use of them during its early missions [10].

7.7. References

[1] Alred, J., and K. Fairchild, Lunar Surface Operations Study, Eagle Engineering Report No. 87-172, NASA Contract NAS9-17878, December 1, 1987.

[2] Alred, J., et. al., Lunar Outpost, (Systems Definition Branch, Advanced Programs Office), NASA Johnson Space Center, Houston, Texas, 1989.

[3] Bate, Roger R., Donald D. Mueller, and Jerry E. White, Fundamentals of Astrodynamics, New York, Dover Publications, Inc., 1971.

[4] Masurky, Harold, G. W. Colton, and Farouk El-Baz, Apollo Over the Moon: A View from Orbit, NASA SP-362, Science and Technical Information Office, NASA, 1978.

[5] Apollo 12 Preliminary Science Report, NASA SP-235, Manned Spacecraft Center, 1970.

[6] Analysis of Apollo 8 Photography and Observations, NASA SP-201, Manned Spacecraft Center, 1969.

[7] Apollo 12 Lunar Landing Mission H-1: Spacecraft Familiarization Document, NASA George C. Marshall Space Flight Center, Huntsville, Alabama, November 7, 1969.

[8] Wertz, James R. and Wiley, J. Larson, ed., Space Mission Analysis and Design, Boston, Kluwer Academic Publishers, 1991.

[9] Buning, Harm, Mission Analysis and Orbital Operations: AERO 542 Coursepack, The University of Michigan, Ann Arbor, 1984.

[10] Evaluation and Comparison of Alternative Communication Architectures for Lunar Exploration, Volume I, Computer Sciences Corporation, NASA Contract NAS5 - 31500, NASA Goddard Space Flight Center, November, 1990.

[11] Apollo 11 Lunar Trajectory Notes, MSC Internal Note No. 69-FM-209, Manned Spacecraft Center, Houston, Texas, July 14, 1969.

[12] Alred, John Ph.D., Eagle Engineering, Interview, February 13, 1991.

[13] Alred, J., Technical Monitor, and M. Roberts, Task Manager, Lunar Lander Conceptual Design,Eagle Engineering Report No. 88-181, NASA Contract NAS9-17878, May 1, 1988.

[14] Private Conversation with Professor Donald T. Greenwood, The University of Michigan, March 7, 1991.

[15] Wiesel, William E., Spacecraft Dynamics, McGraw-Hill, Inc., 1989.

Chapter 8

Conclusion

8.0. Summary

The results presented in this report are the products of a preliminary design study of a Self-Unloading Reusable Lunar Lander. The present UM-Haul design has not been closed, even to preliminary phase standards. It is clear, therefore, that much research remains to be done before the design can be considered for project phase advancement. However, based on the preliminary results obtained by the design Team, the UM-Haul system will be able to successfully fulfill its mission goals.

Rough estimates indicate that the developmental and production costs for one UM-Haul system alone will total nearly 1.3 billion dollars.

8.1. UM-Haul Design Status

In this concluding chapter of the report, it seems fitting to ask how much has actually been done, and where this design would place in a large-scale project life cycle.

A full-scale engineering design project can be seen as consisting of roughly four main phases [1]:

Phase A: Preliminary Design
- Feasibility studies, budgeting, preliminary analysis.

Phase B: Detail design
- In-depth analysis of system, spot developmental needs.

Phase C: Development
- Testing, clear design for final blueprint.

Phase D: Realization
- Manufacturing, assembly and launch.

This report describes the "Phase A" design for a Self-Unloading Reusable Lunar Lander. Due to the academic time constraint imposed upon the Team, however, it was not possible to complete the entire preliminary design phase. In order to assess the current developmental stage of UM-Haul, consider the ideal preliminary design cycle given below [2]:

1. Define quantitative system requirements.
2. Establish a program philosophy.
3. Partition the system.
4. Develop possible mission profiles.
5. Develop models to evaluate feasibility.
6. Estimate critical parameters at all levels.
7. Define issues to be studied.
8. Establish budget for critical parameters.
9. Establish margins for critical parameters.
10. Iterate until design closes with desired margins.

In the following paragraphs, the implementation of these stages for Project UM-Haul will be discussed.

1. Define Quantitative System Requirements: A design project should be based on a list of specific top-level requirements, which, in later stages of the design, should be reflected in all critical subsystem parameters. The requirements for Project UM-Haul can be found in section 1.2.2 of this report.

2. Establish a Program Philosophy: Assess the role of the program in a larger context and the bounds imposed upon it by these circumstances. Example: UM-Haul does not use nuclear propulsion/power as it will be delivering cargo for a future manned lunar base. A full description of the program philosophy is contained in section 1.1.2.

3. Partition the System: Assign subsystem tasks in a logical manner such that group interfaces become clear-cut, both administratively and technically. Refer to the preface of this report for the breakdown of specific technical group responsibilities.

4. Develop Possible Mission Profiles: Generate strategies for achieving the mission goals (i.e. how to get there?) and develop viable design concepts. A summary of this phase is contained in section 2.2.

5. Develop Models to Evaluate Feasibility: Construct simple models (theoretical or physical) of the design concepts to discover and evaluate fundamental problems. Given the Project UM-Haul time constraints, exhaustive evaluation of the design concepts was not possible. However, a brief discussion of this phase is contained in section 2.2.

6. Estimate Critical Parameters at All Levels: For all design concepts under consideration, identify and approximate parameters critical to the success of the mission. Examples of such parameters range from technical aspects such as structural strength and power consumption, to logistical factors like time limits and operational costs. For the sake of conciseness, no exact account of this phase is given in this report; yet it comprised a significant part of the early design work.

7. Define Issues to be Studied: Select methods by which problem issues are to be solved. Within the time budget of all projects, there will be limits to the number of methods one can afford to employ. It is therefore of critical importance to choose the methods with a high promise of useful returns. Much of this success depends on the proper formulation of questions. It is important to remember, however, that most real world (i.e. complex) problems have *no optimum solution*. In Project UM-Haul, these decisions were generally made on the Group Leader level, and references to them can be found throughout the report.

8. Establish Budget for Critical Parameters: Develop a scheme in which all critical parameters are monitored against mandated limits with the continual evolution of the design. Within the severe constraints of Project UM-Haul, no time was found to formalize this process. In compensation, the

small size of the Team facilitated efficient ad hoc communication of critical parameter changes.

9. Establish Margins for Critical Parameters: Assess the accuracy to which the critical parameters are determined. These figures are a measure of the consistency and the completeness of the design. Due to the aforementioned constraints, no systematic effort has been made to chart the margins of UM-Haul.

10. Iterate Until Design Closes with Desired Margins: Repeat points 6-10 until the margins converge. In a preliminary design study, only two to three iterations should be required for plausible accuracy. Project UM-Haul did not allow time for such iterations.

In summary, the progress of the UM-Haul design has been limited to include points 1-8. Any inconsistencies found within this report are likely due to the lack of finalized critical margins and verified parameter convergence. Regardless, based on the preliminary results obtained by the design Team, the UM-Haul system will be able to successfully fulfill its mission goals.

8.2. Future Research and Development

As can be inferred from the preceding discussion of the design status, many important areas remain to be further researched, detailed and developed. Some immediate concerns to be further addressed (by general domain) are listed in the following:

8.2.1. Unloader

- Structure: Finite Elements Analysis (static and dynamic), reliability and redundancy, suspension, transmissions, drive train, lifting mechanisms, deployable Payload legs.

- Power: Thermal management system, power architecture and usage, NaS battery freeze-thaw cycles, solar cell technology, solar array shadowing.

- Controls: Obstacle avoidance system, artificially intelligent guidance and navigation (full autonomy), on-board computer design, task management software, steering, lifting.

8.2.2. Lander

- Structure: Finite Elements Analysis (static and dynamic), landing impact attenuation, reliability and redundancy, propellant tank analysis.

- Propulsion: Main engines and RCS power requirements, detailed propellant delivery system, volumetric boil-off figures.
- Power: Thermal management system, power architecture and usage, Fuel Cell technology.
- Controls: Obstacle avoidance scanner characteristics, attitude control system, guidance and navigation algorithms, flight computer design.

8.2.3. System

- Management: Compilation of critical parameter margins, verification of consistency and completeness, accurate cost analysis.
- Spacecraft Integration: Upkeep of Integrated Control Documents, compliance of system interface specifications, Failure Mode Effect Analysis.
- Communications: Use of Lunar and/or Earth-orbiting relay satellites, optimize link, telemetry specifications.
- Mission Analysis: Burn times, orbital perturbations and stationkeeping, LEO-to-LLO OTV launch timing, far side landings.

8.3. Cost Analysis

A rough estimate of the UM-Haul total cost and systems cost breakdown is shown in Table 8.1:

Table 8.1 - UM-Haul Cost Breakdown

System	Design/Dev ($M)	Production ($M)	Total ($M)
Lander			
Structure	239	19	258
Propulsion	527	17	544
GN&C	188	59	247
Power	66	16	82
Misc.	19	3	22
Total	**1039**	**114**	**1153**
Unloader			
Structure	15	7	22
GN&C	30	15	45
Power	20	7.4	27.4
Motors	5	0.6	5.6
Total	**70**	**30**	**100**
UM-Haul (Dry)	**1109**	**144**	**1253**

The total cost of nearly 1.3 billion dollars does not include intermediate operational costs such as in-orbit assembly and system launch. It should be noted that these figures primarily focus on the hardware part of UM-Haul; accordingly, often significant factors such as ground support infrastructure (personnel) and maintenance costs have not been considered.

8.4. References

[1] Lemke, L. G., Mission and Systems Engineering, NASA Ames; Seminar given at University of Michigan, Ann Arbor, 1/16/91.

[2] Shea, Dr. Joseph, Professor, Systems Engineering - Can it be Taught?, Massachusetts Institute of Technology, Seminar given at the University of Michigan, Ann Arbor, 4/2/91.

Chapter 9

Appendices

Appendix A: Structures

For the analysis of the structural components of the Lander and Unloader, beam theory was used. Beam theory calculations resulted in a value for the maximum stresses and moments the structural members would encounter for a given set of loading conditions [refer to Figure A.1 for the shear and moment diagrams for the Unloader]. These results were used to find the minimum size, and thus the minimum mass, of the given member. This process was then repeated, incorporating the mass of the members into the loading conditions. These calculations were performed until two consecutive iterations were approximately the same. To expedite this analysis, two spreadsheets, using Microsoft Excel, were constructed for the Lander and Unloader [see following pages].

Notes:

1. In each spreadsheet, **h** and **b** refer to the height and base, respectively, of a rectangular cross section, while **h1**,**b1** and **h2**,**b2** refer to the outer and inner dimensions respectively.

2. In the Lander spreadsheet, under the **Platform Spars** column, h1=.203 m for the two outermost spars but h1=0.123 for the inner spars as shown.

3. All units are SI units (meters, kilograms, etc.).

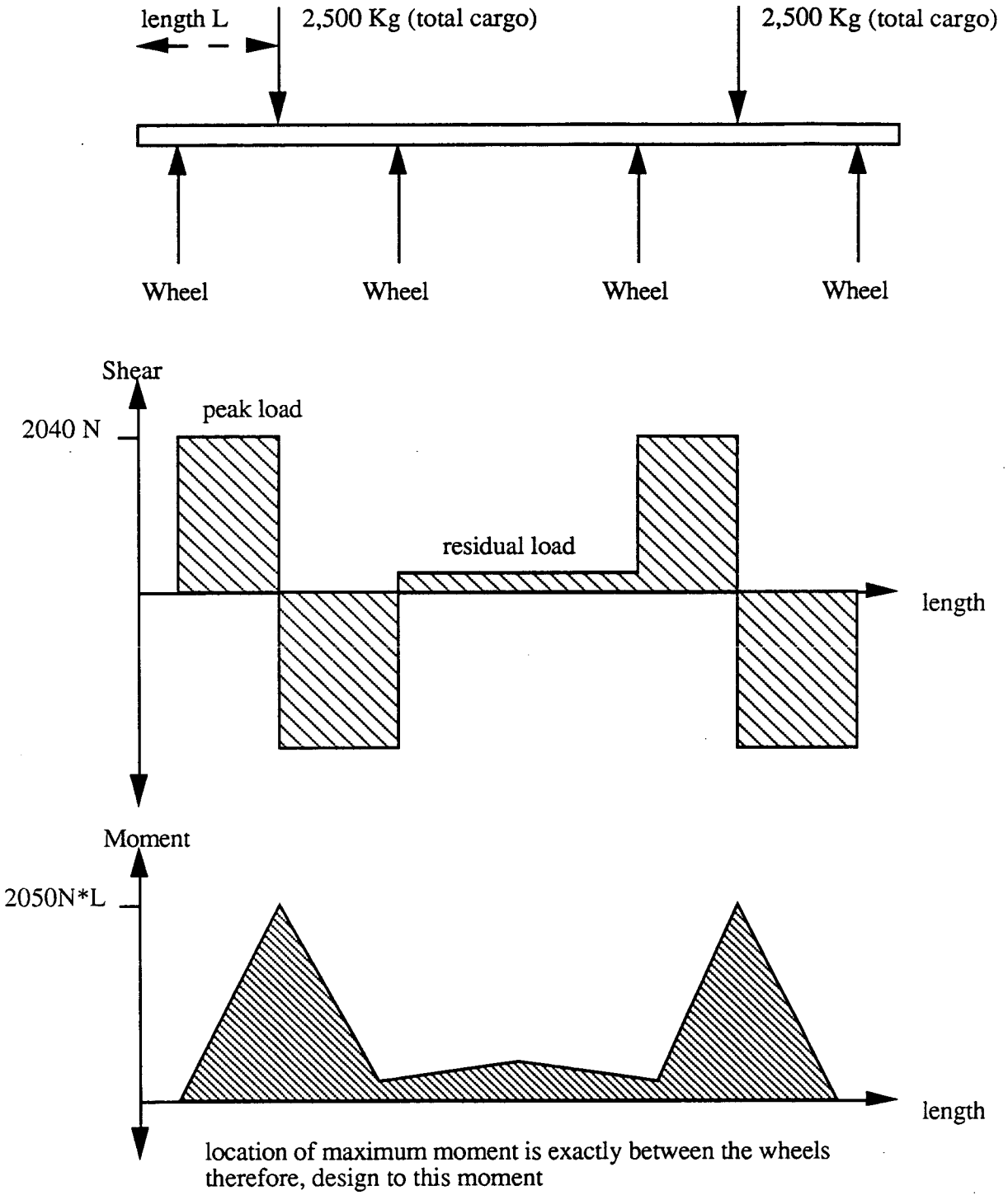

Figure A.1 - Unloader Shear and Moment Diagrams

Cargo	Rocker Joint	Support Rail			Threaded Post	Rail Post		Hard Lock
8439	arclength	length			length	length		length
	0.5	5.787			1.1	1.1		0.65
Material Density	width	outer radius	outer radius	outer radius	outer radius	outer radius	outer r (min)	outer radius
2546	0.25	0.042708684	0.063	0.063	0.036114291	0.041174529	0.062666667	0.034303214
Kg/m3	thickness	inner radius	inner radius	inner radius	inner radius	inner radius	inner r (min)	inner radius
	0.031550794	0.032031513	0.059337888	0.053	0.027085718	0.030880896	0.047	0.025727411
Yield Strength	volume	volume	volume	volume	volume		volume	volume
206666667	0.003943849	0.014508209	0.008145091	0.02108926	0.001702981		0.005937366	0.001051262
	mass each	mass each	mass each	mass each	mass each		mass each	mass each
PI	10.04104005	36.93789908	20.73740117	53.69325636	4.335788762		15.11653325	2.676512776
3.141592654	total mass	total mass	total mass	total mass	total mass		total mass	total mass
	60.2462403	73.87579816	41.47480235	**107.3865127**	17.34315505	0	**60.466133**	**5.353025551**
Structure Mass		(Ro too small)	(thin wall)		(check buckling)	(too small)	(threads fit)	
448.2566714								
Suspension Mass								
140								
					For Buckling		**For Buckling**	
Wheel Mass								
320					length		length	
					1.1		1.1	
Power Mass					outer radius		outer r (min)	
425					0.047168747		0.052414895	
					inner radius		inner r (min)	
Motor Mass					0.03537656		0.047	
70					volume		volume	
					0.002905094		0.001860305	
C & C Mass					mass each		mass each	
35					7.396369787		4.736335471	
					total mass		total mass	
System Mass					**29.58547915**		18.94534188	
1438.256671								

Structural Analysis of Unloader

	Cross Beam		Chassis Beam		Chassis Spar	Rod Truss		Solar Shelding
length	length		length		length	length	width	
3	3		7		2.9196	2.9196	3.4238	
outer radius	outer radius	outer radius	H outer	H outer	H outer	outer radius	outer radius	
0.034303214	0.00399441	0.062666667	0.041118925	0.0762	0.0762	0.009022481	0.009022481	
inner radius	inner radius	inner radius	H inner	H inner	H inner	inner radius	inner radius	
0.025727411	0.002995808	0.0580849	0.030839193	0.0635	0.0635	0	0	
volume	volume	volume	volume	volume	volume	total volume		
0.004851978	0.0000658	0.005214321	0.005177971	0.01241933	0.005179925	0.007982419		
mass each	mass each	mass each	mass each	mass each	mass each	1 truss bar mass	1 truss bar mass	
12.35313589	0.167499252	13.27566016	13.18311348	31.61961418	13.18808937	1.901006237	2.229300299	
total mass	total mass	total mass	total mass	total mass	total mass	total mass		
12.35313589	0.334998505	**26.55132032**	26.36622697	**63.23922836**	**52.75235746**	**20.32323862**		**10**
	(axial str.)	(trans. str.)	(min. size)	(desired size)				(approximated)

Cargo		Platform Beams		Platform Spars	Engine Shrouds	
8439		(tapd.) segment 1,3	segment 2		transverse	axial
		length	length	length	hypt. length	hypt . length
Material Density (kg/m3)		2.297	5	8	2.4	3.15
2546		b1	b1	b1	R1	R1
		0.203	0.203	0.203	0.016198173	0.002290009
Yield Strength		h1	h1	h1	R2	R2
413333334		0.123	0.203	0.123	0.01214863	0.001717506
		b2	b2	b2		
PI		0.1886	0.1886	0.1886		
3.141592654		h2	h2	h2		
		0.101	0.181	0.101		
Structure Mass		area (ave)	area	area	area	area
3409.466527		0.0064964	0.0070724	0.0059204	0.00036063	0.00000721
		I (start)	I	I	I	I
Power Mass (w/ react.)		0.0000153	0.0000483	0.0000153	0.000000037	1.47651E-11
850		volume	volume	volume	volume	volume
		0.014922231	0.035362	0.0473632	0.016069605	0.000516597
PSCI		mass	mass	mass	mass	mass
240		37.99199962	90.031652	120.5867072	40.91321451	1.315255318
		Total Mass	Total Mass	Total Mass	Shroud Mass	Shroud Mass
C & C Mass		379.9199962	450.15826	482.3468288	**163.652858**	5.261021273
86.3						
		Platform Mass				
Propulsion Systems		**1312.425085**				
1077						
Dry Mass						
5662.766527						
Take-Off Propellent	Descent Propellent					
4665	12002					
Take-Off Mass	Total Descent Mass					
10327.76653	30768.76653					
Landing Mass						
18766.76653						
	18931					

Ramp				**Legs**			
main support	truss	plates	side guides	Leg Post	Leg Shell	Support	Pad
length	length	length	length	length	length	length	thickness
4	1.084619749	1	4	3.08	3	2	0.03
R1	R1	width	thickness	R1	R1	R1	R1
0.031430674	0.011290184	0.42	0.005	0.059341016	0.150408848	0.0777229	0.5
R2	R2	thickness	arc	R2	R2	R2	
0.023573006	0	0.003	0.2	0.044505762	0.140408848	0.066064465	
area	area	area	area	area	area	area	area
0.001357799	0.000400453	0.42	0.001	0.00483992	0.00913631	0.005266364	0.785398164
I	I			I	I	I	
0.00000052	0.00000001			0.000006657	0.000096702	0.00001370	
volume	volume	volume	volume	volume	volume	volume	volume
0.005431194	0.004147478	0.00126	0.004	0.014906943	0.027408922	0.010532727	0.023561945
mass	mass	mass	mass	mass	mass	mass	mass
27.65564019	10.55947938	3.20796	10.184	37.95307727	69.78311588	26.81632412	59.98871173
Support Mass	Truss Mass	Plating Mass	Guide Mass	Leg Post Mass	Leg Post Mass	Leg Support	Landing Pads
110.6225608	**42.23791751**	**51.32736**	**81.472**	151.8123091	**279.1324635**	**107.2652965**	**239.9548469**
Ramp Mass					area required		
285.65983826				**Buckling Load**	0.000111238		
				length			
				3.08			
				R1			
				0.140408848			
				R2			
				0.119347521			
				area	mass		
				0.01718707	134.7754934		
				I	Leg Post Mass		
				0.000107855	**539.1019736**		
				volume			
				0.052936172			

Structural Analysis of Lander

Runners				**Truss**	**Thin Plating**
main support	truss	plates	side guides	for various	
length	length	length	length	supports	thickness
8	1.25	1	8		0.001
R1	R1	width	thickness	R1	
0.021328994	0.011837096	0.75	0.005	0.01	
R2	R2	thickness	arc	R2	
0.015996746	0	0.003	0.2	0	
area	area	area	area	area	total area
0.000625272	0.00044019	0.75	0.001	0.000314159	155.9
I	I			I	
0.00000011	0.00000002			0.00000001	
volume	volume	volume	volume	volume	total volume
0.005002173	0.01028284	0.00225	0.008	0.050265482	0.1559
mass	mass	mass	mass	mass	mass
12.7355312	26.18010998	5.7285	20.368	127.9759184	396.9214
Support Mass	Truss Mass	Plating Mass	Guide Mass	Truss Mass	Plate Mass
50.94212478	**104.7204399**	**183.312**	**162.944**	**127.9759184**	**396.9214**
Runner Mass					
501.91856472					

Appendix B: Propulsion

Propellant Mass Requirements

Isp = 470 sec		ΔV=1.929&2.02 km/s		m Unloader = 1502 kg		nominal		cont.&	required		loading
m lander	R ascent	m ascent	m prop asc	R descen	m descent	m prop desn	m prop tota	off-nom	reserves	total	residual	uncertain
(kg)		(kg)	(kg)		(kg)	(kg)	(kg)	(kg)	(kg)	(kg)	(kg)	(kg)
5500	1.520	10640.830	3646.726	1.550	27343.025	9702.195	13348.921	15.018	2002.338	15366.276	230.494	76.831
5600	1.520	10792.798	3698.807	1.550	27578.573	9785.775	13484.582	15.170	2022.687	15522.440	232.837	77.612
5700	1.520	10944.767	3750.888	1.550	27814.122	9869.356	13620.244	15.323	2043.037	15678.603	235.179	78.393
5800	1.520	11096.735	3802.970	1.550	28049.671	9952.936	13755.906	15.475	2063.386	15834.767	237.522	79.174
5900	1.520	11248.703	3855.051	1.550	28285.220	10036.616	13891.567	15.628	2083.735	15990.930	239.864	79.955
6057	**1.520**	**11487.294**	**3938.818**	**1.550**	**28655.031**	**10167.738**	**14104.556**	**15.868**	**2115.683**	**16236.107**	**243.542**	**81.181**
6200	1.520	11704.609	4011.294	1.550	28991.866	10287.258	14298.552	16.086	2144.783	16459.421	246.891	82.297
6250	1.520	11780.593	4037.335	1.550	29109.641	10329.048	14366.383	16.162	2154.957	16537.502	248.063	82.688
6300	1.520	11856.577	4063.376	1.550	29227.415	10370.838	14434.213	16.238	2165.132	16615.584	249.234	83.078
6350	1.520	11932.561	4089.416	1.550	29345.189	10412.628	14502.044	16.315	2175.307	16693.666	250.405	83.468
6400	1.520	12008.546	4115.457	1.550	29462.964	10454.418	14569.875	16.391	2185.481	16771.747	251.576	83.859
6450	1.520	12084.530	4141.497	1.550	29580.738	10496.209	14637.706	16.467	2195.656	16849.829	252.747	84.249
6500	1.520	12160.514	4167.538	1.550	29698.513	10537.999	14705.537	16.544	2205.831	16927.911	253.919	84.640

Propellant Mass Requirements

FINAL			Spherical	Spherical		
TOTAL	m LH2	m LOX	Vol LH2	Vol LOX	Rad. LH2	Rad. LOX
(kg)	(kg)	(kg)	(m^3)	(m^3)	(m)	(m)
15673.602	2239.086	13434.516	31.724	11.811	1.964	1.413
15832.889	2261.841	13571.047	32.046	11.931	1.970	1.418
15992.175	2284.596	13707.579	32.369	12.051	1.977	1.422
16151.462	2307.352	13844.110	32.691	12.171	1.984	1.427
16310.749	2330.107	13980.642	33.014	12.291	1.990	1.432
16560.829	**2365.833**	**14194.996**	**33.520**	**12.479**	**2.000**	**1.439**
16788.609	2398.373	14390.236	33.981	12.651	2.009	1.445
16868.252	2409.750	14458.502	34.142	12.711	2.012	1.448
16947.896	2421.128	14526.768	34.303	12.771	2.016	1.450
17027.539	2432.506	14595.033	34.465	12.831	2.019	1.452
17107.182	2443.883	14663.299	34.626	12.891	2.022	1.455
17186.826	2455.261	14731.565	34.787	12.951	2.025	1.457
17266.469	2466.638	14799.831	34.948	13.011	2.028	1.459

Spreadsheet Definitions

Column 1, "m lander": This is the mass of the Lander (kg) including the Lander's structural mass, and the masses of all other subsystems.

Column 2, "R ascent": This represents the ascent payload ratio.

$$\text{R ascent} = e^{\frac{\Delta V_a}{g_o * Isp}}$$

where ΔV_a is the ascent ΔV in $\frac{m}{s}$

g_o is the value of Earth's gravitational constant, 9.807 $\frac{m}{s^2}$

Isp is specific impulse in seconds

Column 3, "m ascent": This is the mass of the Lander plus the mass of the Unloader and the mass of the ascent propellant. In this configuration, the Lander is ready to take off from the lunar surface and return to orbit. Because payload ratio, R, is also the ratio between the initial mass and final mass,

$$R = \frac{m_i}{m_f}$$

then m ascent can be called the initial mass, and m Lander plus m Unloader would then be the final mass. The m_f occurs when the Lander has returned to lunar orbit with the Unloader but without any ascent propellant.

$$\text{m ascent} = \text{R ascent} * (\text{m Lander} + \text{m Unloader})$$

where m Unloader is the mass of the Unloader in kg.

Column 4, "m prop asc": This is the mass of the ascent propellant in kg. It follows from the definition of m ascent that

$$\text{m prop asc} = \text{m ascent} - (\text{m Lander} + \text{m Unloader})$$

Also included in m prop asc is a small correction for boil-off.

Column 5, "R descent": This is the descent payload ratio.

$$\text{R descent} = e^{\frac{\Delta V_d}{g_o * Isp}}$$

where ΔV_d is the descent ΔV in $\frac{m}{s}$

Column 6, "m descent": This includes m Lander, m Unloader, the 7000 kg payload, m prop asc, and the descent propellant required. Similar to Column 3, if m descent is called the initial mass (when the Lander is ready to descend from orbit to the surface), then the final mass will be m descent without the descent propellant (when the Lander has arrived on the lunar surface). This final mass would simply be m ascent plus the payload mass.

m descent = R descent * (m ascent + 7000 kg payload)

Column 7, "m prop des": This is the descent propellant, computed from

m prop des = m descent - (m ascent + 7000 kg payload)

Column 8, "nominal m prop total": This is the sum of the ascent and descent propellant masses.

nominal m prop total = m prop asc + m prop des

Column 9, "off-nom": This is the allowance for off-nominal performance of the propulsion system, .75% of the nominal propellant total.

off-nom = .0075 * nominal m prop total

Column 10, "cont. & reserve": These two terms represent the propellant required for reserves and contingencies. Both safety factors require 7.5% of the nominal propellant total, for a combined 15% of the nominal propellant total in this column.

cont. & reserve = .15 * nominal m prop total

Column 11, "required total": This is the required propellant mass, or the nominal propellant total plus the safety factors of off-nominal performance, reserves, and contingencies.

required total = nominal m prop total + off-nom + cont. & reserve

Column 12, "residual": This accounts for any propellant trapped in tanks, propellant piping, etc. It is 1.5% of the required total propellant.

residual = .015 * required total

Column 13, "loading uncertain": This is the mass of the propellant required to make up for any loading uncertainty that occurs during refueling, typically .5% of the required total propellant mass.

loading uncertain = .005 * required total

Column 14, "FINAL TOTAL": This is the final mass of propellant required to achieve the required ΔV's and also account for safety and other factors.

FINAL TOTAL = required total + residual + loading uncertain

Tank Calculations

The following is a calculation of the Hydrogen and Oxygen tank volumes, and tank wall thickness' and weights, with and without insulation.

Hydrogen Tanks

The total mass of Hydrogen required for one mission is 2,452 kg. Using four equally sized spherical tanks, this gives a mass of 613 kg per tank. The preliminary volume of the tank is 34.74 m^3 . This is calculated from the equation for the density of Hydrogen (1).

(1) $$\text{Volume} = V1 = \frac{\text{mass Hydrogen}}{\text{density Hydrogen}} = 34.74\ m^3$$

where

mass Hydrogen = 613 kg
density Hydrogen = 70.58 kg/m^3

The volume of the tanks also have to take into account the ullage volume. The ullage volume is calculated to be 2.5% of the total volume of the tank. Therefore, the total volume of the tank is given by equation (2) below.

(2) $$\text{Total Volume} = VT = V1 + (.025) * V1 = 35.61\ m^3$$

The radius of the tanks can then be calculated using the equation for the volume of a sphere, (3).

(3) $$\text{Volume} = \frac{4}{3} * \pi * r^3 = 1.286\ m$$

The thickness of the Hydrogen tanks are calculated next with equation (4) given below.

(4) $$\text{Thickness} = t = \frac{p * r}{2 * Smax * ew} = 0.173\ mm$$

where

p = maximum tank pressure = 82,737.1 Pa
r = radius of tank = 1.286 m
Smax = maximum allowable working stress = 5.59 MPa
ew = approximate weld efficiency of tank material = 0.55

The maximum allowable working stress was calculated by taking the maximum allowable working stress of our tank material, Al-Li 2090 - T87, at 20 K, (615 MPa), and dividing by a factor of safety of 1.1 to get Smax = 559 MPa.
The mass of each tank without insulation was calculated using equation (5).

(5) $$\text{Mass of tank} = mt = 4 * \pi * r^2 * \rho(\text{Al-Li}) * t = 9.16\ kg$$

where

density of Al-Li = 2546.55 kg/m^3
t = thickness of tank = 0.173 mm
r = radius of tank = 1.286 m

The mass of the insulation is 0.99 kg/m^2. The total mass of the insulation on the Hydrogen tanks would then be the mass of the insulation, given above, times the surface area of the tank (6).

(6) $$\text{Mass of Insulation} = mi = (0.99\ kg/m^2) * (4 * \pi * r^2) = 20.64\ kg$$

The total mass of each tank is, therefore, mt + mi, which is 29.8 kg. The mass of the four tanks is 119.2 kg. The radius of each tank with 3.81 cm thick insulation is 1.32 m.

Oxygen Tanks

The total mass of Oxygen needed for each mission is 14,858 kg. This will be divided into two equally sized small tanks , and two equally sized larger tanks. These tanks are cylindrical with spherical ends. The initial volume of Oxygen is given by equation (1).

(1) $$\text{Volume} = V1 = \frac{\text{mass Oxygen}}{\text{density Oxygen}} = 13.06\ m^3$$

where

mass Oxygen = 14,858 kg
density Oxygen = 1137.5 kg/m^3

Again, accounting for the ullage volume, the total volume of the tanks are given by equation (2).

(2) $$\text{Total Volume} = VT = V1 + (.025) * V1 = 13.39\ m^3$$

The length of both the large tank and the small tank is L = 3 m (set by Payload Spacecraft Integration). The radius of the small tank, rs, is 0.4119 m. The radius of the large tank, rL, is 0.81 m. The total volume of each tank is calculated from equation (7).

(7) $$\text{Volume of each tank} = (\frac{4}{3} * \pi * r^3) + (4 * \pi * r * L)$$

with

Total volume of small tank = 1.454 m^3
Total volume of large tank = 5.06 m^3

After calculating the total volume of each tank, the volume of the spherical ends and cylindrical section can be calculated. From there, the mass and thickness of the spherical ends and the cylindrical section can be calculated separately. Calculations of the mass and thickness of the spherical ends will be done first.

Spherical Ends

The volume of one spherical end of each cylindrical tank is given by one half of equation (3). This gives the volume of one spherical end in the small tank as 0.146 m^3 . The volume of one spherical end in the large tank is 1.11 m^3 .

The thickness of the spherical end at the knuckle is given by equation (8). The knuckle is the bottom portion of the spherical end that will be attached to the

cylindrical section. This part must be thicker than the crown, which is the top of the spherical end, in order to be able to handle any welding and attachments located in this area.

(8) $$\text{thickness of knuckle} = tk = \frac{K * p * r}{Smax * ew}$$

where

K = stress factor = 0.67 (for spherical heads)
p = maximum tank pressure = 82,737.1 Pa
r = radius of spherical end
Smax = maximum allowable working stress = 545 MPa
ew = approximate weld efficiency of tank material = 0.55

For the small tank, tk = 0.76 mm. For the large tank, tk = 0.150 mm.

The maximum allowable working stress was calculated by taking the yield stress of Al-Li 2090 - T87 at 78 K (600 MPa) and dividing by a factor of safety of 1.1 to give an Smax = 545 MPa.

The thickness, tc, of the spherical ends at the crown is given by equation (4). For the small tank, tc = 0.057 mm. For the large tank, tc = 0.112 mm.

The mass of the spherical ends is given by one half of equation (5). The mass of the small tank spherical end is 0.154 kg, and the mass of both ends is 0.308 kg. The mass of the large tank spherical end is 1.176 kg, and both ends are 2.352 kg.

The insulation mass is given by equation (6), above. This gives an insulation mass of the small tank of 2.11 kg and an insulation mass of the large tank of 8.162 kg.

The total mass of the small spherical tank ends (both ends) with insulation is therefore 2.42 kg. The total mass of the large spherical tank ends (both ends) with insulation is 10.51 kg.

Cylindrical Section

The thickness and mass of the cylindrical sections can now be calculated for the small and large Oxygen tanks. The volume of the cylindrical section is given by equation (9).

(9) $$\text{Volume cylinder} = L * \pi * r^2$$

The volume of the cylinder of the small tank is 1.16 m^3. The length of the cylindrical section in the small tank is 2.18 m. The volume of the cylinder of the large tank is 2.84 m^3. The length of the cylindrical section of the large tank is 1.38 m. The thickness of the cylindrical section is given by equation (10) below.

(10) $$\text{Thickness of cylinder} = tcy = \frac{p * r}{Smax * ew}$$

where the values of the parameters in equation (10) are the same as for the spherical ends. The thickness of the small tank cylindrical section is 0.114 mm, and the thickness of the large tank cylindrical section is 0.224 mm. The thickness

of the cylindrical sections at the juncture is 5% thicker than the rest of the cylindrical section. The juncture is located at each end of the cylindrical section, and is attached to the spherical ends. It is thicker in order to be able to handle the weld and attachment stresses. The thickness at the juncture is given by equation (11).

(11) $$\text{Thickness at juncture, } tj = tcy + (.05) * tcy$$

Tj for the small tank is 0.120 mm, and tj for the large tank is 0.235 mm.

The mass of the cylindrical sections is given by equation (12).

(12) $$\text{Mass} = mc = (2 * \pi * r * L) * tcy * \rho(\text{Al-Li})$$

The mass of the small tank cylindrical section without insulation is 1.64 kg, and the mass of the large tank is 4.0 kg. The insulation mass of the cylindrical section is given by equation (13).

(13) $$\text{Insulation mass} = 0.99 \text{ kg/m}^2 * (2 * \pi * r * L)$$

This gives an insulation mass of the cylindrical section for the small tank of 5.58 kg, and for the large tank, insulation mass is 6.95 kg. Adding the tank mass and the insulation mass gives the total mass of the cylindrical section. The total mass of the small tank cylindrical section is 7.22 kg, and the total mass of the large tank cylindrical section is 10.95 kg.

Tabulation of all of the calculations gives a total volume for the small Oxygen tank of 1.454 m^3 , and a total mass (spherical ends plus cylindrical section) of 9.64 kg. The total volume of the large tank is 5.06 m^3 , and the total mass is 21.46 kg. The total weight of all four Oxygen tanks is 62.16 kg.

The above equations for the tank calculations (for both the Hydrogen and Oxygen tanks) can be found in References [9] and [10].

Lunar Dust Blast Radius, Sample Calculation

Baseline Data

$\varphi_{base} = 930 \frac{\text{particles}}{\text{cm}^2 * \text{sec}}$

$t_{descent} = 5$ sec

impact crater diameter = 0.005 mm = 0.00005 cm for a 50 μ particle

Scale factor for flux: velocity (and flux) of particles decrease roughly with square root of thrust decrease.

$\frac{33360 \text{ N}}{50000 \text{ N}} = 0.6672$ scale = $k = \sqrt{0.6672} = .8168$

Scaled data

$$\varphi = \varphi_{base} * k = 930 \frac{particles}{cm^2 * sec} * .8168 = 760 \frac{particles}{cm^2 * sec}$$

$$\varphi * t_{descent} = 760 \frac{particles}{cm^2 * sec} * 5 \text{ sec} = 3800 \frac{particles}{cm^2} \text{ or impacts per 1 cm}^2$$

Pitted area from one particle impact = 0.5 * surface area of sphere
$= 0.5 * (4 * \pi * (0.00005/2)^2) = 3.927 \times 10^{-9} \text{ cm}^2$

Pitted area from 3800 impacts = $3800 * 3.927 \times 10^{-9} \text{ cm}^2 = 1.5 \times 10^{-5} \text{ cm}^2$
or .015% of the surface area

After 10 landings, 1.5% of the surface pitted

Appendix C: Mission Analysis

Hohmann Transfer

The optimal method of transfer (lowest fuel consumption) between two coplanar circular orbits is a Hohmann transfer [15]. The Hohmann transfer is used during the rendezvous and the descent for UM-Haul.

Rendezvous

The UM-Haul rendezvous procedure requires a Hohmann transfer between the 111 km altitude parking orbit and the 101 km altitude chase orbit. In this maneuver, the Lander enters an elliptical orbit which is tangent to the two circular orbits at the points of maximum and minimum radii which are called apolune and perilune, respectively (see Figure 7.5). The semimajor axis (a) of the transfer ellipse is:

$$a = \frac{R_1 + R_2}{2} \qquad (C.1)$$

where: R_1 = radius of parking orbit = R_{moon} + altitude = 1849.1 km
R_2 = radius of chase orbit = 1839.1 km

Two velocity changes (ΔV's) required during a Hohmann transfer, and both ΔV's are assumed to be impulsive. The first ΔV is called the Descent to Chase Orbit Initiation (DCOI). This ΔV causes the Lander to leave the parking orbit and inserts the Lander into the transfer orbit at its apolune. The second ΔV is called the Chase Orbit Insertion (COI). This ΔV causes the Lander to leave the transfer orbit at its perilune and inserts the Lander into the chase orbit. Both ΔV's are retrograde because the Lander slows down during each one. The ΔV for DCOI is found by subtracting the speed of the Lander in the two orbits at their tangent point. The Lander in the parking orbit travels at the local circular speed, V_{lc}, of the 111 km altitude orbit. The local circular speed of an orbit is:

$$V_{lc} = \sqrt{\frac{\mu}{R}} \qquad (C.2)$$

where: μ = gravitational constant of the moon = 4902.8 km^3/sec^2

The speed in the elliptical transfer orbit at the tangent point is:

$$\frac{V^2}{\mu} = \frac{2}{R} - \frac{1}{a} \qquad (C.3)$$

Equation (C.3) comes from the conservation of energy. The ΔV for the DCOI maneuver is found using equations (C.1), (C.2), and (C.3):

$$\Delta V_1 = \Delta V_{DCOI} = \sqrt{\frac{2\mu}{R_1} - \frac{2\mu}{R_1 + R_2}} - \sqrt{\frac{\mu}{R_1}} \qquad (C.4)$$

The COI maneuver requires a ΔV of:

$$\Delta V_2 = \Delta V_{COI} = \sqrt{\frac{\mu}{R_2}} - \sqrt{\frac{2\mu}{R_2} - \frac{2\mu}{R_1 + R_2}} \qquad (C.5)$$

Substituting R_1 = 1849.1 km, and R_2 = 1839.1 km gives

$$\Delta V_{DCOI} = \Delta V_{COI} = 2.21 \text{ m/s}$$

The ΔV's for TPI and Braking cause the Lander to execute the same Hohmann transfer in reverse. Thus, the ΔV's are again 2.21 m/s each, but they are posigrade rather than retrograde, because the Lander must speed up to break the pull of the moon's gravity in order to reach a higher altitude. The time required for the Hohmann transfer is found by taking half of the period of the elliptical transfer orbit:

$$T_{Hohmann} = \pi \sqrt{\frac{a^3}{\mu}} \qquad (C.6)$$

Substituting a = 1844.1 km into equation (C.6) gives $T_{Hohmann}$ = 59 minutes, 13 seconds.

Descent

The descent trajectory is similar to a Hohmann transfer. The only difference is that at perilune, instead of circularizing, the Lander slows down to the powered descent speed of 9.8 m/s. The ΔV for the Descent Orbit Insertion (DOI) is found using equation (C.4) with R_2 = 1753.3 km since the perilune of the transfer orbit is at an altitude of 15.2 km. This gives ΔV_{DOI} = 21.8 m/s. Substituting a = 1801.2 km into equation (C.6) gives a time of 57 minutes and 11 seconds for the transfer from DOI to PDI.

Two-Impulse Insertion into the Parking Orbit

The ascent to the parking orbit is accomplished using a two-impulse insertion which will be explained in this section [9].

Transfer Orbit Insertion

The launch phase must provide the Lander with the necessary orbital velocity to insert into an elliptical transfer orbit with its apolune at the parking orbit altitude of 111 km. The velocity required depends on the range angle (ø in Figure C.1), which is the angle between insertion and apolune. In non-dimensional form:

$$\Delta\hat{V} = \frac{\Delta V}{\sqrt{\frac{\mu}{R}}} \qquad (C.7)$$

$$\Delta\hat{V}_1 = \sqrt{\frac{1 + 2\hat{h} - \frac{\hat{h}}{\hat{h} + 1 - \cos\phi}}{1 + \hat{h}}} \qquad (C.8)$$

where: $\hat{h} = \frac{h}{R_{moon}} = 0.064$

The non-dimensional form of the velocity at apolune, $\hat{V}_A$, is given by

$$\hat{V}_A = \sqrt{\frac{1 - \cos\phi}{(1 + \hat{h})(\hat{h} + 1 - \cos\phi)}} \qquad (C.9)$$

and the flight path angle at launch, γ_L, is given by:

$$\cos\gamma_L = \frac{1 + \hat{h}}{\sqrt{(1 + 2\hat{h}) + \frac{2\hat{h}^2}{1 - \cos\phi}}} \qquad (C.10)$$

Figures C.1 and C.2 define the variables introduced above.

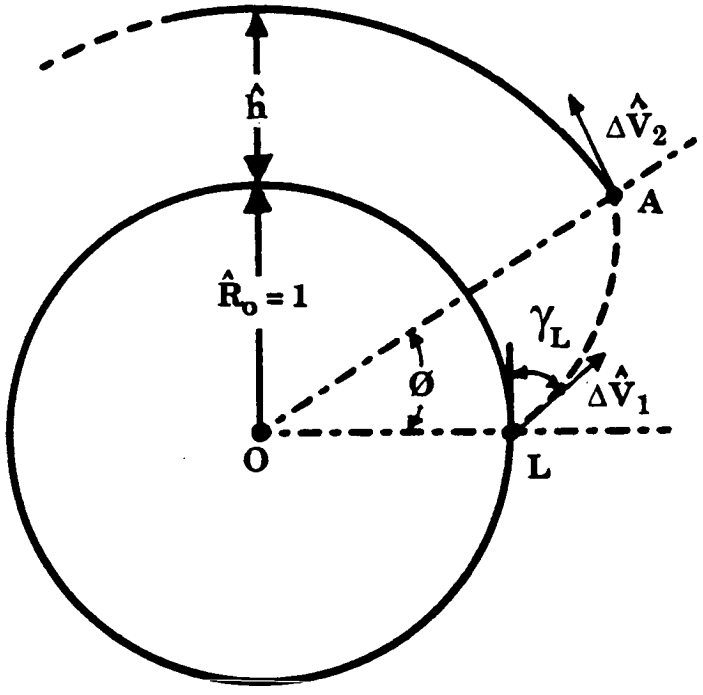

Figure C.1 - Two -Impulse Launch into Circular Orbit

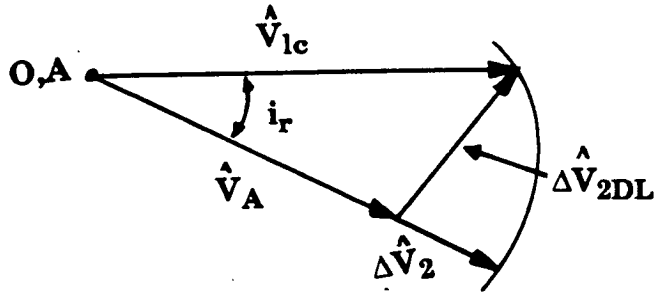

Figure C.2 - The Circularization Dog-Leg Maneuver

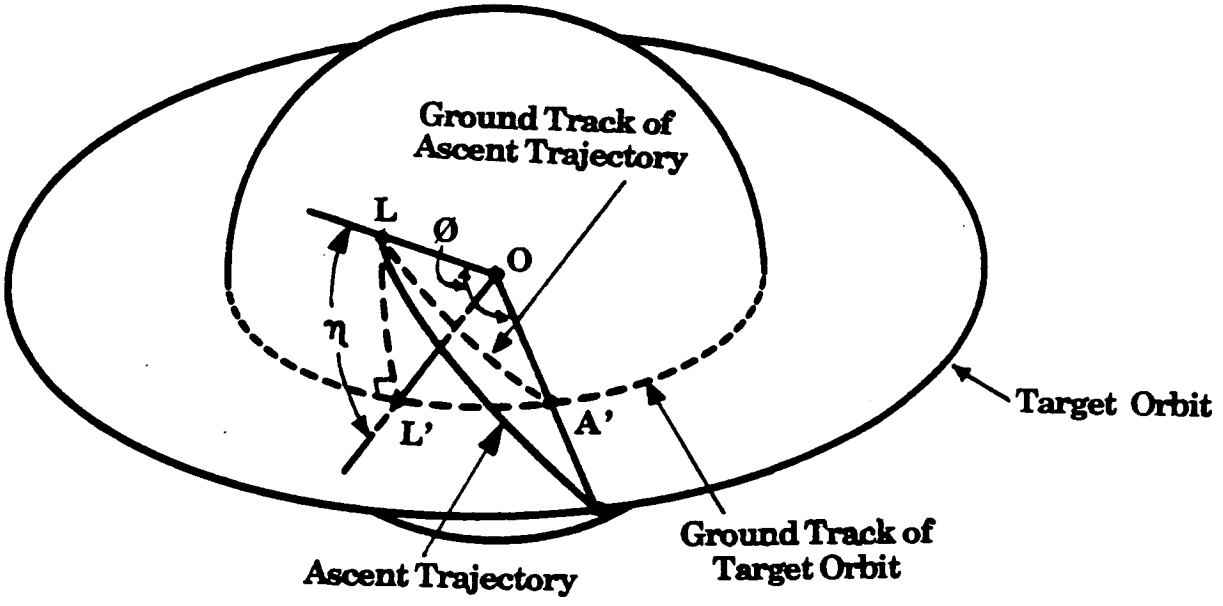

Figure C.3 - Geometry of Orbit Insertion

Dog-Leg Maneuver

In order for all ten UM-Haul landings to occur in lunar daylight, the right ascension of the parking orbit [Ω in Figure 7.10] must remain fixed [see Requirement for a Daylight Landing in Chapter 7]. However, the rotation of the moon causes Ω to increase each time that the Lander ascends to the parking orbit after a certain time on the surface. To correct for this effect, there must be a plane change at the parking orbit altitude. The Lander must also aquire the local circular velocity of the parking orbit to circularize its orbit at that altitude. This combined circularization and plane change, shown in Figures C.2 and C.3 is called a Dog-Leg Maneuver, and the ΔV for this maneuver is:

$$\Delta\hat{V}_{2DL} = \sqrt{\hat{V}_A^2 + \hat{V}_{lc}^2 - 2\hat{V}_A\hat{V}_{lc}\cos i_R} \qquad (C.11)$$

where i_R is the plane change angle. The plane change angle should be minimized in order to minimize the ΔV of the dog-leg maneuver. It turns out that $i_{Rmin} = \eta$, where η is the relative latitude of the landing site to the parking orbit. The relative latitude of the landing site is a measure of how far the landing site is out-of-plane of the parking orbit. The condition $i_{Rmin} = \eta$ corresponds to ø = 90°, and

the total $\Delta\hat{V} = \Delta\hat{V}_1 + \Delta\hat{V}_{2DL}$ is minimized when $\phi = 90°$. Thus, the ascent trajectory will intersect the parking orbit at $\phi = 90°$, and substituting this value into equations (C.8), (C.9), and (C.10) gives:

$$\Delta\hat{V}_1 = 1.6825 \text{ km/s}$$

$$\hat{V}_A = 0.94$$

$$\gamma_L = 3.436°$$

$\Delta\hat{V}_{2DL}$ depends on the relative latitude η, which changes with time due to the rotation of the moon:

$$\sin\eta = \sin i \cos l \sin(\delta + \omega_M t) - \cos i \sin l \qquad \text{(C.12)}$$

where:
- i = orbit inclination
- l = landing site latitude
- ω_M = the angular velocity of the moon = 8.807×10^{-4} rad/sec
- δ = angle between in-plane landing site and intersection of orbit ground track and equator [see Figure 7.10]
- t = surface wait time

The relationship between δ, l, and i is:

$$\sin\delta = \frac{\tan(l)}{\tan(i)} \qquad \text{(C.13)}$$

Since the Lander is always launched into the parking orbit with an inclination equal to the latitude of the next landing site to be visited, i = l, except for the case when the Lander changes landing sites. When the Lander completes its final mission at Mare Nubium (l = 10°), it will be launched into the parking orbit with an inclination equal to the latitude of Lacus Veris (i = 13°). Similarly, when the final mission at Lacus Veris (l = 13°) are complete, the Lander will be launched into the parking with an inclination equal to the latitude of Taurus Littrow (i=20°).

Thus, the angle η and $\Delta\hat{V}_{2DL}$ are both dependent on the surface wait time, the inclination of the orbit, and the latitude of the next landing site. Figure 7.10 is a plot of $\Delta\hat{V}_{2DL}$ as a function of the surface wait time for the various combinations of inclination and latitude. The surface wait time will generally be less than 1.5 days, so the dog-leg maneuver will require ΔV's ranging from 52.8 m/s (i = 10°, l = 10°) to 130.2 m/s (i = 20°, l = 13°).